Problems in Transport theory

by

Anupam Kundu

A Thesis submitted to the
Jawaharlal Nehru University
for the Degree of
Doctor of Philosophy

2010

Raman Research Institute
Bangalore 560 080
India

Certificate:

This is to certify that the thesis entitled **Problems in transport theory** submitted by **Mr. Anupam Kundu** for the award of the degree of Doctor of Philosophy of Jawaharlal Nehru University is his original work. This has not been published or submitted to any other University for any other Degree or Diploma.

Prof. Ravi Subrahmanyan
(Center Chairperson)
Director,
Raman Research Institute,
Bangalore 560 080, INDIA.

Prof. Abhishek Dhar
(Thesis Supervisor)
Raman Research Institute,
Bangalore 560 080, INDIA.

Declaration:

I hereby declare that the work reported in this thesis is entirely original. This thesis is composed independently by me at Raman Research Institute under the supervision of Prof. Abhishek Dhar. I further declare that the subject matter presented in this thesis has not previously formed the basis for the award of any degree, diploma, membership, associateship, fellowship or any other similar title of any university or institution.

(Prof. Abhishek Dhar) (Anupam Kundu)

Theoretical Physics,

Raman Research Institute,

Bangalore 560 080, INDIA.

Acknowledgement:

I would like to thank my supervisor Dr. Abhishek Dhar for his careful guidance throughout my Ph.D. programme. He was always ready to help me in both academic and non-academic matters. I have learnt a lot from him and most importantly how to be patient. He always has encouraged me to think in new ways and gave me a lot of freedom. I would like to convey my sincere regards and respect for his valuable involvement during the period of my graduate research.

Recently, I have worked with Dr. Sanjib Sabhapandit. I had many great discussions with him which helped me a lot in understanding many things in a better way. I enjoyed several tea-time discussions with Dr. Joseph Samuel and Dr. Supurna Sinha. I wish to convey my deep regards to them not only for academic discussions but also for non-academic advice.

It has been a very good stay at RRI doing my PhD work. Lots of people are responsible for making this stay happening, interesting and enjoyable. I would like to acknowledge some of my friends who have helped me in many aspects, namely, Suman, Arnab, Chandrakant, Pragya, Suchana, Alok, Venkat. Apart from research and studies, I spent a lot of happy hours with them. I would also like to thank all the football players of RRI for making many evenings memorable.

I would like to thank my parents and Kalpana for their support and encouragement.

I wish to thank all the people in RRI, administrative as well as academic, for making this stay enjoyable.

Preface

In this thesis we study theoretical problems in transport phenomena. These phenomena include the transport of heat or particles across a system due to the presence of external driving forces such as temperature gradients or electric fields. Some well known laws related to these phenomena are Fourier's law of heat conduction and Ohm's law of electrical conduction. These laws describe normal behaviour of macroscopic systems in nonequilibrium situations where external driving is weak and the system is close to equilibrium. There have been many attempts to understand these laws from a microscopic approach in the same spirit as one derives the thermodynamic properties of a system using equilibrium statistical mechanics. Some of the well known theories that have been developed in this regard are Boltzmann kinetic theory approach and the Green-Kubo formalism. However there are assumptions that go into these approaches and these may not always be valid. Another more recently developed theory is the non-equilibrium Green's function (NEGF) method. In this approach, which is closely related to the Landauer formalism, transport is viewed as a scattering problem in an open system which includes the reservoirs. In addition to these theoretical approaches there have been many attempts to understand heat transport through direct simulations of the microscopic equations of motion of the system with heat baths. These studies suggest Fourier's law is not valid in low dimensional systems and transport is anomalous. Recent developments of nanophysics and mesoscopic physics have made it possible for the experimental study of transport in low-dimensional systems and this provides further motivations for microscopic theoretical analysis. The following problems have been addressed in this thesis:

i) Is Fourier's law valid in higher dimensional disordered harmonic systems? How does heat current across such a system scale with system size in the asymptotic limit ? How does this scaling law depend on boundary conditions?

ii) The applicability of the standard Green-Kubo formula to small systems and systems with anomalous transport is problematic. We derive another linear response result for open classical systems which can be applied to both the above cases. We also obtain an exact analytical

expression for the current-current time correlation function for harmonic chain.

iii) Another related problem studied in this thesis is on the properties of fluctuations of transport current in various systems. An interesting result in this area, valid for systems far from equilibrium, is the so-called fluctuation theorem. This theorem involves rare fluctuations of the transport current whose probabilities are difficult to compute by usual simulations. In this thesis we have developed an algorithm to find probabilities of vary rare events and applied it to non-equilibrium processes involving both heat and particle transport. We have also calculated analytically the large-deviation function corresponding to the heat transfer across a harmonic system.

The plan of the thesis is as follows:

Chapter (1) is an introduction to the thesis. Here in the first part we describe the transport phenomena. Then we briefly discuss the methods and approaches applied to the theoretical study of transport phenomena. We also discuss the problems and limitations associated with these methods. Next part is devoted to some earlier studies relevant to our work. These are theoretical studies as well as simulation studies on heat conduction, which provide motivations for our work.

In Chapter (2) we introduce the Langevin equation and Green's function (LEGF) approach to study heat conduction in harmonic systems. We discuss the approach for harmonic systems in detail because we extensively use this approach and ideas in our work. Briefly, it involves solving a set of generalized Langevin equations by Fourier transforming them and then finding expectation values of observables by taking an average over noise configurations. One finds that the current through the system in the non-equilibrium steady state (NESS) can be written as an integral of a transmission function over all frequencies. The final result is the same as obtained by the NEGF approach and has the form of the Landauer formula. In the last section we discuss heat conduction in one-dimensional disordered harmonic systems where there are some well established results. In the next chapter we extend these ideas for one dimensional systems to understand heat conduction in higher dimensional systems.

Chapter (3) reports extensive numerical studies on heat conduction in two and three dimensional disordered harmonic systems. In this chapter we investigate the asymptotic system size dependence of the average heat current in the NESS. In the first section we use heuristic arguments based on kinetic theory and localization theory to predict the size dependence of the current for different boundary conditions. Next we calculate the current using the Landauer-like formula discussed in chapter (2) and also through direct non-equilibrium simulations. In our numerical approach we computed the transmission coefficient using an efficient algorithm based on the recursive properties of the Green's functions of the system. We also study the nature of the phonon modes of the harmonic system without coupling to heat baths. Finally we compare our numerical result against our heuristic predictions and discuss them.

In the beginning of chapter (4) we discuss the Green-Kubo formalism to study systems near equilibrium. We first briefly describe the existing mechanical derivation of the Green-Kubo formula which gives the response of a system to small external perturbations. Then we discuss the derivation of the corresponding formula for non-mechanical perturbations and the limitations of the use of the formula in small systems and systems with anomalous transport. Next we present our derivation of a similar linear-response formula for general open classical systems. We also give a detailed calculation of the time auto-correlation function of current for a disordered harmonic chain and show that it satisfies our open system formula. Unlike the standard Green-Kubo formula, our linear response result for open systems is valid for small systems and systems with anomalous transport.

Chapter (5) discusses a different problem in transport where we study properties of fluctuations of the heat as well as particle current. In this chapter we analytically compute the large deviation function of the probability distribution of heat transfer over a large time interval across a harmonic chain connected to heat baths. The algorithm is applied to both heat and particle transport. Next we describe an algorithm that we have developed to find the probabilities of very rare events in transport process.

Publications

- (1) Green-Kubo formula for open systems, Anupam Kundu, Abhishek Dhar, Onuttom Narayan, J. Stat. Mech. (2009) L03001

- (2) Heat transport and phonon localization in disordered harmonic crystals, Anupam Kundu, Abhishek Chaudhuri, Dibyendu Roy, Abhishek Dhar, Joel Lebowitz, Herbert Spohn, EPL **90** (2010) 40001.

- (3) Heat transport and phonon localization in mass-disordered harmonic crystals, Abhishek Chaudhuri, Anupam Kundu, Dibyendu Roy, Abhishek Dhar, Joel Lebowitz, Herbert Spohn, PRB **81**, (2010) 064301.

- (4) Time auto-correlation function and Green-kubo formula: A study on disordered harmonic chain, Anupam Kundu, submitted to PRE.

- (5) Algorithm for finding probabilities of rare events and application to non-equilibrium processes, Anupam Kundu, Sanjib Sabhapandit, Abhishek Dhar, Submitted to PRL.

- (6) Large deviation of heat flow in harmonic chains, Anupam Kundu, Sanjib Sabhapandit, Abhishek Dhar, in preparation.

Contents

1 Introduction **1**

1.1 Various approaches in transport theory 2

1.1.1 Drude-Sommerfeld theory 2

1.1.2 Semiclassical Boltzmann kinetic theory: Boltzmann equation . . . 3

1.1.3 Green-Kubo linear response theory 5

1.1.4 Non-equilibrium Green's function formalism 8

1.2 Earlier studies on heat transport 9

1.3 Problems addressed in the thesis 16

2 Heat conduction in harmonic systems **18**

2.1 Generalized Langevin equations and LEGF approach 19

2.2 Stationary solution of the equation of motion and steady state properties . . 24

2.3 Examples of baths 31

2.4 Current in d-dimensional disordered harmonic lattice 34

2.4.1 Transfer matrix approach and recursion relations for Green's functions 38

2.4.2 Current in one dimensional harmonic system: 41

2.4.3 Current in d-dimensional ordered harmonic system 46

3 Study on heat conduction in higher dimensional harmonic system **48**

3.1 Phonon localization 49

3.2 Kinetic theory 51

3.3 System and methods 51

3.4 Heat conduction in disordered harmonic crystals: General considerations . 55
3.5 Results from Numerics and Simulations 61
3.5.1 Results in two dimensions 61
3.5.1.1 Disordered $2D$ lattice without pinning 61
3.5.1.2 Disordered $2D$ lattice with pinning 70
3.5.2 Results in three dimensions 74
3.5.2.1 Disordered $3D$ lattice without pinning 74
3.5.2.2 Disordered $3D$ lattice with pinning 81
3.6 Conclusions 85
3.7 appendix 87

4 Green-Kubo formula for open systems 88

4.1 Proof of the formula for $1D$ lattice model 90
4.2 One dimensional lattice with other baths 95
4.3 Lattice models in higher dimensions 97
4.4 Fluid system coupled to Maxwell baths 99
4.5 Proof of the formula for boundary currents 102
4.5.1 Definition of the model 102
4.5.2 Steady state properties and current calculation 104
4.5.3 Calculation of auto-correlation function 106
4.5.4 Numerical results 108
4.6 Conclusions 113
4.7 appendix 114
4.7.1 Proof of Eq. [4.55] 114
4.7.2 Expressions of K_1s 115

5 Large deviations in transport processes 116

5.1 Large deviation function of heat flow in harmonic chain 117
5.1.1 Derivation 122

5.1.2 Single Brownian particle 129
5.2 Algorithm for finding probabilities of rare events 131
5.2.1 The algorithm 132
5.2.2 Symmetric simple exclusion process 133
5.2.3 Heat conduction 135
5.3 Conclusions 139
5.4 Appendix 139
5.4.1 Expression of the matrix $E(\omega)$: 139
5.4.2 Expressions of the elements of $J(\lambda, \omega)$ and $c(\omega)$: 141

1 Introduction

We know that when an external electric field is applied across a conductor, an electrical current flows across the system. Similarly when a chemical potential difference or a temperature difference is maintained across a system, then particle current or energy current flows through the system. These are examples of transport phenomena. Normally these phenomena are described by phenomenological laws, namely Ohm's law of electrical transport and Fourier's law of thermal transport. For electrical conduction, the current density $\mathbf{j}_e$ through the system is proportional to the applied electrical field $\mathbf{E}$:

$$\mathbf{j}_e = \sigma \mathbf{E} \tag{1.1}$$

and for thermal conduction, the heat current density $\mathbf{j}_{th}$ is proportional to the temperature gradient ∇T:

$$\mathbf{j}_{th} = -\kappa \nabla T. \tag{1.2}$$

The proportionality constants σ and κ are called electrical conductivity and thermal conductivity respectively. These proportionality constants are normally known as transport coefficients. These characterise the transport properties of a macroscopic substance. One of the main interest in the theoretical study of transport phenomena is to understand these laws and compute the transport coefficients from a microscopic point of view. Attempts to derive these laws starting from microscopic description of a system, have been started long back. All these attempts have led to various theoretical techniques. Clearly these are non-equilibrium phenomena and their study also has provided new understanding in non-equilibrium physics. In sec. (1.1) of this chapter we will briefly discuss the different approaches used to understand

charge and energy transport. In Sec. (1.2) we discuss the earlier results in heat conduction. Finally, in Sec. (1.3) we describe the problems addressed in this thesis.

1.1 Various approaches in transport theory

One of the main goals of a complete theory of transport would be to derive linear response formulae such as Eqs. (1.1,1.2) starting from a microscopic description in the usual framework of statistical mechanics. This task seems to be very difficult. The earliest attempts were aimed at finding heat conductivity of gases using kinetic theory. Later Drude applied kinetic theory to gas of conducting electrons in metal to study transport phenomena. In case of thermal conduction in insulating solids Debye applied kinetic theory to gas of phonons. In 1929 R. Peierls formulated Boltzmann equation for phonons to study thermal transport in solids. Since then Peierls-Boltzmann theory became a cornerstone in the theory of thermal conduction in solids. Later several other theoretical approaches were developed to study transport and these include Green-Kubo formalism, Landauer formalism, non-equilibrium Green function formalism etc. In the following we will discuss these approaches.

1.1.1 Drude-Sommerfeld theory

In 1900 Drude made one of the first attempt to derive these phenomenological laws Eq. (1.1) and (1.2) of charge and energy conduction by conducting electrons in metals, starting from a microscopic point of view . He applied kinetic theory of gas to conducting electrons moving in the field of heavy ions which form the underlying lattice. In spite of electron-electron interaction and electron-ion interaction Drude model treats this metallic gas as a neutral dilute gas in which kinetic theory can be applied. The basic assumptions in this theory are [1]: (i) Between successive collisions and in the absence of electromagnetic field the electrons move uniformly in a straight line. (ii) The effect of interactions are taken into account by simply considering that electrons suffer random collisions. As in kinetic theory the collisions are modeled as instantaneous events which alter velocities abruptly. The probability of an electron undergoing a collision in time dt is dt/τ where τ is a phenomenological parameter and

known as relaxation time. (iii) Electrons are assumed to achieve thermal equilibrium with their surroundings only through collisions.

Though the Drude model neglects the details of both the electron-electron and electron-ion interactions, it was quite successful to explain Ohmic behaviour of metallic conductor, Fourier's law of thermal conduction (assuming local thermal equilibrium achieved by collisions) and phenomenological Wiedemann-Franz law. From Drude model one gets explicit forms of the transport coefficients σ and κ in terms of the electron density n, charge e, mass m, mean velocity v and a single phenomenological parameter τ. The expressions for σ and κ are following

$$\sigma = \frac{ne^2\tau}{m}, \tag{1.3}$$

$$\kappa = \frac{1}{3}v^2\tau C_V\,, \tag{1.4}$$

where C_V is the electronic specific heat. We note that the thermal conductivity can also be expressed in terms of mean free path $\ell = v\tau$ as :

$$\kappa = \frac{1}{3}v\ell C_V. \tag{1.5}$$

The ratio $\kappa/\sigma T = 3K_B^2/2e^2$ gives the Lorentz number. Here K_B represents Boltzmann constant. The agreement of this number with experimental results was one of the success of Drude theory. A more correct approach is to use the Fermi-Dirac distribution for the electrons velocities. Using Fermi-Dirac distribution, Sommerfeld obtained a more correct expression for the Lorentz number: $\kappa/\sigma T = \pi^2 K_B^2/3e^2$.

1.1.2 Semiclassical Boltzmann kinetic theory: Boltzmann equation

In kinetic theory picture, one considers a gas of interacting particles which are the carriers of heat or charge. The usual carriers are molecules of a gas, electrons in a metal, phonons in crystalline solid etc. These carriers experience random collisions and Kinetic theory gives an expression for the conductivity in terms of the mean free path ℓ.

The Boltzmann equation approach is a more systematic way of deriving kinetic theory re-

sults. Let us first discuss this for electrons in metals. In this approach one considers electrons at time t labelled by mean position $\mathbf{r}$ and mean momentum $\mathbf{k}$. Between successive collisions electrons are described by a wave packet. One then defines a non-equilibrium distribution function $g(\mathbf{r}, \mathbf{k}, t)$ such that, $g(\mathbf{r}, \mathbf{k}, t) d\mathbf{r} d\mathbf{k}/4\pi^3$ is the number of electrons at time t in the semiclassical phase space volume $d\mathbf{r}d\mathbf{k}$ about the point $\mathbf{r}$, $\mathbf{k}$. It is assumed that between two successive collisions, $\mathbf{r}$ and $\mathbf{k}$ evolve according to the semiclassical equations of motion under the influence of external forces [1, 2, 3].

The time evolution equation of the distribution function $g(\mathbf{r}, \mathbf{k}, t)$ is given by the Boltzmann equation:

$$\begin{aligned} \frac{\partial g}{\partial t} + \mathbf{v}.\nabla_{\mathbf{r}}\, g + \mathbf{F}.\frac{1}{\hbar}\nabla_{\mathbf{k}}\, g &= (\frac{\partial g}{\partial t})_{coll} \\ \text{where, } \mathbf{v} &= \frac{1}{\hbar}\nabla_{\mathbf{k}}\, \mathcal{E}(\mathbf{k}), \end{aligned} \tag{1.6}$$

and $\mathcal{E}(\mathbf{k})$ is the energy dispersion for electrons. In the above equation $\mathbf{F}$ represents the external forces and $(\partial g/\partial t)_{coll}$ represents the contribution from collisions. The collision term in the right hand side of the above equation is calculated using different approximations in different situations. Very often it is calculated using Fermi golden rule. The final result is quite often in the form of the kinetic theory answers $\kappa \sim \int d\mathbf{k} c_{\mathbf{k}} v_{\mathbf{k}} \ell_{\mathbf{k}}$, with an explicit form for the mean free path $\ell_{\mathbf{k}}$. In high temperature regime the main source of collision in metal is the lattice thermal vibrations, whereas impurities are the source of scattering in low temperatures. Surface or boundary scattering are dominant source of scattering in nanostructures like quantum wires, quantum tubes, dots etc. Next we discuss the case of heat conduction in crystalline solids.

In crystalline solids, the dynamical entities are the ions which are arranged (mean positions) in a regular periodic array forming the lattice. At non zero temperature this ions oscillate about their mean positions. The normal modes of the lattice vibrations are called phonons, which are the carriers of heat in metals as well as in electronic insulators. Debye, like Drude, treated this vibrating lattice as a gas of phonons and applied kinetic theory to express the phonon thermal conductivity κ_{ph} in terms of the phonon specific heat per unit vol-

ume c_V^{ph}, mean velocity v and mean free path ℓ as $\kappa_{ph} \sim c_V^{ph} v \ell$. Later Peierls wrote Boltzmann equation for phonons [4] and showed how important anharmonicity, and specifically Umpklapp precesses, is in giving rise to finite lattice thermal conductivity. Solving the Boltzmann equation in the relaxation time approximation gives a simple kinetic theory like expression for the thermal conductivity, $\kappa_{ph} \sim \int d\mathbf{k} c_{\mathbf{k}} v_{\mathbf{k}}^2 \tau_{\mathbf{k}}$, where $\tau_{\mathbf{k}}$ is the time between collisions, and $\mathbf{k}$ refers to different phonon modes of the crystal. The relaxation time $\tau_{\mathbf{k}}$ can get contributions from various sources. In case of phonon conduction the main source of scatterings are impurities and phonon-phonon interactions. Impurity scattering can arise due to the randomness of the masses of the ions and force constants, whereas the phonon-phonon scattering arises due to the higher order terms (beyond quadratic order) in the expansion of inter-particle potential. In three dimensional solids, the Peierls-Boltzmann theory is well-developed [2, 3, 4] and probably quite accurate. Only problem with Peierls-Boltzmann theory is that meaning of $g(\mathbf{r}, \mathbf{k}, t)$ is not very clear since phonons are extended objects. The recent work of Spohn and Lukkarinen [5, 6] tries to give a rigorous basis for the phonon Boltzmann equation.

1.1.3 Green-Kubo linear response theory

Earlier two approaches of transport considers classical or semiclassical motion of interacting carriers with appropriately introduced incoherent scattering mechanisms. Now we discuss a general theory of transport called the Green-Kubo formalism which can be applied to both classical and quantum systems. In this formalism one prepares a system in equilibrium and then applies a small perturbation to the system. Due to this small perturbation the system will be slightly out of equilibrium. In response to the perturbation, the expectation values of observables will change from their equilibrium values. In this formalism one finds this response to linear order in perturbation strength. One finally obtains a formula which provides a relation between the transport coefficients, such as electrical conductivity or the thermal conductivity, and appropriate equilibrium time correlation functions. This formula has been proved both for mechanical perturbations (perturbations in Hamiltonian) and non-mechanical perturbation (perturbation in the boundary condition). Here we briefly sketch the

derivation of this formula for mechanical perturbation.

Let us consider a quantum system in thermodynamic equilibrium which is described by a time-independent Hamiltonian $\hat{H}_0$ and temperature T (inverse temperature is $\beta = 1/K_B T$ where K_B is the Boltzmann constant). We assume that in the long past $t = -\infty$ the perturbation is switched on. Now the total Hamiltonian is

$$\hat{H}_{tot} = \hat{H}_0 + \hat{H}_p \quad \text{where} \quad \hat{H}_p = f(t)\hat{B}. \tag{1.7}$$

In the above expression $f(t)$ represents the strength of the perturbation, for example electric field, magnetic field etc. At $t = -\infty$ the expectation value of any operator $\hat{A}$ is given by

$$\langle \hat{A} \rangle_0 = tr\{\rho_0 \hat{A}\}, \tag{1.8}$$

where, ρ_0 is the equilibrium density matrix. Because of the perturbation the steady state expectation value of $\hat{A}$ will change. The change is given as

$$\delta\langle \hat{A}(t) \rangle = tr\{\delta\rho(t)\hat{A}\}, \quad \text{where,} \quad \delta\rho(t) = \rho(t) - \rho_0. \tag{1.9}$$

We find $\delta\rho(t)$ from the time evolution equation of $\rho(t)$

$$i\hbar \frac{\partial \rho}{\partial t} + [\rho, \hat{H}_{tot}] = 0 \quad \text{with} \quad \rho(-\infty) = \rho_0, \tag{1.10}$$

where, [..] represents commutation operation. Since we want $\delta\rho(t)$ to be linear order in f, we expand above expression and keep terms linear order in f. In the interaction picture ($\hat{A}^I(t) = e^{i\hat{H}_0 t}\hat{A}e^{-i\hat{H}_0 t}$) we get

$$i\hbar \frac{\partial \delta\rho^I}{\partial t} = -[\rho_0, \hat{H}_p^I] \quad \text{with} \quad \delta\rho^I(-\infty) = 0, \tag{1.11}$$

whose formal solution is

$$\begin{aligned} \delta\rho^I(t) &= \frac{i}{\hbar}\int_{-\infty}^{t} dt' [\rho_0, \hat{H}_p^I(t')] \\ &= \frac{i}{\hbar}\int_{-\infty}^{t} dt' \rho_0 \int_0^{\beta} d\lambda [\hat{H}_p^I(t' - i\lambda\hbar), \hat{H}_0] \end{aligned}$$

$$= -\int_{-\infty}^{t} dt' \rho_0 \int_0^{\beta} d\lambda \hat{H}_p^I(t' - i\lambda\hbar). \tag{1.12}$$

In the second line of the above equation we have used the following relation:

$$F(\beta) = [\hat{V}^I(t'), e^{-\beta\hat{H}_0}] = -e^{-\beta\hat{H}_0} \int_0^{\beta} d\lambda [\hat{V}^I(t' - i\lambda\hbar), \hat{H}_0], \tag{1.13}$$

and in the third line we have used the time evolution equation of operators in the interaction picture. Using the above solution given in Eq. (1.12) we calculate $\delta\langle\hat{A}(t)\rangle$ and get

$$\begin{aligned}
\delta\langle\hat{A}(t)\rangle &= -\int_{-\infty}^{t} dt' f(t') \int_0^{\beta} d\lambda tr\{\rho_0 \hat{\bar{B}}^I(t' - i\lambda\hbar)\hat{A}^I(t)\} \\
&= -\int_{-\infty}^{t} dt' f(t') \int_0^{\beta} d\lambda \langle \hat{\bar{B}}^I(t' - i\lambda\hbar)\hat{A}^I(t)\rangle_0 \\
&= \int_{-\infty}^{\infty} \chi_{AB}(t - t') f(t').
\end{aligned} \tag{1.14}$$

where,

$$\chi_{AB}(t - t') = \int_0^{\beta} d\lambda \langle \hat{\bar{B}}^I(t' - i\lambda\hbar)\hat{A}^I(t)\rangle_0 \Theta(t - t') \tag{1.15}$$

Thus the response $\chi_{AB}(t-t') = \delta\langle\hat{A}(t)\rangle/\delta f(t')$ is related to the equilibrium correlation function $C_{AB}(t - t') = \langle \hat{\bar{B}}^I(t' - i\lambda\hbar)\hat{A}^I(t)\rangle_0$. In the classical limit $\hbar \to 0$ which is equivalent to $\beta \to 0$ we may approximate the formula in the second line of Eq. (1.14) as

$$\delta\langle\hat{A}(t)\rangle = -\beta \int_{-\infty}^{t} dt' f(t')\langle \hat{\bar{B}}(t')\hat{A}(t)\rangle_0. \tag{1.16}$$

The results in Eqs. (1.15,1.14) are referred to as the Green-Kubo formula.

Now let us consider the case of electrical conduction in a gas of N electrons contained in a one dimensional box of length L. Let x_l be the position of the l^{th} particle and e be the charge of electron. The density of electrons at x is given by: $\hat{n}(x) = \sum_l \delta(x - x_l)$. Now we perturb the system by applying an electrostatic potential $\phi(x, t)$. The perturbation is written as $\hat{H}_p = e\int_0^L e^{\epsilon t}\phi(x, t)\hat{n}(x, t)$ where ϵ is a positive parameter which controls the rate at which the field is switched on. From continuity equation $\hat{\dot{n}}(x, t) = -\partial\hat{j}(x, t)/\partial x$, one defines the

electrical current as $\hat{j}(x,t) = \sum_l \dot{x}_l \delta(x - x_l)$. If we take $\hat{A} = \hat{j}(x,t)$ then from Eq. (1.16) we get

$$\langle \hat{j}(x,t) \rangle = -e \int_{-\infty}^{t} dt' \int_0^L dx' e^{\epsilon t'} \phi(x',t') \langle \hat{n}(x',t') \hat{j}(x,t) \rangle_0. \tag{1.17}$$

Using continuity equation and doing a partial integration one gets

$$\langle \hat{j}(x,t) \rangle = \beta e \int_{-\infty}^{t} dt' e^{\epsilon t'} \int_0^L dx' E(x') \langle \hat{j}(x,t) \hat{j}(x',t') \rangle. \tag{1.18}$$

where we have ignored boundary terms requiring that currents at the boundaries are zero. One can show that only in the limit $L \to \infty$ then $\epsilon \to 0$, $\langle j(x,t) \rangle \neq 0$ [7]. For constant electric field one defines the electrical conductivity as $\sigma = \langle \hat{j}(x,t) \rangle / E$ and is given by

$$\sigma = \beta e \lim_{\epsilon \to 0} \int_0^\infty dt e^{-\epsilon t} \lim_{L \to \infty} \int_0^L dx' \langle \hat{j}(x,t) \hat{j}(x',0) \rangle. \tag{1.19}$$

In terms of total current $\hat{J} = \int_0^L dx \hat{j}(x)$ the above formula reads as

$$\sigma = \beta e \lim_{\epsilon \to 0} \int_0^\infty dt e^{-\epsilon t} \lim_{L \to \infty} \frac{1}{L} \langle \hat{J}(t) \hat{J}(0) \rangle. \tag{1.20}$$

This is the Green-Kubo formula (GK) for electrical conductivity. As shown by Luttinger [7] one can do a mechanical derivation for thermal conduction and this gives a similar formula for thermal conductivity which looks like

$$\kappa = \frac{1}{K_B T^2} \lim_{\epsilon \to 0} \int_0^\infty dt e^{-\epsilon t} \lim_{L \to \infty} \frac{1}{L} \langle \hat{J}_E(t) \hat{J}_E(0) \rangle, \tag{1.21}$$

where $\hat{J}_E$ is the total energy current.

1.1.4 Non-equilibrium Green's function formalism

The Non-equilibrium Green's function formalism (NEGF) is a highly developed technique. It was first invented in the context of quantum transport to calculate the steady state properties of a finite system connected to reservoirs [8, 9]. The reservoirs are modeled by non-interacting Hamiltonians with infinite degrees of freedom.

As an example consider a system of electrons, which is in contact with reservoirs which are themselves gas of non-interacting electrons. One starts with the system initially decoupled

with the reservoirs, which are in equilibrium at different temperatures and different chemical potentials. The initial state of the system and the decoupled reservoirs are described by a well defined density matrix. Considering that at $t = -\infty$ the couplings of the system with the reservoirs are switched on, one evolves the density matrix with this full Hamiltonian given by

$$\mathcal{H} = \hat{H}_s + \hat{H}_L + \hat{H}_R + \hat{V}_{Ls} + \hat{V}_{Rs} \tag{1.22}$$

where $\hat{H}_s$ is the system Hamiltonian, $\hat{H}_{L,R}$ are Hamiltonians of left and right reservoirs and $\hat{V}_{Ls}$, $\hat{V}_{Rs}$ are couplings of the system with the left and right reservoirs. Now the density matrix of the entire system (system plus reservoir) is evolved for an infinite time so that one eventually reaches a non-equilibrium steady state (NESS). Various physical observables such as currents, densities, etc, can be calculated using this non-equilibrium density matrix. For non-interacting systems one obtains an expression for the steady state current in terms of transmission coefficient of the carriers across the system. These expressions are basically the same expressions that one obtains from the Landauer formalism [10] where, one thinks of the transport through the system as a quantum mechanical scattering process. For noninteracting systems, an equivalent and simpler approach is Langevin equation and Green's function approach (LEGF), where instead of the density matrix one deals with the Heisenberg equations of motion for the dynamical variables. Integrating out the bath degrees of freedom one obtains a Generalised Langevin equation. For classical system the two approaches are like considering the Fokker-Planck approach versus the Langevin approach. It is possible to show that one can get all the results of NEGF, from LEGF approach. We discuss the LEGF approach in chapter (2) in detail.

1.2 Earlier studies on heat transport

As discussed in the beginning of sec. (1.1), one of the goals in the theoretical study of heat transport is to derive Fourier's law from a statistical mechanical calculation. But this task is formidably difficult. As is usual in theoretical physics, the guiding criterion of mathematical

simplicity leads one naturally to consider simple mathematical models which are able to provide more detailed understanding to the necessary and sufficient conditions needed to prove Fourier's law.

One of the commonly used tests of Fourier's law is to look at the dependence of heat current density on the system size. Let j be the heat current density flowing through the system in the steady state due to the small temperature difference ΔT applied across a system of linear size N. Now let us define the finite system conductivity as

$$\kappa_N = \frac{jN}{\Delta T} \ . \tag{1.23}$$

Then the conductivity appearing in Fourier's law is given by

$$\kappa = \lim_{N\to\infty} \lim_{\Delta T\to 0} \kappa_N \ . \tag{1.24}$$

The validity of Fourier's law requires the above limit to be finite and in that case Eq. (1.23) and (1.24) imply that j should scale as N^{-1} in the large N limit (asymptotic limit). But in many cases, especially in low dimensional systems, it is seen that

$$j \ \sim \ N^{-\mu}, \tag{1.25}$$

with $\mu \neq 1$. The thermal conductivity behaves then as $\kappa_N \sim N^{\alpha}$ where $\alpha = 1 - \mu$. For two dimensional systems there are some analytic studies which suggest $\kappa \sim ln(N)$. Fourier's law holds only if $\alpha = 0$. Some important questions are to find the scaling exponent α and to decide the necessary and sufficient conditions for the validity of Fourier's law. Below we give a summery of earlier studies addressing these questions. From now onwards κ_N will be denoted by κ only.

The harmonic crystal is a good starting point for understanding heat transport in solids. In the non-equilibrium case, the problem of heat conduction in a classical ordered 1D harmonic crystal was studied for the first time by Rieder, Lebowitz and Leib (RLL)[11]. Considering the case of stochastic Markovian baths they were able to obtain full phase-space probability distribution in the steady state exactly. Using this distribution they showed that temperature

in the bulk of the system is equal to the mean value of the two bath temperatures and obtained an expression for the steady state current and also showed that in the large system size limit current is independent of system size. Nakazawa (NK) [12] obtained the exact non-equilibrium steady state distribution for an ordered harmonic chain with an onsite harmonic potential at all sites and extended these results in higher dimensions. Results of RLL and NK papers were also obtained by Dhar and Roy [13] using LEGF approach. The conclusion that one draws from these studies is, the heat current in an ordered harmonic lattice is independent of system size $\kappa \sim N$ (for large systems). This result is expected since there is no mechanism for scattering of heat carriers, namely the phonons, and hence transport is ballistic. One then thinks of introducing scattering mechanism to get Fourier's behavior. There are two ways of introducing scattering of phonons (i) introduction of disorder in the system (ii) introduction of anharmonicity which would cause phonon-phonon scattering. Disorder can be introduced in various ways, for example by making the masses of the particles random or by making the spring constants random. Anharmonicity can be introduced by making the interaction force anomg the particles non-linear. First we state earlier results on disordered harmonic systems and next we will give results in interacting (anharmonic) systems.

Disordered harmonic systems: In this case the carriers of heat are the normal modes of lattice vibrations (phonons). Since the normal modes take part in the conduction of heat it is expected that heat conduction in disordered harmonic systems will be strongly affected by the physics of Anderson localization. This was first discovered in disordered electronic systems. Because of multiple scattering electronic states become localized at some point in space, where it's amplitude is significant and it decays exponentially from that point. In fig. (1.1) we show typical examples of extended and localized states, where ξ represents the localization length.

One can thus expect the same kind of physics as in electronic systems where localization was first studied. In fact the problem of finding the normal modes of the disordered harmonic lattice can be directly mapped to that of finding the eigenstates of an electron in a disordered potential and described by the tight binding model (see chapter (3)). The effect of localization

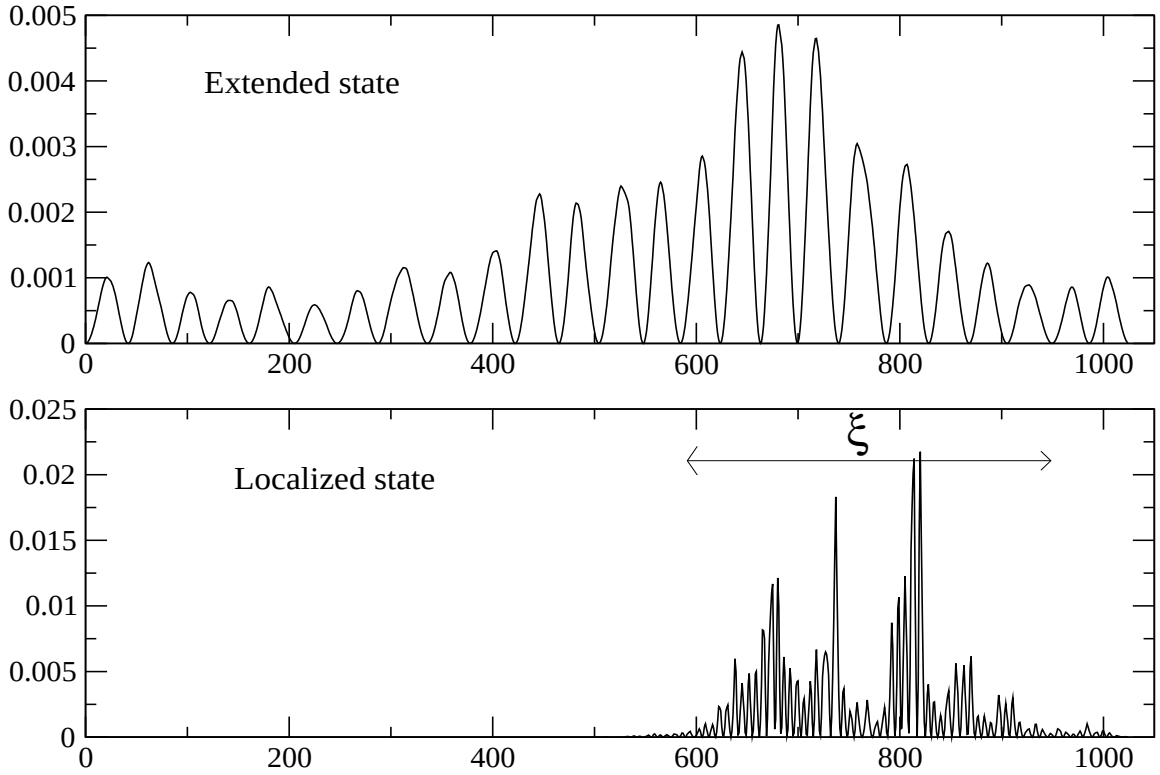

Figure 1.1: Typical plots of an extended state and a localized state with localization length ξ.

on transport in phonon case is much the same as in electron case except for the following two facts : (a) In the absence of external potential, the translational symmetry of the system leads to the fact that low frequency modes are not localized and hence contribute to transport. (b) Secondly, in the phonon case all frequencies participate in transport whereas electron-transport is dominated by electrons near Fermi level. Because of these two differences, the disordered harmonic crystal in one and two dimensions is not a heat insulator in contrast to the electron case.

One of the earlier important work on phonon heat transport in disordered systems was by Matsuda and Ishii (MI) [14] who showed that all high frequency modes in a disordered harmonic chain were exponentially localized and this led to anomalous transport. They also showed that, for small ω the localization length in an infinite chain goes as ω^{-2}. This implies that, localization length for normal modes with frequency $\omega < N^{-1/2}$ is greater than N and these low frequency modes are extended and hence they participate in transport. The disordered harmonic chain has been extensively studied by several authors [15, 16, 17, 18,

19, 20, 21, 22]. Two different models of baths and boundary conditions have been studied: (i)white noise bath (WNB) (ii) Rubin's model of baths (R). In the second model, baths are itself modeled as semi-infinite ordered harmonic chains. One of the main conclusions was that the exponent α depends on the choice of boundary conditions (BCs). For free BC (no external forces acting on the system) one gets $\alpha = 1/2$ while for fixed BC (external forces acting at the boundaries only) one gets $\alpha = -1/2$. Another model was studied by Bolsteri et al. [23], in which they have connected each site of a harmonic chain to a self-consistent reservoirs to introduce scattering of phonons. Bonetto et al.solved this model exactly and proved the existance of local thermal equilibrium and the validity of Fouriers law. Later this model model was again studied by Dhar and Roy [24] using LEGF approach in both the classical and quantum cases.

There are very few studies on the problem of heat conduction in higher dimensional disordered systems. These include study of localization properties in disordered continuous elastic media by John et al. [25] using renormalization group theory, simulation studies on two-dimensional harmonic system with bond-missing disorder by Lei yang [26] and simulation studies on harmonic crystal in 2D with binary mass disorder by Lee and Dhar [27]. In their study John et al. showed that : in one dimension, all modes with $\omega > 1/N^{1/2}$ are localized; in two dimensions, all modes with $\omega > 1/[log(N)]^{1/2}$ are localized and in three dimensions, there is a finite band of frequencies of non-localized states. However, this study was unable to extract the system size dependence of heat current in a disordered lattice in any dimension. By simulating the Langevin equations for two different heat bath models Lee and Dhar obtained different system size dependence of the conductivity. With fixed BCs they obtained $\alpha \approx 0.41$ for white noise baths and for exponentially correlated Gaussian noise bath it is 0.49.

Interacting systems: The other way of introducing scattering of phonons is to include anharmonicity in the system. There are few analytic results for one dimensional interacting systems and all of them are based on the use of Green Kubo formula. Mainly three different approaches have been used to study interacting systems which are: renormalization group (RG)

theory of hydrodynamic equations, mode coupling theory (MCT) and the Peierls-Boltzmann kinetic theory approach. All these theories aim at calculating the equilibrium current-current time auto-correlation $C(t) = \langle j(t)j(0)\rangle$.

Narayan and Ramaswamy [28] introduced the first approach in the study of transport phenomena and used RG theory to study transport phenomena in a one dimensional system of interacting particles described by the following density fields: number, momentum and energy densities respectively, corresponding to the following conserved quantities: total number of particles, total momentum and total energy respectively. Using RG they obtained that $C(t) \sim t^{-2/3}$ for large t and putting a upper cut-off $t_N \sim N$ in the GK formula they obtained $\alpha = 1/3$.

The MCT approach was first introduced by Lepri, Livi and Politi [29] in the study of energy conduction and has subsequently been used by several other authors [29, 30, 31, 32, 33]. In this theory one tries to calculate the slow relaxation of spontaneous fluctuations of long-wave length modes since in low dimensional systems it is related to the long time tails of C(t). Inserting this $C(t)$ into the GK formula (with a cutoff $\propto N$) one obtains the value of α. Predictions are different for different situations. When the anharmonic potential carries a cubic leading power then $\alpha = 1/3$ whereas for a quartic leading order $\alpha = 1/2$. There are many computer simulation attempts on energy transport in FPU chains and other interacting models to sort this disagreement, but different simulations gave various exponents [29, 34, 32, 35, 36, 37, 38]. People have studied joint effects of anharmonicity and disorder on the system size dependence of heat current in FPU chains [39]. Simulation in disordered anharmonic chains by Dhar and Saito [40] found that the asymptotic power law dependence of current on system size always dominated by anharmonicity and got $\alpha = 1/3$.

There are studies in fluid systems with non-linear interactions. A number of studies were made for momentum conserving (translationally invariant) systems using non-equilibrium simulations and using the GK formalism [41, 42, 43, 44, 45, 46, 47]. The values of α obtained in these studies do not match. In momentum non-conserving systems, in addition to interparticle interaction, particles experience external potentials. All studies in these kind of model

systems agree upon Fourier like behaviour in large system size limit [41, 48, 49, 50, 51, 52].

Effects of interaction have been studied in higher dimensional systems both theoretically and numerically. The MCT and hydrodynamic approach predict that for momentum conserving systems, the thermal conductivity diverges logarithmically in two dimensions and finite in three dimension. But reported values of α in various numerical studies in two dimension do not agree [53, 54, 55, 56]. In the presence of pinning all theories predict a finite conductivity in all dimensions. In a very recent simulation, Saito and Dhar [57] provided first verification of Fourier's law in a 3D anharmonic crystal without pinning potential. (For a detailed discussion see [58, 59]). In order to obtain the correct exponent one requires to go to large system sizes and at some point the sizes required are beyond current computational capabilities. In summary, main conclusions of these studies of transport phenomena are following:
(i) Fourier's law is not valid in disordered harmonic crystal in one and two dimensions. The disordered averaged current in NESS decays as a power law with system size and the exponent α is sensitive to boundary condition. In one dimension there are different analytical predictions for α for different boundary conditions. In two and three dimensions only analytical studies are kinetic theory approach and renormalization group theory approach. Prediction of these theories do not match and so far no numerical studies have verified their predictions.
(ii) For interacting systems prediction from mode coupling theory is that $\alpha = 1/3$ if the leading nonlinearity is cubic and $1/2$ if leading nonlinearity is quartic. Hydrodynamic approach predicts that there exists a single universality class with $\alpha = 1/3$. Recent simulation strongly suggest single universality class, with $\alpha = 1/3$, for momentum-conserving interacting systems in one dimension. In two dimension, both the theoretical approaches MCT and hydrodynamic approach predict that for momentum conserving systems, the thermal conductivity diverges logarithmically and finite when there is pinning. Various numerical studies could not verify the logarithmic divergence. All theories predict finite thermal conductivity in three dimension (Fourier's law). This is verified in a recent simulation by Saito and Dhar [57].

1.3 Problems addressed in the thesis

In this section we will discuss the problems studied in the thesis and give the motivation to study those problems. Broadly this thesis comprises (i) application of the LEGF approach to heat conduction in higher dimensional disordered systems, (ii) derivation of Green-Kubo type formula for conductance in open systems and (iii) studies of large deviations in current fluctuations in non-equilibrium situations. Below we discuss these problems.

From the earlier studies discussed in the previous section we see that there are many attempts to find out the value of α in different one dimensional model systems but not much studies in higher dimensional systems, where there is more expectation of getting Fourier like behaviour. In chapter (2,3) of this thesis we study the problem of heat conduction in disordered harmonic crystal in two and three dimensions, where we find the asymptotic size dependence of current. In chapter (2) we first discuss the LEGF approach in detail. Then we show that the Green's function required for the calculation of current satisfies a simple recursion relation. The recursion relation connects Green's functions of systems with different sizes and leads to an efficient numerical technique that can be used in any dimension. In chapter (3) we first give heuristic arguments using the results of both the kinetic theory and renormalization group theory to predict asymptotic system size behaviour of the disorder averaged current in NESS. We then present numerical results based on the direct calculation of the transmission function using the recursive Green's function technique. We also obtain the steady state current by direct non-equilibrium simulation of the corresponding Langevin equations. A comparison is made between the heuristic predictions and our numerical results. In addition to the studies on the open system we have also considered the system in the absence of heat baths. We obtained the normal modes of the isolated disordered lattice numerically, studied their localisation properties and tried to make connections with the results for the open system.

In sec. (1.1.3) we have seen that Green-Kubo formula provides one way to calculate current flowing through the system when it is kept slightly out of equilibrium. We have seen

in the previous section that in many theoretical studies people have used GK formula to find out the exponent α. In chapter (4) we have proved a similar formula for the conductance when the system is connected to heat baths. We prove this formula for a variety of implementations of baths and both for fluid and lattice systems in arbitrary dimensions. In the last section we explicitly calculate the time auto-correlation for boundary currents for a mass disordered harmonic chain connected to Langevin baths and show directly and explicitly that it satisfies an open system GK formula.

Another related problem studied in this thesis is on the properties of fluctuations of transport current in various systems. An interesting result in this area, valid for systems far from equilibrium, is the so-called fluctuation theorem. This theorem involves rare fluctuations of the transport current. These large fluctuations are described by the large deviation function. In the first part of chapter (5) we obtain an exact expression for the large-deviation function of the heat transfer across a harmonic chain over a large time duration. Finding probabilities of large deviations is usually difficult to compute by usual simulations. In the second part of chapter (5), we have developed an algorithm to find probabilities of vary rare events and applied it to two different non-equilibrium processes involving heat and particle transport.

2 Heat conduction in harmonic systems

In the open system description of transport, a system is connected to reservoirs through some system-reservoir couplings. An idealised reservoir acts like a perfect blackbody with zero reflectivity, as used in the Landauer formalism. However in real situations one does not have ideal reservoirs, and it is important to understand the role of reservoirs in transport. Unlike other microscopic approaches such as Boltzmann kinetic theory, or the usual Green-Kubo formalism, where one studies the properties of the system only, the LEGF approach explicitly includes the effect of reservoirs.

In the first three sections of this chapter we introduce and discuss the LEGF approach. In Sec.(2.1) we show the derivation of the generalized quantum Langevin equations for a system coupled to two reservoirs at different temperatures. In Sec. (2.2) we work out the non-equilibrium steady state current expressed in terms of the Green's function of the system. In Sec.(2.3) we discuss various types of baths that are generally used. Next, in Sec. (2.4) we study heat conduction in d-dimensional harmonic lattices using the LEGF approach. One important new result of the thesis is to develop a recursive Green's function technique for evaluation of the phonon transmission function. The recursion relation proved here was earlier known for one-dimensional systems. In Sec. (2.4.1) we give the details of the proof of the recursion relation in higher dimensional systems and discuss its numerical implementation to find the transmission function. Applying this technique we evaluate the transmission coefficient and hence the current for harmonic chain in Sec. (2.4.2). Using the results of ordered harmonic chain from previous section we work out current in d- dimensional harmonic system in Sec. (2.4.3).

2.1 Generalized Langevin equations and LEGF approach

Consider a particle of mass m attached to a spring of stiffness k and kept inside a fluid of temperature T. Then phenomenologically the simplest way to model the effect of the environment (fluid) is to write the following simple classical equation of motion for the particle:

$$m\ddot{x} = -kx - \gamma\dot{x} + \xi(t). \tag{2.1}$$

The last two terms correspond to the dissipation and noise respectively. The noise is assumed to be Gaussian and has the following statistical properties

$$\langle \xi(t) \rangle = 0 \text{ and } \langle \xi(t)\xi(t') \rangle = 2\gamma K_B T \delta(t - t'). \tag{2.2}$$

The last equation is called a fluctuation dissipation relation. In the Eq. (2.1) the dissipation is instantaneous and the noise is δ-correlated in time. Often in real systems the situation is somewhat different and a more appropriate description is given in terms of the generalized Langevin equation, which is:

$$m\ddot{x} = -kx - \int_{-\infty}^{t} dt' \alpha(t - t')\dot{x}(t') + \xi(t) \tag{2.3}$$

where the dissipation term involves memory and the noise $\xi(t)$ is Gaussian but correlated in time. The noise properties are now given by

$$\langle \xi(t) \rangle = 0 \text{ and } \langle \xi(t)\xi(t') \rangle = K_B T \alpha(t - t'). \tag{2.4}$$

One can also write Eq. (2.3) in the following form

$$\begin{aligned} m\ddot{x} &= -(k + \alpha(0))x(t) + \int_{-\infty}^{t} dt' \, \frac{d\alpha(t - t')}{dt'} x(t') + \xi(t) \\ m\ddot{x} &= -(m\omega_s^2)x(t) + \int_{-\infty}^{t} dt' \, \sigma(t - t')x(t') + \xi(t) \end{aligned} \tag{2.5}$$

where we assume that $\lim_{t\to\infty} \alpha(t) = 0$ and have defined $m\omega_s^2 = k + \alpha(0)$, $\sigma(t) = -d\alpha(t)/dt$. The Eq. (2.5) is the generalized Langevin equation (GLE) for a single harmonic oscillator.

Now we present the details of the LEGF formalism in the context of heat conduction, which will essentially involve solving GLEs for a more general multi-particle harmonic system. The GLEs in this case appear automatically by eliminating the bath degrees of freedom from the Heisenberg equations of motion (or Newton's equations of motion) of the system degrees of freedom. This approach was used by Ford-Kac-Mazur [60] to study Brownian motion in coupled oscillators. Dhar and Shastry [61] extended this approach to study transport in electron and phonon systems. They derived the Landauer formula using this approach. In [62], Dhar and Sen showed how one can get NEGF results for non-interacting electrons modeled by tight binding Hamiltonians, using quantum Langevin equations. There are four basic steps of this approach, which are :

- (i) Write down the equation of motion for both system variables and bath variables.
- (ii) Solve the equations corresponding to bath variables and put these solutions back into the equations for system variables. Thus one gets generalised Langevin equations for system variables. The noises present in GLEs depend of the initial values on bath variables which are chosen from appropriate equilibrium distributions.
- (iii) Solve these generalised Langevin equations by Fourier transform technique and write the solution in such a form so that one can easily identify the phonon green's functions which lead to the identification with NEGF results.
- (iv) To find the steady state value of any quantity take average over noise configurations.

Let us illustrate this approach for a quantum harmonic chain of size N connected to two heat baths at two different temperatures. The baths are also taken to be harmonic oscillators. The first site of the chain is coupled to the left reservoir and the last site (N^{th} site) of the system is coupled to the right reservoir. The left and right reservoirs are at temperatures T_L and T_R respectively. The Hamiltonian of the entire system (system and bath) is ([63]):

$$H = \mathcal{H}_C + \mathcal{H}_L + \mathcal{H}_R + \mathcal{V}_L + \mathcal{V}_R$$

$$
\begin{aligned}
\text{where} \quad \mathcal{H}_C &= \sum_{l=1}^{N} \left(\frac{p_l^2}{2m_l} + \frac{k_l x_l^2}{2}\right) + \sum_{l=1}^{N-1} \frac{k(x_{l+1} - x_l)^2}{2} \\
\mathcal{H}_L &= \sum_{i=1}^{N_L} \frac{p_{iL}^2}{2} + \sum_{i=0}^{N_L+1} k_0 \frac{(x_{i+1L} - x_{iL})^2}{2} \quad \text{with} \quad x_{0L} = x_{N_L+1L} = 0 \\
\mathcal{H}_R &= \sum_{n=1}^{N_R} \frac{p_{nR}^2}{2} + \sum_{n=0}^{N_R+1} k_0 \frac{(x_{n+1R} - x_{nR})^2}{2} \quad \text{with} \quad x_{0R} = x_{N_R+1R} = 0 \\
\mathcal{V}_L &= -k' x_1 x_{1L} \quad \text{and} \quad \mathcal{V}_R = -k' x_N x_{1R}
\end{aligned} \tag{2.6}
$$

where $\mathcal{H}_C$, $\mathcal{H}_L$, $\mathcal{H}_R$ represent the Hamiltonians of the chain, the left reservoir and the right reservoir of sizes N, N_L, N_R respectively. The Heisenberg operators x_l, x_{iL} and x_{nR} correspond to the particle displacements (assumed to be scalar) about respective equilibrium positions. The conjugate operators corresponding to x_l, x_{iL} and x_{nR} are p_l, p_{iL} and p_{nR} respectively, which satisfy these commutation relations : $[x_k, p_l] = i\hbar\delta_{kl}$, $[x_{iL}, p_{jL}] = i\hbar\delta_{ij}$ and $[x_{mR}, p_{nR}] = i\hbar\delta_{mn}$. $\mathcal{V}_L$ and $\mathcal{V}_R$ denote the interaction between the system and the two reservoirs respectively. Let us consider that, the matices U^L, U^R diagonalize the Hamiltonians $\mathcal{H}_L$ and $\mathcal{H}_R$ respectively, where $\omega_{\mu L}$ and $\omega_{\mu R}$ are the corresponding eigen frequencies. Then under the variable transformation $x_{iL} = \sum_{\mu=1}^{N_L} U_{i\mu}^L X_{\mu L}$ the Hamiltonian $\mathcal{H}_L$ and $\mathcal{V}_L$ become

$$
\begin{aligned}
\mathcal{H}_L &= \sum_{\mu=1}^{N_L} \Big[\frac{P_{\mu L}^2}{2} + \frac{\omega_{\mu L}^2 X_{\mu L}^2}{2}\Big] \\
\mathcal{V}_L &= -x_1 \sum_{\mu=1}^{N_L} c_{\mu L} X_{\mu L} \quad \text{with} \quad c_{\mu L} = k' U_{1\mu}^L
\end{aligned} \tag{2.7}
$$

and similarly for right reservoir we have

$$
\begin{aligned}
\mathcal{H}_R &= \sum_{\mu=1}^{N_R} \Big[\frac{P_{\mu R}^2}{2} + \frac{\omega_{\mu R}^2 X_{\mu R}^2}{2}\Big] \\
\mathcal{V}_R &= -x_N \sum_{\mu=1}^{N_R} c_{\mu R} X_{\mu R} \quad \text{with} \quad c_{\mu R} = k' U_{1\mu}^R
\end{aligned} \tag{2.8}
$$

The full Hamiltonian in Eq. (2.6) now becomes

$$
H = \mathcal{H}_C + \mathcal{H}_L + \mathcal{H}_R + \mathcal{V}_L + \mathcal{V}_R
$$

$$
\begin{aligned}
\text{where} \quad \mathcal{H}_C &= \sum_{l=1}^{N}\left(\frac{p_l^2}{2m_l}+\frac{k_l x_l^2}{2}\right)+\sum_{l=1}^{N-1}\frac{k(x_{l+1}-x_l)^2}{2} \\
\mathcal{H}_L &= \sum_{\mu=1}^{N_L}\Big[\frac{P_{\mu L}^2}{2}+\frac{\omega_{\mu L}^2 X_{\mu L}^2}{2}\Big] \\
\mathcal{H}_R &= \sum_{\mu=1}^{N_R}\Big[\frac{P_{\mu R}^2}{2}+\frac{\omega_{\mu R}^2 X_{\mu R}^2}{2}\Big] \\
\mathcal{V}_L &= -x_1\sum_{\mu=1}^{N_L} c_{\mu L}X_{\mu L}, \\
\mathcal{V}_R &= -x_N\sum_{\mu=1}^{N_L} c_{\mu R}X_{\mu R}\ . \qquad (2.9)
\end{aligned}
$$

From the above Hamiltonian we obtain the following Heisenberg equations of motion

$$
\begin{aligned}
m_1\ddot{x}_1 &= -k_1x_1-k(x_1-x_2)+\sum_{\mu=1}^{N_L}c_{\mu L}X_{\mu L} \\
m_l\ddot{x}_l &= -k_lx_l-k(2x_l-x_{l-1}-x_{l+1}) \qquad 1<l<N \\
m_N\ddot{x_N} &= -k_Nx_N-k(x_N-x_{N-1})+\sum_{\mu=1}^{N_R}c_{\mu R}X_{\mu R}, \qquad (2.10)
\end{aligned}
$$

for the system degrees of freedom, and

$$
\begin{aligned}
\ddot{X}_{\mu L} &= -\omega_{\mu L}^2X_{\mu L}+c_{\mu L}x_1, \ \ \mu=1 \text{ to } N_L \\
\ddot{X}_{\mu R} &= -\omega_{\mu R}^2X_{\mu R}+c_{\mu R}x_N, \ \ \mu=1 \text{ to } N_R, \qquad (2.11)
\end{aligned}
$$

for the bath degrees of freedom. We first solve the equations of motion of the bath degrees of freedom by considering them to be linear inhomogeneous equations. We assume that the system reservoir interaction is switched on at time t_0. The solutions of the equations of motion of the reservoir variables in Eq. (2.11), for $t > t_0$, are given by

$$
\begin{aligned}
X_{\mu L}(t) &= \cos\omega_{\mu L}(t-t_0)\,X_{\mu L}(t_0)+\frac{\sin\omega_{\mu L}(t-t_0)}{\omega_{\mu L}}\dot{X}_{\mu L}(t_0)+\int_{t_0}^{t}dt'\,\frac{\sin\omega_{\mu L}(t-t')}{\omega_{\mu L}}\,c_{\mu L}x_1(t') \\
X_{\mu R}(t) &= \cos\omega_{\mu R}(t-t_0)\,X_{\mu R}(t_0)+\frac{\sin\omega_{\mu R}(t-t_0)}{\omega_{\mu R}}\dot{X}_{\mu R}(t_0)+\int_{t_0}^{t}dt'\,\frac{\sin\omega_{\mu R}(t-t')}{\omega_{\mu R}}\,c_{\mu R}x_N(t') \qquad (2.12)
\end{aligned}
$$

Plugging these solutions into the system's equations of motion in Eq. (2.10) we get

$$
\begin{aligned}
m_1\ddot{x}_1 &= -k_1x_1 - k(x_1 - x_2) + \int_{t_0}^{t} dt'\ \sigma_1^+(t-t')x_1(t') + \eta_1(t) \\
m_l\ddot{x}_l &= -k_lx_l - k(2x_l - x_{l-1} - x_{l+1}) \qquad 1 < l < N \\
m_N\ddot{x}_N &= -k_Nx_N - k(x_N - x_{N-1}) + \int_{t_0}^{t} dt'\ \sigma_N^+(t-t')x_N(t') + \eta_N(t) \\
\text{where}\ \ \sigma_1^+(t) &= \sum_{\mu=1}^{N_L} \frac{c_{\mu L}^2}{\omega_{\mu L}} \sin(\omega_{\mu L}t)\Theta(t)\ , \quad \sigma_N^+(t) = \sum_{\mu=1}^{N_R} \frac{c_{\mu R}^2}{\omega_{\mu R}} \sin(\omega_{\mu R}t)\Theta(t) \\
\text{and}\ \ \eta_1(t) &= \sum_{\mu=1}^{N_L} c_{\mu L}[\cos\omega_{\mu L}(t-t_0)\ X_{\mu L}(t_0) + \frac{\sin\omega_{\mu L}(t-t_0)}{\omega_{\mu L}}\dot{X}_{\mu L}(t_0)] \\
\eta_N(t) &= \sum_{\mu=1}^{N_R} c_{\mu R}[\cos\omega_{\mu R}(t-t_0)\ X_{\mu R}(t_0) + \frac{\sin\omega_{\mu R}(t-t_0)}{\omega_{\mu R}}\dot{X}_{\mu R}(t_0)]\ , \qquad (2.13)
\end{aligned}
$$

and where the function $\Theta(t)$ is the Heaviside step function. We can easily see that the above equations are in the form of the generalized Langevin equation (Eq. (2.5)). The noises η_1 and η_N involve initial positions and momenta of the reservoir particles. The statistical properties of the noises are determined by the statistical properties of the initial configurations of the reservoirs. It is assumed that at time t_0 the left and right reservoirs were in thermal equilibrium at temperatures T_L and T_R respectively. The population of the normal modes of the isolated reservoirs is given by the phonon distribution functions $f_b(\omega, T_{L,R}) = 1/[e^{\hbar\omega/k_BT_{L,R}} - 1]$. Using these distribution functions it can be easily shown that the equilibrium correlations are given by (for the left reservoir):

$$
\begin{aligned}
&\langle\omega_{\mu L}^2 X_{\mu L}^2(0)\rangle = \langle\dot{X}_{\mu L}^2(0)\rangle = \frac{\hbar\omega_{\mu L}}{2}\coth(\frac{\hbar\omega_{\mu L}}{2K_BT_L}) \\
&\langle[X_{\mu L}(0)\dot{X}_{\mu L}(0) + \dot{X}_{\mu L}(0)X_{\mu L}(0)]\rangle = 0\ . \qquad (2.14)
\end{aligned}
$$

Using these correlations the noise correlations come out to be

$$
\begin{aligned}
\langle\eta_1(t)\rangle &= 0\ \text{ where }\ \frac{1}{2}[\langle\eta_1(t)\eta_1(t') + \eta_1(t')\eta_1(t)\rangle] = K_BT_LK_L(t-t') \\
\text{where}\ \ K_L(t) &= \sum_{\mu=1}^{N_L} \frac{c_{\mu L}^2}{\omega_{\mu L}^2}\cos(\omega_{\mu L}t)\frac{\hbar\omega_{\mu L}}{2k_bT_L}\coth(\frac{\hbar\omega_{\mu L}}{2K_BT_L}). \qquad (2.15)
\end{aligned}
$$

Similar relations hold for the right reservoir.

2.2 Stationary solution of the equation of motion and steady state properties

In the limits of infinite reservoir sizes and $t_0 \to -\infty$, the easiest way to obtain the steady state properties is to solve the equations in (2.13) by Fourier transform. Thus defining the Fourier transforms

$$\begin{aligned} \tilde{x}_l(\omega) &= \frac{1}{2\pi}\int_{-\infty}^{\infty} dt\; x_l(t)\; e^{i\omega t} \\ \tilde{\eta}_{1,N}(\omega) &= \frac{1}{2\pi}\int_{-\infty}^{\infty} dt\; \eta_{1,N}(t)\; e^{i\omega t} \\ \sigma^{+}_{1,N}(\omega) &= \int_{-\infty}^{\infty} dt\; \sigma^{+}_{1,N}(t)\; e^{i\omega t} \end{aligned} \tag{2.16}$$

we get from Eq. (2.13)

$$\begin{aligned} -m_1\omega^2\tilde{x}_1(\omega) &= -k_1\tilde{x}_1 - k(\tilde{x}_1 - \tilde{x}_2) + \sigma^{+}_1(\omega)\tilde{x}_1(\omega) + \tilde{\eta}_1(\omega) \\ -m_l\omega^2\tilde{x}_l(\omega) &= -k_l\tilde{x}_l - k(2\tilde{x}_l - \tilde{x}_{l-1} - \tilde{x}_{l+1}) \qquad 1 < l < N \\ -m_N\omega^2\tilde{x}_N(\omega) &= -k_N\tilde{x}_N - k(\tilde{x}_N - \tilde{x}_{N-1}) + \sigma^{+}_N(\omega)\tilde{x}_N(\omega) + \tilde{\eta}_N(\omega)\;. \end{aligned} \tag{2.17}$$

where the new noise $\tilde{\eta}_{1,N}(\omega)$ have the following correlations in the Fourier space

$$\begin{aligned} \frac{1}{2}[\langle\tilde{\eta}_{1,N}(\omega)\tilde{\eta}_{1,N}(\omega') &+ \tilde{\eta}_{1,N}(\omega')\tilde{\eta}_{1,N}(\omega)\rangle] = \frac{K_B T_{L,R}}{2\pi}\tilde{K}_{L,R}(\omega)\;\delta(\omega+\omega') \\ \text{where}\;\; \tilde{K}_{L,R}(\omega) &= \frac{\hbar}{K_B T_{L,R}} Im[\sigma^{+}_{1,N}(\omega)]\;\coth(\frac{\hbar\omega}{2k_B T_{L,R}}). \end{aligned} \tag{2.18}$$

One can also show that

$$\langle\tilde{\eta}_{1,N}(\omega)\tilde{\eta}_{1,N}(\omega')\rangle = \frac{\hbar\; Im[\sigma^{+}_{1,N}(\omega)]}{2\pi}\;[1 + f_b(\omega, T_{L,R})]\;\delta(\omega+\omega'). \tag{2.19}$$

Now we write the equations (2.17) in the following matrix form

$$[-M\omega^2 + \Phi - \Sigma^{+}_L(\omega) - \Sigma^{+}_R(\omega)]\tilde{X}(\omega) = \tilde{\eta}_L(\omega) + \tilde{\eta}_R(\omega), \tag{2.20}$$

where, X, η are column vector with elements $[X]^T = (x_1, x_2, ...x_N)$, $[\eta]^T = (\eta_L, 0, ...0, \eta_R)$ and $\Sigma^{+}_L(\omega)$, $\Sigma^{+}_R(\omega)$ are $N \times N$ matrices whose only non-vanishing elements are $[\Sigma^{+}_L]_{11} = \sigma^{+}_1$,

$[\Sigma_R^+]_{NN} = \sigma_N^+$. $[\Phi]_{N\times N}$ represents a tridiagonal matrix with elements $[\Phi]_{i,j} = (2k + k_0)\delta_{i,j} - k\delta_{i-1,j} - k\delta_{i+1,j}$ for $i = 2$ to $N-1$ and $[\Phi]_{1,j} = (2k+k_0)\delta_{1,j} - k\delta_{2,j}$, $[\Phi]_{N,j} = (2k+k_0)\delta_{N,j} - k\delta_{N-1,j}$ for $j = 1$ to N. From the imaginary part of each element of Σ_L^+ and Σ_R^+, we construct two more matrices Γ_L^+ and Γ_R^+ respectively, *i.e.* $\Gamma_{L,R}(\omega) = Im[\Sigma_{L,R}^+(\omega)]$.

From Eq. (2.20) we get $\tilde{X}(\omega) = G^+(\omega)[\tilde{\eta}_L(\omega) + \tilde{\eta}_R(\omega)]$, where

$$\begin{aligned}
G^+(\omega) &= \frac{1}{-M\omega^2 + \Phi - \Sigma_L^+(\omega) - \Sigma_R^+(\omega)} \\
\langle \tilde{\eta}_L(\omega)\tilde{\eta}_L^T(\omega')\rangle &= \frac{\hbar\Gamma_L(\omega)}{2\pi}\,[1 + f_b(\omega, T_L)]\,\delta(\omega + \omega'), \\
\langle \tilde{\eta}_R(\omega)\tilde{\eta}_R^T(\omega')\rangle &= \frac{\hbar\Gamma_R(\omega)}{2\pi}\,[1 + f_b(\omega, T_R)]\,\delta(\omega + \omega'), \\
\langle \tilde{\eta}_L(\omega)\tilde{\eta}_R^T(\omega')\rangle &= 0, \;\; \Gamma_{L,R}(\omega) = Im[\Sigma_{L,R}^+(\omega)].
\end{aligned} \tag{2.21}$$

Using $\tilde{X}(\omega)$ we write the solution of the GLEs of the system in steady state as

$$X(t) = \int_{-\infty}^{\infty} d\omega\, \tilde{X}(\omega)\, e^{-i\omega t}. \tag{2.22}$$

Connections to Green's function: Now we will show that the function $G^+(\omega)$ can be identified as Green's function while $\Sigma_{L,R}^+$ can be identified as self energy corrections. Since the chain and baths are collections of harmonic oscillators and the interactions among the bath and the chain are quadratic, the Hamiltonian of the entire system in Eq. (2.9) can be expressed as a quadratic Hamiltonian given by:

$$\begin{aligned}
H &= \frac{1}{2}\dot{Y}^T M\dot{Y} + \frac{1}{2}Y^T\bar{\Phi}Y \\
&= \mathcal{H}_C + \mathcal{H}_L + \mathcal{H}_R + \mathcal{V}_L + \mathcal{V}_R \\
\text{where}\quad \mathcal{H}_C &= \frac{1}{2}\dot{X}_C^T M_C\dot{X}_C + \frac{1}{2}X_C^T\Phi_C X_C\,, \\
\mathcal{H}_L &= \frac{1}{2}\dot{X}_L^T M_L\dot{X}_L + \frac{1}{2}X_L^T\Omega_L^2 X_L\,, \\
\mathcal{H}_R &= \frac{1}{2}\dot{X}_R^T M_R\dot{X}_R + \frac{1}{2}X_R^T\Omega_R^2 X_R\,, \\
\mathcal{V}_L &= X_C^T V_L X_L, \quad \mathcal{V}_R = X_C^T V_R X_R\,,
\end{aligned} \tag{2.23}$$

where M denotes the mass matrix of the entire system and $\bar{\Phi}$ denotes the force constant

matrix of the quadratic interactions among the particles of the entire system (chain plus baths). Here, M_L and M_R represent the mass matrices of the left and right reservoirs. Since all particles in both reservoirs have unit masses, M_L and M_R are identity matrices of dimensions $N_L \times N_L$ and $N_R \times N_R$ respectively. The eigenvalues of the two reservoirs are denoted by the matrices Ω_L^2 and Ω_R^2. Here V_L represents a $N \times N_L$ matrix whose only non-vanishing elements are $[V_L]_{1,\mu} = c_{\mu L} = U^L_{1\mu}$, and V_R represents a $N \times N_R$ matrix whose only non-vanishing elements are $[V_R]_{1,\mu} = c_{\mu R} = U^R_{1\mu}$.

The equations of motion for particles of the entire system are :

$$M\ddot{Y} = -\bar{\Phi}Y. \tag{2.24}$$

If $\mathcal{G}^+(t)$ denotes the Green's function of the entire system, then $\mathcal{G}^+(t)$ satisfies

$$M\ddot{\mathcal{G}}^+(t) + \bar{\Phi}\mathcal{G}^+(t) = \delta(t)I \ . \tag{2.25}$$

It is easy to verify that $\mathcal{G}^+(t) = \mathcal{G}(t)\Theta(t)$ where $\mathcal{G}(t)$ satisfies the equation $M\ddot{\mathcal{G}}(t) + \bar{\Phi}\mathcal{G}(t) = 0$ with the initial conditions $\mathcal{G}(0) = 0$, $\dot{\mathcal{G}}(0) = M^{-1}$. The Fourier transform $\mathcal{G}^+(\omega) = \int_{-\infty}^{\infty} dt\mathcal{G}^+(t)e^{i\omega t}$ of $\mathcal{G}^+(t)$ satisfies the equation

$$[-M(\omega + i\epsilon)^2 + \bar{\Phi}]\mathcal{G}^+(\omega) = I \ . \tag{2.26}$$

The isolated reservoir Green's functions are given by

$$\begin{aligned} g_L^+(\omega) &= \frac{1}{-(\omega + i\epsilon)^2 M_L + \Omega_L^2} \\ g_R^+(\omega) &= \frac{1}{-(\omega + i\epsilon)^2 M_R + \Omega_R^2} \ . \end{aligned} \tag{2.27}$$

The Green's function element $\mathcal{G}^+_{r,s}$ is defined between any pair of points r and s on the entire system of chain and baths. We are interested in evaluating $\mathcal{G}^+(\omega)$ only between points on the chain. To do that, let us define some notations for various Green's Functions as follows:

- $G_C^+(\omega)$ represents the part of $\mathcal{G}^+(\omega)$ whose elements are non-zero only if both the indices represents points on the chain.

- $G_L^+(\omega)$ represents the part of $\mathcal{G}^+(\omega)$ whose elements are non-zero only if both the indices represents points on the left reservoir.

- $G_R^+(\omega)$ represents the part of $\mathcal{G}^+(\omega)$ whose elements are non-zero only if both the indices represents points on the right reservoir.

- $G_{CL}^+(\omega)$ represents the part of $\mathcal{G}^+(\omega)$ whose elements are non-zero only if one index represents a point on the chain while the other one represents point on the left reservoir.

- $G_{CR}^+(\omega)$ represents the part of $\mathcal{G}^+(\omega)$ whose elements are non-zero only if one index represents a point on the chain while the other one represents point on the right reservoir.

- $G_{LR}^+(\omega)$ represents the part of $\mathcal{G}^+(\omega)$ whose elements are non-zero only if one index represents a point on the left reservoir while the other one represents point on the right reservoir.

Now using the above notations and Eq. (2.27) we can write Eq. (2.26) in the following matrix form :

$$\begin{pmatrix} -M_C\,(\omega+i\epsilon)^2\hat{I}+\Phi_C & V_L & V_R \\ V_L^T & -M_L\,(\omega+i\epsilon)^2\hat{I}+\Omega_L^2 & 0 \\ V_R^T & 0 & -M_R\,(\omega+i\epsilon)^2\hat{I}+\Omega_R^2 \end{pmatrix} \times \begin{pmatrix} G_C^+ & G_{CL}^+ & G_{CR}^+ \\ G_{LC}^+ & G_L^+ & G_{CR}^+ \\ G_{RC}^+ & G_{RL}^+ & G_R^+ \end{pmatrix} = \begin{pmatrix} \hat{I} & 0 & 0 \\ 0 & \hat{I} & 0 \\ 0 & 0 & \hat{I} \end{pmatrix}. \tag{2.28}$$

This gives the following equations:

$$\begin{aligned} [-M_C\,(\omega+i\epsilon)^2\hat{I}+\Phi_C]G_C^+ + V_L G_{LC}^+ + V_R G_{RC}^+ &= \hat{I} \\ V_L^T G_C^+ + [-M_L\,(\omega+i\epsilon)^2\hat{I}+\Omega_L^2]G_{LC}^+ &= 0 \\ V_R^T G_C^+ + [-M_R\,(\omega+i\epsilon)^2\hat{I}+\Omega_R^2]G_{RC}^+ &= 0. \end{aligned} \tag{2.29}$$

From the last two equations we get $G_{LC}^+(\omega) = -g_L^+(\omega)V_L^T G_C^+(\omega)$ and $G_{RC}^+(\omega) =$

$-g_R^+(\omega)V_R^T G_C^+(\omega)$. Using this in the first equation then gives [24, 62]

$$
\begin{aligned}
&[-M_C\,(\omega+i\epsilon)^2\hat{I}+\Phi_C-V_L g_L^+(\omega)V_L^T-V_R g_R^+(\omega)V_R^T]G_C^+(\omega)=\hat{I}\\
&\Rightarrow G_C^+(\omega)=\frac{1}{[-M_C\,(\omega+i\epsilon)^2\hat{I}+\Phi_C-\Sigma_L^+(\omega)-\Sigma^+(\omega)]}\\
&\text{where}\;\;\Sigma_L^+(\omega)=V_L g_L^+(\omega)V_L^T=\sum_{\mu=1}^{N_L}\frac{(U_{1\mu}^L)^2}{-(\omega+i\epsilon)^2M_L+\Omega_L^2}\\
&\text{and}\;\;\Sigma_R^+(\omega)=V_R g_R^+(\omega)V_R^T=\sum_{\mu=1}^{N_R}\frac{(U_{1\mu}^R)^2}{-(\omega+i\epsilon)^2M_R+\Omega_R^2}.
\end{aligned}
\tag{2.30}
$$

Now comparing the second line of Eq. (2.30) with the third line of Eq. (2.21) we identify that $G^+(\omega)=G_C^+(\omega)$, and $\Sigma_{L,R}^+$ are self energy corrections.

Steady state properties: In general, the steady state is represented by the invariant probability distribution of the phase space variables. But it can also be represented by the various cumulants obtained in the steady state. In the case of heat conduction in harmonic systems with correlated noise, it is difficult to obtain the full distribution. However we can calculate a few cumulants which represent various physical quantities. For example, those quantities could be the energy current, local kinetic energy etc. Below we present the calculation of steady state current.

To define the local energy current inside the chain we first define the local energy density associated with the l^{th} particle (or energy at the lattice site l) as follows (such that $H=\sum_{l=1}^{N}\epsilon_l$) [58].

$$
\begin{aligned}
\epsilon_1 &= \frac{p_1^2}{2m_1}+\frac{k_1x_1^2}{2}+\frac{k}{4}(x_1-x_2)^2\,,\\
\epsilon_l &= \frac{p_l^2}{2m_l}+\frac{k_lx_l^2}{2}+\frac{k}{4}[\,(x_{l-1}-x_l)^2+(x_l-x_{l+1})^2\,]\,,\quad \text{for}\;\; l=2,3...N-1\\
\epsilon_N &= \frac{p_N^2}{2m_N}+\frac{k_Nx_N^2}{2}+\frac{k}{4}(x_{N-1}-x_N)^2\,.
\end{aligned}
\tag{2.31}
$$

Taking the time derivative of these equations, using Eq. (2.13) and after some straightforward manipulations, we get the continuity equations which are given by:

$$
\dot{\epsilon}_1 = -j_{2,1}+j_{1,L}
$$

$$
\begin{aligned}
\dot{\epsilon}_l &= -j_{l+1,l} + j_{l,l-1} \quad \text{for } l = 2, 3...N-1 \\
\dot{\epsilon}_N &= j_{N,R} + j_{N,N-1}\,, \qquad (2.32)\\
\text{with } j_{l,l-1} &= \frac{1}{2}(v_{l-1} + v_l) f_{l,l-1} \qquad (2.33)\\
\text{where } f_{l,l+1} &= -f_{l+1,l} = -k(x_l - x_{l+1})
\end{aligned}
$$

is the force that the $(l+1)^{\text{th}}$ particle exerts on the l^{th} particle and $v_l = \dot{x}_l$. From the above equations one can identify $j_{l,l-1}$ to be the energy current from site $l-1$ to l. The terms $j_{1,L}$ and $j_{N,R}$ are respectively the rate of energy flow from the left or right reservoir into the boundary particles. It is easy to verify that

$$
\begin{aligned}
j_{1,L}(t) &= \dot{X}_C^T V_L X_L = \dot{x}_1(t)\Big[\int_{t_0}^{t} dt' \sigma_1^+(t-t') x_1(t') + \eta_1(t)\Big] \\
\text{and } j_{N,R}(t) &= \dot{X}_C^T V_R X_R = \dot{x}_N(t)\Big[\int_{t_0}^{t} dt' \sigma_N^+(t-t') x_N(t') + \eta_N(t)\Big]. \qquad (2.34)
\end{aligned}
$$

Using the fact that in the steady state $\langle \dot{\epsilon}_l \rangle = 0$, we get

$$
\mathcal{J} = \langle j_{1,L} \rangle = \langle j_{2,1} \rangle = \langle j_{3,2} \rangle = ... \langle j_{N,N-1} \rangle = -\langle j_{N,R} \rangle\,. \qquad (2.35)
$$

Now we proceed to calculate $\mathcal{J} = \langle j_{1,L} \rangle$.

$$
\begin{aligned}
\mathcal{J} &= \Big\langle \dot{x}_1(t)\Big[\int_{t_0}^{t} dt'\ \sigma_1^+(t-t') x_1(t') + \eta_1(t)\Big]\Big\rangle \\
&= \int_{t_0}^{t} dt' \left\langle \dot{X}^T(t) \Sigma_L^+(t-t') X(t') \right\rangle + \left\langle \dot{X}^T(t) \eta_L(t) \right\rangle \\
&= -i \int_{-\infty}^{\infty} d\omega \int_{-\infty}^{\infty} d\omega'\ e^{i(\omega+\omega')t}\ \omega \Big\langle \tilde{X}^T(\omega) \Sigma_L i^+(\omega') \tilde{X}(\omega') + \tilde{X}^T(\omega) \tilde{\eta}_L(\omega') \Big\rangle \\
&= -i \int_{-\infty}^{\infty} d\omega \int_{-\infty}^{\infty} d\omega'\ e^{i(\omega+\omega')t}\ \omega \Big\langle Tr\left[\tilde{X}(\omega') \Sigma_L^+(\omega') \tilde{X}^T(\omega)\right] + Tr\left[\tilde{\eta}_L^T(\omega') \tilde{X}(\omega)\right] \Big\rangle.
\end{aligned} \qquad (2.36)
$$

Using the solution in Eq. (2.21) we get

$$
\begin{aligned}
\mathcal{J} = -i \int_{-\infty}^{\infty} d\omega \int_{-\infty}^{\infty} d\omega'\ e^{i(\omega+\omega')t}\ \omega \Big(& Tr\Big[\Sigma_L^+(\omega') G^+(\omega) \Big\langle \big(\tilde{\eta}_L(\omega') + \tilde{\eta}_R(\omega') \big) \\
& \big(\tilde{\eta}_L^T(\omega) + \tilde{\eta}_R^T(\omega) \big) \Big\rangle G^{+T}(\omega)\Big] + Tr\Big[\Big\langle \tilde{\eta}_L(\omega') \big(\tilde{\eta}_L^T(\omega) + \tilde{\eta}_R^T(\omega) \big) \Big\rangle G^{+T}(\omega)\Big]\Big).
\end{aligned}
$$

Now consider that part of $\mathcal{J}$, say $\mathcal{J}_R$, which depends only on T_R . Clearly this is:

$$\begin{aligned}\mathcal{J}_R &= -i\int_{-\infty}^{\infty} d\omega \int_{-\infty}^{\infty} d\omega'\, e^{i(\omega+\omega')t}\, \omega\, Tr\left[G^{+T}(\omega)\Sigma_L^{+}(\omega')G^{+}(\omega')\Big\langle\, \tilde{\eta}_R(\omega')\tilde{\eta}_R^{T}(\omega)\,\Big\rangle\right] \\ &= -i\int_{-\infty}^{\infty} d\omega\, Tr\left[G^{+T}(\omega)\Sigma_L^{+}(-\omega)G^{+}(-\omega)\Gamma_R(\omega)\right]\frac{\hbar\,\omega}{\pi}\,[1+f_b(\omega,T_R)].\end{aligned}$$

The real part of $\mathcal{J}_R$ is

$$\mathcal{J}_R = -\int_{-\infty}^{\infty} d\omega\, Tr\left[G^{+T}(\omega)\Gamma_L(-\omega)G^{+}(-\omega)\Gamma_R(\omega)\right]\frac{\hbar\,\omega}{\pi}\,[1+f_b(\omega,T_R)].$$

Including the contribution from the terms involving T_L , and noting that the current has to vanish for $T_L = T_R$, it is clear that the net current will then be given by

$$\mathcal{J} = \int_{-\infty}^{\infty} d\omega\, Tr\left[G^{+T}(\omega)\Gamma_L(-\omega)G^{+}(-\omega)\Gamma_R(\omega)\right]\frac{\hbar\,\omega}{\pi}[f_b(\omega,T_L)-f_b(\omega,T_R)]\,. \tag{2.37}$$

Once $G^{+}(\omega)$ is identified as the system's Green's function in the open situation (connected to baths) the above expression is the same expression as one obtains in the NEGF [64] formalism. The above expression for the current is of the Landauer form and has been derived using various other approaches such as scattering theory [65, 66] and the nonequilibrium Green's function formalism [67, 68].

The classical limit is obtained by taking the high temperature limit so that $\frac{\hbar}{k_B T} \to 0$. In this limit the current in NESS is given by

$$\begin{aligned}\mathcal{J} &= \frac{K_B(T_L-T_R)}{\pi}\int_{-\infty}^{\infty} d\omega\, Tr\left[G^{+T}(\omega)\Gamma_L(-\omega)G^{+}(-\omega)\Gamma_R(\omega)\right] \\ &= \frac{K_B(T_L-T_R)}{2\pi}\int_{0}^{\infty} d\omega\, \mathcal{T}(\omega) \\ \text{where}\qquad &\mathcal{T}(\omega) = 4\, Tr\left[G^{+T}(\omega)\Gamma_L(-\omega)G^{+}(-\omega)\Gamma_R(\omega)\right].\end{aligned} \tag{2.38}$$

The quantity $\mathcal{T}(\omega)$ is known as transmission coefficient.

Here, we have presented the formalism for a simple one dimensional harmonic chain in such a way that one can easily generalize the formalism for more general systems and higher dimensional systems. (See [24] for general harmonic systems and [62] for tight binding model of electrons.) All of the above derivations will go through for situations more general than a

simple one-dimensional chain, as long as one can write the Hamiltonian for the entire system (the system plus the baths and the interactions of the system with the baths) in a quadratic form as in Eq. (2.23). So far, this approach has mostly been used to study conduction for non-interacting systems; a drawback of this approach is that it is not easy to extend the results to interacting systems.

2.3 Examples of baths

From Eq. (2.13) it is clear that, once the informations about the bath and noise correlations are given one can always start just by writing a set of generalized Langevin equations to obtain the steady state properties. In the equation (2.13), the bath information is given by $\sigma(t) = -\frac{d\alpha(t)}{dt}$. In the Fourier domain this relation reads $\sigma^+(\omega) = i\omega\alpha^+(\omega) + \alpha(0)$, which implies that $Im[\sigma^+(\omega)] = \omega Re[\alpha^+(\omega)] = \Gamma(\omega)$. Below we present $\sigma^+(\omega)$, $\Gamma(\omega)$ for some baths commonly used in theoretical studies.

Ohmic bath: For ohmic baths one chooses

$$\alpha(t) = \frac{\gamma}{t} e^{-|t|/\tau} \tag{2.39}$$

which in Fourier domain becomes

$$\begin{aligned} \alpha^+(\omega) &= \frac{\gamma}{1+\omega^2\tau^2} + i\frac{\omega\gamma\tau}{1+\omega^2\tau^2} \\ \text{and} \qquad \sigma^+(\omega) &= \alpha(0) + i\omega\alpha^+(\omega)\,. \end{aligned} \tag{2.40}$$

In the limit $\tau \to 0$ we get the Langevin bath

$$\alpha(t) = 2\gamma\delta(t), \quad \alpha^+(\omega) = \gamma\,. \tag{2.41}$$

In this case, $\alpha(0) \to \infty$. However one can absorb this in the definition of the spring constant.

Rubin model: The heat bath in this model is a harmonic chain connected to the system at one end. For simplicity let us consider the system to be a harmonic oscillator of mass m_s and

frequency ω_0. The Hamiltonian of the whole system is written as :

$$\begin{aligned} H_s &= \frac{p^2}{2m_s} + \frac{1}{2}m_s\omega_0^2\, x^2 \\ H_b &= \sum_{l=1}^{N_b} \frac{p_{lb}^2}{2m} + \sum_{l=0}^{N_b+1} k_0 \frac{(x_{l+1b} + x_{lb})^2}{2} + \sum_{l=1}^{N_b} \frac{1}{2}k_1 x_{lb}^2 \\ H_{sb} &= -k' x x_{1b} \end{aligned} \tag{2.42}$$

We transform to normal mode coordinates using $x_{lb} = \sum_\alpha U_{l\alpha} X_{\alpha b}$ and $p_{lb} = \sum_\alpha U_{l\alpha} P_{\alpha b}$, where

$$\begin{aligned} U_{l\alpha} &= \Big(\frac{2}{N_b+1}\Big)^{\frac{1}{2}} sin(lq_\alpha) \text{ with } q_\alpha = \frac{\pi\alpha}{N_b+1}, \;\; \alpha = 1, 2, .., N_b \\ \text{and } \omega_\alpha^2 &= \frac{k_o}{m}\Big(4sin^2(q_\alpha/2) + \frac{k_1}{k_o}\Big). \end{aligned} \tag{2.43}$$

Now, in terms of the new variables $X_{\alpha b}$ and $P_{\alpha b}$ the Hamiltonians H_b and H_{sb} look like

$$\begin{aligned} H_b &= \sum_{\alpha=1}^{N_b} [\frac{P_{\alpha b}^2}{2m} + \frac{1}{2}m\omega_\alpha^2\, X_{\alpha b}^2] \\ H_{sb} &= -\sum_{\alpha=1}^{N_b} c_\alpha\, x\, X_{\alpha b} \\ \text{where } c_\alpha &= k'\Big(\frac{2}{N_b+1}\Big)^{\frac{1}{2}} sin(q_\alpha). \end{aligned} \tag{2.44}$$

The equations of motion of the system and bath variables are

$$\begin{aligned} m_s\ddot{x} &= -m_s\omega_0^2\, x + \sum_{\alpha=1}^{N_b} c_\alpha\, X_{\alpha b} \\ \ddot{X}_{\alpha b} &= -\omega_\alpha^2\, X_{\alpha b} + c_\alpha\, x\, . \end{aligned} \tag{2.45}$$

As earlier, solving the equations of motion for bath variables and plugging back those solutions into the equation of motion of the system, we get

$$\begin{aligned} m_s\ddot{x} &= -m_s\omega_0^2\, x + \int_{-t_0}^{t} dt'\, \sigma(t-t')\, x(t') + \xi(t) \\ \text{where } \sigma(t) &= \sum_{\alpha=1}^{N_b} \frac{c_\alpha^2}{\omega_\alpha}\, sin(\omega_\alpha\, t)\, , \\ \text{and } \xi(t) &= \sum_{\alpha=1}^{N_b} c_\alpha [cos(\omega_\alpha\, t)\, X_{\alpha b}(t_0) + \frac{sin(\omega_\alpha\, t)}{\omega_\alpha}\, \dot{X_{\alpha b}}(t_0)]\, . \end{aligned} \tag{2.46}$$

We are interested in $\sigma^+(\omega) = \int_0^\infty dt\ \sigma(t)\ e^{i\ \omega\ t}$ whose imaginary part is given by

$$Im[\sigma^+(\omega)] = \Gamma(\omega) = \pi \sum_{\alpha=1}^{N_b} \frac{c_\alpha^2}{2\ \omega_\alpha}[\delta(\omega - \omega_\alpha) - \delta(\omega + \omega_\alpha)]. \tag{2.47}$$

For $\omega > 0$ and $\sqrt{\frac{k_1}{m}} < \omega < \sqrt{\frac{k_0}{m}}\sqrt{(4 + \frac{k_1}{k_0})}$,

$$\begin{aligned}
\Gamma(\omega) &= \frac{2\ k'^2}{(N_b + 1)} \sum_q \frac{sin^2(q)}{\omega_q}\ \delta(\omega - \omega_q) \\
&= k'^2 \int_0^\pi dq\ \frac{sin^2(q)}{\omega_q}\ \delta(\omega - \omega_q) \\
&= \frac{k'^2\ m}{k_0}\ sin(q_0) \quad \text{where,} \quad sin(q_0/2) = \sqrt{\frac{m}{4k_0}(\omega^2 - \frac{k_1}{m})},
\end{aligned} \tag{2.48}$$

To get the real part of $\sigma^+(\omega)$ we use the Kramers-Kronig relations and get

$$\begin{aligned}
Re[\sigma^+(\omega)] &= \frac{2}{\pi} \int_0^\infty d\omega' \frac{\omega'}{\omega'^2 - \omega^2}\ \Gamma(\omega') \\
&= \frac{2}{\pi} \int_{\sqrt{\frac{k_1}{m}}}^{\sqrt{\frac{k_0}{m}}\sqrt{(4+\frac{k_1}{m})}} d\omega' \frac{\omega'}{\omega'^2 - \omega^2}\ \Gamma(\omega')
\end{aligned} \tag{2.49}$$

Now, making the variable transformation $cos(\beta) = (1 - \frac{m\omega'^2}{2k_0} + \frac{k_1}{2k_0})$, we get

$$\begin{aligned}
Re[\sigma^+(\omega)] &= \frac{mk'^2}{\pi k_0} \int_0^\pi d\beta \frac{sin^2(\beta)}{x_0 - cos(\beta)} \quad \text{where,} \quad x_0 = (1 + \frac{k_1}{2k_0} - \frac{m\omega^2}{2k_0}) \\
&= \frac{mk'^2}{k_0}\ cos(q_0) \quad \text{for} \quad \sqrt{\frac{k_1}{m}} < \omega < \sqrt{\frac{k_0}{m}}\ \sqrt{(4 + \frac{k_1}{k_0})} \\
&= -\frac{mk'^2}{k_0}\ e^{-\nu_1} \quad \text{for} \quad |\omega| > \sqrt{\frac{k_0}{m}}\ \sqrt{(4 + \frac{k_1}{k_0})} \\
&= \frac{mk'^2}{k_0}\ e^{-\nu_2} \quad \text{for} \quad -\sqrt{\frac{k_1}{m}} < \omega < \sqrt{\frac{k_1}{m}} \\
\text{where} \quad cosh(\nu_1) &= (\frac{m\omega'^2}{2k_0} - \frac{k_1}{2k_0} - 1) \ \text{ and } \ cosh(\nu_2) = (1 + \frac{k_1}{2k_0} - \frac{m\omega'^2}{2k_0}).
\end{aligned} \tag{2.50}$$

Finally collecting the real and imaginary parts we get

$$\begin{aligned}
\sigma^+(\omega) = \frac{mk'^2}{k_0}\ e^{iq_0} \ \text{ for } \ &\sqrt{\frac{k_1}{m}} < \omega < \sqrt{\frac{k_0}{m}}\ \sqrt{(4 + \frac{k_1}{k_0})} \\
&\text{and} \ -\sqrt{\frac{k_0}{m}}\ \sqrt{(4 + \frac{k_1}{k_0})} < \omega < -\sqrt{\frac{k_1}{m}}
\end{aligned}$$

$$= -\frac{mk'^2}{k_0}\, e^{-\nu_1} \quad \text{for } |\omega| > \sqrt{\frac{k_0}{m}}\ \sqrt{(4+\frac{k_1}{k_0})}$$
$$= \frac{mk'^2}{k_0}\, e^{-\nu_2} \quad \text{for } -\sqrt{\frac{k_1}{m}} < \omega < \sqrt{\frac{k_1}{m}}. \tag{2.51}$$

2.4 Current in d-dimensional disordered harmonic lattice

In this section we consider heat conduction in d-dimensional classical harmonic lattice. For simplicity we consider only the case where longitudinal and transverse vibration modes are decoupled, allowing us to describe the displacement at each site by a scalar variable. Also we restrict our study to d-dimensional hypercubic lattices. Let us denote the lattice points by the vector $\mathbf{n} = \{n_1, n_2, ..., n_d\}$ with $n_\nu = 1, 2, ..., d$. The displacement of a particle at the lattice site $\mathbf{n} = (n_1, \mathbf{n}')$ is given by $x_\mathbf{n}$. In the harmonic approximation the system Hamiltonian is given by

$$\begin{aligned} H &= \sum_{\mathbf{n}} \frac{1}{2} m_\mathbf{n} \dot{x}_\mathbf{n}^2 + \sum_{n_1=1}^{N-1} \sum_{\mathbf{n}',\hat{\mathbf{e}}} \frac{k}{2} (x_\mathbf{n} - x_{\mathbf{n}+\hat{\mathbf{e}}})^2 \\ &\quad + \frac{k_o}{2} \sum_{\mathbf{n}} x_\mathbf{n}^2 + \frac{k'}{2} \sum_{\mathbf{n}'} x_{(1,\mathbf{n}')}^2 + \frac{k'}{2} \sum_{\mathbf{n}'} x_{(N,\mathbf{n}')}^2 \,, \end{aligned} \tag{2.52}$$

where $\hat{\mathbf{e}}$ refers to the $2d$ nearest neighbors of any site and we impose different boundary conditions which will be specified later. The parameter k_o represents the spring constant of the external pinning potential whereas k' is the spring constant of the external potential at the boundary $n_1 = 1$ and $n_1 = N$. The mass of the particle at site $\mathbf{n}$ is denoted by $m_\mathbf{n}$.

We couple all the particles at $n_1 = 1$ and $n_1 = N$ to heat reservoirs, at temperatures T_L and T_R respectively, and use periodic boundary conditions in the other $(d-1)$ directions. The heat conduction takes place along the $\nu = 1$ direction. Each layer with constant n_1 consists of $N' = N^{d-1}$ particles. The heat baths are modeled by white noise Langevin equations of motion for the particles coupled to the baths. The equations of motion are given by:

$$m_\mathbf{n} \ddot{x}_\mathbf{n} = -\sum_{\hat{\mathbf{e}}} k(x_\mathbf{n} - x_{\mathbf{n}+\hat{\mathbf{e}}}) - k_o x_\mathbf{n} + \delta_{n_1,1}(-\gamma \dot{x}_\mathbf{n}$$

$$+ \eta^L_{\mathbf{n}'} - k' x_{\mathbf{n}}) + \delta_{n_1,N}(-\gamma \dot{x}_{\mathbf{n}} + \eta^R_{\mathbf{n}'} - k' x_{\mathbf{n}}) \,, \tag{2.53}$$

where the dissipative and noise terms are related by the usual fluctuation dissipation relations

$$\begin{aligned} \langle \eta^L_{\mathbf{n}'}(t) \eta^L_{\mathbf{l}'}(t') \rangle &= 2\gamma k_B T_L \delta(t-t') \delta_{\mathbf{n}'\mathbf{l}'} \,, \\ \langle \eta^R_{\mathbf{n}'}(t) \eta^R_{\mathbf{l}'}(t') \rangle &= 2\gamma k_B T_R \delta(t-t') \delta_{\mathbf{n}'\mathbf{l}'} \,. \end{aligned} \tag{2.54}$$

The particles at the surfaces $n_1 = 1, N$ experience additional harmonic pinning potentials with spring constants k' arising from coupling to the heat reservoirs. We consider two kinds of boundary conditions at the surfaces connected to reservoirs: (i) fixed BCs $k' > 0$ and (ii) free BCs $k' = 0$. A schematic of the models and the different boundary conditions is given in Fig. (2.1).

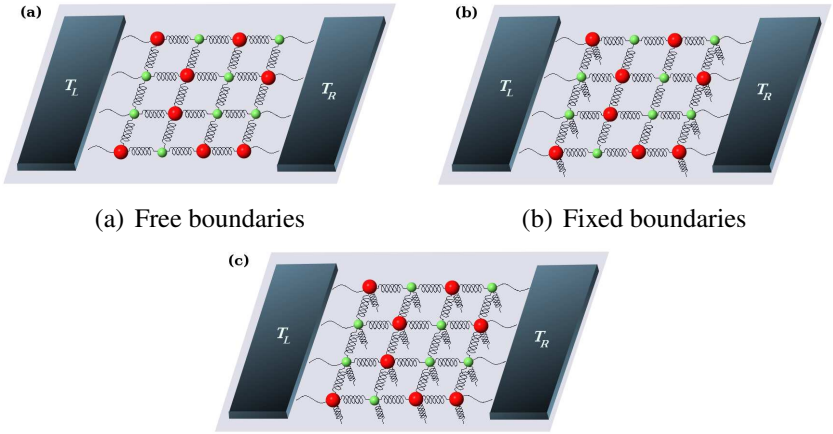

(a) Free boundaries (b) Fixed boundaries

(c) Pinned lattice

Figure 2.1: A schematic diagram of a two-dimensional mass-disordered lattice of particles connected by harmonic springs and connected to heat baths at temperatures T_L and T_R. Red and green colours indicate particles of different masses. Pinning refers to the presence of a spring attaching a particle to the substrate. In (a) there is no pinning, in (b) boundary particles are pinned and in (c) all sites are pinned.

The two different BCs emerge naturally if we model the heat reservoirs themselves by infinite ordered harmonic crystals. One then obtains Langevin type equations on eliminating the bath degrees of freedom. Fixed BCs correspond to reservoirs with properties different from the system (*e.g.* different spring constants) and in this case one finds that effectively the particles at the boundaries (those coupled to reservoirs) experience an additional harmonic

pinning potential. Free BCs correspond to the case where the reservoir is simply an extension of the system (without disorder) and in this case the end particles are unpinned.

Driven by the reservoirs at two different temperatures T_L and T_R, the system reaches a nonequilibrium steady state. We are mainly interested in the steady state heat current. Given the Langevin equations of motion Eq (2.53), one can find a formal general expression for the current. Let us denote by X a column vector with N^d elements consisting of the displacements at all lattice sites. Similarly let $\dot{X}$ represent the vector for velocities at all sites. Then we can write the Hamiltonian in Eq. (2.52) in the compact form as in Eq. (2.23), $H = \frac{1}{2}\dot{X}^T \mathcal{M}\dot{X} + \frac{1}{2}X^T \mathcal{V} X$, which defines the diagonal mass matrix $\mathcal{M}$ and the force constant matrix $\mathcal{V}$. Now following the four steps of LEGF formalism one gets an expression for the current $\mathcal{J}$ in terms of the transmission coefficient $\mathcal{T}(\omega)$.

It is convenient to express all the results in terms of dimensionless variables. These variables are as follows: force-constants are measured in units of k, masses in units of the average mass $\bar{m}$, time in units of the inverse frequency $\Omega_o^{-1} = (\bar{m}/k)^{1/2}$, displacements are in units of the lattice spacing a, friction constant γ in units of $\bar{m}\Omega$, and finally, temperature is measured in units of $\bar{m}a^2\Omega_o^2/k_B$. With this notation, we write the steady state current per bond from the left to the right reservoir from Eq. (2.38) [24, 17] :

$$\mathcal{J} = \frac{\Delta T}{4\pi N'} \int_{-\infty}^{\infty} d\omega \mathcal{T}(\omega) \,, \tag{2.55}$$

$$\text{where } \mathcal{T}(\omega) = 4\, Tr[\mathcal{I}_L(\omega)\mathcal{G}^+(\omega)\mathcal{I}_R(\omega)\mathcal{G}^-(\omega)] \,, \tag{2.56}$$

$$\mathcal{G}^+(\omega) = [-\omega^2 \mathcal{M} + \mathcal{V} - \mathcal{S}_L^+ - \mathcal{S}_R^+]^{-1} \,, \;\; \mathcal{G}^- = [\mathcal{G}^+]^*$$

$$\mathcal{I}_L = Im[\mathcal{S}_L^+] \,, \text{ and } \mathcal{I}_R = Im[\mathcal{S}_R^+] \tag{2.57}$$

and $\Delta T = T_L - T_R$. The matrices $\mathcal{S}_L^+$ and $\mathcal{S}_R^+$ represent the coupling of the system to the left and right reservoirs respectively, and can be written as $N \times N$ block matrices where each block is a $N' \times N'$ matrix. The block structures are as follows:

$$\mathcal{S}_L^+ = \begin{pmatrix} \Sigma_L^+ & 0 & ... & 0 \\ 0 & 0 & \dots & 0 \\ 0 & 0 & \dots & 0 \end{pmatrix}, \mathcal{S}_R^+ = \begin{pmatrix} 0 & 0 & \dots & 0 \\ 0 & 0 & \dots & 0 \\ 0 & 0 & ... & \Sigma_R^+ \end{pmatrix}, \tag{2.58}$$

where

$$\Sigma_L^+ = \Sigma_R^+ = i\gamma\omega I \,, \tag{2.59}$$

I is a $N' \times N'$ unit matrix, and 0 is a $N' \times N'$ matrix with all elements equal to zero. Similarly the matrices $\mathcal{M}$ and $\mathcal{V}$ have the following block structure:

$$\mathcal{M} = \begin{pmatrix} M_1 & 0 & ... & 0 \\ 0 & M_2 & \dots & 0 \\ 0 & 0 & \dots & 0 \\ 0 & 0 & .. & M_N \end{pmatrix}, \; \mathcal{V} = \begin{pmatrix} \Phi & -I & \dots & 0 \\ -I & \Phi & \dots & 0 \\ 0 & 0 & \dots & 0 \\ 0 & 0 & .. - I & \Phi \end{pmatrix}, \tag{2.60}$$

where M_n denotes the diagonal mass-matrix for the $n_1 = n$ layer and Φ is a force-constant matrix whose off-diagonal terms correspond to coupling to sites within a layer. Hence the matrix $\mathcal{G}^{-1} = [-\mathcal{M}\omega^2 + \mathcal{V} - \mathcal{S}_L^+ - \mathcal{S}_R^+]$ has the following structure:

$$[\mathcal{G}]^{-1} = \begin{pmatrix} a_1 & -I & 0 & ... & 0 \\ -I & a_2 & -I & 0 \dots & 0 \\ ... & ... & ... & ... & ... \\ 0 & ... 0 & -I & a_{N-1} & -I \\ 0 & ... & 0 & -I & a_N \end{pmatrix}, \tag{2.61}$$

where $a_l = -M_l\omega^2 + \Phi - \delta_{l,1}\Sigma_L^+ - \delta_{l,N}\Sigma_R^+$. With the form of $\mathcal{S}_{L,R}^+$ given in Eqs. (2.58)and (2.59), we find that the expression for the transmission coefficient reduces to the following form:

$$\begin{aligned} \mathcal{T}(\omega) &= 4\, Tr[\Gamma_L(\omega) G_N^+(\omega) \Gamma_R(\omega) G_N^-(\omega)] \,, \\ &\text{where } \Gamma_{L,R} = Im[\Sigma_{L,R}^+] \end{aligned} \tag{2.62}$$

and G_N^+ is the $(1,N)^{\text{th}}$ block element of $\mathcal{G}$ and $G_N^- = [G_N^+]^\dagger$. We now show that G_N^+ satisfies some simple recursion relations and using those recursion relations the transmission coefficient $\mathcal{T}(\omega)$ can be expressed as a product of random matrices.

2.4.1 Transfer matrix approach and recursion relations for Green's functions

Here we will see that because of the block tridiagonal nature of the force constant matrix one can find simple recursion relations among the elements of Green's function. Before doing that we first introduce some notations. Let $\mathcal{Y}^{(l,l+n-1)}$ with $1 \leq n \leq N-l+1$ denote a $n \times n$ tridiagonal block matrix whose diagonal entries are $a_l, a_{l+1}, ...a_{l+n-1}$, where each a_l is a $N' \times N'$ matrix. The off-diagonal entries are given by $-I$. For an arbitrary block matrix $\mathcal{A}^{(l,m)}$, $\mathcal{A}^{(l,m)}_{(i,j)}$ will denote the block sub-matrix of $\mathcal{A}^{(l,m)}$ beginning with i^{th} block row and column and ending with the j^{th} block row and column, while $A^{(l,m)}_{i,j}$ will denote the $(i,j)^{th}$ block element of $\mathcal{A}^{(l,m)}$. Also $\mathcal{I}_n$ will denote a $n \times n$ block-diagonal matrix with diagonal elements I.

The inverse of $\mathcal{Y}^{(1,N)}$ is denoted by $[\mathcal{Y}^{(1,N)}]^{-1} = \mathcal{G}^{(1,N)}$ and satisfies the equation:

$$\mathcal{Y}^{(1,N)}\,\mathcal{G}^{(1,N)} \;=\; \mathcal{I}_N\,.$$

According to our notation, we have $\mathcal{G}^{(1,N)} = \mathcal{G}^{+}$ and $G^{(1,N)}_{1,N} = G^{+}_{N}$. The matrix $\mathcal{Y}^{(1,N)}$ has the following structure:

$$\mathcal{Y}^{(1,N)} = \begin{pmatrix} \mathcal{Y}^{(1,N-1)} & \mathcal{W}_N \\ \mathcal{W}_N^T & a_N \end{pmatrix}, \tag{2.63}$$

where $\mathcal{W}_N^T = (0, 0, ..., -I)$ is a $1 \times N-1$ block vector. We then write Eq. (2.63) in the form

$$\begin{pmatrix} \mathcal{Y}^{(1,N-1)} & \mathcal{W}_N \\ \mathcal{W}_N^T & a_N \end{pmatrix}\begin{pmatrix} \mathcal{G}^{(1,N)}_{(1,N-1)} & \mathcal{U}_N \\ \mathcal{U}_N^T & G^{(1,N)}_{N,N} \end{pmatrix} = \begin{pmatrix} \mathcal{I}_{N-1} & 0 \\ 0 & I \end{pmatrix}, \tag{2.64}$$

where $\mathcal{U}_N^T = [G^{(1,N)T}_{1,N}, G^{(1,N)T}_{2,N} ..., G^{(1,N)T}_{N-1,N}]$ is a $1 \times N-1$ block vector. From Eq (2.64) we get the four following equations:

$$\begin{aligned} \mathcal{Y}^{(1,N-1)}\,\mathcal{G}^{(1,N)}_{(1,N-1)} + \mathcal{W}_N\,\mathcal{U}_N^T &= \mathcal{I}_{N-1}\,, \\ \mathcal{W}_N^T\,\mathcal{G}^{(1,N)}_{(1,N-1)} + a_N\,\mathcal{U}_N^T &= 0\,, \\ \mathcal{Y}^{(1,N-1)}\,\mathcal{U}_N + \mathcal{W}_N\,G^{(1,N)}_{N,N} &= 0\,, \\ \mathcal{W}_N^T\,\mathcal{U}_N + a_N\,G^{(1,N)}_{N,N} &= I\,. \end{aligned} \tag{2.65}$$

Noting that $[\mathcal{Y}^{(1,N-1)}]^{-1} = \mathcal{G}^{(1,N-1)}$ and using the third equation above and the form of $\mathcal{W}_N$, we get:

$$\begin{aligned} \mathcal{U}_N &= -\mathcal{G}^{(1,N-1)}\mathcal{W}_N G^{(1,N)}_{N,N} \,, \\ \text{or } G^{(1,N)}_{i,N} &= G^{(1,N-1)}_{i,N-1} G^{(1,N)}_{N,N} \,, \text{ for } i = 1, 2, ..., N-1. \end{aligned} \tag{2.66}$$

From the fourth equation in Eq. (2.65) we get:

$$G^{(1,N)}_{N-1,N} = a_N \, G^{(1,N)}_{N,N} - I \,. \tag{2.67}$$

We will now use Eqs. (2.66),(2.67) to obtain a recursion relation for $G^{(1,N)}_{1,N} = G^{+}_{N}$ in Eq. (2.62)], which is the main object of interest. Let us define $P^{(l,n)} = [G^{(l,n)}_{1,n-l+1}]^{-1}$ where $\mathcal{G}^{(l,m)} = [\mathcal{Y}^{(l,m)}]^{-1}$. Then setting $i = 1$ in Eq. (2.66) and taking an inverse on both sides we get:

$$P^{(1,N)} = [G^{(1,N)}_{N,N}]^{-1} \, P^{(1,N-1)}. \tag{2.68}$$

Setting $i = N-1$ in Eq. (2.66) we get $G^{(1,N)}_{N-1,N} = G^{(1,N-1)}_{N-1,N-1} G^{(1,N)}_{N,N}$ and using this in Eq. (2.67) we get $[G^{(1,N)}_{N,N}]^{-1} = [a_N - G^{(1,N-1)}_{N-1,N-1}]$. Inserting this in the above equation we finally get our required recursion relation:

$$P^{(1,N)} = a_N P^{(1,N-1)} - P^{(1,N-2)} \,. \tag{2.69}$$

The initial conditions for this recursion are: $P^{(1,0)} = I_M$ and $P^{(1,1)} = a_1$. By proceeding similarly as before we can also obtain the following recursion relation:

$$P^{(n,N)} = P^{(n+1,N)} a_1 - P^{(n+2,N)} \,, \quad n = 1, 2, ..., N-1 \,, \tag{2.70}$$

and $P^{(1,N)}$ can be recursively obtained using the initial conditions $P^{(N+1,N)} = I_M$ and $P^{(N,N)} = a_N$. Given the set $\{a_i\}$, by iterating either of the above equations one can numerically find $P^{(1,N)}$ and then invert it to find $G^{(1,N)}_{1,N}$.

However this scheme runs into accuracy problems since the numerical values of the matrix elements of the iterates grow rapidly. We describe now a different way of performing the

recursion which turns out to be numerically more efficient. We first define

$$r_N = P^{(1,N)}[P^{(1,N-1)}]^{-1} \ . \tag{2.71}$$

From Eq. (2.69) we immediately get:

$$r_N = a_N - \frac{1}{r_{N-1}} \ , \tag{2.72}$$

with the initial condition $r_1 = a_1$. Then $G_{1,N}^{(1,N)}$ is given by:

$$\begin{aligned} G_{1,N}^{(1,N)} &= [P^{(1,N)}]^{-1} = [r_N r_{N-1} ... r_1]^{-1} \\ &= r_1^{-1} r_2^{-1} ... r_N^{-1} \ . \end{aligned} \tag{2.73}$$

This form where at each stage r_l^{-1} is evaluated turns out to be numerically more accurate.

Finally, we show that one can express $G_{1,N}^{(1,N)}$ in the form of a product of matrices. The product form is such that the system and reservoir contributions are separated. First, we note that the form of the matrices a_l for our specific problem is: $a_l = c_l - \delta_{l,1}\Sigma_1 - \delta_{l,N}\Sigma_N$ where $c_l = -M_l\omega^2 + \Phi$. We define system-dependent matrices $Q^{(1,n)}$, $Q^{(n,N)}$ by replacing a_1, a_N by c_1, c_N in the recursions for P's. Thus $Q^{(1,n)} = P^{(1,n)}(a_1 \to c_1, a_N \to c_N)$ and $Q^{(n,N)} = P^{(n,N)}(a_1 \to c_1, a_N \to c_N)$. Clearly Q's satisfy the same recursion as the P's with a_l replaced by c_l. Then using Eqs. (2.69),(2.70), and similar equations for the Qs' we get:

$$\begin{aligned} & P^{(1,N)} \\ = \ & Q^{(1,N)} - Q^{(2,N)}\,\Sigma_1 - \Sigma_N\,Q^{(1,N-1)} + \Sigma_N\,Q^{(2,N-1)}\,\Sigma_1 \\ = \ & (1 \quad -\Sigma_N) \begin{pmatrix} Q^{(1,N)} & -Q^{(2,N)} \\ Q^{(1,N-1)} & -Q^{(2,N-1)} \end{pmatrix} \begin{pmatrix} 1 \\ \Sigma_1 \end{pmatrix} . \end{aligned} \tag{2.74}$$

From the recursion relations for the Qs', it is easy to see that

$$\begin{aligned} & \begin{pmatrix} Q^{(1,N)} & -Q^{(2,N)} \\ Q^{(1,N-1)} & -Q^{(2,N-1)} \end{pmatrix} \\ = \ & \begin{pmatrix} a_N & -I \\ I & 0 \end{pmatrix} \begin{pmatrix} Q^{(1,N-1)} & -Q^{(2,N-1)} \\ Q^{(1,N-2)} & -Q^{(2,N-2)} \end{pmatrix} \\ = \ & \hat{T}_N \hat{T}_{N-1} ... \hat{T}_1 \ , \end{aligned} \tag{2.75}$$

where

$$\hat{T}_l \;=\; \begin{pmatrix} a_l & -I \\ I & 0 \end{pmatrix}. \tag{2.76}$$

From Eq. (2.74) we then obtain $P^{(1,N)}$ and from which we get $G_N^+ = [P^{(1,N)}]^{-1}$. Using this and noting that the baths are white noise Langevin baths we get

$$\mathcal{J} \;=\; \frac{K_B(T_L - T_R)}{\pi N'} \int_{-\infty}^{\infty} d\omega\, \omega^2\, \gamma^2\, Tr\left[[P^{+*}_{1,N}(\omega) P^{+T}_{1,N}(\omega)]^{-1}\right]. \tag{2.77}$$

Comparing the above equation with Eq. (2.55), we get

$$\mathcal{T}(\omega) = 4\omega^2\, \gamma^2\, Tr\left[[P^{+*}_{1,N}(\omega) P^{+T}_{1,N}(\omega)]^{-1}\right]. \tag{2.78}$$

2.4.2 Current in one dimensional harmonic system:

For 1D chain the Hamiltonian in Eq. (2.52) looks like

$$H = \sum_{l=1}^{N}\left[\frac{1}{2}m_l\dot{x}_l^2 + \frac{1}{2}k_o x_l^2\right] + \sum_{l=1}^{N-1}\frac{1}{2}k(x_{l+1} - x_l)^2 + \frac{1}{2}k'(x_1^2 + x_N^2)\,, \tag{2.79}$$

and the corresponding langevin equations look like

$$\begin{aligned} m_1\ddot{x}_1 &= -(k' + k_o)x_1 - k(x_1 - x_2) + \gamma\dot{x}_1 + \eta_1(t) \\ m_l\ddot{x}_l &= -k_o x_l - k(2x_l - x_{l-1} - x_{l+1}), \qquad 1 < l < N \\ m_N\ddot{x}_N &= -(k' + k_o)x_N - k(x_N - x_{N-1}) + \gamma\dot{x}_N + \eta_N(t) \end{aligned} \tag{2.80}$$

In the classical case, the steady state heat current from left to right reservoir is obtained from Eq. (2.77) [17, 13]

$$\begin{aligned} \text{where } \mathcal{T}_N(\omega) &= \gamma^2\omega^2|G_N|^2\,, \\ G_N(\omega) &= [P^{(1,N)}]^{-1}(\omega), \\ \mathcal{V}_{lm} &= (1 + k' + k_o)\,\delta_{l,m} - \delta_{l,m-1} \qquad \text{for} \quad l = 1\,, \end{aligned}$$

$$
\begin{aligned}
&= -\delta_{l,m+1} + (2 + k_o)\,\delta_{l,m} - \delta_{l,m-1} \quad \text{for} \quad 2 \le l \le N-1\,, \\
&= (1 + k' + k_o)\,\delta_{l,m} - \delta_{l,m+1} \qquad \text{for} \quad l = N\,, \\
\Sigma_{lm} &= i\gamma\omega\delta_{lm}[\delta_{l1} + \delta_{lN}]\,,
\end{aligned}
$$

All the variables and parameters in the above expressions are now dimensionless quantities and $[P^{(1,N)}]^{-1}$ is now just a complex number. It is easy to identify that

$$
P^{(1,N)} = \Delta_N \tag{2.81}
$$

where Δ_N is the determinant of the matrix $Z = [-\omega^2\mathcal{M} + \mathcal{V} - \Sigma]$.

Disordered case: This has been extensively studied and is well understood [14, 15, 17, 19, 22, 69]. The matrix formulation explained in the last section leads to a clear analytic understanding of the main results. From the products of N random matrices of size (2×2) one calculates $P^{(1,N)}$ numerically and hence $\mathcal{T}(\omega)$. Clearly $\mathcal{T}(\omega)$ and $\mathcal{J}$ will be different for different disorder realisations. Since we will mostly be interested in disorder averages of these quantities we need to introduce some notation for the disorder average. We consider $[x]$ to be the disorder average of the quantity x. We denote disordered averaged $\mathcal{T}_N(\omega)$ and $\mathcal{J}$ by $T(\omega) = [\mathcal{T}]$ and $J = [\mathcal{J}]$ respectively.

There are three observations that enable one to determine the asymptotic system size dependence of the current. These are:

(i)$P^{(1,N)} = [G_N^+]^{-1}$ given by Eqs. (2.74), (2.76) is a complex number which can be expressed in terms of the product of N random 2×2 matrices. Using Furstenberg's theorem it can be shown that for almost all disorder realizations, the large N behaviour of $P^{(1,N)}$ for fixed $\omega > 0$ is $|P^{(1,N)}| \sim e^{bN\omega^2}$, where $b > 0$ is a constant. This is to be understood in the sense that $\lim_{N\to\infty}(1/N)\log|P^{1,N)}| \sim b\omega^2$ for $\omega \to 0$. Since $\mathcal{T}(\omega) \sim |P^{(1,N)}|^{-2} \sim e^{-2bN\omega^2}$, this implies that transmission is significant only for low frequencies $\omega \lesssim \omega_c(N) \sim 1/N^{1/2}$. The current is therefore dominated by the small ω behaviour of $T(\omega)$.

(ii) The second observation made in [19] is that the transmission for $\omega < \omega_c(N)$ is ballistic in the sense that $T(\omega)$ is insensitive to the disorder. This can be seen in fig. (2.2) where the

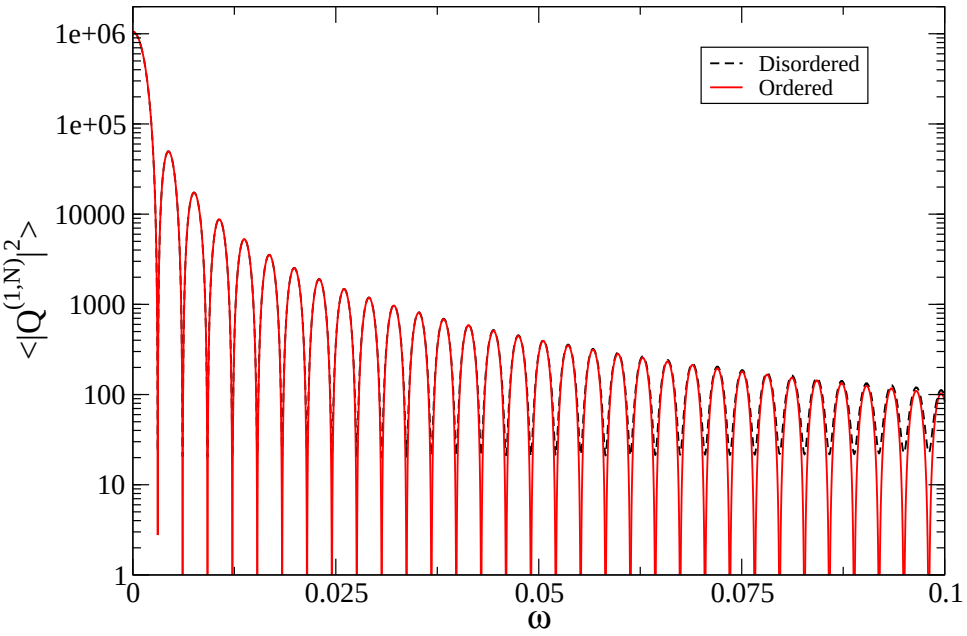

Figure 2.2: Frequency dependence of $[|Q^{(1,N)}|]$ at small ω for $\Delta = 0.2$ and $N = 1024$ with fixed BC is compared with the same for an ordered chain. In disordered case $|Q^{(1,N)}|^2$ is averaged over 10^4 different realisation of masses.

disorder average of $|Q^{(1,N)}|^2$ for a chain of length $N = 1024$ is plotted along with the same for an ordered chain.

(iii) The final important observation is that the form of the prefactors of $e^{-bN\omega^2}$ in $T(\omega)$ for $\omega < \omega_c(N)$ depends strongly on boundary conditions and bath properties [19, 22]. For the white noise Langevin baths, one finds $T(\omega) \sim \omega^2 e^{-bN\omega^2}$ for fixed BC and $T(\omega) \sim \omega^0 e^{-bN\omega^2}$ for free BC [22]. This difference arises because of the scattering of long wavelength modes by the boundary pinning potentials. Now, the asymptotic N dependence of the disorder averaged current in the NESS will be

$$\begin{aligned} J &\sim \int_0^{\omega_c(N)} T(\omega) \\ &\sim N^{-\frac{1}{2}} \text{ for free BC} \\ &\sim N^{-\frac{3}{2}} \text{ for fixed BC.} \end{aligned} \tag{2.82}$$

In Fig. (2.3), we plot numerical results showing $\mathcal{T}(\omega)$ for the $1D$ mass-disordered lattice with both fixed and free boundary conditions. We consider a binary mass disordered crystal

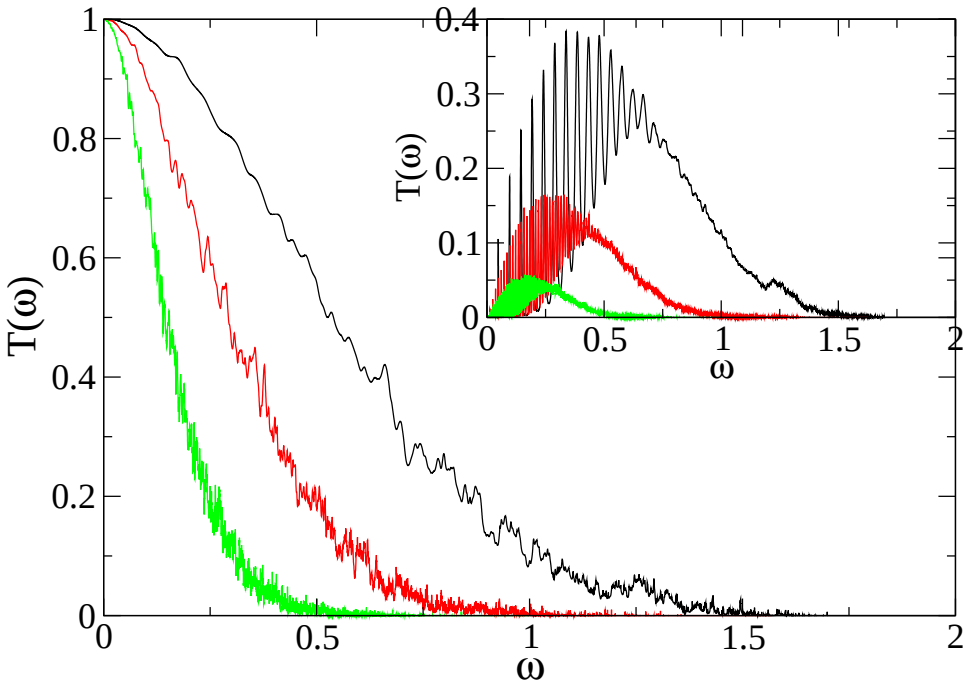

Figure 2.3: $1D$ unpinned case with both free and fixed (INSET) boundary conditions: plot of the disorder averaged transmission $T(\omega)$ versus ω for $\Delta = 0.4$. The various curves (from top to bottom) correspond to lattices of sizes $N = 64, 256, 1024$ respectively.

in which we set the masses of exactly half the particles at randomly chosen sites to be $\bar{m} - \Delta$ and the rest to be $\bar{m} + \Delta$. Thus Δ gives a measure of the disorder. One can clearly see the two features discussed above, namely (i) dependence of frequency cut-off on system size and (ii) dependence of the form of $T(\omega)$ on boundary conditions. Using the three observations made above it is easy to arrive at the conclusion that $J \sim N^{-3/2}$ for fixed BC and $J \sim N^{-1/2}$ for free BC. In the presence of a pinning potential the low-frequency modes are suppressed and one obtains a heat insulator with $J \sim e^{-cN}$, with c a constant [69] (see also [21] and references therein).

Ordered case: In this case, masses of all the particles are the same (say, m). Hence one can write a closed form expression for Δ_N. After some straightforward calculations and rearrangements one can show that [11]:

$$\Delta_N \;=\; [a(q)\sin Nq + b(q)\cos Nq]/\sin q\,, \tag{2.83}$$

$$
\begin{aligned}
\text{where } a(q) &= [2-\gamma^2\omega^2+k'^2-2k']\cos q + 2k' - 2 - 2i\gamma\omega[1+(k'-1)\cos q]\,, \\
b(q) &= [\gamma^2\omega^2 - k'^2 + 2k']\sin q + 2i\gamma\omega(k'-1)\sin q\,, \\
2\cos q &= -m\omega^2 + k_o + 2\,. \qquad (2.84)
\end{aligned}
$$

From the relation in Eq. (2.84), it is clear that for frequencies outside the phonon band $k_o \le m\omega^2 \le k_o + 2$ the wave vector q becomes imaginary and hence, from Eq. (2.83), we note that the transmission coefficient $\mathcal{T}(\omega)$ decays exponentially with N. Hence, for large N we need to consider only the range $0 < q < \pi$ and the current is given by:

$$
J_C = \frac{2\gamma^2(T_L - T_R)}{\pi}\int_0^\pi dq \left|\frac{d\omega}{dq}\right| \frac{\omega_q^2}{|\Delta_N|^2}\,, \qquad (2.85)
$$

with $m\omega_q^2 = k_o + 2[1-\cos(q)]$. We now state the following result. For any two well-behaved functions $g_1(q)$ and $g_2(q)$

$$
\lim_{N\to\infty}\int_0^\pi dq \frac{g_1(q)}{1+g_2(q)\sin Nq} = \int_0^\pi dq \frac{g_1(q)}{[1-g_2^2(q)]^{1/2}}\,. \qquad (2.86)
$$

There are three steps required to prove this result: (i) expand the factor $1/[1+g_2(q)\sin(Nq)]$ (valid for $|g|<1$ in the integration range), (ii) take the $N\to\infty$ limit, (iii) resum the resulting series. It is easy to see that the Eq. (2.85) has the same structure as the left hand side of Eq. (2.86) once we note that Δ_N can be written as

$$
\begin{aligned}
|\Delta_N|^2 &= (|a|^2+|b|^2)[1+r\sin(2Nq+\phi)]/[2\sin^2(q)] \\
\text{where} &\qquad r\cos\phi = (ab^* + a^*b)/(|a|^2+|b|^2) \\
\text{and} &\qquad r\sin\phi = (|b|^2-|a|^2)/(|a|^2+|b|^2). \qquad (2.87)
\end{aligned}
$$

Hence using Eq. (2.86) and simplifying, we get [22]:

$$
\begin{aligned}
J_C &= \frac{\gamma k^2 k_B(T_L-T_R)}{\pi m}\int_0^\pi \frac{\sin^2 q\, dq}{\Lambda - \Omega\cos q} \\
&= \frac{\gamma k^2 k_B(T_L-T_R)}{m\Omega^2}(\Lambda - \sqrt{\Lambda^2-\Omega^2})\,, \qquad (2.88) \\
\text{where } \Lambda &= 2k(k-k') + k'^2 + \frac{(k_o+2k)\gamma^2}{m} \text{ and } \Omega = 2k(k-k') + \frac{2k\gamma^2}{m}\,.
\end{aligned}
$$

2.4.3 Current in d-dimensional ordered harmonic system

The current in a d-dimensional ordered lattice can be calculated by using the observation that the problem of heat conduction in a d-dimensional ordered harmonic lattice can be related to heat conduction across N^{d-1} independent ordered harmonic chains with different onsite potentials. Hence the transmission coefficient $\mathcal{T}(\omega)$ for the d-dimensional lattice can be expressed as a sum of the transmission coefficients of the $1D$ chains. Now we will see how one can relate the d-dimensional problem to a one dimensional problem. The Hamiltonian of the d-dimensional system is given in sec. (2.4). We recall that $x_{\mathbf{n}}$ is the displacement of a particle at the lattice site $\mathbf{n} = (n_1, \mathbf{n}')$. Let us consider that for each $\mathbf{n}$ there exists a $\mathbf{q} = (q_1, q_2, ..., q_{d-1}, q_d) = (q_1, \mathbf{q}')$ with $q_\alpha = \frac{2\pi l}{N}$ where l goes from 1 to N such that

$$\frac{1}{N^{d-1}} \sum_{\mathbf{q}'} e^{i\mathbf{q}'.\mathbf{n}'_1} \, e^{i\mathbf{q}'.\mathbf{n}'_2} = \delta_{\mathbf{n}'_1,\mathbf{n}'_2} \tag{2.89}$$

Now, if we define

$$x_{n_1}(\mathbf{q}') = \frac{1}{N^{\frac{d-1}{2}}} \sum_{\mathbf{n}'} x_{(n_1,\mathbf{n}')} \, e^{i\mathbf{q}'.\mathbf{n}'}, \tag{2.90}$$

then one can show that, for each $\mathbf{q}'$, $x_{n_1}(\mathbf{q}')$ satisfies a Langevin equation corresponding to a one-dimensional Hamiltonian with the onsite spring constant replaced by

$$\lambda(\mathbf{q}') = k_o + 2k(d - 1 - \sum_{\alpha=2,..,d} cos\ q_\alpha). \tag{2.91}$$

Hence in the ordered case the d-dimensional harmonic system can be decomposed into N^{d-1} harmonic chains. For $N \to \infty$, the heat current $J(\mathbf{q}')$ for each mode with given $\mathbf{q}'$ is then simply given by Eq.(2.88) with k_o replaced by $\lambda(\mathbf{q}')$. The heat current per bond is then given by:

$$J = \frac{1}{N^{d-1}} \sum_{\mathbf{q}'} J(\mathbf{q}') \, . \tag{2.92}$$

The above result also holds for finite lengths in the transverse direction. For infinite trans-

verse lengths, we get $J = \int ... \int_0^{2\pi} d\mathbf{q} J(\mathbf{q})/(2\pi)^{d-1}$. Heat conduction in higher dimensional disordered harmonic systems is studied in the next chapter.

3 Study on heat conduction in higher dimensional harmonic system

In the previous chapter we have discussed the LEGF formalism and applied it to one dimensional harmonic chain to find out the system size dependence of the NESS current J. We also mentioned results on heat conduction in one dimensional systems, from which we conclude that system size scaling of the NESS current strongly depends on the boundary conditions and also on the presence of pinning potentials. There have been theoretical as well as computational studies on finding the system size dependence of heat current in NESS. All the studies suggest that Fourier's law is not valid in one and two dimensional systems, even in the presence of anharmonic interactions, unless the system is also subjected to an external substrate pinning potential. It is generally expected that the system size scaling of J will be less sensitive to boundary conditions as we go to higher and higher dimensions. Based on empirical evidence, it is also expected that average energy current J in NESS through a system in a slab geometry, should be proportional to N^{-1}. In this chapter we present numerical studies on heat conduction through disordered harmonic lattices in two and three dimensions.

Here we report results of heat conduction studies in $2D$ and $3D$ disordered harmonic lattices with scalar displacements and connected to heat baths modeled by Langevin equations with white noise. In crystalline solids the carriers of heat are phonons, which are normal modes of lattice vibrations. Transport properties of these modes will be affected by Anderson localization [70] and by phonon scattering in anharmonic lattices. We pay particular attention to the interplay between localization effects, boundary effects, and the role of long wavelength modes. The steady state heat current is given exactly as an integral over all fre-

quencies of a phonon transmission coefficient as shown in Eq. (2.38). Using this formula and heuristic arguments, based on localization theory and kinetic theory results, we estimate the system size dependence of the current.

Numerically we use two different approaches to study the nonequilibrium stationary state. The first is a numerical one which relies on the result that the current can be expressed in terms of a transmission coefficient. We saw in Eq. (2.38) that the transmission coefficient can be written in terms of phonon Green's functions. Using the recursion relations of the Green's functions (discussed in sec. (2.4.1) we implement efficient numerical schemes to evaluate this transmission coefficient. The second approach is through direct nonequilibrium simulations of the Langevin equations of motion and finding the steady state current and temperature profiles. We have also studied properties of the isolated system, *i.e.*, of the disordered lattice without coupling to heat baths, and looked at the normal mode frequency spectrum and the wavefunctions. One measure of the degree of localization of the normal modes of the isolated system is the so-called inverse participation ratio [IPR, defined in Eq. (3.11) below]. We have carried out studies of the IPR and linked these with results from the transmission study.

The rest of the chapter is organized as follows. In Sec. (3.1) and Sec. (3.2) we discuss earlier studies on phonon localization and kinetic theory results in phonon transport respectively. In the beginning of Sec. (3.3) we describe the specific model studied which is followed by discussions on quantities studied and approaches used in this chapter. Heuristic arguments and our predictions on asymptotic system size dependence of current are given in Sec. (3.4). In Sec. (3.5) we present results from both the numerical approach and from nonequilibrium simulations which is followed by conclusion in Sec. (3.6).

3.1 Phonon localization

This is closely related to the electron localization problem. The effect of localization on linear waves in disordered media has been most extensively studied in the context of the Schrödinger equation for non-interacting electrons moving in a disordered potential. Looking at the eigenstates and eigenfunctions of the isolated system of a single electron in a

disordered potential one finds that, in contrast to the spatially extended Bloch states in periodic potentials, there are now many eigenfunctions which are exponentially localized in space. It was argued by Mott and Twose [73] and by Borland [74], and proven rigorously by Goldsheid *et al.* [75], that in one dimension all states are exponentially localized. In two dimensions there is no proof but it is believed that again all states are localized. In three dimensions there is expected to be a transition from extended to localized states as the energy is moved towards the band edges [76]. The transition from extended to localized states, which occurs when the disorder is increased, changes the system from a conductor to an insulator. The connection between localization and heat transport in a crystal is complicated by the fact that phonons of all frequencies can contribute to energy transmission across the system. In particular, account has to be taken of the fact that low frequency phonon modes are only weakly affected by disorder and always remain extended. The heat current carried by a mode which is localized on a length scale ℓ, decays with system length N as $e^{-N/\ell}$. This ℓ depends on the phonon frequency, and low frequency modes for which $\ell \sim N$ will therefore be carriers of the heat current. The net current then depends on the nature of these low frequency modes and their scattering due to boundary conditions (BCs).

A renormalization group study in a disordered continuum elastic media by John *et al.* [17] found that in 1D and 2D all non-zero frequency phonons are localized. They studied the spreading of an energy pulse to define a frequency dependent diffusivity $D_0(\omega)$. From the behaviour of $D_0(\omega)$ under renormalization one can obtain a differential recursion relation for the resistivity. This relation shows that in the large system size limit the RG flow is towards infinity for dimensions ≤ 2, in contrast to $d = 3$ where the flow is towards zero as long as ω is less than some fixed value, independent of system size. Hence all finite-frequency modes in one and two dimensions are localized. From the differential recursion relations one finds that for $d = 1$ and $d = 2$ the localization length in $\omega \to 0$ limit diverges as $\sim\ 1/\omega^2$ and $\sim\ e^{1/\omega^2}$ respectively. In $3D$ there exists a frequency, independent of system size, above which all states are localized while states below that frequency are extended. Hence for a system of size N there will be a cut-off frequency ω_c^L (which depends on N for $d \leq 2$) above which all

the modes are localized. In different dimensions ω_c^L is given by

$$\begin{aligned} \omega_c^L &\sim N^{-1/2} \text{ for } d = 1 \\ &\sim [log(N)]^{-1/2} \text{ for } d = 2 \\ &\sim \text{ nonzero value independent of } N \text{ for } d = 3 \end{aligned} \tag{3.1}$$

However this study does not make any statements on the system size dependence of the conductivity.

3.2 Kinetic theory

If one considers the low frequency extended phonons, then the effect of disorder is weak and in dimensions $d > 1$ one expects that localization effects can be neglected and kinetic theory should be able to provide an accurate description. In this case one can think of Rayleigh scattering of phonons. This gives an effective mean free path $\ell_K(\omega) \sim \omega^{-(d+1)}$ [see chapter (1)] , for dimensions $d > 1$, and a diffusion constant $D(\omega) = v\ell_K(\omega)$ where v, the sound velocity, can be taken to be constant. For a finite system of linear dimension N we have $D(\omega) = vN$ for $\omega \lesssim N^{-1/(d+1)}$. Kinetic theory then predicts

$$\kappa = \int_{N^{-1}}^{\omega_{\max}} d\omega \rho(\omega) D(\omega) \, , \tag{3.2}$$

where $\rho(\omega) \sim \omega^{d-1}$ is the density of states and we get $\kappa \sim N^{1/(d+1)}$, implying $\mu = d/(d+1)$. The divergence of the phonon mean free path at low frequencies and the resulting divergence of the thermal conductivity of a disordered harmonic crystal has been discussed in the literature and it has been argued that anharmonicity is necessary to make κ finite [77, 2].

3.3 System and methods

Here we consider heat conduction across a d-dimensional hyper-cubic lattice which is connected to two Langevin heat baths at the two ends of it. The model was defined in Sec. (2.4) in detail. For completeness, we recall the Hamiltonian of the system and the corresponding

Langevin equations. The Hamiltonian of the system is given by

$$\begin{aligned} H &= \sum_{\mathbf{n}} \frac{1}{2} m_{\mathbf{n}} \dot{x}_{\mathbf{n}}^2 + \sum_{n_1=1}^{N-1} \sum_{\mathbf{n}',\hat{\mathbf{e}}} \frac{k}{2} (x_{\mathbf{n}} - x_{\mathbf{n}+\hat{\mathbf{e}}})^2 \\ &\quad + \frac{k_o}{2} \sum_{\mathbf{n}} x_{\mathbf{n}}^2 + \frac{k'}{2} \sum_{\mathbf{n}'} x_{(1,\mathbf{n}')}^2 + \frac{k'}{2} \sum_{\mathbf{n}'} x_{(N,\mathbf{n}')}^2 \,, \end{aligned} \tag{3.3}$$

and the Langevin equation are given by

$$\begin{aligned} m_{\mathbf{n}} \ddot{x}_{\mathbf{n}} = &- \sum_{\hat{\mathbf{e}}} k(x_{\mathbf{n}} - x_{\mathbf{n}+\hat{\mathbf{e}}}) - k_o x_{\mathbf{n}} + \delta_{n_1,1}(-\gamma \dot{x}_{\mathbf{n}} \\ &+ \eta_{\mathbf{n}'}^L - k' x_{\mathbf{n}}) + \delta_{n_1,N}(-\gamma \dot{x}_{\mathbf{n}} + \eta_{\mathbf{n}'}^R - k' x_{\mathbf{n}}) \,. \end{aligned} \tag{3.4}$$

The meaning of all the variables and quantities appearing in the above two equations is explained in sec. (2.4). For a particular disorder configuration the steady state current per bond from left to right reservoir has the following form (Eq. (2.55))

$$\mathcal{J} = \frac{\Delta T}{4\pi N'} \int_{-\infty}^{\infty} d\omega \mathcal{T}(\omega) \,, \tag{3.5}$$

where

$$\mathcal{T}(\omega) = 4\, Tr[\mathcal{I}_L(\omega) \mathcal{G}^+(\omega) \mathcal{I}_R(\omega) \mathcal{G}^-(\omega)] \,, \tag{3.6}$$

$$\begin{aligned} \mathcal{G}^+(\omega) &= [-\omega^2 \mathcal{M} + \mathcal{V} - \mathcal{S}_L^+ - \mathcal{S}_R^+]^{-1} \,, \ \mathcal{G}^- = [\mathcal{G}^+]^* \\ \mathcal{I}_L &= Im[\mathcal{S}_L^+] \,, \text{ and } \mathcal{I}_R = Im[\mathcal{S}_R^+] \end{aligned} \tag{3.7}$$

and $\Delta T = T_L - T_R$. The specific form of $\mathcal{S}_{L,R}^+$ for our system described by Eqs. (3.4) was given in Eq. (2.58). The matrix $\mathcal{G}^+(\omega)$ can be identified as the phonon Green's function of the system with self-energy corrections due to the baths [24]. The integrand in Eq. (3.5) $\mathcal{T}(\omega)$ can be thought of as the transmission coefficient of phonons at frequency ω from the left to the right reservoir. It will vanish, when $N \to \infty$, at values of ω for which the disorder averaged density of states is zero. Note that due to the harmonic nature of the forces the dependence of the heat flux on the reservoir temperatures enters only through the term ΔT in Eq. (3.5).

Numerical approach: In sec 2.4.1, we have described how $\mathcal{T}$ can be expressed in a form amenable to accurate numerical computation. The system sizes we study are sufficiently large so that $\mathcal{T}(\omega)$ has appreciable values only within the range of frequencies of normal modes of the isolated system, *i.e.*, corresponding to $\gamma = 0$ in the equation of motion (Eq. (2.53)). Outside this range we find that the transmission rapidly goes to zero. By performing a discrete sum over the transmitting range of frequencies we do the integration in Eq. (3.5) to obtain the heat current density $\mathcal{J}$. In evaluating the discrete sum over ω, step sizes of $\delta\omega = 0.01 - 0.0001$ are used and we verified convergence in most cases. With our choice of units we have $k = 1, \bar{m} = 1$ and we fixed $\Delta T = 1$. Different values of the mass variance Δ and the on-site spring constant k_o were studied for two and three dimensional lattices of different sizes. It is expected that the value of the exponent μ will not depend on γ and in our calculations we mostly set $\gamma = 1$, except when otherwise specified.

Simulation approach: The simulations of Eq. (3.4) are performed using a velocity-Verlet scheme as given in [78]. The current and temperature profiles in the system are obtained from the following time averages in the nonequilibrium steady state:

$$\begin{aligned}
\mathcal{J}_1 &= \frac{1}{N'}\sum_{\mathbf{n}'}\frac{\gamma}{m_{(1,\mathbf{n}')}}\left[T_L - m_{(1,\mathbf{n}')}\langle \dot{x}^2_{(1,\mathbf{n}')}\rangle\right], \\
\mathcal{J}_n &= -\frac{1}{N'}\sum_{\mathbf{n}'}\langle\, [x_{(n,\mathbf{n}')} - x_{(n-1,\mathbf{n}')}]\, \dot{x}_{(n,\mathbf{n}')}\,\rangle\,, \\
&\qquad\qquad n = 2, 3, ..., N\,, \\
\mathcal{J}_{N+1} &= -\frac{1}{N'}\sum_{\mathbf{n}'}\frac{\gamma}{m_{(N,\mathbf{n}')}}\left[T_R - m_{(N,\mathbf{n}')}\langle \dot{x}^2_{(N,\mathbf{n}')}\rangle\right]\,, \\
T_n &= \frac{1}{N'}\sum_{\mathbf{n}'} m_{(n,\mathbf{n}')}\langle\, \dot{x}^2_{(n,\mathbf{n}')}\,\rangle\,, \quad n = 1, 2, ..., N\,.
\end{aligned}$$

We then obtained the average current $\mathcal{J} = (\sum_{n=1}^{N+1}\mathcal{J}_N)/(N+1)$. In the steady state one has $\mathcal{J}_n = \mathcal{J}$ for all n and stationarity can be tested by checking how accurately this is satisfied. We chose a step size of $\Delta t = 0.005$ and equilibrated the system for over 10^8 time steps. Current and temperature profiles were obtained by averaging over another 10^8 time steps. The parameters $T_L = 2.0, T_R = 1.0$ are kept fixed and different values of the mass variance Δ and the on-site spring constant k_o are simulated.

Disorder averaged T_n is denoted by $[T_n]$. Note that disorder average of any quantity is denoted by [...]. We also define the disorder averaged transmission per bond with the notation

$$T(\omega) = \frac{1}{N'}[\mathcal{T}(\omega)] \, . \tag{3.8}$$

Numerical analysis of eigenmodes and eigenfunctions: We have studied the properties of the normal modes of the disordered harmonic lattices in the absence of coupling to reservoirs, again with both free and fixed boundary conditions. The d-dimensional lattice has $p = 1, 2, ..., N^d$ normal modes and we denote the displacement field corresponding to the p^{th} mode by $a_{\mathbf{n}}(p)$ and the corresponding eigenvalue by ω_p^2. The normal mode equation corresponding to the Hamiltonian in Eq. (3.3) is given by:

$$m_{\mathbf{n}}\omega_p^2 a_{\mathbf{n}} = (2d + k_o)a_{\mathbf{n}} - \sum_{\hat{\mathbf{e}}} a_{\mathbf{n}+\hat{\mathbf{e}}} \, , \tag{3.9}$$

where the $a_{\mathbf{n}}$ satisfy appropriate boundary conditions. Introducing variables $\psi_{\mathbf{n}}(p) = m_{\mathbf{n}}^{1/2} a_{\mathbf{n}}(p)$, $v_{\mathbf{n}} = (2d + k_o)/m_{\mathbf{n}}$ and $t_{\mathbf{n},\mathbf{l}} = 1/(m_{\mathbf{n}} m_{\mathbf{l}})^{1/2}$ for nearest neighbour sites $\mathbf{n}$, $\mathbf{l}$ the above equation transforms to the following form:

$$\omega_p^2 \psi_{\mathbf{n}}(p) = v_{\mathbf{n}}\psi_{\mathbf{n}}(p) - \sum_{\mathbf{l}} t_{\mathbf{n},\mathbf{l}}\psi_{\mathbf{l}}(p) \, . \tag{3.10}$$

This has the usual structure of an eigenvalue equation for a single electron moving in a d-dimensional lattice corresponding to a tight-binding Hamiltonian with nearest neighbour hopping $t_{\mathbf{n},\mathbf{l}}$ and on-site energies $v_{\mathbf{n}}$. Note that $t_{\mathbf{n},\mathbf{l}}$ and $v_{\mathbf{n}}$ are correlated random variables, hence the disorder-energy diagram might differ considerably from a single band Anderson tight-binding model.

We have numerically evaluated all eigenvalues and eigenstates of the above equation for finite cubic lattices of size upto $N = 64$ in $2D$ and $N = 16$ in $3D$. One measure of the degree of localization of a given mode is the inverse participation ratio (IPR) defined as follows:

$$P^{-1} = \frac{\sum_{\mathbf{n}} a_{\mathbf{n}}^4}{(\sum_{\mathbf{n}} a_{\mathbf{n}}^2)^2} \, . \tag{3.11}$$

For a completely localized state, *i.e.* $a_{\mathbf{n}} = \delta_{\mathbf{n},\mathbf{n}_0}$, P^{-1} takes the value 1. On the other hand for

a completely delocalized state, for which $a_{\mathbf{n}} = N^{-d/2} e^{i\mathbf{n}.\mathbf{q}}$ where $\mathbf{q}$ is a wave vector, P^{-1} takes the value N^{-d}. We will present numerical results for the IPR calculated for all eigenstates of given disorder realizations, in both $2D$ and $3D$. Finally we will show some results for the density of states, $\rho(\omega)$, of the disordered system defined by:

$$\rho(\omega) = \sum_{p} \delta(\omega_p - \omega) \; . \tag{3.12}$$

The density of states of disordered binary mass harmonic crystals was studied numerically by Payton and Visscher in 1967 [80] and reviewed by Dean in 1972 [81].

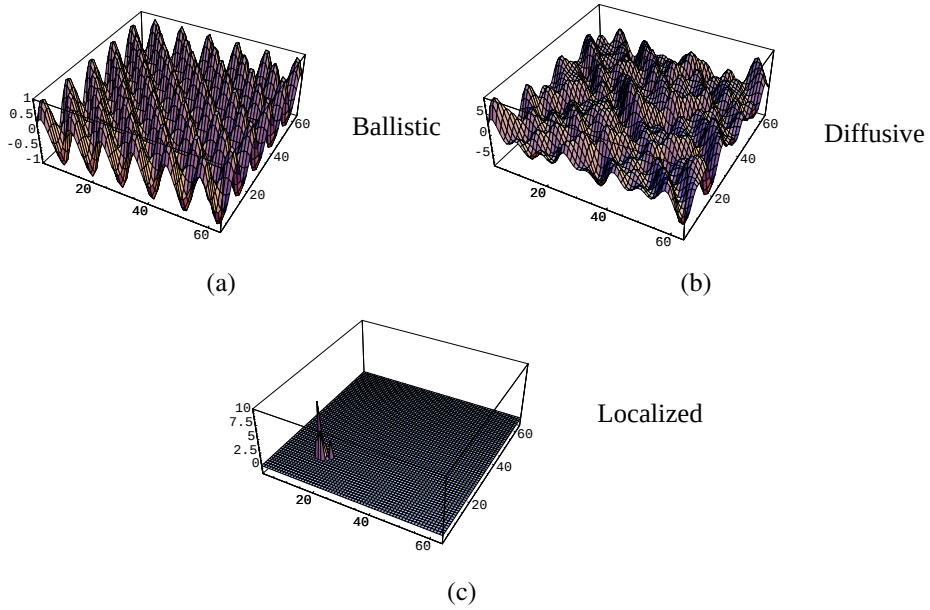

Figure 3.1: Three different types of modes

3.4 Heat conduction in disordered harmonic crystals: General considerations

Here we will try to extend the analysis of the $1D$ case (given in the previous chapter) to higher dimensions. For this we will use inputs from both kinetic theory and the theory of phonon localization. The main point of our arguments involves the assumption that normal modes can be classified as ballistic, diffusive or localized. The classification refers both to the character of the eigenfunctions as well as to their transmission properties. Ballistic

modes are spatially extended and approximately periodic; their transmission is independent of system size. Diffusive modes are extended but non-periodic and their transmission decays as $1/N$. For localized modes transmission decays exponentially with N. In the context of kinetic theory calculations, the ballistic modes are the low frequency modes with phonon mean free path $\ell_K(\omega) \gtrsim N$, and their contribution to the current leads to divergence of the thermal conductivity. Here we carefully examine the effect of both free and fixed boundary conditions on these modes.

In the presence of an external pinning potential low frequency modes are suppressed, hence one expects qualitative differences in transport properties. The pinned system has often been used as a model system to study the validity of Fourier's law. It has no translational invariance and is thus more closely related to the problem of electrons moving in a random potential. Using localization theory we determine the frequency region where states are localized. The lowest frequency states with $\omega \to 0$ will be ballistic and we use kinetic theory to determine the fraction of extended states which are ballistic. We assume that at sufficiently low frequencies the effective disorder is always weak (even when the mass variance Δ is large) and one can still use kinetic theory. Corresponding to the three observations made above for the $1D$ case we now make the following arguments:

(i) From localization theory one expects all fixed non-zero frequency states in a $2D$ disordered system to be localized when the size of the system goes to infinity. As discussed in Sec. (3.1), localization theory gives us a frequency cut-off $\omega_c^L = (\ln N)^{-1/2}$ in $2D$ above which states are localized. In $3D$ one obtains a finite frequency cut-off ω_c^L independent of system size above which states are localized.

(ii) For the unpinned case with finite N there will exist low frequency states below ω_c^L, in both $2D$ and $3D$, which are extended states. These states are either diffusive or ballistic. Ballistic modes are insensitive to the disorder and their transmission coefficients are almost the same as for the ordered case. To find the frequency cut-off below which states are ballistic we use kinetic theory results (see Sec. (1.1.2)). For the low-frequency extended states we expect kinetic theory to be reliable and this gives us a mean free path for phonons $\ell_K \sim$

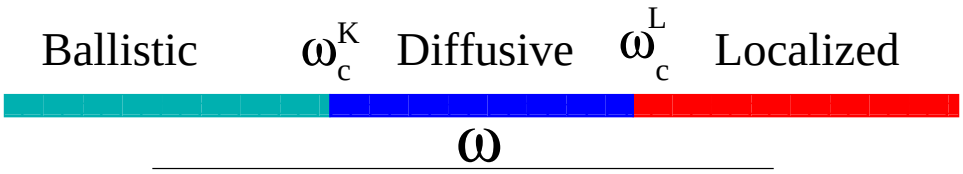

Figure 3.2: Frequency spectrum

$\omega^{-(d+1)}$. This means that for low frequencies $\omega \lesssim \omega_c^K = N^{-1/(d+1)}$ we have $\ell_K(\omega) > N$ and phonons transmit ballistically. We now proceed to calculate the contribution of these ballistic modes to the total current. This can be obtained by looking at the small ω form of $T_N(\omega)$ for the ordered lattice. States with frequency lying between $[\omega_c^K, \omega_c^L]$ are assumed to be diffusive while making predictions about the system size dependence of current. Fig. (3.2) schematically describes the nature of the modes at different ranges.

(iii) For the ordered lattice $T(\omega)$ is typically a highly oscillatory function with the oscillations increasing with system size. An effective transmission coefficient in the $N \to \infty$ limit can be obtained by considering the integrated transmission. This asymptotic *effective* low-frequency form of $T(\omega)$, for the ordered lattice can be calculated using methods described in [22] and is given by:

$$\begin{aligned} T(\omega) &\sim \omega^{d+1}, \quad \text{fixed BC} \\ T(\omega) &\sim \omega^{d-1}, \quad \text{free BC}, \end{aligned} \tag{3.13}$$

the result being valid for $d = 1, 2, 3$ [82].

Using the above arguments we then get the ballistic contribution to the total current density (for the unpinned case) as:

$$\begin{aligned} J_{\text{ball}} &\sim \int_0^{\omega_c^K} d\omega\, \omega^{d+1} \sim \frac{1}{N^{(d+2)/(d+1)}}, \quad \text{fixed BC}, \\ &\sim \int_0^{\omega_c^K} d\omega\, \omega^{d-1} \sim \frac{1}{N^{d/(d+1)}}, \quad \text{free BC}. \end{aligned} \tag{3.14}$$

We can now make predictions for the asymptotic system size dependence of total current density in two and three dimensions.

Two dimensions: From localization theory one expects that all finite frequency modes $\omega \gtrsim$

$\omega_c^L = (\ln N)^{-1/2}$ are localized and their contribution to the total current falls exponentially with system size. Our kinetic theory arguments show that the low frequency extended states with $\omega_c^K \lesssim \omega \lesssim \omega_c^L$ are diffusive (where $\omega_c^K = N^{-1/3}$) while the remaining modes with $\omega \lesssim \omega_c^K$ are ballistic. The diffusive contribution to total current will then scale as $J_{\rm diff} \sim (\ln N)^{-1/2} N^{-1}$. The ballistic contribution depends on BCs and is given by Eq. (3.14). This gives $J_{\rm ball} \sim N^{-4/3}$ for fixed BC and $J_{\rm ball} \sim N^{-2/3}$ for free BC. Hence, adding all the different contributions, we conclude that asymptotically:

$$\begin{aligned} J &\sim \frac{1}{(\ln N)^{1/2} N}, \quad \text{fixed BC, } d = 2, \\ &\sim \frac{1}{N^{2/3}}, \qquad \text{free BC, } d = 2. \end{aligned} \tag{3.15}$$

In the presence of an onsite pinning potential at all sites the low frequency modes get cut off and all the remaining states are localized, we expect:

$$J \sim e^{-bN}, \qquad \text{pinned}, \ d = 2, \tag{3.16}$$

where b is some positive constant.

Three dimensions: In this case localization theory tells us that modes with $\omega \gtrsim \omega_c^L$ are localized and ω_c^L is independent of N. From kinetic theory we find that the extended states with $\omega_c^K \lesssim \omega \lesssim \omega_c^L$ are diffusive (with $\omega_c^K = N^{-1/4}$) and those with $\omega \lesssim \omega_c^K$ are ballistic. The contribution to current from diffusive modes scales as $J_{\rm diff} \sim N^{-1}$. The ballistic contribution (from states with $\omega \lesssim N^{-1/4}$) is obtained from Eq. (3.14) and gives $J_{\rm ball} \sim N^{-5/4}$ for fixed BC and $J_{\rm ball} \sim N^{-3/4}$ for free BC. Hence, adding all contributions, we conclude that asymptotically:

$$\begin{aligned} J &\sim \frac{1}{N}, \qquad \text{fixed BC}, \ d = 3, \\ &\sim \frac{1}{N^{3/4}}, \qquad \text{free BC}, \ d = 3. \end{aligned} \tag{3.17}$$

In the presence of an onsite pinning potential at all sites the low frequency modes get cut off and, since in this case the remaining states form bands of diffusive and localized states,

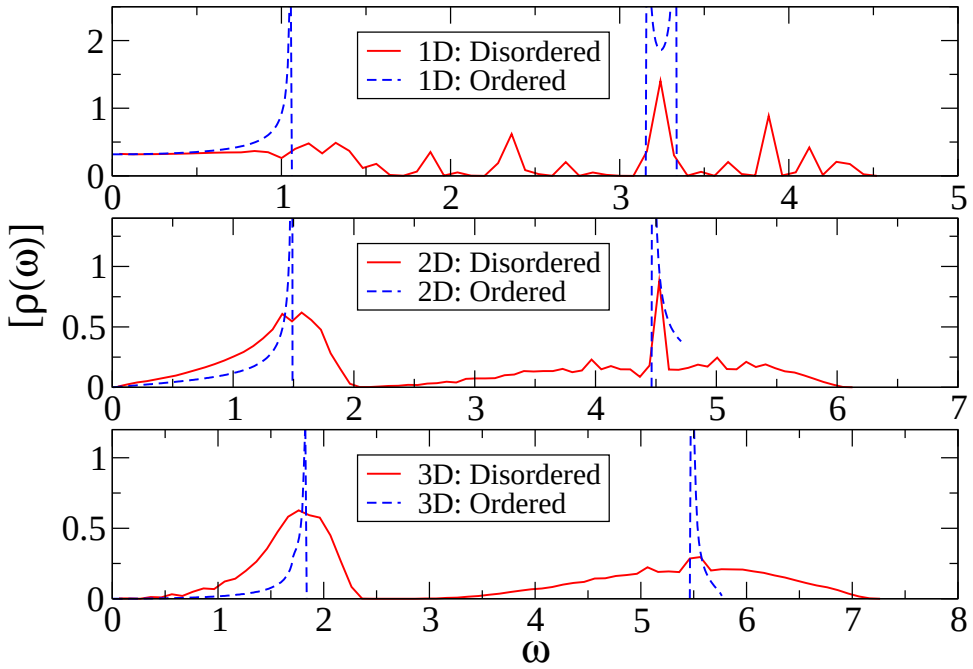

Figure 3.3: Unpinned lattices with fixed BC in one direction and periodic BC in all others. Disorder averaged density of states obtained numerically from the eigenvalues of several disorder realizations in $1D, 2D$ and $3D$ for lattice sizes $N = 4096, 64, 16$ respectively. Note that the low frequency behaviour is unaffected by disorder and one has ω^{d-1} as $\omega \to 0$. We set $\Delta = 0.8, k = 1$ and averaged over 30 realizations in $1D$ and over 10 realizations in $2D$ and $3D$. In $2D$ and $3D$ there is not much variation in $\rho(\omega)$ for different disorder samples. Also shown are the density of states for the binary mass ordered lattices.

hence we expect:

$$J \sim \frac{1}{N}\,, \qquad \text{pinned}\,,\ d = 3. \tag{3.18}$$

Thus in $3D$ both the unpinned lattice with fixed boundary conditions and the pinned lattice are expected to show Fourier type of behaviour as far as the system size dependence of the current is concerned.

Note that for free BC, the prediction for the current contribution from the ballistic part $J_{\text{ball}} \sim N^{-d/(d+1)}$ is identical to that from kinetic theory discussed earlier. This agreement can be traced to the small ω form of $T(\omega) \sim \omega^{d-1}$ for free BC [see Eq. (3.13)] which is identical to the form of the density of states $\rho(\omega)$ used in kinetic theory. The typical form of density of

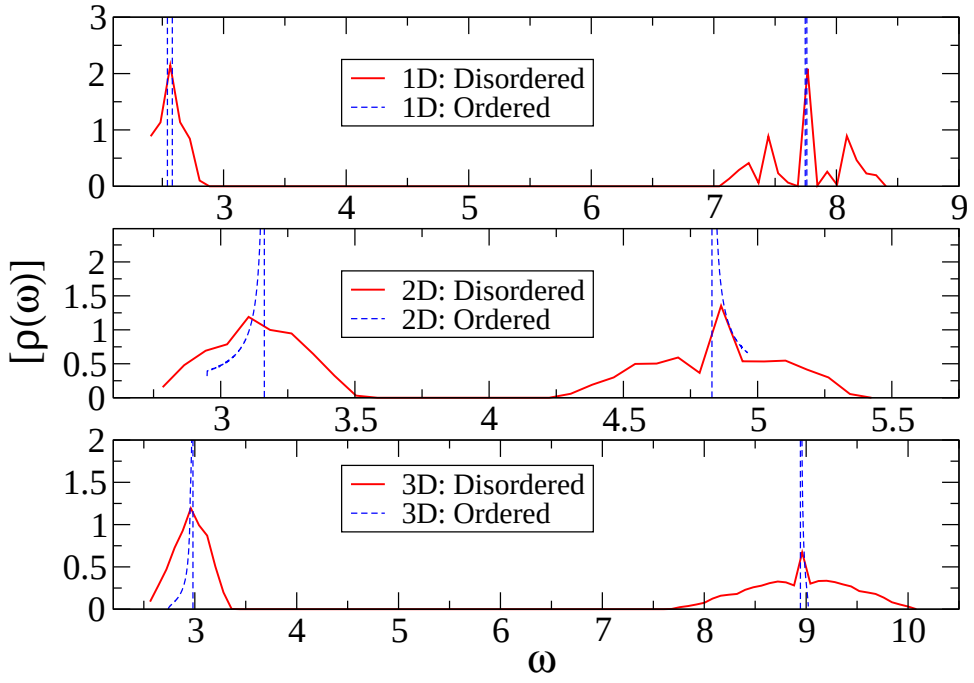

Figure 3.4: Pinned lattices: Disorder averaged density of states obtained numerically from the eigenvalues of several disorder realizations in $1D, 2D$ and $3D$ for lattice sizes $N = 4096, 64, 16$ respectively. Note that low frequency modes are absent. We set $k = 1, k_o = 10.0$ and $\Delta = 0.4$ in $2D$ and $\Delta = 0.8$ in $1D, 3D$. Averages were taken over 30 realizations in $1D$ and 10 realizations in $2D, 3D$. We find that in $2D$ and $3D$ there is not much variation in $\rho(\omega)$ for different disorder samples. Also shown are the density of states for the binary mass ordered lattices.

states for ordered and disordered lattices in different dimensions is shown in Fig. (3.3) and we can see that the low frequency form is similar in both cases and has the expected ω^{d-1} behaviour. However it seems reasonable to expect that, since the transport current phonons are injected at the boundaries, in kinetic theory one needs to use the *local density of states* evaluated at the boundaries. For fixed BC this will then give rise to an extra factor of ω^2 (from the squared wavefunction) and then the kinetic theory prediction matches with those given above.

We note that the density of states in Fig. (3.3) show apparent gaps in the middle ranges of ω for $d = 2, 3$. These might be expected to disappear when the size of the system goes to infinity when there should be large regions containing only masses of one type [17, 69].

These regions will however be rare. In Fig. (3.4) we show plots of the density of states for the ordered and disordered harmonic lattices in the presence of pinning. In this case the gaps in the spectrum are more pronounced and, for large enough values of k_o and Δ, may be present even in the thermodynamic limit.

3.5 Results from Numerics and Simulations

We now present the numerical and simulation results for transmission coefficients, heat current density, temperature profiles and IPRs for the disordered harmonic lattice in various dimensions. The numerical scheme for calculating J is both faster and more accurate than nonequilibrium simulations. Especially, for strong disorder, equilibration times in nonequilibrium simulations become very large and in such cases only the numerical method can be used. However we also show some nonequilibrium simulation results. Their almost perfect agreement with the numerical results provides additional confidence in the accuracy of our results. In Sec. (3.5.1) we give the results for the $2D$ lattice for the unpinned case with both fixed and free boundary conditions and then for the pinned case. In Sec. (3.5.2) we present the results for the three dimensional case with and without substrate pinning potentials.

3.5.1 Results in two dimensions

In this section we consider $N \times N$ square lattices with periodic BCs in the $\nu = 2$ direction and either fixed or free BCs in the conducting direction ($\nu = 1$). One of the interesting questions here is as to how the three properties for the $1D$ case discussed in second chapter get modified for the $2D$ case.

3.5.1.1 Disordered $2D$ lattice without pinning

Fixed BC: we have computed the transmission coefficients and the corresponding heat currents for different values of Δ and for system sizes from $N = 16 - 1024$. The number of averages varied from over 100 samples for $N = 16$ to about two samples for $N = 1024$. In Figs. (3.5,3.6,3.7) we plot the disorder averaged transmission coefficient for three differ-

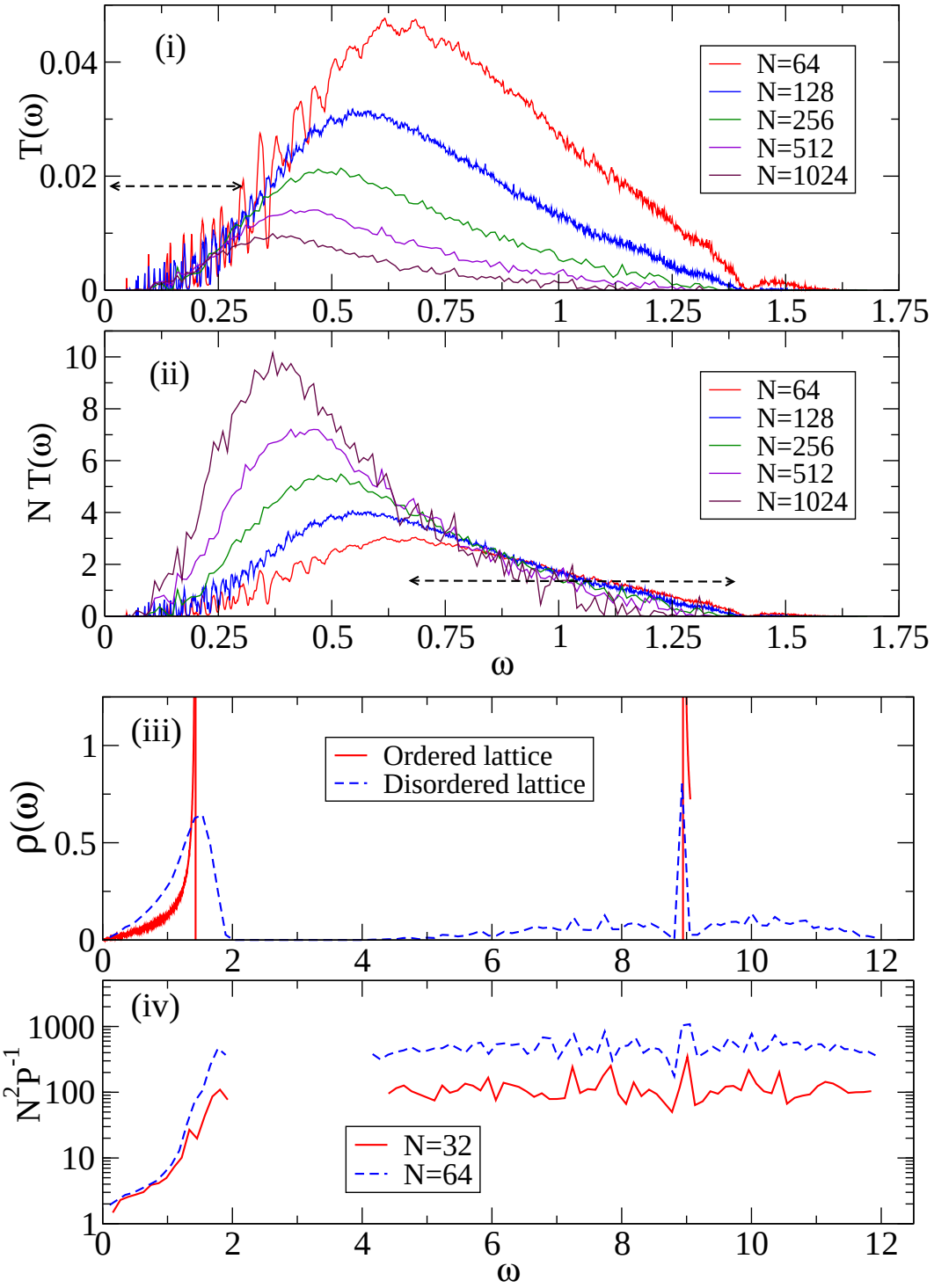

Figure 3.5: $2D$ unpinned case with fixed BC for $\Delta = 0.95$. (i) Plot of the disorder averaged transmission $T(\omega)$ versus ω. (ii) Plot of $NT(\omega)$. The range of frequencies for which $T(\omega) \sim 1/N$ is indicated by the dashed line. (iii) Plot of $\rho(\omega)$ for binary mass ordered and single disordered sample. (iv) Plot of N^2P^{-1} for single samples (smoothed data). We see that even though the allowed normal modes occur over a large frequency band $\approx$ (0 – 12), transmission takes place in a small band $\approx$ (0 – 1.25) and is negligible elsewhere. The IPR plots confirm that the non-transmitting states correspond to localized modes. In (i) we see that ω_c^L is slowly decreasing with inrease of N.

ent disorder strengths, $\Delta = 0.95$, $\Delta = 0.8$ and $\Delta = 0.2$, for different system sizes. The corresponding plots of IPRs as a function of normal mode frequency ω_p, for single disorder realizations, are also given. From the IPR plots we get an idea of the typical range of allowed normal mode frequencies and their degree of localization. Low IPR values which scale as N^{-2} imply extended states while large IPR values which do not change much with system size denote localized states. In Fig. (3.6) we also show typical plots of small IPR and large IPR wavefunctions. From Figs. (3.5,3.6,3.7) we make the following observations:

(i) As expected we see significant transmission only over the range of frequencies with extended states. Thus in Fig. (3.5) for $\Delta = 0.95$ we see that, while there are normal modes in the range $\omega \approx (0 - 12)$, transmission is appreciable only in the range $\omega \approx (0 - 1.5)$ and this is also roughly the range where the IPR data shows a N^{-2} scaling behaviour. This can also be seen in Fig. (3.6) where the inset shows the decay of $T(\omega)$ in the localized region. Unlike the $1D$ case we see a very weak dependence on system size of the upper frequency cut-off ω_c^L beyond which states are localized and transmission is negligible. As discussed earlier, localization theory predicts $\omega_c^L \sim (\ln N)^{-1/2}$ but this may be difficult to observe numerically. The overall transmission function $T_N(\omega)$ decreases with increasing system size, with $T(\omega) \sim 1/N$ at higher frequencies and $T(\omega) \sim N^0$ at the lowest frequencies.

(ii) In Fig. (3.7) we have also plotted $T(\omega)$ for the ordered binary mass case and we note that over a range of small frequencies, $T(\omega)$ for the disordered case is very close to the curve for the ordered case, which means that these modes are ballistic. As expected from the arguments in Sec. (3.4) we roughly find $T(\omega) \sim \omega^3$ at small frequencies. The remaining transmitting states are either diffusive (with a $1/N$ scaling) or are in the cross-over regime between diffusive and ballistic and so do not have a simple scaling.

We next look at the integrated transmission which gives the net heat current. The system size dependence of the disorder averaged current J for different values of Δ is shown in Fig. (3.8). For the case $\Delta = 0.2$, we also show simulation results and one can see that there is excellent agreement with the numerical results. For $\Delta = 0.2$ we get an exponent $\mu \approx 0.6$ which is close to the value obtained earlier in [27] for a similar disorder strength.

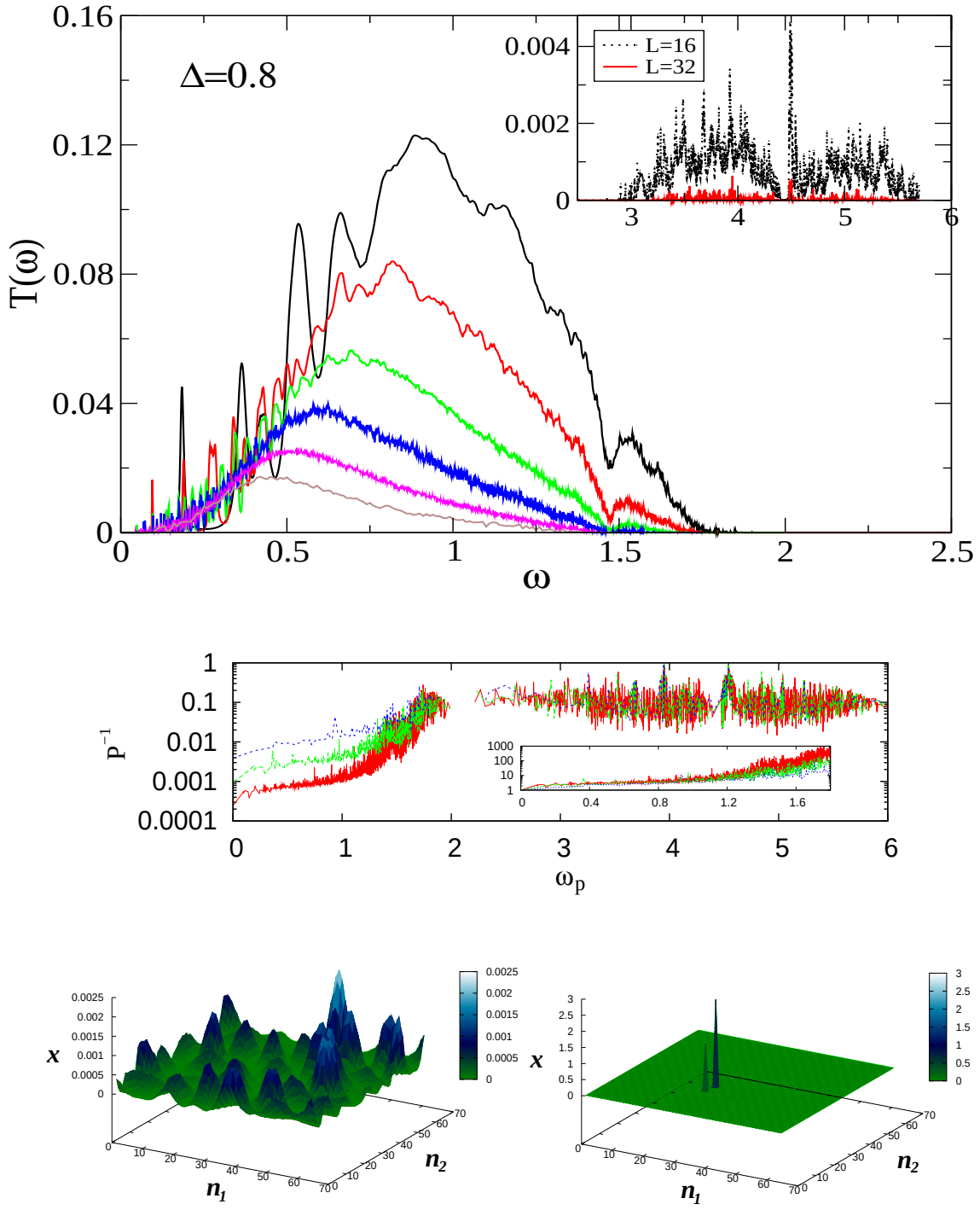

Figure 3.6: $2D$ unpinned case with fixed BC for $\Delta = 0.8$. TOP: Plot of the disorder averaged transmission $T(\omega)$ versus ω. The various curves (from top to bottom) correspond to square lattices with $N = 16, 32, 64, 128, 256, 512$ respectively. We see again that most modes are localized and transmission takes place over a small range of frequencies. BOTTOM: Plot shows the IPR (P^{-1}) as a function of normal mode-frequency ω_p for the $2D$ lattice with $\Delta = 0.8$. The curves are for $N = 16$ (blue), 32 (green) and 64 (red). The inset plots N^2P^{-1} and the collapse at low frequencies shows that these modes are extended. Also shown are two typical normal modes for one small (left) and one large value of P^{-1} for $N = 64$.

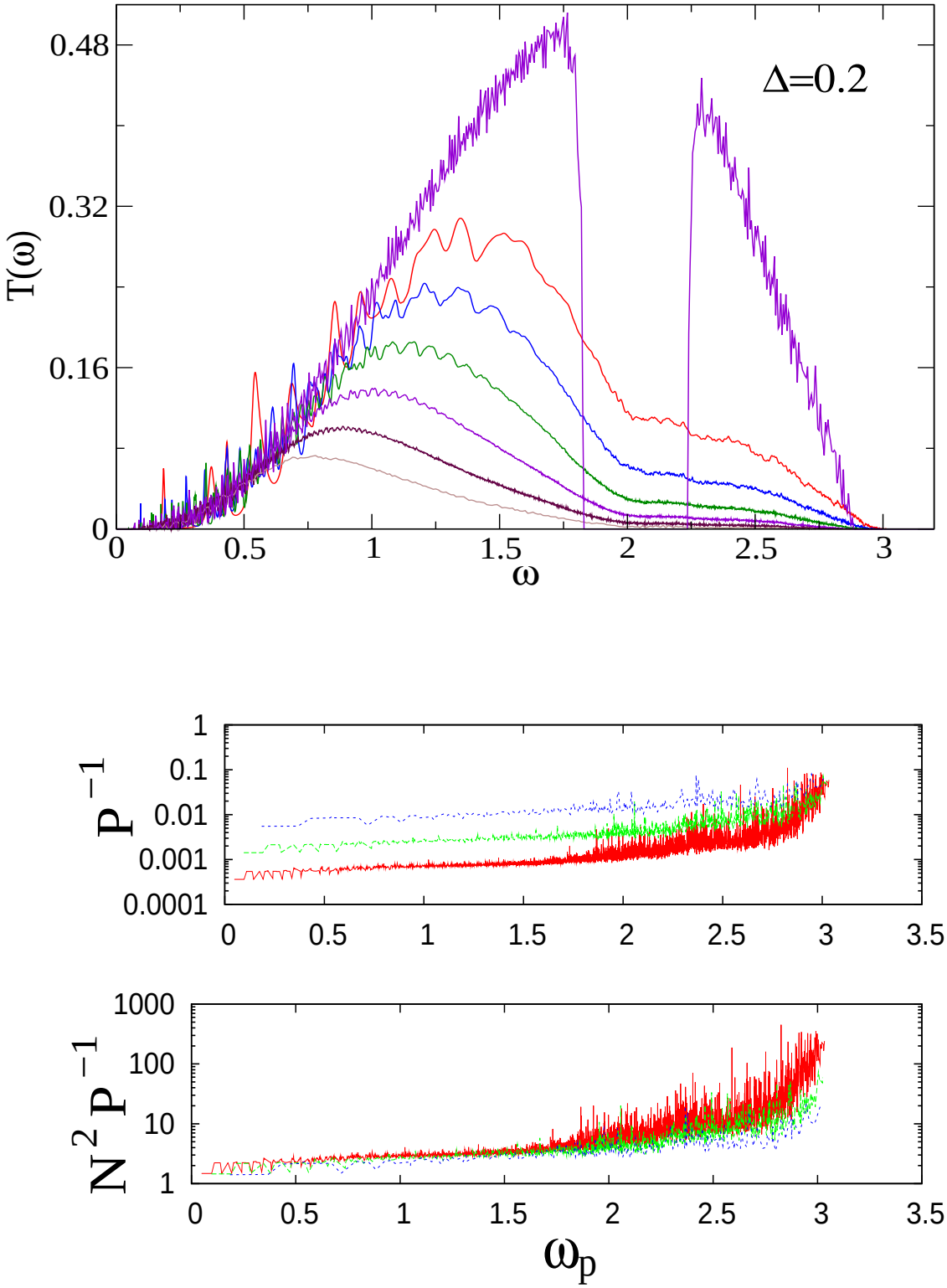

Figure 3.7: $2D$ unpinned case with fixed BC for $\Delta = 0.2$. TOP: Plot of the disorder averaged transmission $T(\omega)$ versus ω. The upper-most curve corresponds to a binary-mass ordered lattice with $N = 128$ while the remaining curves (from top to bottom) correspond to square lattices with $N = 16, 32, 64, 128, 256, 512$ respectively. BOTTOM: Plot shows the IPR (P^{-1}) and scaled IPR ($N^2 P^{-1}$) as a function of normal mode-frequency ω_p. The curves are for $N = 16$ (blue), 32 (green) and 64 (red).

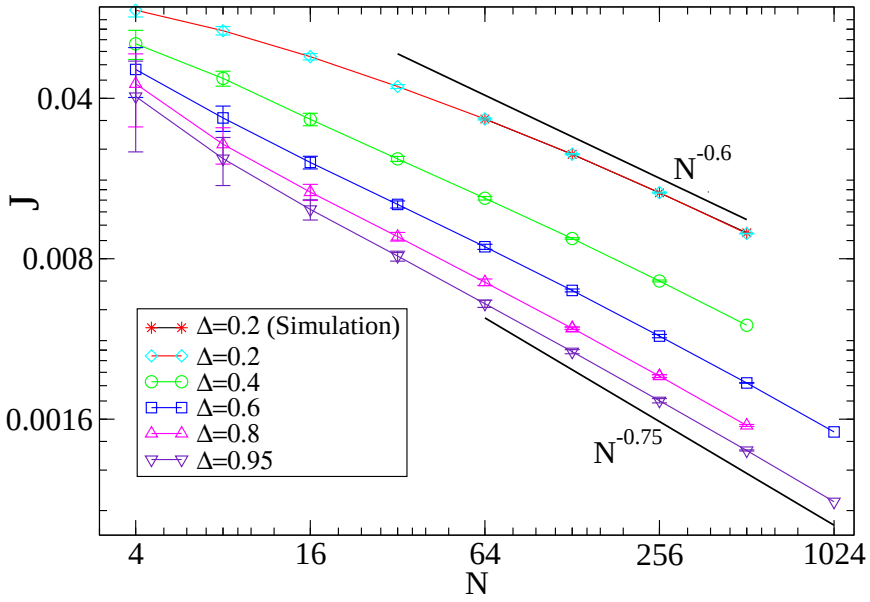

Figure 3.8: $2D$ unpinned lattice with fixed BC. Plot of disorder-averaged current J versus system size for different values of Δ. The error-bars show the actual standard deviations from sample-to-sample fluctuations. Numerical errors are much smaller. For $\Delta = 0.2$, simulation data is also plotted.

However with increasing disorder we see that this value changes and seems to settle to around $\mu \approx 0.75$. It seems reasonable to expect (though we have no rigorous arguments) that there is only one asymptotic exponent and for small disorder one just needs to go to very large system sizes to see the true value. In Fig. (3.9) we show temperature profiles obtained from simulations for lattices of different sizes with $\Delta = 0.2$. The jumps at the boundaries indicate that the asymptotic size limit has not yet been reached. This is consistent with our result that the exponent μ obtained at $\Delta = 0.2$ is different from what we believe is the correct asymptotic value (obtained at larger values of Δ). We do not have temperature plots at strong disorder where simulations are difficult.

Thus contrary to the arguments in Sec. (3.4) which predicted $J \sim (\ln N)^{-1/2} N^{-1}$ we find a much larger current scaling as $J \sim N^{-0.75}$. It is possible that one needs to go to larger system sizes to see the correct scaling.

Free BC: In this case from the arguments in Sec. (3.4) we expect ballistic states to contribute most significantly to the current density giving $J \sim N^{-2/3}$.

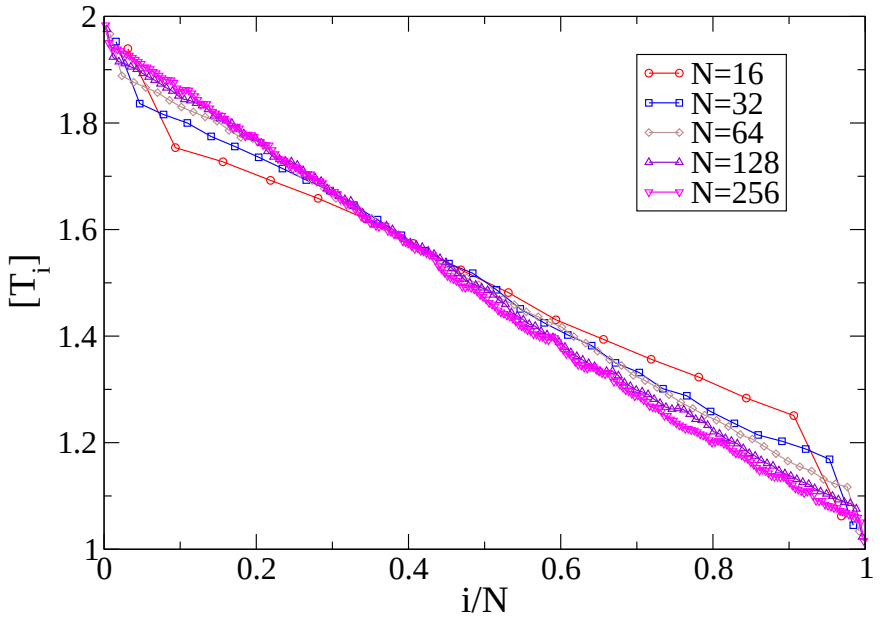

Figure 3.9: $2D$ unpinned case with fixed BC for $\Delta = 0.2$. Plot of disorder-averaged temperature profile $[T_i]$ for different system sizes obtained from simulations.

In Figs. (3.10,3.11) we plot the disorder averaged transmission coefficient for $\Delta = 0.8$ and $\Delta = 0.2$ for different system sizes. Qualitatively these results look very similar to those for fixed boundaries. However transmission is now significantly larger in the region of extended states. The behaviour at frequencies $\omega \to 0$ is also different and we now find $T(\omega) \sim \omega$ in contrast to $T(\omega) \sim \omega^3$ for fixed boundaries. From the plots of IPRs in Fig. (3.10) we note that there is not much qualitative difference with the fixed boundary plots except in the low frequency region.

The system size dependence of the disorder averaged current J for two different values of Δ is shown in Fig. (3.12). For $\Delta = 0.2$ we get an exponent $\mu \approx 0.5$ while for the stronger disorder case $\Delta = 0.8$ we see a different exponent $\mu \approx 0.6$. Again we believe that the strong disorder value of $\mu = 0.6$ is closer to the value of the true asymptotic exponent. This value is close to the expected $\mu = 2/3$ for free BC and significantly different from the value obtained for fixed BC ($\mu \approx 0.75$). Thus the dependence of the value of μ on boundary conditions exists even in the $2D$ case.

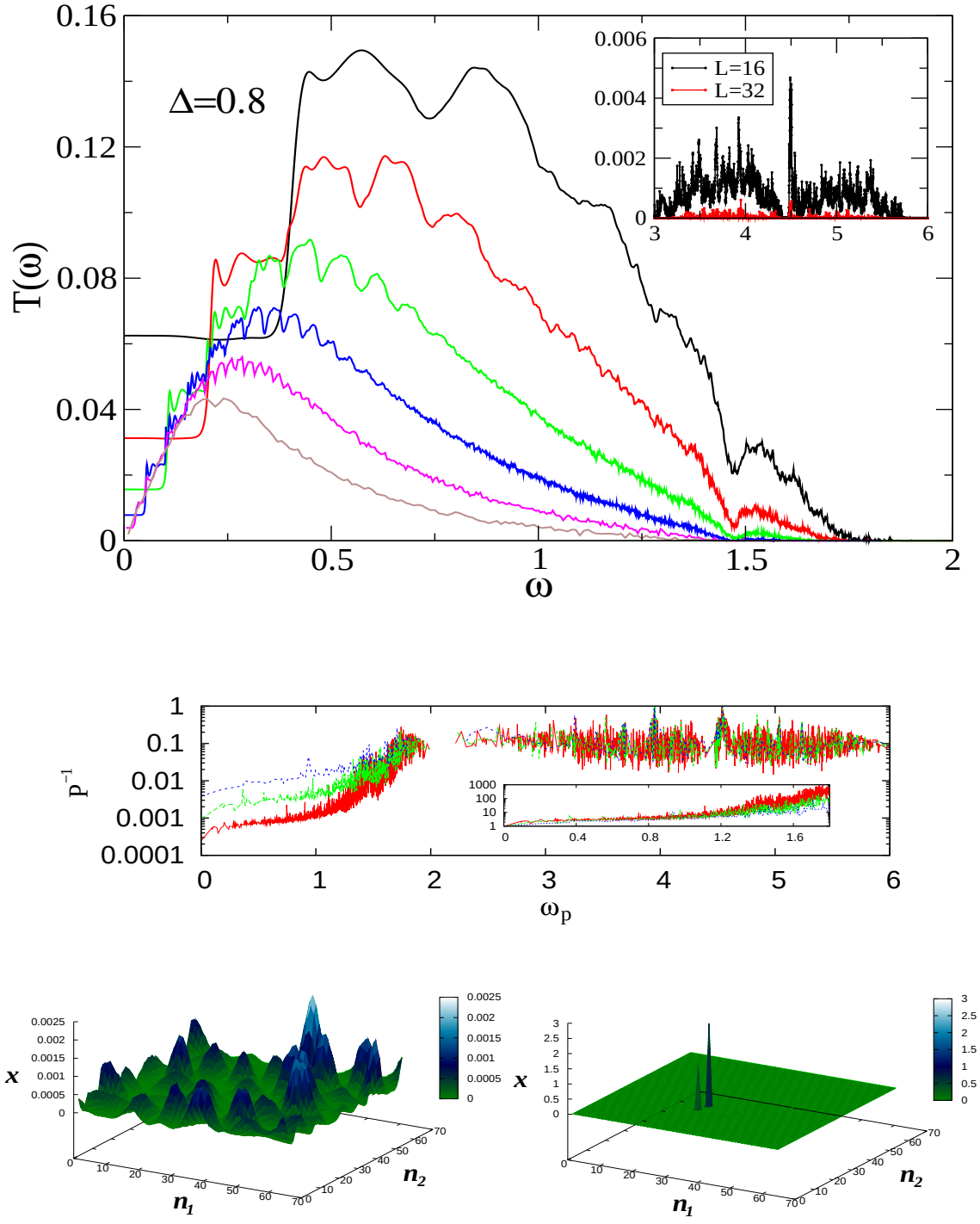

Figure 3.10: $2D$ unpinned case with free BC for $\Delta = 0.8$. TOP: Plot of the disorder averaged transmission $T(\omega)$ versus ω. The various curves (from top to bottom) correspond to square lattices with $N = 16, 32, 64, 128, 256, 512$ respectively. We see that transmission takes place in a small band $\approx (0-2)$ of the full range $\approx (0-6)$ of normal modes and, as can be seen in the inset, is negligible elsewhere. BOTTOM: Plot shows the IPR (P^{-1}) as a function of normal mode-frequency ω_p. The curves are for $N = 16$ (blue), 32 (green) and 64 (red). In the inset we plot $N^2 P^{-1}$ and the collapse at low frequencies shows that low frequency modes are extended. Also shown are two typical normal modes for one small (left) and one large value of P^{-1} for $N = 64$.

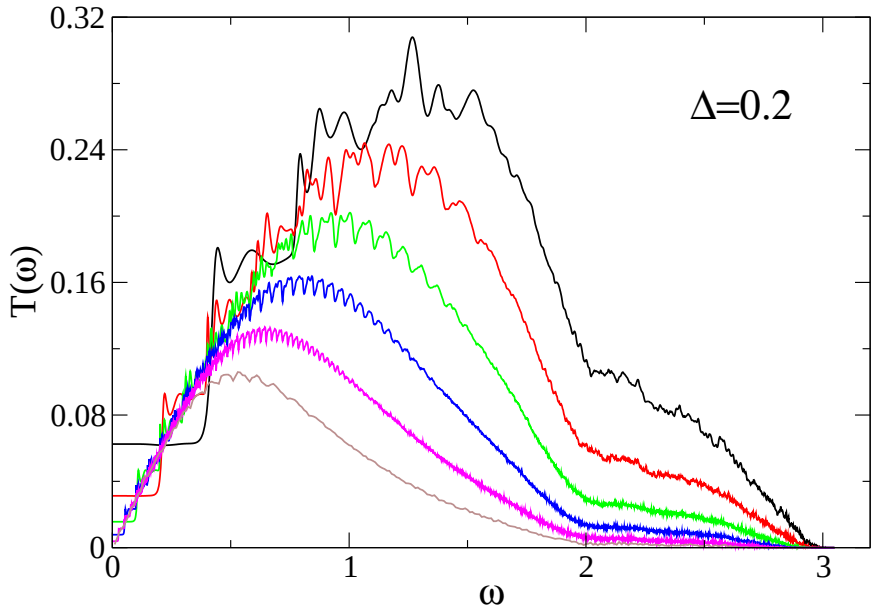

Figure 3.11: $2D$ unpinned case with free BC for $\Delta = 0.2$. Plot of the disorder averaged transmission $T(\omega)$ versus ω. The curves (from top to bottom) are for $N = 16, 32, 64, 128, 256, 512$ respectively. Note the linear form at small ω.

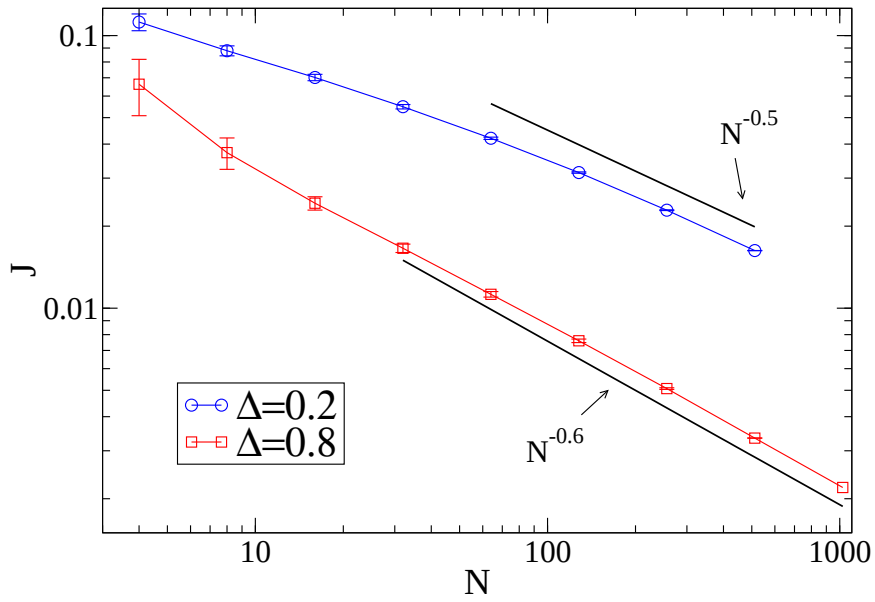

Figure 3.12: $2D$ unpinned case with free BC. Plot of disorder-averaged current J versus system size for two different values of Δ. The error-bars show standard devations due to sample-to-sample fluctuations. Numerical errors are much smaller.

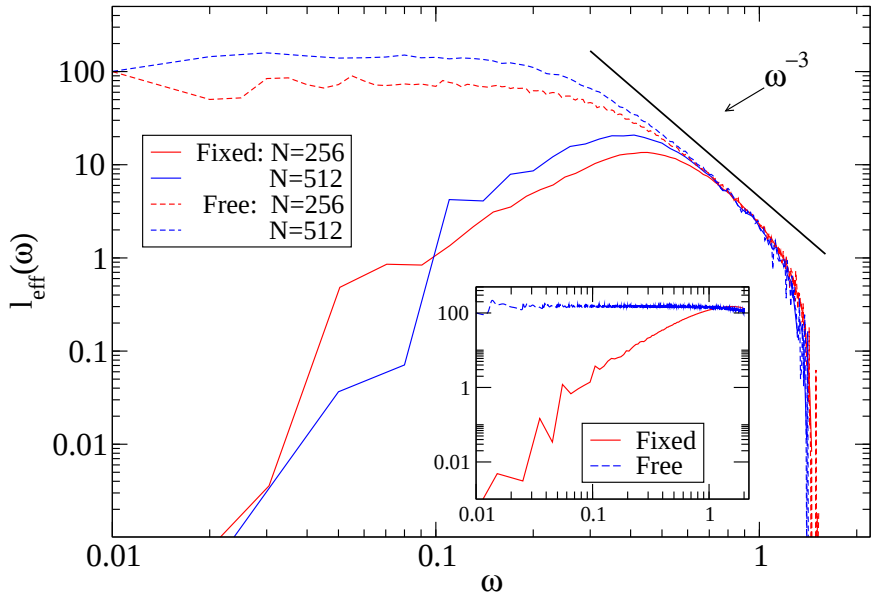

Figure 3.13: Plot of the effective mean-free path $l_{\text{eff}} = NT(\omega)/\omega^{d-1}$ in $2D$ with $\Delta = 0.8$. The insets show ℓ_{eff} for the ordered lattices with a single mass. An ω^{-3} behaviour is observed in a small part of the diffusive region.The fixed BC data is highly oscillatory and has been smoothed.

For the case of free BCs, we find that the values of $T(\omega)$ in the diffusive regime matches with those for fixed BCs but are completely different in the ballistic regime. This is seen in Fig. (3.13) where we plot the effective mean free path $l_{\text{eff}}(\omega) = NT(\omega)/w^{d-1}$ in the low-frequency region [this is obtained by comparing Eq. (2.55) with the kinetic theory expression for conductivity Eq. (3.2)]. For free BC, l_{eff} is roughly consistent with the kinetic theory prediction $l_{\text{eff}}^{-1} \sim N^{-1} + \ell_K{}^{-1}(\omega)$ but the behaviour for fixed BC is very different. The inset of Fig. (3.13) plots l_{eff} for the equal mass ordered case and we find that in the ballistic regime it is very close to the disordered case, an input that we used in the heuristic derivation. The numerical data also confirms that for small ω, $T(\omega) \sim \omega$ for free BCs and as ω^3 for fixed BCs. The transmission for fixed BC shows rapid oscillations which increase with system size, and arise from scattering and interference of waves at the interfaces.

3.5.1.2 Disordered $2D$ lattice with pinning

We now study the effect of introducing a harmonic pinning potential at all sites of the lattice. It is expected that this will cut off low frequency modes and hence one should see strong

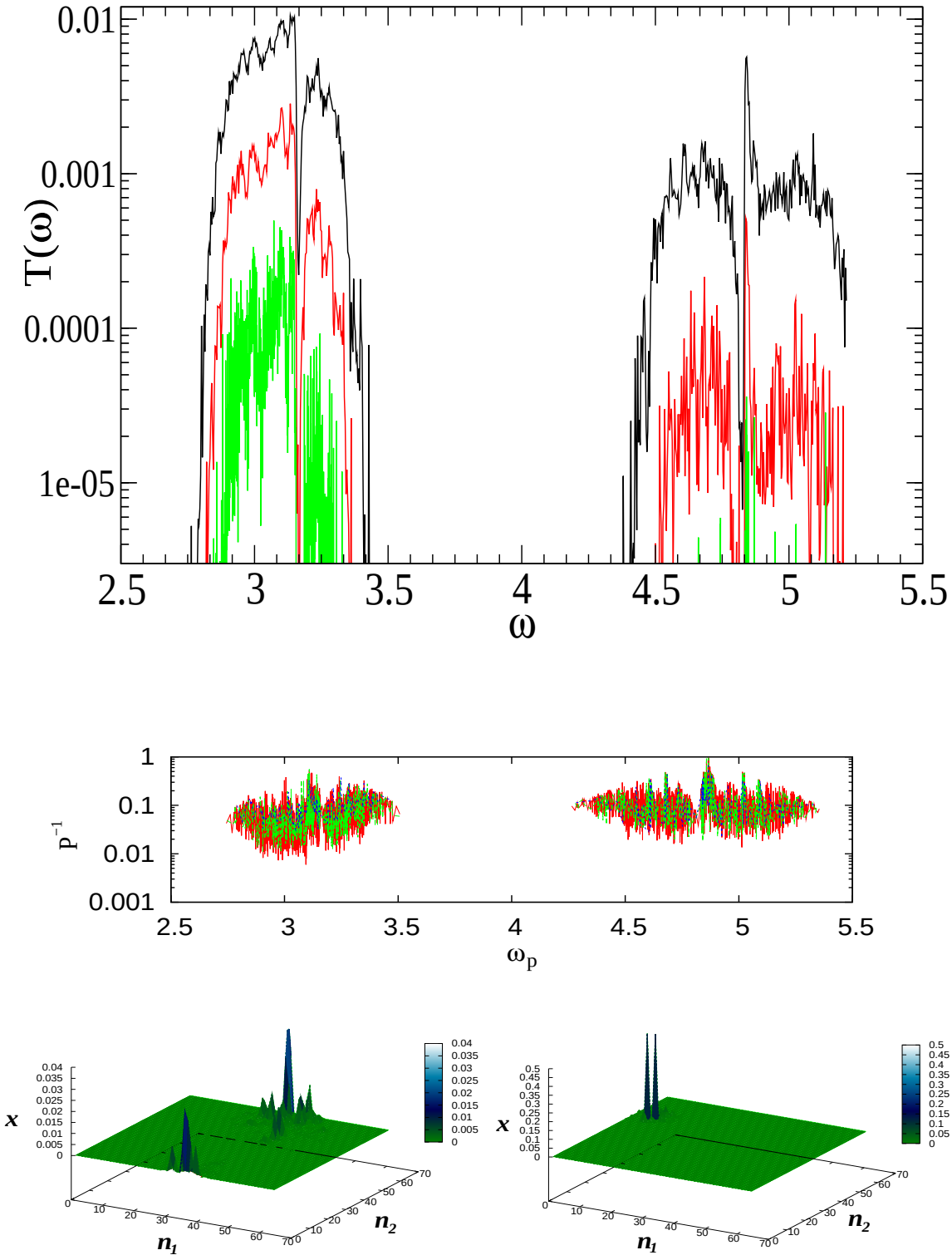

Figure 3.14: $2D$ pinned case for $\Delta = 0.4$ and $k_o = 10.0$. TOP: Plot of the disorder averaged transmission $T(\omega)$ versus ω. The various curves (from top to bottom) correspond to lattices with $N = 16, 32, 64$ respectively. Here we choose $\gamma = \sqrt{10}$. BOTTOM: Plot of the IPR (P^{-1}) as a function of normal mode-frequency ω_p. The curves are for $N = 16$ (blue), 32 (green) and 64 (red). Also shown are two typical normal modes for one small (left) and one large value of P^{-1} for $N = 64$.

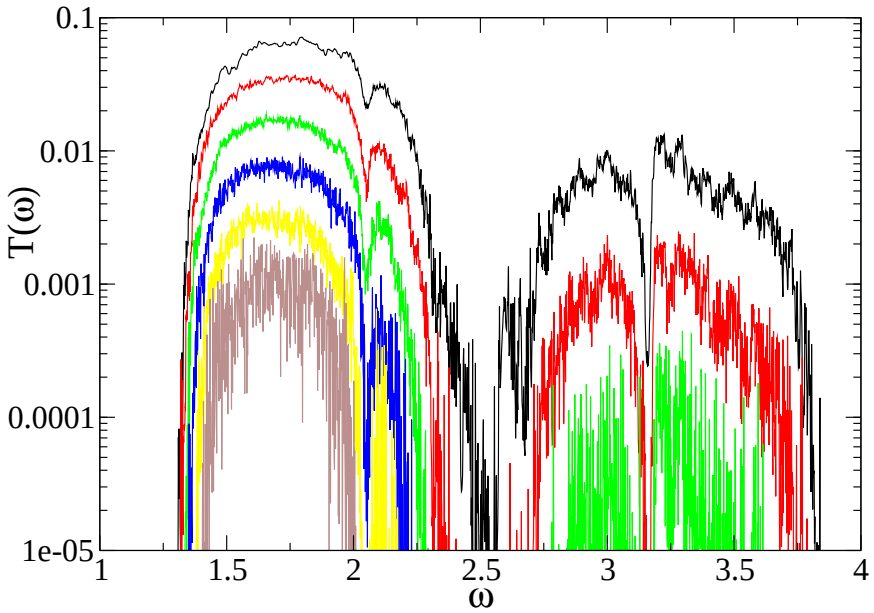

Figure 3.15: $2D$ pinned case for $\Delta = 0.4$ and $k_o = 2.0$. Plot of the disorder averaged transmission $T(\omega)$ versus ω . The various curves (from top to bottom) are for $N = 16, 32, 64, 128, 256, 512$ respectively. Here we choose $\gamma = \sqrt{2}$.

localization effects. The localization length ℓ will decrease both with increasing Δ and increasing k_o (in $1D$, heuristic arguments give $\ell \sim 1/(\Delta^2 k_o)$ [21]). In Figs. (3.14,3.15) we plot the transmission coefficients for two cases with on-site potentials $k_o = 10.0$ and $k_o = 2.0$ respectively, and $\Delta = 0.4$. We also plot the IPR in Fig. (3.14). Unlike in the unpinned case we now find that the transmission coefficients are much smaller and fall more rapidly with system size.

From the plot of P^{-1} we find that for all the modes, the value of P^{-1} does not change much with system size which implies that all modes are localized. The allowed frequency bands correspond to the transmission bands. The two wavefunctions plotted in Fig. (3.14) correspond to one relatively small and one large P^{-1} value and clearly show that both states are localized.

The system size dependence of the integrated current is shown in Fig. (3.16) for the two parameter sets. The values of $\mu \approx 1.6,\ 3.65$ for the two sets indicate that at large enough length scales one will get a current falling exponentially with system size and hence we

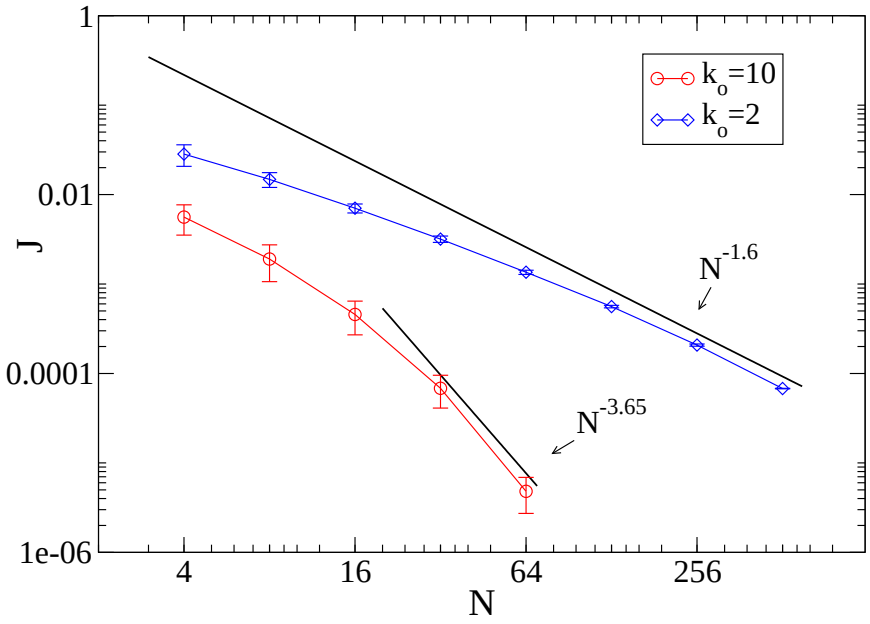

Figure 3.16: $2D$ pinned case for $\Delta = 0.4$. Plot of disorder-averaged current J versus system size for two different values of k_o. Error bars show standard deviation due to disorder and numerical errors are much smaller. Note that the standard deviation do not decrease with system size for higher k_o.

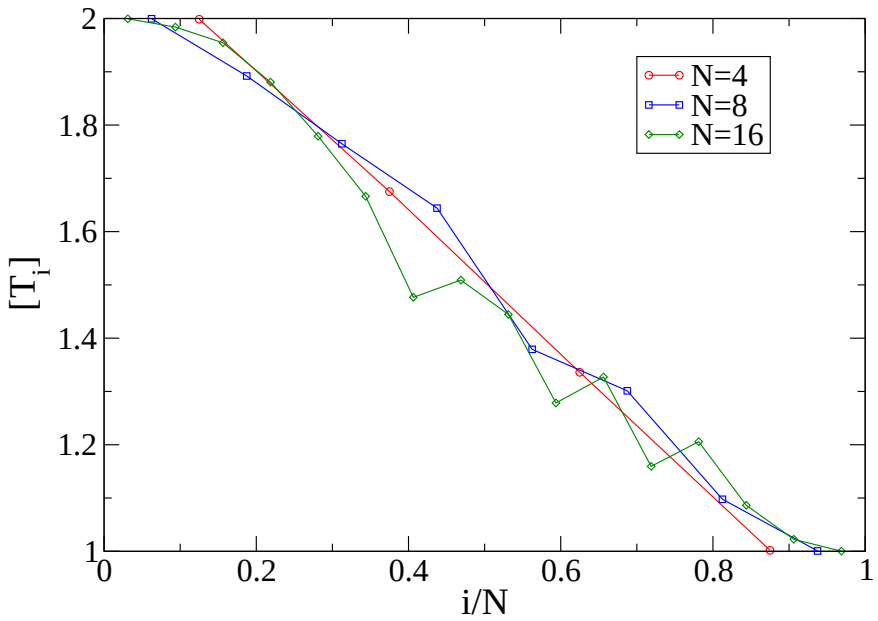

Figure 3.17: $2D$ pinned case for $\Delta = 0.4$ and $k_o = 10.0$. Plot of disorder-averaged temperature profile $[T_i]$ for different system sizes. The plots are from simulations and here we choose $\gamma = \sqrt{10}$.

have an insulating phase. In Fig. (3.17) we plot the temperature profiles for the set with $\Delta = 0.4, k_o = 10.0$. In this case it is difficult to obtain steady state temperature profiles from simulations for larger system sizes. The reason is that the temperature (unlike current) gets contributions from all modes (both localized and extended) and equilibrating the localized modes takes a long time.

3.5.2 Results in three dimensions

In this section we mostly consider $N \times N \times N$ lattices with periodic boundary conditions in the $\nu = 2, 3$ directions. Some results for $N \times N_2 \times N_3$ lattices with $N_2 = N_3 < N$ will also be described. Preliminary results for the case of free BCs are given and indicate that there is no dependence of the exponent μ on BCs. It is not clear to us whether this is related to the boundedness of the fluctuations in $x_{\mathbf{n}}$ and the decay of the correlations between $x_{\mathbf{n}}$ and $x_{\mathbf{l}}$ (like $|\mathbf{n} - \mathbf{l}|^{-1}$) in $d = 3$ and their growth (with N) in $d < 3$.

3.5.2.1 Disordered $3D$ lattice without pinning

Fixed BC: we have used both the numerical approach and simulations for sizes up to $32 \times 32 \times 32$ for which we have data for $T(\omega)$. For larger systems the matrices become too big and we have not been able to use the numerical approach. Hence, for larger system sizes we have only performed simulations, including some on $N \times N_2 \times N_2$ lattices. For these cases only the current J is obtained. The number of averages varies from over 100 samples for $N = 16$ to two samples for $N = 64$. In Figs. (3.18,3.19) we plot the disorder averaged transmission coefficient for two different disorder strengths, $\Delta = 0.8$ and $\Delta = 0.2$, for different system sizes. The corresponding plots of IPRs as a function of normal mode frequency ω_p, for single disorder realizations, are also given. From the IPR plots we get an idea of the typical range of allowed normal mode frequencies and their degree of localization. Low IPR values which scale as N^{-3} imply extended states while large IPR values which do not change much with system size denote localized states.

From Figs. (3.18,3.19) we make the following observations.

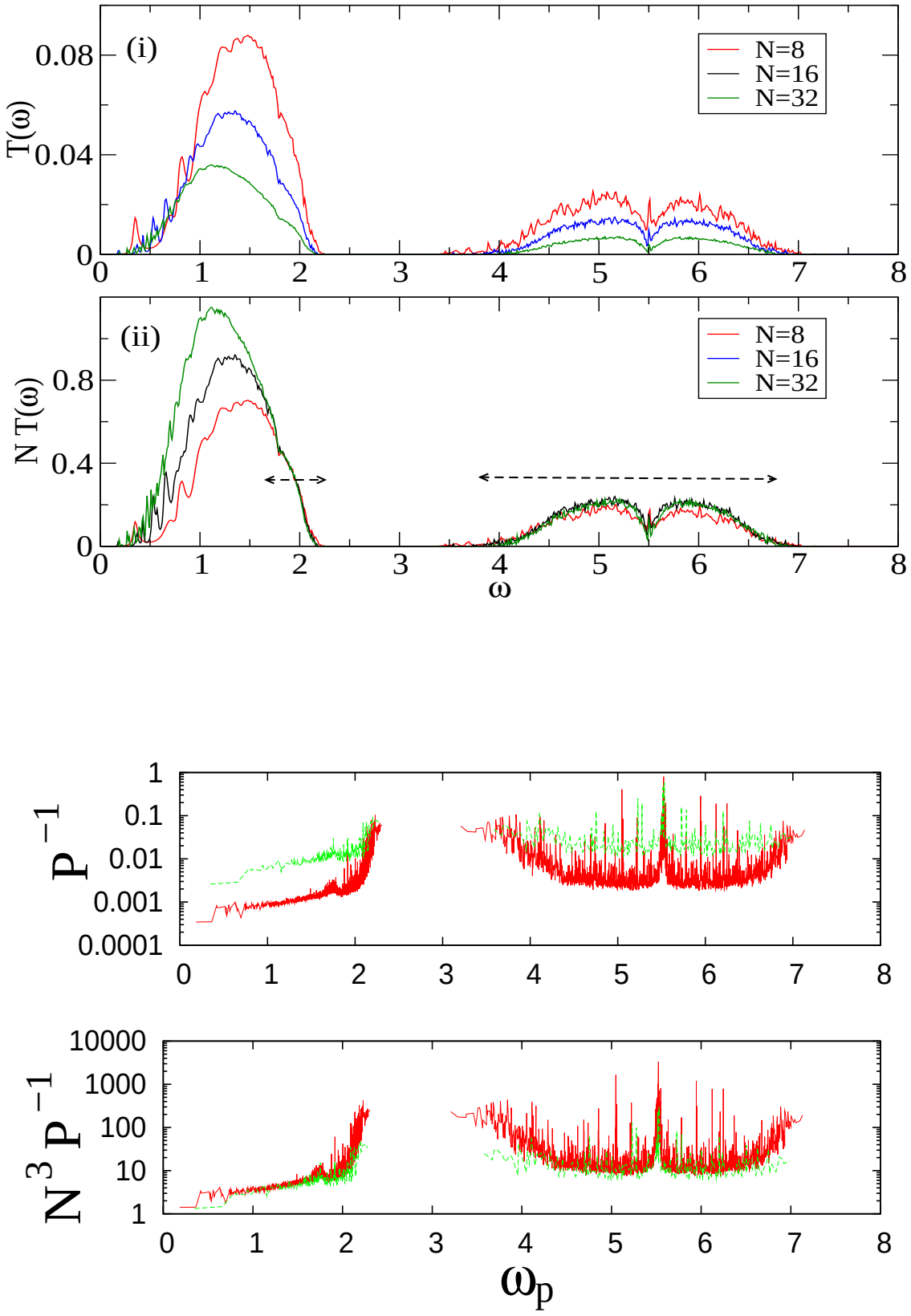

Figure 3.18: $3D$ unpinned case with fixed BC for $\Delta = 0.8$. TOP: Plot of the disorder averaged transmission $T(\omega)$ versus ω. The inset shows the same data multiplied by a factor of N. BOTTOM: Plot of the IPR (P^{-1}) and scaled IPR ($N^3 P^{-1}$) as a function of normal mode-frequency ω_p for a fixed disorder-realization. The curves are for $N = 8$ (green) and 16 (red).

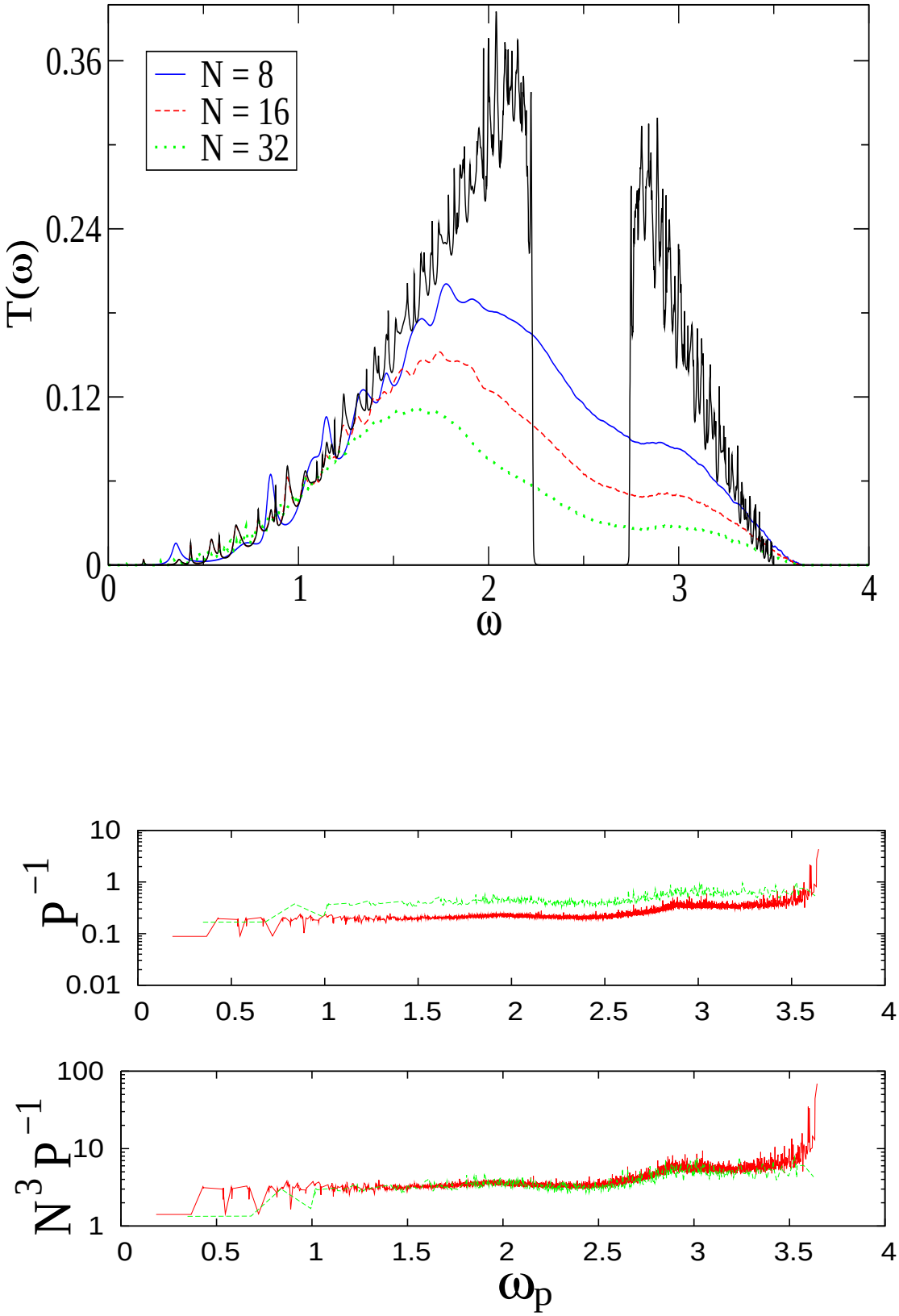

Figure 3.19: $3D$ unpinned case with fixed BC for $\Delta = 0.2$. TOP: Plot of the disorder averaged transmission $T(\omega)$ versus ω. The uppermost curve is the transmission curve for the binary mass ordered lattice for $N = 16$. BOTTOM: Plot of IPR (P^{-1}) and scaled IPR ($N^3 P^{-1}$) as a function of normal mode-frequency ω_p for a fixed disorder realization. The curves are for $N = 8$ (green) and 16 (red).

(i) From the $3D$ data it is clear that the effect of localization is weaker than in $1D$ and $2D$. Both for $\Delta = 0.2$ and $\Delta = 0.8$ we find that there is transmission over almost the entire range of frequencies of the allowed normal modes. From the IPR plots we see that for $\Delta = 0.2$ most states are extended except for a small region in the high frequency band-edge. For $\Delta = 0.8$ the allowed modes form two bands and one finds significant transmission over almost the full range. At the band edges (except the one at $\omega = 0$) there are again localized states. It also appears that there are some large IPR states interspersed within the high frequency band. As in the $2D$ case and unlike the $1D$ case, the frequency range over which transmission takes place does not change with system size, only the overall magnitude of transmission coefficient changes.

(ii) The plot of $NT(\omega)$ in Fig. (3.18) shows the nature of the extended states. The high frequency band and a portion of the lower frequency band have the scaling $T(\omega) \sim N^{-1}$ and hence correspond to diffusive states. In the lower-frequency band the fraction of diffusive states seems to be increasing with system size but it is difficult to verify the $\omega_c^K \sim N^{-1/4}$ scaling. The ballistic nature of the low-frequency states is confirmed in Fig. (3.19) where we see that $T(\omega)$ for the binary-mass ordered and disordered lattices match for small ω [with a $T(\omega) \sim \omega^4$ dependence].

In Fig. (3.20) we show the system size dependence of the disorder averaged current density J for the two cases with weak disorder strength ($\Delta = 0.2$) and strong disorder strength ($\Delta = 0.8$). The results for cubic lattices of sizes up to $N = 32$ are from the numerical method while the results for larger sizes are from simulations. We find an exponent $\mu \approx 0.6$ at small disorder and $\mu \approx 0.75$ at large disorder strength. As in the $2D$ case here too we believe that at small disorder, the asymptotic system size limit will be reached at much larger system sizes and that the exponent obtained at large disorder strength is probably close to the true asymptotic value. The value ($\mu = 0.75$) does not agree with the prediction ($J \sim N^{-1}$) made from the heuristic arguments in Sec. (3.4). A study of larger system sizes is necessary to confirm whether or not the asymptotic size limit has been reached.

The data point at $N = 128$ for the set with $\Delta = 0.2$ in Fig. (3.20) actually corresponds to

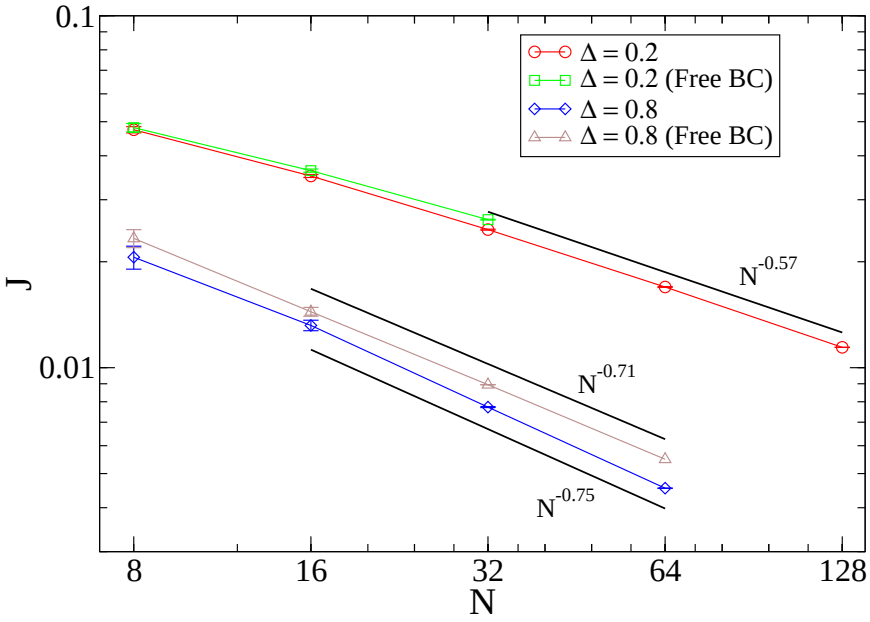

Figure 3.20: $3D$ unpinned case with fixed and free BCs. Plot of disorder-averaged current J versus system size for two different values of Δ. The data for $\Delta = 0.2$ is from simulations. The error-bars show standard deviations due to disorder and numerical errors are smaller.

a lattice of dimensions $128 \times 48 \times 48$ and we believe that the current value is very close to the expected fully $3D$ value. To see this point, we have plotted in Fig. (3.21) results from nonequilibrium simulations with $N \times N_2 \times N_2$ lattices with $N_2 \leq N$.

Finally, in Fig. (3.22) we show temperature profiles (for single disorder realizations) obtained from simulations for lattices of different sizes and with $\Delta = 0.2$. The jumps at the boundaries again indicate that the asymptotic system size limit has not been reached even at the largest size.

Free BC: In this case from the arguments in Sec. (3.4) we expect ballistic states to contribute most significantly to the current density giving $J \sim N^{-3/4}$.

In Fig. (3.23) we plot the disorder averaged transmission coefficient for $\Delta = 0.8$ for different system sizes. The transmission function is very close to that for the fixed boundary case except in the frequency region corresponding to non-diffusive states. At $\omega \to 0$ we now expect, though it is hard to verify from the data, that $T(\omega) \sim \omega^2$ in contrast to $T(\omega) \sim \omega^4$ for

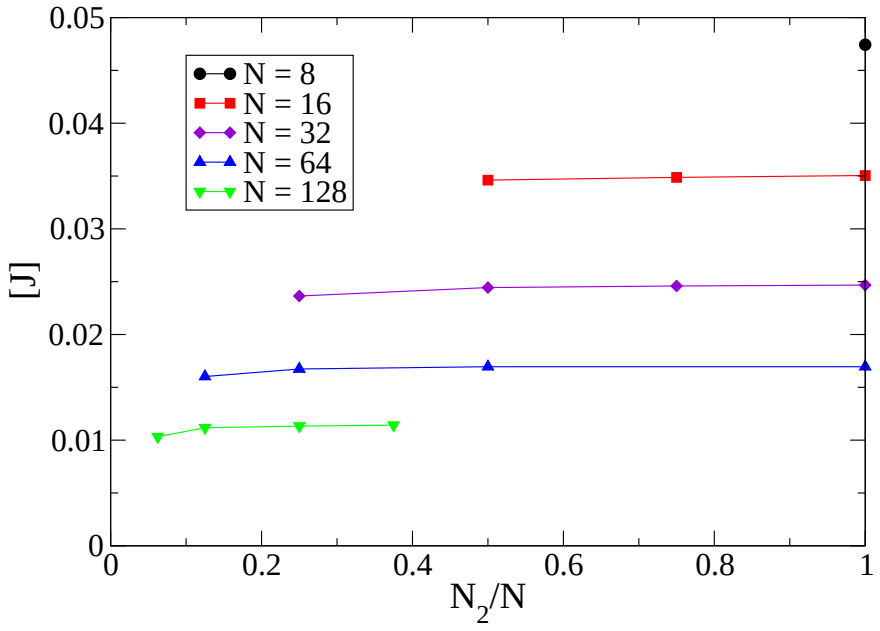

Figure 3.21: $3D$ unpinned case with fixed BC for $\Delta = 0.2$. Plot of disorder-averaged current density J (with the definition $J = I/N_2^2$) versus N_2/N for different fixed values of N. We see that the 3D limiting value is reached at quite small values of N_2/N.

fixed boundaries.

The system size dependence of the disorder averaged current J for two different values of Δ is shown in Fig. (3.20). We find that the current values are quite close to the fixed BC case and the exponent obtained at the largest system size studied for this case is $\mu \approx 0.71$. This value is close to the expected $\mu = 3/4$ for free BC.

We now compare the transmission coefficient for free and fixed BCs in the ballistic regime. This is plotted in Fig. (3.24) where we show the effective mean free path $l_{\rm eff}(\omega) = NT(\omega)/w^{d-1}$ in the low-frequency region. As in the $2D$ case we again find that for free BCs, $l_{\rm eff}$ is roughly consistent with the kinetic theory prediction $l_{\rm eff}^{-1} \sim N^{-1} + {\ell_K}^{-1}(\omega)$ and the behaviour for fixed BCs is very different. The inset of Fig. (3.24) plots $l_{\rm eff}$ for the equal mass ordered case and we find that in the ballistic regime it is very close to the disordered case. The numerical data confirms the input in our theory on the form of $T(\omega)$ for small ω, *i.e.* $T(\omega) \sim \omega^2$ for free BCs and as ω^4 for fixed BCs. The transmission for fixed BC shows rapid oscillations which increase with system size, and arise from scattering and

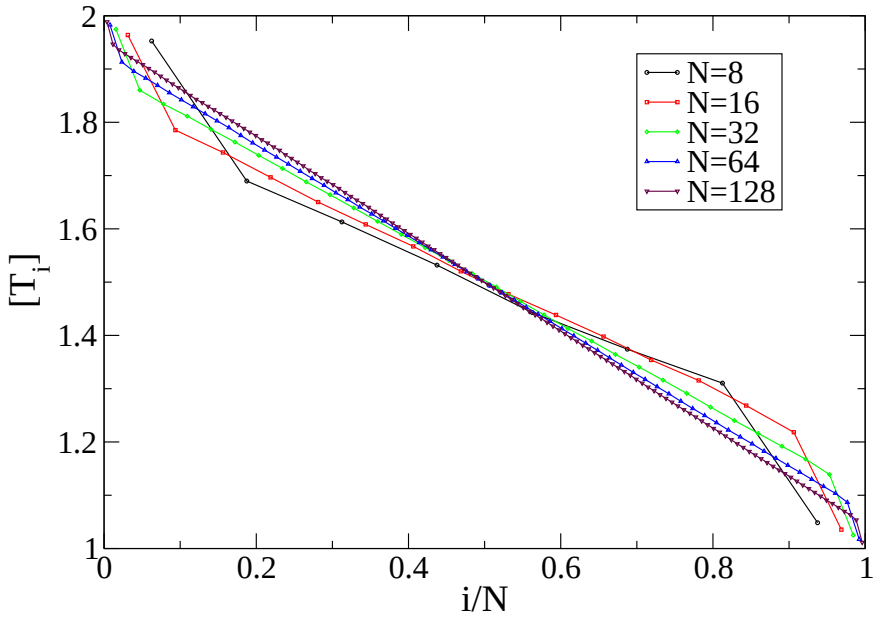

Figure 3.22: $3D$ unpinned case with fixed BC for $\Delta = 0.2$. Plot of temperature profile T_i in a single disorder realization for different system sizes. The plots are from simulations.

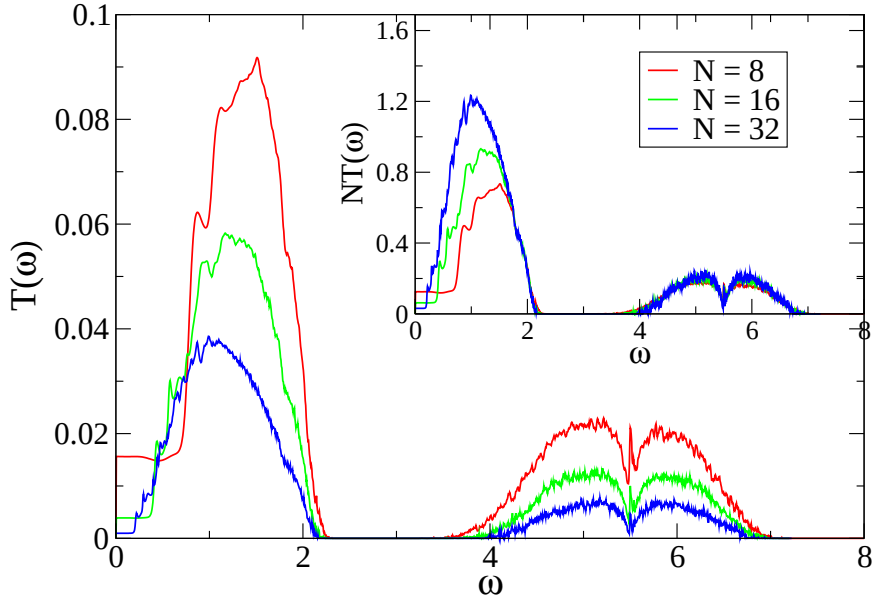

Figure 3.23: $3D$ unpinned case with free BC for $\Delta = 0.8$. Plot of the disorder averaged transmission $T(\omega)$ versus ω. The inset shows the same data multiplied by a factor of N.

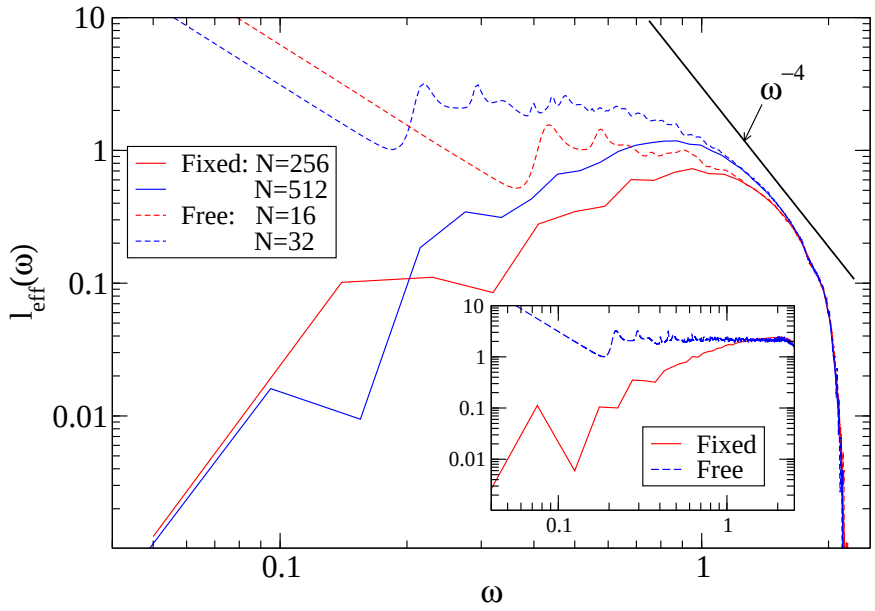

Figure 3.24: Plot of the effective mean-free path $l_{\text{eff}} = NT(\omega)/\omega^{d-1}$ in $3D$ with $\Delta = 0.8$ for fixed and free BCs. The insets show ℓ_{eff} for the ordered system with a single mass. An ω^{-4} behaviour is observed in a small part of the diffusive region.The fixed BC data is highly oscillatory and has been smoothed.

interference of waves at the interfaces.

3.5.2.2 Disordered $3D$ lattice with pinning

For the pinned case, we again use both the numerical method and simulations for sizes up to $N = 32$. For $N = 64$ only nonequilibrium simulation results are reported.

In Figs. (3.25,3.26) we plot the disorder averaged transmission coefficient for $\Delta = 0.2$ and $\Delta = 0.8$ with $k_o = 10.0$. The corresponding IPRs P^{-1} and scaled IPRs N^3P^{-1} are also shown.

From the IPR plots we notice that the spectrum of the $3D$ disordered pinned chain has a similar interesting structure as in the $2D$ case with two bands and a gap which is seen at strong disorder. However unlike the $2D$ case where all states were localized, here the IPR data indicates that most states except those at the band edges are diffusive. We see localized states at the band edges and also there seem to be some localized states interspersed among the extended states within the bands. The insets in Figs. (3.25,3.26) show that there is a reasonable N^{-1} scaling of the transmission data in most of the transmitting region. This is clearer at larger system sizes. Thus, unlike the unpinned case where low frequency extended

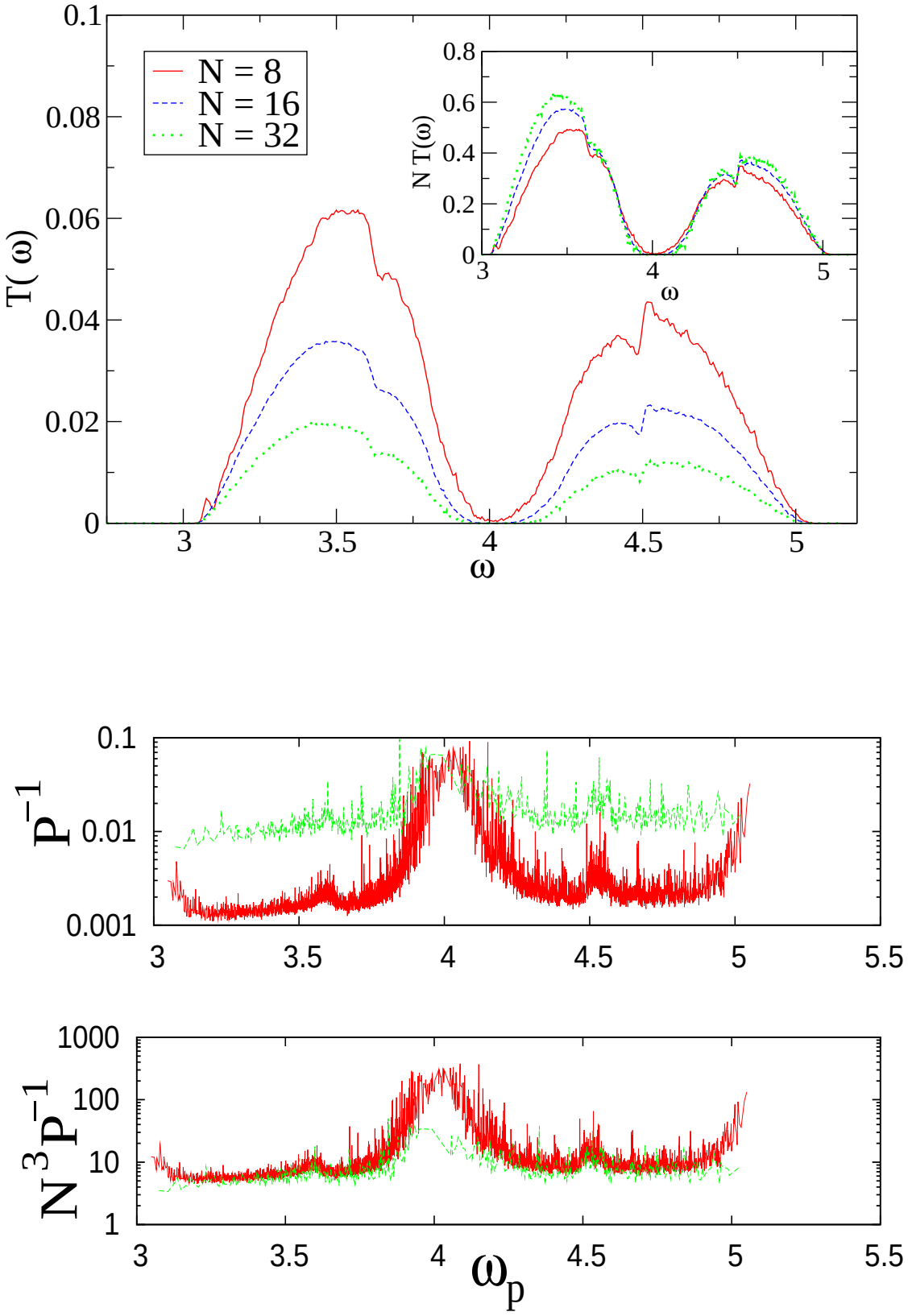

Figure 3.25: $3D$ pinned case for $\Delta = 0.2$ and $k_o = 10.0$. TOP: Plot of the disorder averaged transmission $T(\omega)$ versus ω. BOTTOM: Plot of the IPR (P^{-1}) and scaled IPR (N^3P^{-1}) as a function of normal mode-frequency ω_p. The curves are for $N = 8$ (green) and 16 (red).

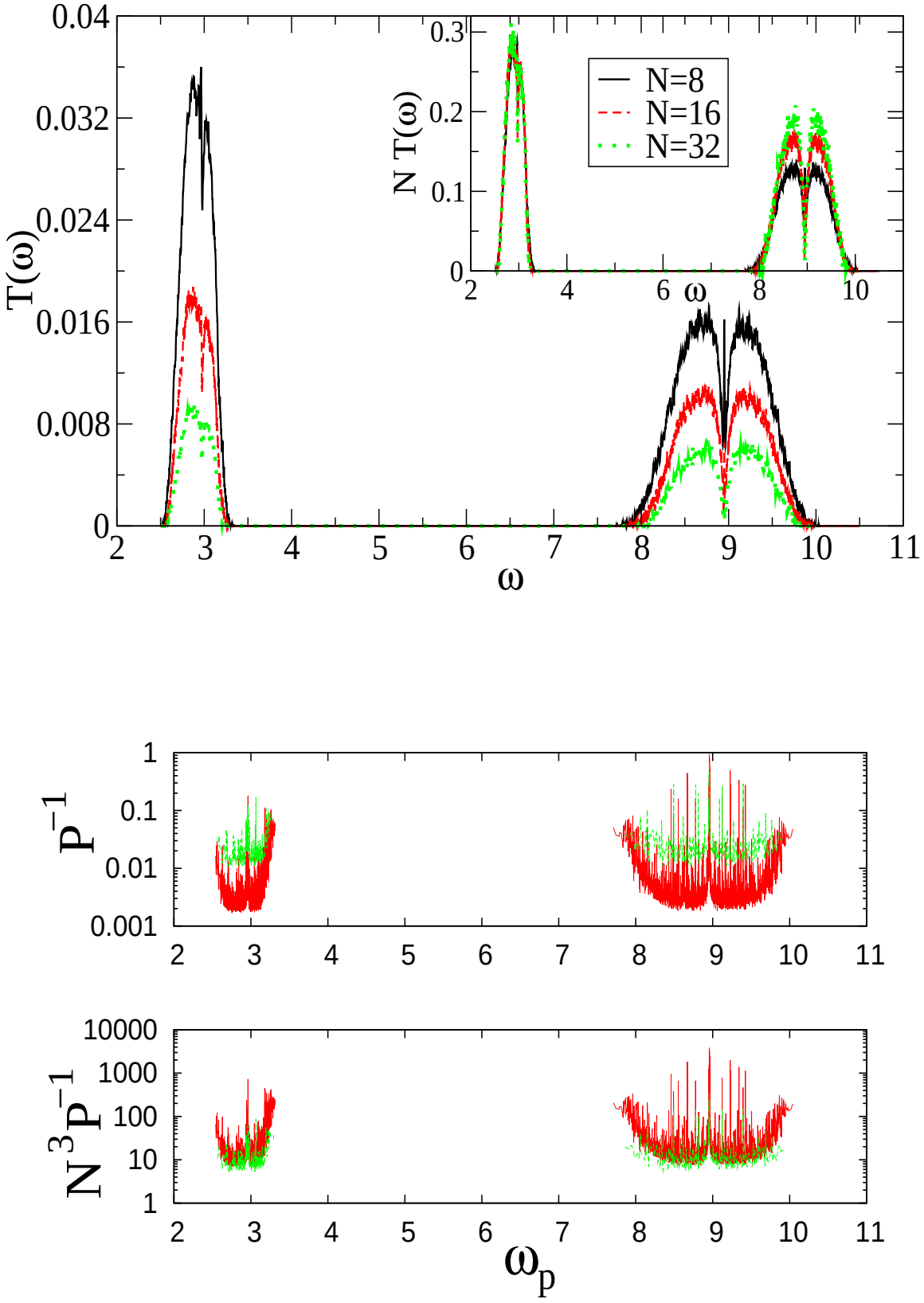

Figure 3.26: $3D$ pinned case for $\Delta = 0.8$ and $k_o = 10.0$. TOP: Plot of the disorder averaged transmission $T(\omega)$ versus ω. BOTTOM: Plot of the IPR (P^{-1}) and scaled IPR (N^3P^{-1}) as a function of normal mode-frequency ω_p. The curves are for $N = 8$ (green) and 16 (red).

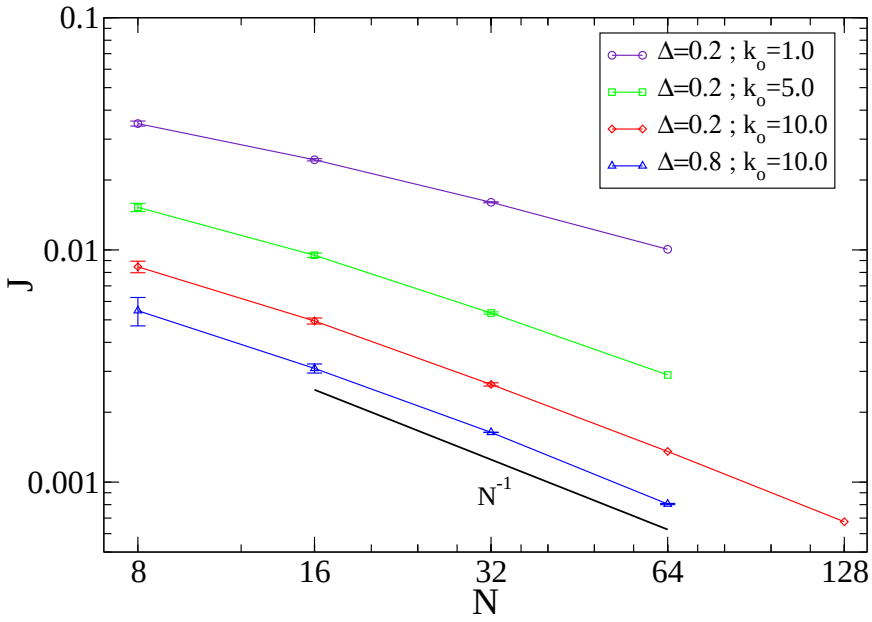

Figure 3.27: $3D$ pinned case. Plot of disorder-averaged current J versus system size for different values of k_o and Δ. The data sets for $\Delta = 0.2$ for different values of k_o are from simulations while the data for $\Delta = 0.8$ is from numerics.

states were ballistic or super-diffusive, here we find that there is no transmittance at small ($\omega \to 0$) frequencies and that all states are diffusive.

From the above discussion we expect Fourier's law to be valid in the $3D$ pinned disordered lattice. The system size dependence of the disorder averaged current J for different disorder strengths is plotted in Fig. (3.27). For all the parameter sets the exponent obtained is close to $\mu = 1$ corresponding to a finite conductivity and validity of Fourier's law. The temperature profiles plotted in Fig. (3.28) have small boundary temperature jumps and indicate that the asymptotic size limit has already been reached.

One might expect that at very strong disorder, all states should become localized and then one should get a heat insulator. The parameter set corresponding to Fig. (3.26) corresponds to strong disorder and for this we still find a significant fraction of extended states. Thus for the binary mass case it appears that there are always extended states. We have some results for the case with a continuous mass distribution (masses are chosen from a uniform distribution between $1-\Delta$ and $1+\Delta$). In this case we find that the effect of disorder is stronger

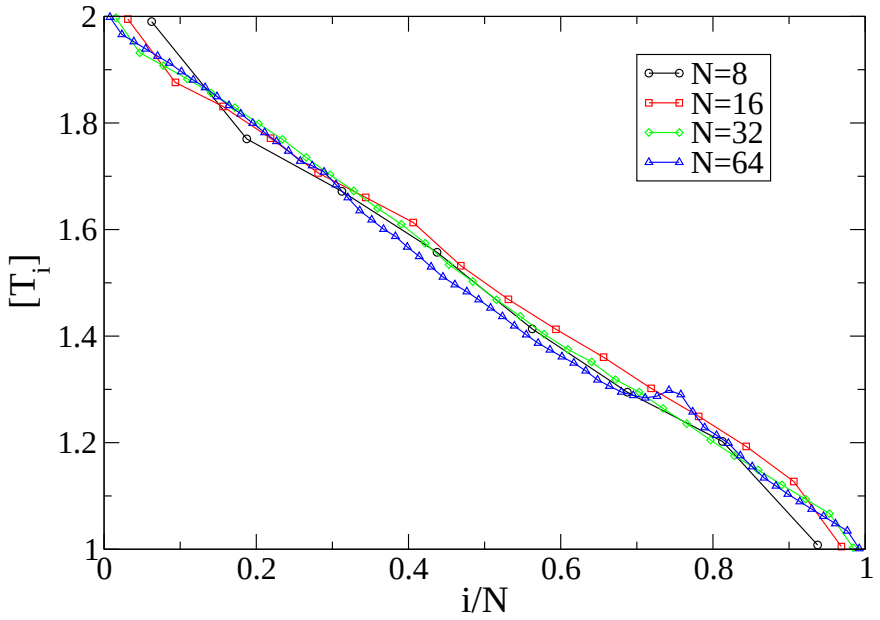

Figure 3.28: $3D$ pinned case for $\Delta = 0.2$ and $k_o = 10.0$. Plot of temperature profile T_i in a single disorder realization for different system sizes. The plots are from simulations.

and the transmission at all frequencies is much reduced compared to the binary mass case. However we cannot see the exponential decrease in transmission with system size and so it is not clear if an insulating behaviour is obtained. Further numerical studies are necessary to understand the asymptotic behaviour.

3.6 Conclusions

We have studied heat conduction in isotopically disordered harmonic lattices with scalar displacements in two and three dimensions. The main question addressed is the system size dependence of the heat current, which is computed using Green's function based numerical methods as well as nonequilibrium simulations. We have tried to understand the size dependence by looking at the phonon transmission function $T(\omega)$ and examining the nature of the energy transport in different frequency regimes. We also described a heuristic analytical calculation based on localization theory and kinetic theory and compared their predictions with our numerical and simulation results. This comparison is summarized in Table (3.1).

	$d = 2$		$d = 3$	
	Analytical	Numerical	Analytical	Numerical
Pinned	$\exp(-bN)$	$N^{-3.7}$	N^{-1}	$N^{-1.0}$
Fixed	$N^{-1}(\ln N)^{-1/2}$	$N^{-0.75}$	N^{-1}	$N^{-0.75}$
Free	$N^{-2/3}$	$N^{-0.6}$	$N^{-3/4}$	$N^{-0.71}$

Table 3.1: The table summarizes the main results. The numerical (and nonequilibrium simulation) results obtained are compared, in two and three dimensions, with the analytical predictions obtained from our heuristic arguments. The error bar for the numerically obtained exponent values is of the order ± 0.02. This error is estimated from the errors in the last few points of the J-versus-N data. NB: The system sizes used may well be far from asymptotic.

The most interesting findings of this work are:

(i) For the unpinned system we find that in $2D$ there are a large number of localized modes for which phonon transmission is negligible. In $3D$ the number of localized modes is much smaller. The extended modes are either diffusive or ballistic. Our analytic arguments show that the contribution of ballistic modes to conduction is dependent on BCs and is strongly suppressed for the case of fixed BCs, the more realistic case. In $3D$ this leads to diffusive modes dominating for large system sizes and Fourier's law is satisfied. Thus a finite heat conductivity is obtained for the $3D$ disordered harmonic crystal without the need of invoking anharmonicity as is usually believed to be necessary [77, 2]. This is similar to what one obtains when one adds stochasticity to the time evolution in the bulk as shown by [83]. Our numerical results verify the predictions for free BCs and we believe that much larger system sizes are necessary to verify the fixed BC results (this is also the case in $1D$ [19, 22]).

(ii) In two dimensions the pinned disordered lattice shows clear evidence of localization and we obtain a heat insulator with exponential decay of current with system size.

(iii) Our result for the $3D$ pinned disordered lattice provides the first microscopic verification of Fourier's law in a three dimensional system. For the binary mass distribution we do not see a transition to insulating behaviour with increasing disorder. For a continuous mass distribution we find that the current is much smaller (than the binary mass case with the same value of Δ) but it is not clear whether all states get localized and if an insulating phase

exists.

3.7 appendix

Kinetic theory: Kinetic theory becomes valid in the limit of small disorder. Its basic object is the Wigner function, f, which describes the phonon density in phase space and is governed by the transport equation

$$\frac{\partial}{\partial t} f(r,k,t) + \nabla\omega(k) \cdot \nabla_r f(r,k,t) = Cf(r,k,t)\,. \tag{3.19}$$

Here $r \in \mathbb{R}^d$ (boundary conditions could be imposed), $k \in [-\pi,\pi]^d$ is the wave number of the first Brioullin zone, ω is the dispersion relation of the constant mass harmonic crystal, and C is the collision operator. It acts only on wave numbers and is given by

$$\begin{aligned} Cf(k) = \quad & (2\pi)^{-d+1}\omega(k)^2\Delta^2 \int_{[-\pi,\pi]^d} dk' \\ & \delta(\omega(k)-\omega(k'))(f(k')-f(k))\,. \end{aligned} \tag{3.20}$$

We refer to [6] for a derivation. In the range of validity of (3.19), (3.20) we can think of phonons as classical particles with energy ω and velocity $\nabla\omega(k)$. They are scattered by the impurities from k to dk' with the rate

$$(2\pi)^{-d+1}\omega(k)^2\Delta^2\delta(\omega(k)-\omega(k'))dk'. \tag{3.21}$$

Collisions are elastic. We distinguish the following cases

(i) no pinning potential. Here for small k one has $\omega(k) = |k|$ and $|\nabla\omega(k)| = 1$. From (3.20) the total scattering rate behaves as $|k|^{d+1}$. This is the basis for the discussion in connection with Eq. (3.2).

(ii) pinning potential. In this case $\omega(k) = \omega_0 + k^2$ for small k. The prefactor in (3.20) can be replaced by ω_0^2. The velocity is k and the scattering is isotropic with rate $|k|^{d-2}$. Thus the diffusion coefficient results as $D(k) \cong |k|^{-d+4}$ which vanishes as $|k| \to 0$ for $d = 2, 3$. Hence there is no contribution to the thermal conductivity from the small k modes.

4 Green-Kubo formula for open systems

The Green-Kubo formula [84, 85] is a cornerstone of the study of transport phenomena. In sec. (1.1.3) we saw that for a system governed by Hamiltonian dynamics, the currents that flow in response to small applied fields can be related to the equilibrium correlation functions of the currents. For the case of heat transport the Green-Kubo formula (in the classical limit) gives:

$$\kappa = \frac{1}{K_B T^2} \lim_{\epsilon \to 0} \int_0^\infty dt e^{-\epsilon t} \lim_{L \to \infty} \frac{1}{L} \langle \hat{J}_E(t) \hat{J}_E(0) \rangle, \tag{4.1}$$

where κ is the thermal conductivity of a system of linear dimension L at temperature T. For a d-dimensional system this formula can be written as:

$$\kappa = \frac{1}{K_B T^2} \lim_{\epsilon \to 0} \int_0^\infty dt e^{-\epsilon t} \lim_{L \to \infty} \frac{1}{L^d} \langle \hat{J}_E(t) \hat{J}_E(0) \rangle. \tag{4.2}$$

The autocorrelation function on the right hand side is evaluated in equilibrium, without a temperature gradient. Since in this chapter we will be talking about heat current J_E only, for the rest of the chapter we denote it by J. The total heat current in the system is $J(t) = \int j(\mathbf{x}, t) d\mathbf{x}$, where $j(\mathbf{x}, t)$ is the heat flux density. The order of the limits in Eq. (4.2) is important. With the correct order of limits, one can calculate the correlation functions with arbitrary boundary conditions and apply Eq. (4.2) to obtain the response of an open system with reservoirs at the ends. There have been a number of derivations of Eq. (4.2) by various authors [84, 85, 86]. In the introduction of this thesis we have presented one such derivation.

There are several situations where the Green-Kubo formula in Eq. (4.2) is not applicable. For example, for the small structures that are studied in mesoscopic physics, the thermo-

dynamic limit is meaningless, and one is interested in the conductance of a specific finite system. Secondly, in many low dimensional systems, heat transport is anomalous and the thermal conductivity diverges [59]. In such cases it is impossible to take the limits as in Eq. (4.2); one is there interested in the thermal conductance as a function of L instead of an L-independent thermal conductivity. The usual procedure that has been followed in the heat conduction literature is to put a cut-off at $t_c \sim L$, in the upper limit in the Green-Kubo integral [59]. There is no rigorous justification of this assumption. A related case is that of integrable systems, where the infinite time limit of the correlation function in Eq. (4.2) is non-zero. Another way of using the Green-Kubo formula for finite systems is to include the infinite reservoirs also while applying the formula and this was done, for example, by Allen and Ford [87] for heat transport and by Fisher and Lee [88] for electron transport. Both these cases are for non-interacting systems and the final expression for conductance is what one also obtains from the nonequilibrium Green's function approach, a formalism of transport commonly used in the mesoscopic literature. More recently, it has been shown that Green-Kubo like expressions for finite open systems can be derived rigorously by using the steady state fluctuation theorem (SSFT) [89, 90, 91, 92].

There are mainly two parts of this chapter. In this first part of this chapter, we derive a Green-Kubo like formula for open systems, without invoking the SSFT. Our proof applies to all classical systems, of arbitrary size and dimensionality, with a variety of commonly used implementations of heat baths. The proof consists in first solving the equation of motion for the phase space probability distribution to find the $O(\Delta T)$ correction to the equilibrium distribution function. The average current at this order can then be expressed in terms of the equilibrium correlation $\langle J(t)J_{fp}(0)\rangle$, where J_{fp} is a specified current operator. Secondly we use the energy continuity equations to relate two different current-current correlation functions, namely $\langle J(0)J(t)\rangle$ and $\langle J(0)J_b(t)\rangle$ where J_b is an instantaneous current operator involving heat flux from the baths. Finally one relates $\langle J(0)J_b(t)\rangle$ to $\langle J(0)J_{fp}(t)\rangle$ and then, using time-reversal invariance, to $\langle J(t)J_{fp}(0)\rangle$. For baths with stochastic dynamics, time-reversal invariance follows from the detailed balance principle, which is an essential requirement of

our proof.

In the second part we obtain an exact expression for the time auto-correlation function for heat current in the NESS for a mass disordered harmonic chain of arbitrary length, expressed in terms of the non-equilibrium Green's functions. We show that it satisfies the GK formula derived in the first section. Using this correlation function we also calculate the asymptotic system size scaling of fluctuations in current in NESS.

The entire chapter is organised as follows. In Sec. (4.1) we present our proof of the formula for $1D$ lattice model in detail and outline the proof for other baths in Sec. (4.2). In Sec. (4.3) we extend our proof for higher dimensional lattice models. We also prove this formula for fluid system coupled to Maxwell baths in Sec. (4.4). Finally in Sec. (4.5) we present the calculation of time autocorrelation function and prove that it also satisfies a similar open system formula.

4.1 Proof of the formula for $1D$ lattice model

We first give a proof of our linear response result for a $1D$ lattice model with white noise Langevin baths. We consider the following general Hamiltonian:

$$H = \sum_{l=1}^{N} \left[\frac{m_l v_l^2}{2} + V(x_l) \right] + \sum_{l=1}^{N-1} U(x_l - x_{l+1}) \,, \tag{4.3}$$

where $\mathbf{x} = \{x_l\}$, $\mathbf{v} = \{v_l\}$ with $l = 1, 2...N$ denotes displacements of the particles about their equilibrium positions and their velocities, and $\{m_l\}$ denotes their masses. The particles at the ends are connected to two white noise heat baths of temperatures T_L and T_R respectively. The equations of motion of the system are given by:

$$m_l \dot{v}_l \;\; = \;\; f_l - \delta_{l,1}[\gamma^L v_1 - \eta^L] - \delta_{l,N}[\gamma^R v_N - \eta^R \,], \tag{4.4}$$

where $f_l = -\partial H/\partial x_l$, and $\eta^{L,R}(t)$ are Gaussian noise terms with zero mean and satisfying the fluctuation dissipation relations: $\langle \eta^{L,R}(t)\eta^{L,R}(t')\rangle = 2\gamma^{L,R}k_B T_{L,R}\delta(t-t')$. There are three stages toward proving the open system GK formula.

First stage : In the first part of the proof we obtain an expression for the nonequilibrium

steady state average $\langle J\rangle_{\Delta T}$, at linear order in ΔT, and then we relate this to the equilibrium correlation function $\langle J(t)J(0)\rangle$. The $\langle ...\rangle$ denotes a thermal equilibrium average. Time-dependent equilibrium correlation functions require an averaging both over initial conditions as well as over paths. In the Fokker-Planck representation this can be obtained using the time-evolution operator, while in the Langevin representation thermal noise occurs explicitly and has to be averaged over. Corresponding to the stochastic Langevin equations in Eq. (4.4), one has a Fokker-Planck (FP) equation for the phase space distribution $P(\mathbf{x},\mathbf{v},t)$. Setting $T_L = T + \Delta T/2$ and $T_R = T - \Delta T/2$ we write the FP equation in the following form:

$$\frac{\partial P(\mathbf{x},\mathbf{v},t)}{\partial t} = \hat{L}P(\mathbf{x},\mathbf{v},t) + \hat{L}^{\Delta T}P(\mathbf{x},\mathbf{v},t)\ , \tag{4.5}$$

$$\text{where}\quad \hat{L}(\mathbf{x},\mathbf{v}) = \hat{L}^H + \sum_{l=1,N}\frac{\gamma^l}{m_l}\frac{\partial}{\partial v_l}\left(v_l + \frac{k_BT}{m_l}\frac{\partial}{\partial v_l}\right)$$

$$\hat{L}^{\Delta T}(\mathbf{v}) = \frac{k_B\Delta T}{2}\left(\frac{\gamma^L}{m_1^2}\frac{\partial^2}{\partial v_1^2} - \frac{\gamma^R}{m_N^2}\frac{\partial^2}{\partial v_N^2}\right), \tag{4.6}$$

where $\hat{L}^H = -\sum_l[\ v_l\ \partial/\partial x_l + (f_l/m_l)\ \partial/\partial v_l\ ]$ is the Hamiltonian Liouville operator and $\gamma^1 = \gamma^L, \gamma^N = \gamma^R$. For $\Delta T = 0$ the steady state solution of the FP equation is known and is just the usual equilibrium Boltzmann distribution $P_0 = e^{-\beta H}/Z$, where $Z = \int d\mathbf{x}d\mathbf{v}e^{-\beta H}$ is the canonical partition function [$\beta = (k_BT)^{-1}$]. It is easily verified that $\hat{L}P_0 = 0$. For $\Delta T \neq 0$, we solve Eq. (4.5) by perturbation theory, starting from the equilibrium solution at time $t = -\infty$. Writing $P(\mathbf{x},\mathbf{v},t) = P_0 + p(\mathbf{x},\mathbf{v},t)$, we obtain the following solution at $O(\Delta T)$:

$$p(\mathbf{x},\mathbf{v},t) = \int_{-\infty}^{t} dt'\ e^{\hat{L}(t-t')}\ \hat{L}^{\Delta T}\ P_0(\mathbf{x},\mathbf{v})\ = \Delta\beta\int_{-\infty}^{t} dt'\ e^{\hat{L}(t-t')}\ J_{fp}(\mathbf{v})\ P_0(\mathbf{x},\mathbf{v})\ ,$$

$$\text{with } J_{fp}(\mathbf{v}) = (\Delta\beta\ P_0)^{-1}\hat{L}^{\Delta T}P_0 = -\frac{\gamma^L}{2}\left[v_1^2 - \frac{k_BT}{m_1}\right] + \frac{\gamma^R}{2}\left[v_N^2 - \frac{k_BT}{m_N}\right]. \tag{4.7}$$

To define the current operator, one first defines the local energy density at the lth site: $\epsilon_l = m_lv_l^2/2 + V(x_l) + \frac{1}{2}[U(x_{l-1} - x_l) + U(x_l - x_{l+1})]$. Taking a time derivative gives the energy continuity equation

$$d\epsilon_l/dt + j_{l+1,l} - j_{l,l-1} \quad = \quad j_{1,L}\ \delta_{l,1} + j_{N,R}\ \delta_{l,N}\ , \tag{4.8}$$

$$\text{where} \quad j_{l+1,l} \;=\; \frac{1}{2}(v_l + v_{l+1}) f_{l+1,l}$$

gives the current from the lth to the $l+1$th site ($f_{l+1,l}$ is the force on $l+1$th particle due to lth particle). We define the total current flowing through the system as $J = \sum_{l=1}^{N-1} j_{l+1,l}$. The expectation value of the total current is then given by:

$$\begin{aligned}
\langle J \rangle_{\Delta T} &= \int d\mathbf{x} d\mathbf{v}\; J\; p(\mathbf{x}, \mathbf{v}) \\
&= \Delta\beta \int_0^\infty dt \int d\mathbf{x} d\mathbf{v}\; J\; e^{\hat{L}t}\; J_{fp}\; P_0 \\
&= \Delta\beta \int_0^\infty dt\; \langle J(t) J_{fp}(0) \rangle \; . \qquad (4.9)
\end{aligned}$$

Second stage : In this part we prove

$$\langle J(t) J_{fp}(0) \rangle = -\langle J(0) J_{fp}(t) \rangle. \qquad (4.10)$$

Eq. (4.10) is a statement of time-reversal symmetry. To prove this we write $\langle J_{fp}(t) J(0) \rangle = \int dq \int dq' J_{fp}(q) J(q') P_0(q') W(q, t|q', 0)$ where $W(q, t|q', 0)$ denotes the transition probability from $q' = (\mathbf{x}', \mathbf{v}')$ to $q = (\mathbf{x}, \mathbf{v})$ in time t. Then, using the detailed balance principle, $W(\mathbf{x}, \mathbf{v}, t|\mathbf{x}', \mathbf{v}', 0) P_0(\mathbf{x}', \mathbf{v}') = W(\mathbf{x}', -\mathbf{v}', t|\mathbf{x}, -\mathbf{v}, 0) P_0(\mathbf{x}, -\mathbf{v})$ (see [93, 94, 95]) and the fact that J is odd in the velocities while J_{fp} is even, one gets $\langle J_{fp}(t) J(0) \rangle = -\langle J_{fp}(0) J(t) \rangle$ as follows.

$$\begin{aligned}
\langle J_{fp}(t) J(0) \rangle_T \quad &= \int dq \int dq' J_{fp}(q) J(q') P_0(q') W(q, t|q', 0) \\
&= \int dq \int dq' J_{fp}(q') J(q) P_0(q) W(q', t|q, 0) \\
&= \int dq \int dq' J_{fp}(q') J(q) P_0(\mathbf{x}', -\mathbf{v}') W(\mathbf{x}, -\mathbf{v}, t|\mathbf{x}', -\mathbf{v}', 0) \\
&= \int dq \int dq' J_{fp}(\mathbf{x}', -\mathbf{v}') J(\mathbf{x}, -\mathbf{v}) P_0(q') W(q, t|q', 0) \\
&= -\langle J(t) J_{fp}(0) \rangle_T \; , \qquad (4.11)
\end{aligned}$$

where we have interchanged q and q' in the second line and used detailed balance in the third line. Finally in the fourth line we have reversed all the velocity variables and used the fact that $J(\mathbf{x}, \mathbf{v})$ is odd under velocity reversal while J_{fp} is not. The Eq. (4.10) can be

proved in a direct but equivalent way which is as follows: An integration by parts followed by the transformation $\mathbf{v} \to -\mathbf{v}$ yields: $\langle J(t)J_{fp}(0)\rangle = \int d\mathbf{x}d\mathbf{v}Je^{\hat{L}t}J_{fp}P_0 = \int d\mathbf{x}d\mathbf{v}J_{fp}P_0e^{\bar{\hat{L}}t}J = -\int d\mathbf{x}d\mathbf{v}J_{fp}P_0e^{\hat{L}^\dagger t}J$ where $\hat{T}\bar{\hat{L}} = \hat{L}^\dagger = \hat{L}^H - \sum_{l=1,N}\ [v_l - (\beta m_l)^{-1}\partial_{v_l}](\gamma^l/m_l)\partial_{v_l}$ and $\hat{T}$ denotes time reversal. We now note the operator identities $\hat{L}P_0 = P_0\hat{L}^\dagger$ and consequently $e^{\hat{L}t}P_0 = P_0e^{\hat{L}^\dagger t}$ which can be proved using the form of P_0. Using this in the above equation immediately gives: $\langle J(t)J_{fp}(0)\rangle = -\int d\mathbf{x}d\mathbf{v}J_{fp}e^{\hat{L}t}JP_0 = -\langle J(0)J_{fp}(t)\rangle$. Using this relation in Eq. (4.9) we get

$$\langle J\rangle_{\Delta T} \quad = \quad \frac{\Delta T}{K_BT^2}\ \int_0^\infty dt\ \langle J_fp(t)J(0)\rangle\ . \tag{4.12}$$

Third stage : Here we prove the following relations

$$\int_0^\infty dt\langle J(t)J(0)\rangle \quad = \quad (N-1)\int_0^\infty dt\langle J(0)J_b(t)\rangle\ . \tag{4.13}$$

$$\text{and} \qquad \langle J(0)J_b(t)\rangle \quad = \quad \langle J(0)J_{fp}(t)\rangle \tag{4.14}$$

which together complete the proof. For this let us define the current variable J_b as the mean of the instantaneous heat currents flowing into the system from the left reservoir and flowing out of the system to the right reservoir. Thus we have

$$J_b(t) \quad = \quad \frac{1}{2}(j_{1,L} - j_{N,R}) \tag{4.15}$$

$$\text{where} \quad j_{1,L}(t) \quad = \quad -\gamma^L v_1^2(t) + \eta^L(t)v_1(t)\ ,$$

$$j_{N,R}(t) \quad = \quad -\gamma^R v_N^2(t) + \eta^R(t)v_N(t)\ . \tag{4.16}$$

It is easy to note that $\langle J(0)\rangle = 0$. Now we prove

$$\langle J(0)\eta^L(t)v_1(t)\rangle = \langle J(0)\eta^R(t)v_N(t)\rangle = 0\ . \tag{4.17}$$

To prove this we use Novikov's theorem [96] which says: if $\{\eta_i\}$ be a set of arbitrary Gaussian noise variables with $\langle\eta_i(t)\eta_j(t')\rangle = K_{ij}(t,t')$ and $H[\eta]$ be a functional of the noise variables, then

$$< \eta_i(t)H[\eta] > \quad = \quad \sum_j \int \langle\eta_i(t)\eta_j(t')\rangle \left\langle\frac{\delta H[\eta]}{\delta\eta_j(t')}\right\rangle dt'\ ,$$

where $\delta H[\eta]/\delta\eta_j(t')$ represents a functional derivative of $H[\eta]$ with respect to η. Using the fact $\langle J(0)\rangle = 0$ and Eq. (4.17) we get Eq. (4.14).

To prove Eq. (4.13) let us define $D_l(t) = \sum_{k=1}^{l} \epsilon_k - \sum_{k=l+1}^{N} \epsilon_k$ for $l = 1, 2, ...N-1$. Then from the continuity equation Eq. (4.8) one can show that

$$dD_l/dt = -2j_{l+1,l}(t) + 2J_b(t) \; . \tag{4.18}$$

We multiply this equation by $J(0)$, take a steady state average, and integrate over time from $t = 0$ to ∞. Since $D_l J$ has an odd power of velocity, we get $\langle D_l(0)J(0)\rangle = 0$. Also $\langle D_l(\infty)J(0)\rangle = \langle D_l(\infty)\rangle \langle J(0)\rangle = 0$, and using these we immediately get $\int_0^\infty dt\langle j_{l+1,l}(t)J(0)\rangle = \int_0^\infty dt\langle J_b(t)J(0)\rangle$. Summing over all bonds thus proves Eq. (4.13). Now using Eq. (4.14) first and then Eq. (4.13) we write Eq. (4.12) as :

$$\langle J\rangle_{\Delta T} \;\; = \;\; \frac{\Delta T}{K_B T^2} \, \frac{1}{N-1} \, \int_0^\infty dt \, \langle J(t)J(0)\rangle \; . \tag{4.19}$$

Dividing both sides of the above equation by $(N-1)$ and defining the steady state current per bond between the reservoir and the system as $\bar{j} = J/(N-1)$ we write Eq.(4.19) as

$$\langle \bar{j}\rangle_{\Delta T} = \frac{\Delta T}{k_B T^2} \int_0^\infty dt\langle \bar{j}(t)\bar{j}(0)\rangle \;\; . \tag{4.20}$$

Finally the conductance is given by

$$G = \lim_{\Delta T\to 0} \frac{\langle \bar{j}\rangle_{\Delta T}}{\Delta T} = \frac{1}{k_B T^2} \int_0^\infty dt\langle \bar{j}(t)\bar{j}(0)\rangle \;\; . \tag{4.21}$$

Except the proofs of Eq. (4.10) and Eq. (4.14), other parts of the proof are quite general and independent of the heat baths used. Proofs of Eq. (4.10) and Eq. (4.14) depend on the specific bath chosen. In the next section we extend the proof to the cases where the noises from the baths are exponentially correlated in time and noises are obtained by coupling the lattice Hamiltonian to a deterministic bath model. Later we also give the proof of this formula for fluid systems.

4.2 One dimensional lattice with other baths

We outline the proof for two other models of baths coupled to the lattice Hamiltonian. These are (i) the Nose-Hoover bath and (ii) a Langevin bath with exponentially correlated noise.

Nose-Hoover bath: In this case the equations of motion are:

$$m_l \dot{v}_l = f_l - \delta_{l,1}\zeta_L v_1 - \delta_{l,N}\zeta_R v_N, \tag{4.22}$$

where $\zeta_{L,R}$ are themselves dynamical variables satisfying the equations of motion:

$$\begin{aligned} \dot{\zeta_L} &= \frac{1}{\theta_L}(\frac{m_1 v_1^2}{k_B T_L} - 1) \\ \dot{\zeta_R} &= \frac{1}{\theta_R}(\frac{m_N v_N^2}{k_B T_R} - 1) \end{aligned}$$

For small ΔT, we then write an equation of motion for the extended distribution function $P(\mathbf{x}, \mathbf{v}, \zeta_L, \zeta_R, t)$. This has the same form as Eq. (4.5) but now with:

$$\begin{aligned} \hat{L}^T &= \hat{L}^H + \frac{\zeta_L}{m_1}\frac{\partial}{\partial v_1}v_1 - \frac{1}{\theta_L}\frac{\partial}{\partial \zeta_L}\left(\frac{m_1 v_1^2}{k_B T} - 1\right) \\ &+ \frac{\zeta_R}{m_N}\frac{\partial}{\partial v_N}v_N - \frac{1}{\theta_R}\frac{\partial}{\partial \zeta_R}\left(\frac{m_N v_N^2}{k_B T} - 1\right) \\ \hat{L}^{\Delta T} &= \frac{\Delta T}{2k_B T^2}\left(\frac{m_1 v_1^2}{\theta_L}\frac{\partial}{\partial \zeta_L} - \frac{m_N v_N^2}{\theta_R}\frac{\partial}{\partial \zeta_R}\right). \end{aligned} \tag{4.23}$$

If $T_L = T_R = T$, it is easy to verify that the equilibrium phase space density is given by:

$$\hat{P}_0 = P_0(\mathbf{x}, \mathbf{v})\ \exp\left[-\tfrac{1}{2}\left(\frac{\theta_L \zeta_L^2}{m_1} + \frac{\theta_R \zeta_R^2}{m_N}\right)\right], \tag{4.24}$$

and we assume that there is convergence to this distribution. Acting with $\hat{L}^{\Delta T}$ on this, we then obtain:

$$J_{fp} = -\frac{1}{2}(v_1^2 \zeta_L - v_N^2 \zeta_R)\,. \tag{4.25}$$

On the other hand, since $-\zeta_L v_1$ is the force from the left reservoir on the first particle, hence $j_{1,L} = -\zeta_L v_1^2$ and similarly, $j_{N,R} = -\zeta_R v_R^2$. Hence from the definition of J_b in Eq. (4.15), we obtain $J_{fp} = -J_b$. This gives Eq. (4.14) with a minus sign on the right hand side *i.e.* $\langle J(0)J_b(t)\rangle = -\langle J(0)J_{fp}(t)\rangle$. Now proceeding as in the second stage of the proof we get

$\langle J(t)J_{fp}(0)\rangle = \langle J(0)J_{fp}(t)\rangle$ without the minus sign (as there in Eq. (4.10)). This can be seen from Eqs.(4.22) and (4.23). Under time reversal $(x, v, \zeta) \to (x, -v, -\zeta)$, and since J, J_{fp} both are odd under time reversal, there is no minus sign in Eq.(4.11). Rest of the proof is similar to the previous case.

Exponentially correlated bath: A simple way of realizing exponentially correlated heat baths is to consider the following set of equations of motion:

$$m_i \dot{v}_l = f_l + \delta_{l,1} y_L + \delta_{l,N} y_R \,, \tag{4.26}$$

where y_L, y_R satisfy the following equations of motion:

$$\dot{y}_L = -\frac{y_L}{\nu^L \gamma^L} - \gamma^L v_1 + \eta^L$$
$$\dot{y}_R = -\frac{y_R}{\nu^R \gamma^R} - \gamma^R v_N + \eta^R \,,$$

where $\eta^{L,R}$ are Gaussian white noise satisfying $\langle \eta^{L,R}(t)\eta^{L,R}(t')\rangle = 2k_B T_{L,R}/\nu^{L,R}\delta(t-t')$. Assuming that the baths are coupled to the system at time $t = -\infty$, the solution of the above equations is:

$$\begin{aligned} y_L &= -\gamma^L \int_{-\infty}^{t} dt' e^{-(t-t')/(\nu^L\gamma^L)} v_1(t') + \xi^L(t) \\ y_R &= -\gamma^R \int_{-\infty}^{t} dt' e^{-(t-t')/(\nu^R\gamma^R)} v_N(t') + \xi^R(t) \\ \text{where } \xi^L &= \int_{-\infty}^{t} dt' e^{-(t-t')/(\nu^L\gamma^L)} \eta^L(t') \\ \xi^R &= \int_{-\infty}^{t} dt' e^{-(t-t')/(\nu^R\gamma^R)} \eta^R(t') \,. \end{aligned}$$

The noise variables $\xi^{L,R}$ satisfy $\langle \xi^{L,R}(t)\xi^{L,R}(t')\rangle = k_B T_{L,R}\gamma^{L,R} e^{-|t-t'|/(\nu^{L,R}\gamma^{L,R})}$, and so we verify that $y_{L,R}$ are of the required form of exponentially correlated baths.

In this case we write a Fokker-Planck equation for the probability distribution for $P(\mathbf{x}, \mathbf{v}, y_L, y_R)$ and the forms of $\hat{L}^T$ and $\hat{L}^{\Delta T}$ are given by:

$$\begin{aligned} \hat{L}^T &= \hat{L}^H - \frac{y_L}{m_1}\frac{\partial}{\partial v_1} + \gamma^L v_1 \frac{\partial}{\partial y_L} + \frac{\partial}{\partial y_L}\left(\frac{y_L}{\nu^L\gamma^L} + \frac{k_B T}{\nu^L}\frac{\partial}{\partial y_L}\right) \\ &- \frac{y_R}{m_N}\frac{\partial}{\partial v_N} + \gamma^R v_N \frac{\partial}{\partial y_R} + \frac{\partial}{\partial y_R}\left(\frac{y_R}{\nu^R\gamma^R} + \frac{k_B T}{\nu^R}\frac{\partial}{\partial y_R}\right) \,, \end{aligned}$$

$$\hat{L}^{\Delta T} = \frac{k_B \Delta T}{2} \left(\frac{1}{\nu^L} \frac{\partial^2}{\partial y_L^2} - \frac{1}{\nu^R} \frac{\partial^2}{\partial y_R^2} \right) . \tag{4.27}$$

One can verify that the equilibrium distribution is, in this case, given by:

$$\hat{P}_0 = P_0(\mathbf{x}, \mathbf{v}) \ \exp\left[-\frac{1}{2} \left(\frac{y_L^2}{\gamma^L} + \frac{y_R^2}{\gamma^R} \right) \right] , \tag{4.28}$$

while J_{fp} is given by:

$$J_{fp} = \frac{1}{2\nu^L} \left[\frac{y_L^2}{(\gamma^L)^2} - \frac{k_B T}{\gamma^L} \right] - \frac{1}{2\nu^R} \left[\frac{y_R^2}{(\gamma^R)^2} - \frac{k_B T}{\gamma^R} \right] . \tag{4.29}$$

Now using the equation

$$\frac{d}{dt} \left(\frac{y_L^2}{2\gamma^L} \right) = -\frac{y_L^2}{\nu_L (\gamma^L)^2} - y_L v_1 + \frac{y_L \eta^L}{\gamma^L} , \tag{4.30}$$

and the fact that $\langle J(0) y_L(t) \eta^L(t) \rangle_T = 0$, it follows that:

$$\int_0^\infty dt \ \left\langle J(0) \frac{y_L^2(t)}{\nu^L (\gamma^L)^2} \right\rangle_T = - \int_0^\infty dt \langle J(0) y_L(t) v_1(t) \rangle_T ,$$

and a similar result for the right reservoir. From the equations of motion Eq. (4.26), we get $j_{1,L} = y_L v_1$, $j_{N,R} = y_R v_N$. Hence from the above equation and from the definitions of J_b in Eq. (4.15), and of J_{fp} in Eq. (4.29), we again get $\langle J(0) J_{fp}(t) \rangle_T = \langle J(0) J_b(t) \rangle_T$. The other steps of the proof are the same as for the white-noise case.

4.3 Lattice models in higher dimensions

In this section we give a generalization of the derivation to arbitrary dimensions, for the case of white noise reservoirs. The extension to the baths in sec. (4.2) is straightforward. We consider a system of particles with mean positions on a d-dimensional hypercubic lattice with points represented by $\mathbf{l} = (l_1, l_2, ..., l_d)$ where $l_\alpha = 1, 2...N$ with $\alpha = 1, 2, .., d$. The Hamiltonian of the system is given by:

$$H = \sum_{\mathbf{l}} \left[\frac{m_{\mathbf{l}} \ \mathbf{v}_{\mathbf{l}}^2}{2} + V(\mathbf{x}_{\mathbf{l}}) \right] + \sum_{<\mathbf{l},\mathbf{k}>} U(\mathbf{x}_{\mathbf{l}} - \mathbf{x}_{\mathbf{k}}) , \tag{4.31}$$

where $\mathbf{x_l}$ and $\mathbf{v_l}$ are the d-dimensional displacement about lattice positions and velocity vectors respectively, of the particle at $\mathbf{l}$ and $<\mathbf{l},\mathbf{k}>$ denotes nearest neighbors. Heat conduction takes place in the $\alpha = \nu$ direction because of heat baths at temperature T_L and T_R that are attached to all lattice points on the two hypersurfaces $l_\nu = 1$ and $l_\nu = L$. The corresponding Langevin equations of motion are:

$$m_{\mathbf{l}}\dot{\mathbf{v}}_{\mathbf{l}} = \mathbf{f}_{\mathbf{l}} + \delta_{l_\nu,1}[\boldsymbol{\eta}^L_{\mathbf{l}'} - \gamma^L_{\mathbf{l}'}\mathbf{v}_{\mathbf{l}}] + \delta_{l_\nu,L}[\boldsymbol{\eta}^R_{\mathbf{l}'} - \gamma^L_{\mathbf{l}'}\mathbf{v}_{\mathbf{l}'}]\,, \tag{4.32}$$

where $\mathbf{l} = (l_\nu, \mathbf{l}')$, so that $\mathbf{l}'$ denotes points on a constant l_ν hypersurface. The noise terms at different lattice points and in different directions are assumed to be uncorrelated, and satisfy the usual fluctuation-dissipation relations. We define the local energy as:

$$\epsilon_{\mathbf{l}}(t) = \frac{1}{2}m_{\mathbf{l}}\ \mathbf{v}^2_{\mathbf{l}} + V(\mathbf{x_l}) + \frac{1}{2}\sum_{\hat{\mathbf{e}}} U(\mathbf{x_l} - \mathbf{x}_{\mathbf{l}+\hat{\mathbf{e}}})\,, \tag{4.33}$$

where the sum is over all the $2d$ unit vectors $\hat{\mathbf{e}}$ which specify the nearest neighbours of the site $\mathbf{l}$. The corresponding continuity equations are easily found to be:

$$\begin{aligned}
\dot{\epsilon}_{(1,\mathbf{l}')} &= \sum_{\hat{\mathbf{e}}'} j_{(1,\mathbf{l}'),(1,\mathbf{l}')+\hat{\mathbf{e}}'} + j^L_{(1,\mathbf{l}')} \\
\dot{\epsilon}_{\mathbf{l}} &= \sum_{\hat{\mathbf{e}}} j_{\mathbf{l},\mathbf{l}+\hat{\mathbf{e}}}, \quad \text{for } \ l_\nu = 2,3...N-1 \\
\dot{\epsilon}_{(N,\mathbf{l}')} &= \sum_{\hat{\mathbf{e}}'} j_{(N,\mathbf{l}'),(N,\mathbf{l}')+\hat{\mathbf{e}}'} + j^R_{(N,\mathbf{l}')} \\
\text{where } \ j_{\mathbf{l},\mathbf{l}+\hat{\mathbf{e}}} &= \frac{1}{2}\sum_\alpha f^\alpha_{\mathbf{l},\mathbf{l}+\hat{\mathbf{e}}}\,(v^\alpha_{\mathbf{l}} + v^\alpha_{\mathbf{l}+\hat{\mathbf{e}}})\,, \\
j^L_{(1,\mathbf{l}')} &= -\gamma^L_{\mathbf{l}'}\mathbf{v}^2_{(1,\mathbf{l}')} + \boldsymbol{\eta}^L_{\mathbf{l}'}.\mathbf{v}_{(1,\mathbf{l}')} \\
j^R_{(N,\mathbf{l}')} &= -\gamma^R_{\mathbf{l}'}\mathbf{v}^2_{(N,\mathbf{l}')} + \boldsymbol{\eta}^R_{\mathbf{l}'}.\mathbf{v}_{(N,\mathbf{l}')}\,,
\end{aligned} \tag{4.34}$$

where $\mathbf{f}_{\mathbf{l},\mathbf{k}}$ denotes the force on particle at $\mathbf{l}$ by particle at $\mathbf{k}$, and $\sum_{\hat{\mathbf{e}}'}$ is a sum over neighbors but excluding points on $l_\nu = 0, N+1$. Further, if we define $\epsilon_{l_\nu} = \sum_{\mathbf{l}'}\epsilon_{(l_\nu,\mathbf{l}')}$, then these satisfy equations of the $1D$ form:

$$\begin{aligned}
\dot{\epsilon}_1 &= -j^\nu_{2,1}(t) + j^\nu_{1,L}(t) \\
\dot{\epsilon}_{l_\nu} &= j^\nu_{l_\nu,l_\nu-1}(t) - j^\nu_{l_\nu+1,l_\nu}(t) \quad \text{for } \ l_\nu = 2,3...N-1
\end{aligned}$$

$$\dot{\epsilon_N} = j^\nu_{N,N-1}(t) + j^\nu_{N,R}(t)$$
$$\text{where} \quad j^\nu_{l_\nu,l_\nu-1} = \sum_{\mathbf{l}'} j_{(l_\nu,\mathbf{l}'),(l_\nu-1,\mathbf{l}')}$$
$$j^\nu_{1L} = \sum_{\mathbf{l}'} j^L_{(1,\mathbf{l}')} \,, \quad j^\nu_{1R} = \sum_{\mathbf{l}'} j^R_{(N,\mathbf{l}')} \,. \tag{4.35}$$

Defining now the total current operator as $J^\nu = \sum_{l_\nu=1}^{N-1} j^\nu_{l_\nu+1,l_\nu}$ where $j^\nu_{l_\nu+1,l_\nu}$ is the heat current flowing in the ν direction between the l_ν'th and $l_\nu + 1$'th hypersurfaces, and the boundary current operator

$$J^\nu_b \;=\; -(j^\nu_{1L} - j^\nu_{NR})/2 = \frac{1}{2}\sum_{\mathbf{l}'} \left\{ \left[\gamma^L_{\mathbf{l}'} \mathbf{v}^2_{(1,\mathbf{l})} - \boldsymbol{\eta}^L_{\mathbf{l}'}.\mathbf{v}_{(1,\mathbf{l}')} \right] - \left[\gamma^R_{\mathbf{l}'} \mathbf{v}^2_{(N,\mathbf{l}')} - \boldsymbol{\eta}^R_{\mathbf{l}'}.\mathbf{v}_{(N,\mathbf{l}')} \right] \right\} \,, \tag{4.36}$$

and by following the same steps as in the $1D$ case, we can again prove the analogue of Eq. (4.13). In this case this is $\int_0^\infty dt \langle J^\nu(t) J^\nu(0)\rangle = (N-1)\int_0^\infty dt \langle J^\nu(0) J^\nu_b(t)\rangle$.

The Fokker-Planck equation corresponding to the Langevin equations in Eq. (4.32) have the same form as Eq. (4.5) with:

$$L^{\Delta T} = \frac{k_B \Delta T}{2} \sum_{\mathbf{l}'} \left[\frac{\gamma^L_{(1,\mathbf{l}')}}{m^2_{(1,\mathbf{l}')}} \nabla^2_{\mathbf{v}_{(1,\mathbf{l}')}} - \frac{\gamma^R_{(N,\mathbf{l}')}}{m^2_{(N,\mathbf{l}')}} \nabla^2_{\mathbf{v}_{(N,\mathbf{l}')}} \right] . \tag{4.37}$$

As in the $1D$ case, the deviation of the expectation value of any observable $A(\mathbf{x}, \mathbf{v})$ from its stationary value is given by $\Delta T/(k_B T^2) \int_0^\infty dt \, \langle A(t) \, J^\nu_{fp}(0)\rangle_T$, where now:

$$J^\nu_{fp} \;=\; \frac{1}{2}\sum_{\mathbf{l}'} \left\{ \gamma^L_{\mathbf{l}'} \left[\mathbf{v}^2_{(1,\mathbf{l})} - \frac{d k_B T}{m_{(1,\mathbf{l}')}} \right] - \gamma^R_{\mathbf{l}'} \left[\mathbf{v}^2_{(N,\mathbf{l}')} - \frac{d k_B T}{m_{(N,\mathbf{l}')}} \right] \right\} \,. \tag{4.38}$$

With J^ν_b and J^ν_{fp} given by Eqs. (4.36,4.38), it is clear that we can repeat the arguments for the $1D$ case. We then get $\langle J^\nu(0) J^\nu_b(t)\rangle = \langle J^\nu(0) J^\nu_{fp}(t)\rangle = -\langle J^\nu(t) J^\nu_{fp}(0)\rangle$, where the last step requires use of the detailed balance principle. Thus we finally have the required results corresponding to Eqs. (4.9,4.10,4.13,4.14), from which we get the required formula, which is of the same form as Eq. (4.21) with i replaced by $I^\nu = J^\nu/(N-1)$.

4.4 Fluid system coupled to Maxwell baths

We first consider a $1D$ system of particles in a box of length L. The end particles (1 and N) interact with baths at temperatures T_L and T_R respectively. Whenever the first particle

hits the left wall it is reflected back with a random velocity chosen from the distribution: $\Pi(v) = m_1\,\beta_L\,\theta(v)\,v\,\exp[-\beta_L m_1 v^2/2]$, with a similar rule at the right end. Otherwise the dynamics is Hamiltonian.

We find the FP current by noting that $J_{fp} = (\Delta\beta)^{-1}[\partial_t P/P]_{P=P_0}$. There are two parts to the evolution of the phase space density: the Hamiltonian dynamics inside the system, and the effect of the heat baths. After a small time interval ϵ, the phase space density $P(\mathbf{x};\mathbf{v};t+\epsilon)$ is

$$\begin{aligned}
&= \beta_L m_1 e^{-\frac{1}{2}\beta_L m_1 v_1^2}\int_0^\infty P(0,\mathbf{x}'-\mathbf{v}'\epsilon;-v_0,\mathbf{v}'-\mathbf{a}'\epsilon;t)v_0 dv_0 \\
&\qquad\qquad \text{for } x_1 < v_1\epsilon \\
&= \beta_R m_N e^{-\frac{1}{2}\beta_R m_N v_N^2}\int_0^\infty P(\mathbf{x}'-\mathbf{v}'\epsilon,L;\mathbf{v}'-\mathbf{a}'\epsilon,v_0;t)v_0 dv_0 \\
&\qquad\qquad \text{for } x_N > L + v_N\epsilon \\
&= P(\mathbf{x}-\mathbf{v}\epsilon,\mathbf{v}-\mathbf{a}\epsilon,t) \qquad \text{otherwise}
\end{aligned} \tag{4.39}$$

where the primed variables in the first and second lines leave out particles 1 and N respectively. (Note that since $0 < x_1$ and $x_N < L$, the conditions in the second and third lines imply $v_1 > 0$ and $v_N < 0$.)

If $T_L = T_R = T$, and $P(\mathbf{x},\mathbf{v},t) = P_0$, the equilibrium phase space density for the temperature T, then the phase space density at time $t+\epsilon$ is the same. Now if $T_{L,R} = T \pm \Delta T/2$, with $P(\mathbf{x},\mathbf{v},t)$ still equal to P_0, then

$$P(\mathbf{x};\mathbf{v};t+\epsilon) \;=\; P_0 + \frac{\Delta T}{2T}\Big[(\tfrac{1}{2}\beta m_1 v_1^2 - 1)\theta(v_1\epsilon - x_1) - (\tfrac{1}{2}\beta m_N v_N^2 - 1)\theta(x_N - L - v_N\epsilon)\Big]P_0.$$

Dividing by ϵ throughout and taking $\epsilon \to 0$, we see that

$$J_{fp} \;=\; -\frac{1}{2}(\tfrac{1}{2}m_1 v_1^2 - k_B T)v_1\delta(x_1)\theta(v_1) - \frac{1}{2}(\tfrac{1}{2}m_N v_N^2 - k_B T)v_N\delta(x_N - L)\theta(-v_N). \tag{4.40}$$

We have to use continuum energy density $\epsilon(x,t)$ and current $j(x,t)$, and the total heat current is now $J = \int j(x)dx$ instead of $\sum j_{i+1,i}$. The continuity equation is still valid, and defining $D(x,t) = \int_0^x dx'\epsilon(x',t) - \int_x^L \epsilon(x',t)$ and $A(t) = \int_0^L dx D(x)$, we get the analogue of Eq. (4.13):

$$\int_0^\infty \langle J(t)J(0)\rangle dt = L\int_0^\infty \langle J_b(t)J(0)\rangle dt. \tag{4.41}$$

Here $J_b = \frac{1}{2}[j_{1,L} - j_{N,R}]$ as before, and

$$\begin{aligned} j_{1,L} &= \tfrac{1}{2} m_1 v_1 (v_{1,L}^2 - v_1^2)\, \delta(x_1)\theta(-v_1) \\ j_{N,R} &= \tfrac{1}{2} m_N v_N (v_{N,L}^2 - v_L^2)\, \delta(x_N - L)\theta(v_N)\ . \end{aligned}$$

The δ-functions enforce the condition that the particle is colliding with the bath, and $v_{1,L}$ and $v_{N,R}$ are the random velocities with which they emerge from the collision. Invoking detailed balance, using the explicit forms of J_{fp} and J_b, and the fact that $J(0)$ is uncorrelated with $v_{1,L}, v_{N,R}$ we can show that $\langle J(0)J_b(t)\rangle = -\langle J(t)J_{fp}(0)\rangle$. Using this relation and Eq. (4.41) in Eq. (4.9), we obtain Eq. (4.21) with $(N-1)$ replaced with L.

The generalization to a d-dimensional system is straightforward. First, any particle can interact with the baths at the ends if it reaches $x = 0$ or $x = L$. Including the effect of the components of the velocity transverse to the heat-flow direction the derivation of Eq. (4.40) gets modified and gives

$$J_{fp} = \sum_l \Big[-\frac{1}{2}(\tfrac{1}{2} m_l \mathbf{v}_l^2 - \tfrac{1}{2}(d+1)k_B T) v_l^\nu \delta(x_l^\nu)\theta(v_l^\nu) - \frac{1}{2}(\tfrac{1}{2} m_l \mathbf{v}_l^2 - \tfrac{1}{2}(d+1)k_B T) v_l^\nu \delta(x_l^\nu - L)\theta(-v_l^\nu)\Big].$$

The expression for J_b changes similarly, so that the final result of the previous paragraph is still valid.

All the above derivations of open system GK formula for different systems uses Fokker-Planck description of stochastic systems and hence is only applicable for those currents which can be expressed solely in terms of phase space variables (*e.g.* currents inside the bulk of the system). Since boundary currents naturally involve noises explicitly, derivation given in this section is not applicable to them. The general expectation is that, even for boundary currents, one can prove an open finite system GK formula as given in Eq.(4.21). In the next section we explicitly calculate boundary current-current auto correlation function in the context of heat transport for a finite mass disordered harmonic chain in NESS and show that integration of the equilibrium correlation function gives the NESS current.

4.5 Proof of the formula for boundary currents

Time correlation functions are useful quantities in the study of transport processes. They are related to various transport coefficients. For example, the diffusion constant of a Brownian particle is given by the integral of the equilibrium velocity-velocity time auto-correlation function. Similarly the friction coefficient of an over-damped particle is also related to the time correlation function of the instantaneous force experienced by the particle. There are few examples where exact time auto-correlation functions in equilibrium state have been obtained for many-particle systems. For Hamiltonian systems some examples of exact calculations are velocity auto-correlation function for ordered harmonic lattices [97] and for a one dimensional gas of elastically colliding hard rods [98]. Recently authors of [99] have shown explicitly that integration of the heat current auto-correlation function gives the current in non-equilibrium steady state for a two particle harmonic system. In this section we obtain an exact expression for the time auto-correlation function for heat current in the NESS for a disordered harmonic chain of arbitrary length, expressed in terms of the non-equilibrium Green's functions. We show that it satisfies the GK formula derived in previous section. Using this correlation function we also calculate the asymptotic system size scaling of fluctuations in current in NESS.

4.5.1 Definition of the model

We consider a chain of oscillators of N particles described by the Hamiltonian H :

$$H = \sum_{l=1}^{N}[\frac{1}{2}m_l\dot{x}_l^2 \quad + \quad \frac{1}{2}k_o x_l^2] + \sum_{l=1}^{N-1}\frac{1}{2}k(x_{l+1}-x_l)^2 + \frac{1}{2}k'(x_1^2+x_N^2)\,, \tag{4.42}$$

where x_l are displacements of the particles about their equilibrium positions, k, k_0 are the inter-particle and on-site spring constants respectively, and m_l is mass of the l^{th} particle. k' is the spring constant of the potentials at the boundaries. For different values of k' and k_0 we get different boundary-conditions (BCs). If k' and k_0 both are zero we get free BC, otherwise we get fixed BC ($k' \neq 0$ and $k_0 = 0$) and pinned case ($k_0 \neq 0$). The particles 1 and N

are connected to two white noise heat baths of temperatures T_L and T_R respectively. The equation of motion of the l^{th} particle is given by [19]

$$\begin{aligned} m_l\ddot{x}_l &= -k(2x_l - x_{l-1} - x_{l+1}) - k_o x_l - \delta_{l,1}[(k'-k)x_l + \gamma_L\dot{x}_1 - \eta_L] \\ &\quad -\delta_{l,N}[(k'-k)x_l + \gamma_R\dot{x}_N - \eta_R\ ] \\ \text{where} &\quad l = 1, 2...N \ \text{ and } \ x_0 = x_{N+1} = 0 \end{aligned} \tag{4.43}$$

where $\eta_{L,R}(t)$ are Gaussian noise terms with zero mean and satisfy the following fluctuation dissipation relations

$$\begin{aligned} \langle\eta_{L,R}(t)\eta_{L,R}(t')\rangle &= 2\gamma_{L,R}k_B T_{L,R}\delta(t-t') \\ \langle\eta_L(t)\eta_R(t')\rangle &= 0, \quad \langle\eta_{L,R}(t)\rangle = 0 \end{aligned} \tag{4.44}$$

We first define the local energy density associated with the l^{th} particle (or energy at the lattice site l) as earlier:

$$\begin{aligned} \epsilon_1 &= \frac{p_1^2}{2m_1} + \frac{k_o x_1^2}{2} + \frac{k' x_1^2}{2} + \frac{k}{4}(x_1 - x_2)^2\ , \\ \epsilon_l &= \frac{p_l^2}{2m_l} + \frac{k_o x_l^2}{2} + \frac{k}{4}[\ (x_{l-1} - x_l)^2 + (x_l - x_{l+1})^2\ ]\ , \\ &\qquad \text{for } \ l = 2, 3...N-1 \\ \epsilon_N &= \frac{p_N^2}{2m_N} + \frac{k_o x_N^2}{2} + \frac{k' x_N^2}{2} + \frac{k}{4}(x_{N-1} - x_N)^2\ . \end{aligned} \tag{4.45}$$

Taking time derivative of these energy densities we write continuity equations, from which we get two instantaneous currents $j_{1,L}$ and $j_{N,R}$ which are flowing from the left and right reservoirs into the system respectively. These currents are given by [59, 58]

$$\begin{aligned} j_{1,L}(t) &= -\gamma_L\dot{x}_1^2(t) + \eta_L(t)\dot{x}_1(t)\ , \\ \text{and } \ j_{N,R}(t) &= -\gamma_R\dot{x}_N^2(t) + \eta_R(t)\dot{x}_N(t)\ . \end{aligned} \tag{4.46}$$

4.5.2 Steady state properties and current calculation

In order to obtain the steady state properties we have to find out the steady state solution of the Eq. (4.43). For that we write Eq. (4.43) in Matrix form as:

$$M\ddot{X} + \Gamma\dot{X} + \Phi X = \eta(t), \tag{4.47}$$

where,X, η are column vectors with elements $[X]^T = (x_1, x_2, ...x_N)$, $[\eta]^T = (\eta_L, 0, ...0, \eta_R)$ and Γ is a $N \times N$ matrix with only non-vanishing elements $[\Gamma]_{11} = \gamma_L$, $[\Gamma]_{NN} = \gamma_R$. $[\Phi]_{N\times N}$ represents a tridiagonal matrix with elements [13]

$$\begin{aligned}
\Phi_{lm} &= (k + k' + k_o)\delta_{l,m} - k\delta_{l,m-1} \ \text{ for } l = 1 \\
&= -k\delta_{l,m-1} + (2k + k_o)\delta_{l,m} - k\delta_{l,m+1} \\
&\qquad \text{for } \ 2 \leq l \leq N-1 \\
&= (k + k' + k_o)\delta_{l,j} - k\delta_{l,m+1} \ \text{ for } l = N \ ,
\end{aligned} \tag{4.48}$$

and $M_{lm} = m_l\delta_{lm}$ where m_l is chosen uniformly from the range $[1-\Delta, 1+\Delta]$. If $\mathcal{G}^+(t)$ denotes the Green's function of the entire system then $\mathcal{G}^+(t)$ satisfies

$$M\ddot{\mathcal{G}}^+(t) + \Gamma\dot{\mathcal{G}}^+(t) + \Phi\mathcal{G}^+(t) = \delta(t)I \ , \tag{4.49}$$

It is easy to verify that $\mathcal{G}^+(t) = G(t)\Theta(t)$ where $G(t)$ satisfies the homogeneous equation

$$M\ddot{G} + \Gamma\dot{G} + \Phi G = 0 \ , \tag{4.50}$$

with the initial conditions $G(0) = 0$, $\dot{G}(0) = M^{-1}$. Here $\Theta(t)$ is the Heaviside function. Assuming that the heat baths have been switched on at $t = -\infty$ we write the steady state solution of Eq. (4.47) as

$$X(t) = \int_{-\infty}^{t} dt' G(t-t')\eta(t'). \tag{4.51}$$

For equilibration we require that $G(t) \to 0$ as $t \to \infty$. From Eq.(4.51), we get

$$\dot{x}_1(t) = \int_{-\infty}^{t} dt_1 \Big[\dot{G}_{11}(t-t_1)\eta_L(t_1) + \dot{G}_{1N}(t-t_1)\eta_R(t_1)\Big] \ . \tag{4.52}$$

Next we calculate $\mathcal{J} = \langle j_{1,L} \rangle$ in the NESS. Here $\langle ... \rangle$ denotes the average over the noise variables $\eta_L(t)$ and $\eta_R(t)$. Putting $\dot{x}_1(t)$ from Eq. (4.52) in the expression of $j_{1,L}(t)$ in Eq. (4.46) and using the noise correlation in Eq. (4.44) we get :

$$\begin{aligned}\mathcal{J} &= -\gamma_L \int_{-\infty}^{t} dt_1 \int_{-\infty}^{t} dt_2 \Big[\dot{G}_{11}(t-t_1)\dot{G}_{11}(t-t_2) \times \langle \eta_L(t_1)\eta_L(t_2)\rangle \\ &+ \dot{G}_{1N}(t-t_1)\dot{G}_{1N}(t-t_2) \times \langle \eta_R(t_1)\eta_R(t_2)\rangle \Big] + \int_{-\infty}^{t} dt_1 \dot{G}_{11}(t-t_1)\langle \eta_L(t)\eta_L(t_1)\rangle \\ &= 2\gamma_L K_B \Big[\frac{T_L}{2}\dot{G}_{11}(0) - (\gamma_L T_L A_1(0) + \gamma_R T_R A_N(0)) \Big], \end{aligned} \tag{4.53}$$

where we have used the definition

$$A_i(t) = \int_0^\infty dt' \dot{G}_{1i}(t+t')\dot{G}_{1i}(t') \qquad \forall \quad t \, . \tag{4.54}$$

We now note the following identity (for proof see appendix)

$$\gamma_L A_1(t) + \gamma_R A_N(t) = \frac{\dot{G}_{11}(t)}{2}, \tag{4.55}$$

which can be obtained from Eqs.(4.54,4.50). Using this in Eq. (4.53) we get

$$\mathcal{J} = 2\gamma_L \gamma_R K_B (T_L - T_R) A_N(0) \, . \tag{4.56}$$

If we go to the frequency (ω) space using the following definition

$$G^+(\omega) = \int_0^\infty dt \, G(t) e^{i\omega t}, \tag{4.57}$$

we can identify that

$$A_i(t) = \frac{1}{2\pi} \int_{-\infty}^{\infty} \omega^2 |G^+_{1i}(\omega)|^2 e^{i\omega t}, \tag{4.58}$$

and

$$G^+(\omega) = \Big[-M\omega^2 + i\omega\Gamma + \Phi \Big]^{-1}. \tag{4.59}$$

With this identification we see that the expression given in Eq. (4.56) reduces to the form

$$\mathcal{J} = \frac{K_B(T_L - T_R)}{2\pi} \int_0^\infty d\omega \, \mathcal{T}(\omega), \tag{4.60}$$

where

$$\mathcal{T}(\omega) = 4\gamma_L\gamma_R\,\omega^2|G^+_{1N}(\omega)|^2, \tag{4.61}$$

is the transmission coefficient for frequency ω. The above expression for the current $\mathcal{J}$ is seen to be identical to the well-known expression for the current given in [17, 24].

In the next section we proceed to obtain the time auto-correlation function $C_{\Delta T}(t, t')$ defined as:

$$C_{\Delta T}(t, t') = \langle j_{1,L}(t) j_{1,L}(t')\rangle - \langle j_{1,L}\rangle^2, \tag{4.62}$$

in the NESS. The subscript ΔT represents the difference between the temperature at the two ends *i.e.* $\Delta T = T_L - T_R$. In the stationary state $\langle j_L(t) j_L(t')\rangle$ will be a function of $|t - t'|$ only. Hence we set $t' = 0$. If we take $\Delta T = 0$ in the expression of $C_{\Delta T}(t)$ we get the equilibrium auto-correlation which is denoted by $C_0(t)$ and we show that integral of $C_0(t)$ is related to the average current $\langle j_L\rangle$, whereas integral of $C_{\Delta T}(t)$ is related to its fluctuations in the NESS.

4.5.3 Calculation of auto-correlation function

Using the forms of $j_{1,L}$ from Eq. (4.46) we write current current auto-correlation $\langle j_{1,L}(t) j_{1,L}(0)\rangle$ for $t > 0$ as:

$$\begin{aligned}
\langle j_{1,L}(t) j_{1,L}(0)\rangle &= J_{L1} + J_{L2} + J_{L2} + J_{L4}\,, \\
\text{where} \qquad & J_{L1} = \gamma_L^2\langle \dot{x}_1^2(t)\dot{x}_1^2(0)\rangle, \quad J_{L2} = -\gamma_L\langle \eta_L(t)\dot{x}_1(t)\dot{x}_1^2(0)\rangle, \\
& J_{L3} = -\gamma_L\langle \eta_L(0)\dot{x}_1^2(0)\dot{x}_1(t)\rangle, \quad J_{L4} = \langle \eta_L(t)\dot{x}_1(t)\eta_L(0)\dot{x}_1(0)\rangle.
\end{aligned} \tag{4.63}$$

Now we will calculate all these J's using Eq. (4.52) and Eq. (4.44). We will present the calculation of J_{L1} explicitly and state the results for other J's. Putting the form of $x_1(t)$ in the expression of J_{L1} in Eq. (4.63) we get

$$J_{L1} = \gamma_L^2 \int_{-\infty}^{t} dt_1 \int_{-\infty}^{t} dt_2 \int_{-\infty}^{0} dt_3 \int_{-\infty}^{0} dt_4 \times K_1(t_1, t_2, t_3, t_4, t), \tag{4.64}$$

where $K_1(t_1,t_2,t_3,t_4,t) =$

$$\Big\langle [\dot{G}_{11}(t-t_1)\eta_L(t_1) + \dot{G}_{1N}(t-t_1)\eta_R(t_1)] \quad \times [\dot{G}_{11}(t-t_2)\eta_L(t_2) + \dot{G}_{1N}(t-t_2)\eta_R(t_2)]$$
$$\times [\dot{G}_{11}(-t_3)\eta_L(t_3) + \dot{G}_{1N}(-t_3)\eta_R(t_3)] \quad \times [\dot{G}_{11}(-t_4)\eta_L(t_4) + \dot{G}_{1N}(-t_4)\eta_R(t_4)]\Big\rangle \,. \quad (4.65)$$

After taking the average over noises and using their Gaussian property, we get

$$K_1(t_1,t_2,t_3,t_4,t) = 4\Big(K_1^{(1)}(t_1,t_2,t_3,t_4,t)\delta(t_1-t_2)\delta(t_3-t_4) + \quad (4.66)$$
$$K_1^{(2)}(t_1,t_2,t_3,t_4,t)\delta(t_1-t_3)\delta(t_2-t_4) \; + \; K_1^{(3)}(t_1,t_2,t_3,t_4,t)\delta(t_1-t_4)\delta(t_2-t_3)\Big)$$

where expressions for these K_1s are given in appendix. Putting the expression of $K_1(t_1,t_2,t_3,t_4,t)$ in Eq. (4.64) and arranging the terms we get

$$J_{L1} = 4\gamma_L^2 K_B^2[\{\gamma_L T_L A_1(0) + \gamma_R T_R A_N(0)\}^2 + 2\{\gamma_L T_L A_1(t) + \gamma_R T_R A_N(t)\}^2], \quad (4.67)$$

where we have used the definitions of $A_i(t)$ in Eq. (4.54). Similarly we calculate other J's and their expressions are

$$\begin{aligned}
J_{L2} &= -4\gamma_L^2 T_L K_B^2[\frac{1}{2}\dot{G}_{11}(0)\{\gamma_L T_L A_1(0) + \gamma_R T_R A_N(0)\}, \\
J_{L3} &= -4\gamma_L^2 T_L K_B^2[\frac{1}{2}\dot{G}_{11}(0)\{\gamma_L T_L A_1(0) + \gamma_R T_R A_N(0)\} \\
&+ 2\dot{G}_{11}(t)\{\gamma_L T_L A_1(t) + \gamma_R T_R A_N(t)\}], \\
J_{L4} &= 4\gamma_L T_L K_B^2[\delta(t)\{\gamma_L T_L A_1(t) + \gamma_R T_R A_N(t)\} + \gamma_L T_L\{\frac{1}{4}\dot{G}_{11}^2(0)\}] \,. \quad (4.68)
\end{aligned}$$

Collecting all the expressions for J's from Eqs. (4.67) and (4.68) in Eq. (4.63) and subtracting $\langle j_{1,L}\rangle^2$ we finally obtain

$$\begin{aligned}
C_{\Delta T}(t) &= 4\gamma_L T_L K_B^2\{\gamma_L T_L A_1(0) + \gamma_R T_R A_N(0)\}\delta(t) \\
&- 8{\gamma_L}^2 K_B^2[\{\gamma_L T_L A_1(t) + \gamma_R T_R A_N(t)\} \times \{T_L\gamma_L A_1(t) + (2T_L - T_R)\gamma_R A_N(t)\}] \,, \\
&= 4\gamma_L T_L K_B^2\{\gamma_L T_L A_1(0) + \gamma_R T_R A_N(0)\}\delta(t) - g_{\Delta T}(t) \quad (4.69) \\
\text{where } g_{\Delta T}(t) &= 8{\gamma_L}^2 K_B^2[\{\gamma_L T_L A_1(t) + \gamma_R T_R A_N(t)\} \\
&\times \{T_L\gamma_L A_1(t) + (2T_L - T_R)\gamma_R A_N(t)\}] \,, \quad (4.70)
\end{aligned}$$

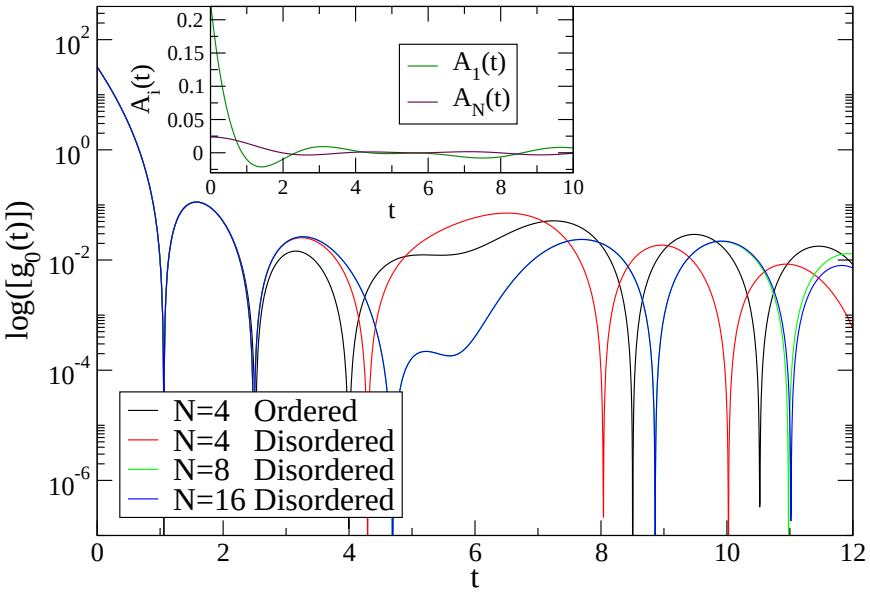

Figure 4.1: Plots of $[g_0(t)]$ vs. t for $N = 4$ and $N = 8$. The parameters for the figure are $T_L = 2.0, T_R = 2.0, k = 1.0, k_0 = 0.0, k' = 0.0, \gamma_L = \gamma_R = 2.5$ and $\Delta = 0.4$. Here $[g_0(t)]$ denotes disorder averaged $g_0(t)$. The average is done over 100 disorder realisations. Inset shows the plots of $A_1(t)$ and $A_N(t)$ for $N = 8$ for a single disorder configuration.

and we have used the identity in Eq. (4.55). From the above expression of $g_{\Delta T}(t)$ we note that $g_0(t)$ is always positive. Thus we have obtained a closed form expression for the non-equilibrium current-current auto-correlation function expressed in terms of the Green's function for a disordered harmonic chain of length N. The delta function appearing in the above equation is purely due to the white nature of the noises. More generally one can define the current operator on any bond on the harmonic chain. However the detailed form of the bond-correlation function is quite different from that of the boundary-correlation function. The notable difference that we find is the absence of the δ-function peak. We have verified that the integral of bond-correlation agrees with the value for the boundary-correlation.

4.5.4 Numerical results

In this section we plot the function $g_{\Delta T}(t) = 4\gamma_L T_L K_B^2\{\gamma_L T_L A_1(0) + \gamma_R T_R A_N(0)\}\delta(t) - C_{\Delta T}$. To find the functional form of $g_{\Delta T}(t)$ we need to know the functional forms of the functions $A_i(t)$. These functions can be obtained by Fourier transforming $\omega^2|G_{1i}(\omega)|^2$ as shown in Eq. (4.58).

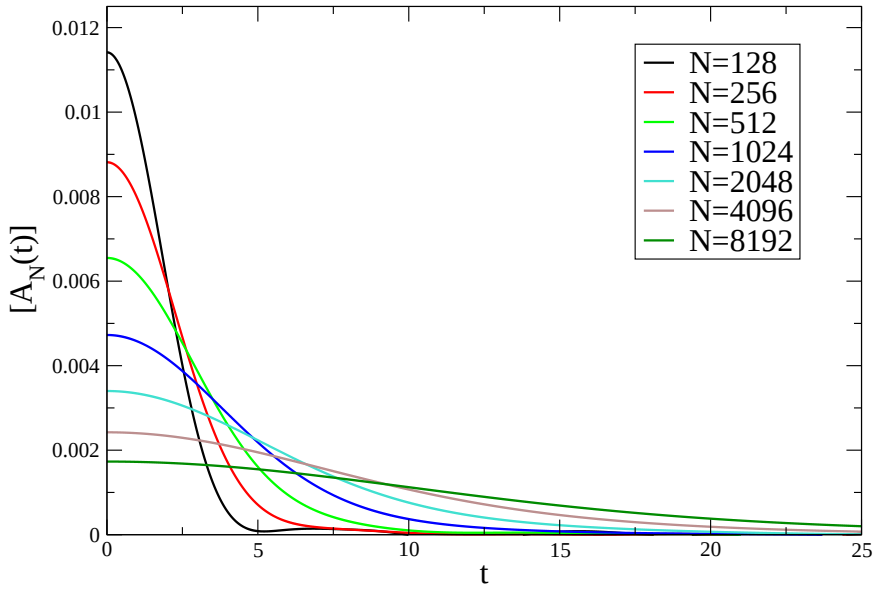

Figure 4.2: Plots of $[A_N(t)]$ vs. t for different system sizes. The parameters for the figure are same as those for Fig. 4.1. $\Delta = 0.4$.

For a general N-particle mass disordered chain it is difficult to find analytical expressions for the functions $|G^+_{ij}(\omega)|^2$. For the ordered case $G^+_{ij}(\omega)$ can be obtained analytically using the tridiagonal nature of the force matrix Φ (see for example Refn. [13]). However in case of disordered chain, $G^+_{1N}(\omega)$ and $G^+_{11}(\omega)$ can be obtained through transfer matrix approach in which $G^+_{1N}(\omega)$ and $G^+_{11}(\omega)$ are expressed in terms of a product of N random matrices [19]. We numerically evaluate $G^+_{1N}(\omega)$ and $G^+_{11}(\omega)$ using this transfer matrix approach. We observe that at large $\omega > \omega_d = \sqrt{\frac{km}{N\sigma^2}}$, $[|G^+_{1N}(\omega)|^2]$ decays as $e^{-aN\omega^2}$ (a is a positive constant) where $m = [m_l]$ and $\sigma^2 = [(m_l - m)^2]$. Here [...] denotes disorder average. This behaviour was proved analytically by Matsuda and Ishi [14] and was first observed numerically by Dhar [19]. A further observation made by Dhar was that for $\omega < \omega_d$ disordered average of $|G^+_{1N}(\omega)|^2$ is almost identical to that of an ordered chain for both the BCs (discussed in detail in chapter (2)). Another observation which we made is that for $\omega > \omega_m$ the function $|G^+_{11}(\omega)|^2$ decays as $1/\omega^4$, where ω_m is the maximum normal mode frequency. This $1/\omega^4$ behaviour can be easily obtained through the transfer matrix approach. For small frequencies disorder average of $|G^+_{11}(\omega)|^2$ oscillates with ω and is again identical to that of ordered chain. Here we make use of these observations.

After integrating Eq. (4.58) numerically, we obtain $A_i(t)$ and $G_{ij}(t)$ and hence $g_0(t)$ for different system sizes with different disorder configurations. In Fig. 4.1 we plot $[g_{\Delta T}(t)]$ versus t for system sizes $N = 4,\ 8$ and 16 with free BC. We observe that the correlation functions for two system sizes remain almost identical at short times and start being different significantly after some time scale. These observations can be made by looking at the dominant contributions of $\omega^2|G^+_{1i}(\omega)|^2$ in the integrand of Eq. (4.58) for fixed t. At large ω the function $|G^+_{1N}(\omega)|^2$ decays as $e^{-aN\omega^2}$ (a is a positive constant)[14, 19] whereas $|G^+_{11}(\omega)|^2$ decays as $1/\omega^4$. At small frequencies both $G^+_{1N}(\omega)$ and $G^+_{11}(\omega)$ are oscillating functions of ω and the frequency of oscillation increases with system size N. As a result $A_1(t)$ is independent of system size N at small times and starts depending on N after some time scale, where contribution from small ω becomes important. Whereas, in case of $A_N(t)$, only a small range of ω contributes to the Fourier transform of $\omega^2|G^+_{1N}(\omega)|^2$(Eq. (4.58)). For large N, at small times $A_1(t)$ is much larger that $A_N(t)$ and contributes most in $g_0(t)$, which makes $g_0(t)$ to be independent of N at small times. Inset in Fig. 4.1 compares $A_1(t)$ and $A_N(t)$ for $N = 8$. In the next paragraph we will see that physically interesting quantities like current, fluctuations in current in NESS are related to the time integral of $C_{\Delta T}(t)$ and this integral depends only on $A_N(t)$, though $A_1(t)$ has dominant contribution in the correlation function itself. Hence it is more relevant to see the behaviour of $A_N(t)$ with system size N. In Fig. 4.2 we plot $[A_N(t)]$ for different system sizes. Here we prefer to give plots of disorder-averaged quantities.

Let $Q(\tau) = \int_o^\tau dt\, j_{1,L}(t)$ be the heat transfer in duration τ from left reservoir to the system. Using stationarity property of the correlation function it is easy to show that the 2^{nd} order cumulant of $Q(\tau)$ is related to $C_{\Delta T}(t)$ as

$$\lim_{\tau\to\infty} \frac{\langle Q^2(\tau)\rangle_c}{\tau} = \int_0^\infty dt C_{\Delta T}(t). \tag{4.71}$$

Now integrating the expression of $C_{\Delta T}(t)$ given in Eq. (4.69) from 0 to ∞ and again using the identity in Eq.(4.55) we get

$$\int_0^\infty dt C_{\Delta T}(t) \;=\; 2\gamma_L\gamma_R T_L T_R K_B^2 A_N(0) + 8\gamma_L^2\gamma_R^2 K_B^2 (T_L - T_R)^2 \int_0^\infty dt\, A_N^2(t)\,. \tag{4.72}$$

In the frequency space the Eq. (4.72) can be written as an integration over ω of the transmission coefficient $\mathcal{T}(\omega)$ defined in Eq. (4.61) and we obtain

$$\int_0^\infty dt C_{\Delta T}(t) = \frac{K_B^2 T_L T_R}{2\pi} \int_0^\infty d\omega\, \mathcal{T}(\omega) + \frac{K_B^2 (T_L - T_R)^2}{4\pi} \int_0^\infty d\omega\, \mathcal{T}^2(\omega)\,. \quad (4.73)$$

This expression matches with the expression given in [100] for quantum mechanical systems in the high temperature limit. Now if we put $T_L = T_R = T$ in the expression in Eq. (4.72) and use Eq.(4.56) we get a relation between the current in the non-equilibrium steady state and the equilibrium correlation function similar to the GK relation given in Eq. (4.20) of the previous section

$$\int_0^\infty dt C_0(t) = \frac{K_B^2 T^2}{2\pi} \int_0^\infty d\omega\, \mathcal{T}(\omega) = K_B T^2 \frac{\mathcal{J}}{(T_L - T_R)}, \quad (4.74)$$

where $C_0(t)$ is the equilibrium auto-correlation function for the open system. The inset of Fig. 4.3 shows the system size dependence of the disorder average of current.

In general for large system sizes $[\mathcal{J}]$ and $[\frac{\langle Q^2(\tau)\rangle_c}{\tau}]$ scale with N as $N^{-\beta}$ and $N^{-\alpha}$ respectively. Using the frequency dependence of $T(\omega) = [\mathcal{T}(\omega)]$ and $[\mathcal{T}^2(\omega)]$ one can predict the values of α and β for different BC's. By computing $[\mathcal{J}]$ in NESS, several authors have already studied asymptotic size dependence of $[\mathcal{J}]$. Rubin and Greer [101] obtained $\beta = 1/2$ for free BC, which was latter proved rigorously by Verheggen[102]. Casher and Lebowitz [17] studied the same model and obtained a lower bound for $[\mathcal{J}] \geq N^{-3/2}$ and simulations by Rich and Vischer [103] confirmed the exponent to be $\beta = 3/2$. Later Dhar[19] obtained $\mathcal{J}$ for both the boundary conditions using Langevin Equation and Green Function approach and obtained $\beta = 1/2$ for free BC and $\beta = 3/2$ for fixed BC. Here we follow the same procedure described in [19] to find the asymptotic size dependence of $[\frac{\langle Q^2(\tau)\rangle_c}{\tau}]$ from the expression given in Eq. (4.73).

We numerically observe that for both the BCs $[\mathcal{T}^2(\omega)]$ is much smaller than $T(\omega)$ for each N. Hence, in determining the asymptotic N dependence, dominant contribution comes from the integration of $T(\omega)$ over ω. To determine α, we use the fact (discussed in the first paragraph of this section) that for ω greater than $\omega_d \sim N^{-1/2}$, $T(\omega)$ decays exponentially

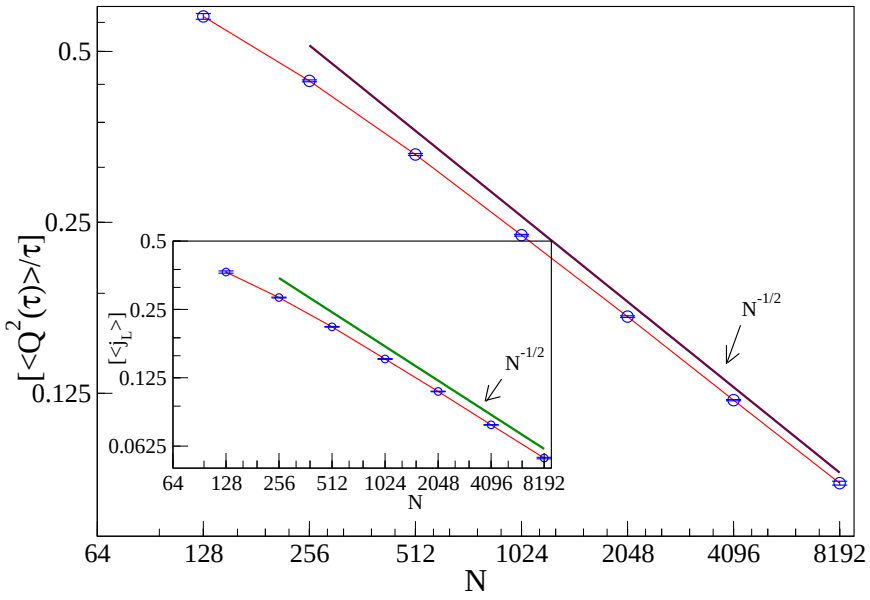

Figure 4.3: This figure shows the dependence of non-equilibrium current fluctuation on system size for free BC. The parameters for the figure are same as those for Fig. 4.1 except $T_L = 3.0$ and $T_R = 2.0$. Inset shows the dependence of non-equilibrium current on system size for free BC. Disorder average is taken over 100 different disorder realizations. Standard deviation corresponding to each point is smaller that the size of the point symbol.

as $e^{-aN\omega^2}$, whereas for $\omega < \omega_d$, $T(\omega)$ is almost identical to $\mathcal{T}_o(\omega)$ of an ordered chain. It is shown in chapter (3) shown that transmission coefficient of an ordered chain, denoted by $\mathcal{T}_o(\omega)$, is independent of ω for free BC and goes as ω^2 for fixed BC. Now putting these forms of $\mathcal{T}_o(\omega)$ and integrating up to $\omega_d \sim N^{-1/2}$ we get $\alpha = 1/2$ for free BC and $3/2$ for fixed BC. We see that the asymptotic size dependence of current fluctuation is same as that of NESS current. We numerically evaluate the RHS of Eq. (4.72) for free BC and obtain $\frac{\langle Q^2(\tau)\rangle_c}{\tau}$ for $\tau \to \infty$ for different system sizes. In Fig. 4.3 we plot $[\frac{\langle Q^2(\tau)\rangle_c}{\tau}]$ versus system size N, which shows that the fluctuation in current scales with system size as $N^{-1/2}$, when both ends of the chain are free. In the pinned case, since there are no low frequency modes, $T(\omega)$ decays exponentially and hence fluctuations in current decay exponentially with N.

4.6 Conclusions

In this chapter we have derived an exact expression for the linear response conductance in a system connected to heat baths. Our results are valid in arbitrary dimensions and have been derived both for a solid where particles execute small displacements about fixed lattice positions as well as for a fluid system where the motion of particles is unrestricted, and various heat bath models have been considered. We also have given an expression for the boundary current-current correlation for a one dimensional mass-disordered harmonic system in NESS. The correlation function has been expressed in terms of the phonon Green's functions which are easy to evaluate numerically. We show that the integration of equilibrium correlation function gives current satisfying the finite size open system Green-Kubo formula whereas the integration of non-equilibrium correlation function gives information about current fluctuation in the NESS.

The important differences with the usual Green-Kubo formula are worth noting. In the present formula, one does not need to first take the limit of infinite system size; the result is valid for finite systems. The fact that a sensible answer is obtained even for a finite system (unlike the case for the usual Green-Kubo formula) is because here we are dealing with an open system. Secondly the correlation function here has to be evaluated *not* with Hamiltonian dynamics, but for an open system evolving with heat bath dynamics. Finally we note that unlike the usual derivation of the Green-Kubo formula where the assumption of local thermal equilibrium is crucial, the present derivation requires no such assumption. The results are thus valid even for integrable Hamiltonian models, the only requirement being that they should attain thermal equilibrium when coupled to one or more heat reservoirs all at the same temperature.

Our derivation here is based on using both the microscopic equations of motion and also the equation for the phase space distribution. The broad class of systems and heat baths for which we have obtained our results strongly suggests that they are valid whenever detailed balance is satisfied.

4.7 appendix

4.7.1 Proof of Eq. [4.55]

Let us first define few quantities:

$$\tilde{G} \;=\; M^{\frac{1}{2}} G M^{\frac{1}{2}},\;\; \tilde{\Gamma} = M^{-\frac{1}{2}}\Gamma M^{-\frac{1}{2}} \;\text{ and }\; \tilde{\Phi} = M^{-\frac{1}{2}}\Phi M^{-\frac{1}{2}}$$

Using this above definitions Eq. (4.50) can be written as

$$\ddot{\tilde{G}}(t) + \tilde{\Gamma}\dot{\tilde{G}}(t) + \tilde{\Phi}\tilde{G}(t) = 0. \tag{4.75}$$

We use the above equation to evaluate $\frac{d}{dt'}[\dot{\tilde{G}}^T(t')\dot{\tilde{G}}(t'+t)]$ and get

$$\frac{d}{dt'}[\dot{\tilde{G}}^T(t')\dot{\tilde{G}}(t'+t)] \;=\; -2\dot{\tilde{G}}^T(t')\tilde{\Gamma}\dot{\tilde{G}}(t'+t) + \frac{d}{dt'}[\tilde{G}^T(t')\tilde{\Phi}\tilde{G}(t'+t)].$$

Now integrating both side of the above equation over $t' = 0$ to $t' = \infty$ we get

$$\dot{\tilde{G}}(t) = 2\int_0^\infty dt' \dot{\tilde{G}}^T(t')\tilde{\Gamma}\dot{\tilde{G}}(t'+t). \tag{4.76}$$

To the above equation we have used the following: $\dot{G}(0) = M^{-1}$, $G(0) = 0$, $G(t) \to 0$ as $t \to \infty$. Now we know that $\Gamma_{ij} = (\frac{\gamma_L}{m_1}\delta_{i1} + \frac{\gamma_R}{m_N}\delta_{iN})\delta_{ij}$. Taking $(11)^{th}$ element on the both side of the matrix equation (4.76) we get

$$\begin{aligned}\frac{\dot{G}_{11}(t)}{2} \;&=\; \int_0^\infty dt'[\gamma_L \dot{G}_{11}(t')\dot{G}_{11}(t'+t) + \gamma_R \dot{G}_{1N}(t')\dot{G}_{1N}(t'+t)] \\ &=\; \gamma_L A_1(t) + \gamma_R A_N(t).\end{aligned} \tag{4.77}$$

4.7.2 Expressions of K_1s

$$\begin{aligned}K_1^{(1)}(t_1,t_2,t_3,t_4,t) \;=\; &[\gamma_L^2 T_L^2 \dot{G}_{11}(t-t_1)\dot{G}_{11}(t-t_2)\dot{G}_{11}(-t_3)\dot{G}_{11}(-t_4) \\ &+\gamma_R^2 T_R^2 \dot{G}_{1N}(t-t_1)\dot{G}_{1N}(t-t_2)\dot{G}_{1N}(-t_3)\dot{G}_{1N}(-t_4) \\ &+\gamma_L T_L \gamma_R T_R\{\dot{G}_{1N}(t-t_1)\dot{G}_{1N}(t-t_2)\dot{G}_{11}(-t_3)\dot{G}_{11}(-t_4) \\ &+\dot{G}_{11}(t-t_1)\dot{G}_{11}(t-t_2)\dot{G}_{1N}(-t_3)\dot{G}_{1N}(-t_4)\}],\end{aligned}$$

$$
\begin{aligned}
K_1^{(2)}(t_1,t_2,t_3,t_4,t) &= [\gamma_L^2 T_L^2 \dot{G}_{11}(t-t_1)\dot{G}_{11}(t-t_2)\dot{G}_{11}(-t_3)\dot{G}_{11}(-t_4) \\
&\quad +\gamma_R^2 T_R^2 \dot{G}_{1N}(t-t_1)\dot{G}_{1N}(t-t_2)\dot{G}_{1N}(-t_3)\dot{G}_{1N}(-t_4) \\
&\quad +\gamma_L T_L \gamma_R T_R \{\dot{G}_{1N}(t-t_1)\dot{G}_{11}(t-t_2)\dot{G}_{1N}(-t_3)\dot{G}_{11}(-t_4) \\
&\quad +\dot{G}_{11}(t-t_1)\dot{G}_{1N}(t-t_2)\dot{G}_{11}(-t_3)\dot{G}_{1N}(-t_4)\}]
\end{aligned}
$$

and

$$
\begin{aligned}
K_1^{(3)}(t_1,t_2,t_3,t_4,t) &= [\gamma_L^2 T_L^2 \dot{G}_{11}(t-t_1)\dot{G}_{11}(t-t_2)\dot{G}_{11}(-t_3)\dot{G}_{11}(-t_4) \\
&\quad +\gamma_R^2 T_R^2 \dot{G}_{1N}(t-t_1)\dot{G}_{1N}(t-t_2)\dot{G}_{1N}(-t_3)\dot{G}_{1N}(-t_4) \\
&\quad +\gamma_L T_L \gamma_R T_R \{\dot{G}_{11}(t-t_1)\dot{G}_{1N}(t-t_2)\dot{G}_{1N}(-t_3)\dot{G}_{11}(-t_4) \\
&\quad +\dot{G}_{1N}(t-t_1)\dot{G}_{11}(t-t_2)\dot{G}_{11}(-t_3)\dot{G}_{1N}(-t_4)\}].
\end{aligned}
$$

5 Large deviations in transport processes

In this chapter our interest is in predicting probabilities of rare fluctuations in transport processes. A number of interesting results have been obtained recently on large fluctuations away from typical ones in nonequilibrium systems. These results include various fluctuation theorems[104, 105, 106, 107, 108, 109, 100] and the Jarzynski relation [110]. In the context of transport one typically considers an observable, say Q, such as the total number of particles or heat transferred across an object with an applied chemical potential or temperature difference respectively. For a given observation time τ this is a stochastic variable and one is naturally interested in its probability distribution $R(Q,\tau)$. Various general results that have been obtained for $R(Q,\tau)$ give some quantitative measure of the probability of rare fluctuations. Usually, for large τ the probabilities of large fluctuations show scaling behavior $P(Q,\tau) \sim e^{-\tau F(Q/\tau)}$. The function $F(q)$ is called the large deviation function which provides informations about the tails of the distribution *i.e.* the probabilities of large fluctuations. For a few model systems exact results have been obtained for the large deviation function $F(q)$ [108, 109, 100]. Very often the characteristic function of $P(Q,\tau)$, given by $\langle e^{-\lambda Q}\rangle$ also has a similar scaling $\langle e^{-\lambda Q}\rangle \sim e^{\tau\mu(\lambda)}$, where $\mu(\lambda)$ is defined as $\mu(\lambda) = \lim_{\tau\to\infty} \tau^{-1} \ln\langle e^{-\lambda Q}\rangle$. The large deviation function $F(q)$ is related to $\mu(\lambda)$ by a Legendre transformation. Often it is easier to calculate $\mu(\lambda)$ rather than $F(q)$ directly. One can then obtain $F(q)$ from $\mu(\lambda)$ by doing Legendre transform. In the first section of this chapter we calculate $\mu(\lambda)$ corresponding to the distribution of heat flow across a harmonic chain. We express $\mu(\lambda)$ as an integration of some function of the phonon transmission coefficient $\mathcal{T}(\omega)$.

Computing the tails of $P(Q,\tau)$ for any system is also difficult both in experiments and in

computer simulations, since the generation of rare events requires a large number of trials. Recently an efficient algorithm has been proposed [111] to compute the function $\mu(\lambda)$. In the second section of this chapter we present an algorithm for generating rare events very often and computing their probabilities. The algorithm proposed here is complementary to the one discussed in [111] in the sense that we obtain $P(Q,\tau)$ directly whereas [111] obtains $\mu(\lambda)$ directly. However, as has been pointed out in [112] there may be problems in obtaining the tails of $\mu(\lambda)$ using the algorithm of [111]. Our algorithm, based on the idea of importance sampling, computes $P(Q,\tau)$ for any given τ and accurately reproduces the tails of the distribution. Algorithms based on importance sampling have earlier been proposed for the study of transition rate processes [113, 114, 115].

This chapter is organised as follows. In Sec.(5.1) we present the calculation of $\mu(\lambda)$ for the heat flow across a harmonic system. In the subsection (5.1.1) we calculate $\mu(\lambda)$ for a harmonic chain of length N. Then in subsection (5.1.2) we discuss the case of single Brownian particle as an example with small discussion on the case of two particles connected by harmonic spring. In the last section (5.2) we present the algorithm of finding the probabilities of rare events. First we develop the algorithm on general basis and we apply this algorithm to different transport processes in the next few subsections.

5.1 Large deviation function of heat flow in harmonic chain

We consider a mass disordered harmonic chain of N particles described by the Hamiltonian H :

$$H = \sum_{l=1}^{N} \frac{1}{2} m_l v_l^2 + \frac{1}{2} \sum_{l=1}^{N} \sum_{m=1}^{N} \Phi_{lm} x_l x_m \tag{5.1}$$

where x_l is displacement of l^{th} particle about its equilibrium position, v_l is its velocity, m_l is its mass and Φ represents the force constant matrix. The particles 1 and N are connected to two white noise heat baths of temperatures T_L and T_R respectively. The equation of motion

of the l^{th} particle is given by [19]

$$\dot{x}_l = v_l \; ; \qquad m_l \dot{v}_l = -\sum_{m=1}^{N} \Phi_{lm} x_m + \delta_{l,1}[-\gamma_L v_1 + \eta_L] + \delta_{l,N}[-\gamma_R v_N + \eta_R \,]$$
$$\text{where} \quad l = 1, 2...N \;\text{ and }\; x_0 = x_{N+1} = 0 \tag{5.2}$$

and $\eta_{L,R}(t)$ are Gaussian noise terms with zero mean and related to the dissipative terms through the relations

$$\begin{aligned} \langle \eta_{L,R}(t)\eta_{L,R}(t')\rangle &= 2\gamma_{L,R}T_{L,R}\delta(t-t') \\ \langle \eta_L(t)\eta_R(t')\rangle &= 0, \quad \langle \eta_{L,R}(t)\rangle = 0. \end{aligned} \tag{5.3}$$

Since the potentials are quadratic in positions, it is convenient to write the set of equations in Eq. (5.2) in the form of linear matrix equation as follows:

$$\dot{\boldsymbol{X}} = \boldsymbol{V}, \;\; \boldsymbol{M}\dot{\boldsymbol{V}} = -\boldsymbol{\Gamma V} - \Phi \boldsymbol{X} + \eta(t), \tag{5.4}$$

where $\boldsymbol{X} = (x_1, x_2, ..., x_N)^T$, $\boldsymbol{V} = (v_1, v_2, ..., v_N)^T$ and $\boldsymbol{M} = \text{diag}(m1, m2, \ldots, m_N)$ is the diagonal mass matrix. The diagonal matrix $\boldsymbol{\Gamma}$ describes the dissipation, $\boldsymbol{\Gamma}_{i,j} = \delta_{i,j}(\delta_{i,1}\gamma_L + \delta_{i,N}\gamma_R)$, and $\boldsymbol{\eta}_i(t) = \delta_{i,1}\eta_L(t) + \delta_{i,N}\eta_R(t)$. In some time duration τ there will be a net amount of heat transfer $Q(\tau)$ between the left reservoir and the system in the steady state. This is given by

$$Q(\tau) = \int_0^\tau [\eta_L(t) - \gamma_L v_1(t)] v_1(t)\, dt. \tag{5.5}$$

Clearly, $Q(\tau)$ is a random variable whose value depends on the realization of noise $\{\boldsymbol{\eta(t)} : 0 \le t \le \tau\}$ and on the initial condition. Here we are interested in the probability distribution of $Q(\tau)$ given that the initial conditions are chosen from the non-equilibrium steady state (NESS) of the system. We denote this distribution by $R(Q, \tau)$. We are mainly interested in probabilities of large fluctuations in Q for large τ ($\tau \to \infty$). Often it is difficult to obtain an analytical expression for the probability density function (pdf) $R(Q, \tau)$, but it is easier to find the characteristic function of $Q(\tau)$, defined as $\langle e^{-\lambda Q}\rangle = \int dQ\; exp(-\lambda Q)\; R(Q, \tau) = \widetilde{R}(\lambda, \tau)$.

Let the pdf of $Q(t)$ for given initial and final configurations of the system be denoted by $P(Q, U, t|U_0)$ where, $\boldsymbol{U} = [\boldsymbol{V}^T, \boldsymbol{X}^T]^T$ represents the state of the system *i.e.* velocities and

positions of all the particles at some time t. In some cases, for example harmonic chain with open boundaries, a steady state distribution does not exist with $\boldsymbol{U} = [\boldsymbol{V}^T, \boldsymbol{X}^T]^T$. In such cases one has to chose $\boldsymbol{U}$ properly, like for open boundary case $\boldsymbol{U} = [\boldsymbol{V}^T, x_2 - x_1, ..., x_N - x_{N-1}]^T$. The distribution $P(Q, U, t|U_0)$ satisfies the following Fokker-Planck equation :

$$\begin{aligned}\frac{\partial P}{\partial t} &= \Big[\sum_{l=1}^{2N} \frac{\partial}{\partial U_l}\frac{\langle \Delta U_l\rangle}{\Delta t} + \frac{\partial}{\partial Q}\frac{\langle \Delta Q\rangle}{\Delta t} + \sum_{l=1}^{2N}\sum_{m=1}^{2N}\frac{\partial^2}{\partial U_l \partial U_m}\frac{\langle \Delta U_l \Delta U_m\rangle}{\Delta t} \\ &+ \sum_{l=1}^{2N}\frac{\partial^2}{\partial U_l Q}\frac{\langle \Delta U_l \Delta Q\rangle}{\Delta t} + \frac{\partial^2}{\partial Q^2}\frac{\langle \Delta Q^2\rangle}{\Delta t}\Big] P(Q, U, t|U_0)\ ; \quad \text{with } \Delta t \to 0\ , \end{aligned} \tag{5.6}$$

where the moments are calculated using the Langevin equations (5.4) and heat equation given in Eq. (5.5). After calculating the moments we get

$$\begin{aligned}\frac{\partial P}{\partial t} &= \mathcal{L}_Q\ P(Q, U, t|U_0) \\ \text{where } \mathcal{L}_Q &= \sum_{l=1}^{N}\Big[\frac{\partial H}{\partial x_l}\frac{\partial}{\partial v_l} - \frac{\partial H}{\partial v_l}\frac{\partial}{\partial x_l}\Big] \\ &+ \gamma_L \frac{\partial}{\partial v_1} v_1 + \gamma_R \frac{\partial}{\partial v_N} v_N + (\gamma_L v_1^2 - \gamma_L T_L)\frac{\partial}{\partial Q} \\ &+ \gamma_L T_L \frac{\partial^2}{\partial v_1^2} + \gamma_R T_R \frac{\partial^2}{\partial v_N^2} + \gamma_L T_L v_1^2 \frac{\partial^2}{\partial Q^2} + 2\gamma_L T_L \frac{\partial^2}{\partial v_1 \partial Q} v_1. \end{aligned} \tag{5.7}$$

Let the characteristic function of Q corresponding to $P(Q, U, t|U_0)$ is defined as

$$\widetilde{P}(\lambda, U, t|U_0) = \langle e^{-\lambda Q}\delta(U(t) - U)\rangle_{U_0} = \int dQ\ exp(-\lambda Q)\ P(Q, U, t|U_0). \tag{5.8}$$

The evolution equation corresponding to $\widetilde{P}(\lambda, U, t|U_0)$ is obtained by Fourier transforming both sides of Eq. (5.7) and is given by

$$\begin{aligned}\frac{\partial \widetilde{P}}{\partial t} &= \mathcal{L}_\lambda\ \widetilde{P}(\lambda, U, t|U_0) \\ \text{where } \mathcal{L}_\lambda &= \sum_{l=1}^{N}\Big[\frac{\partial H}{\partial x_l}\frac{\partial}{\partial v_l} - \frac{\partial H}{\partial v_l}\frac{\partial}{\partial x_l}\Big] \\ &+ \gamma_L \frac{\partial}{\partial v_1} v_1 + \gamma_R \frac{\partial}{\partial v_N} v_N + (\gamma_L v_1^2 - \gamma_L T_L)\ \lambda \\ &+ \gamma_L T_L \frac{\partial^2}{\partial v_1^2} + \gamma_R T_R \frac{\partial^2}{\partial v_N^2} + \gamma_L T_L v_1^2 \lambda^2 + +2\gamma_L T_L \lambda \frac{\partial}{\partial v_1} v_1. \end{aligned} \tag{5.9}$$

The solution of the above equation can formally be written down in the eigenbases of the

Fokker-Planck operator $\mathcal{L}_\lambda$, and the large t behavior is dominated by the term having the largest eigenvalue $\mu(\lambda)$, i.e.,

$$\widetilde{P}(\lambda, U, t|U_0) \approx \chi(\boldsymbol{U}_0, \lambda)\Psi(\boldsymbol{U}, \lambda)\, \exp[t\, \mu(\lambda)] \tag{5.10}$$

where $\Psi(\boldsymbol{U}, \lambda)$ is the eigenfunction corresponding to the largest eigenvalue, i.e., $\mathcal{L}_\lambda \Psi(\boldsymbol{U}, \lambda) = \mu(\lambda)\Psi(\boldsymbol{U}, \lambda)$, and $\chi(\boldsymbol{U}_0, \lambda)$ is the projection of the initial state onto eigenstate corresponding to the eigenvalue $\mu(\lambda)$. The existence of a unique steady state of the system demands that for $\lambda = 0$ the largest eigenvalue $\mu(0) = 0$. Moreover, $\chi(\boldsymbol{U}_0, 0) = 1$ and $\Psi(\boldsymbol{U}, 0)$ is the steady state pdf, which is a Gaussian in our case with the covariance matrix $\lim_{t\to\infty}\langle \boldsymbol{U}\boldsymbol{U}^T\rangle$. Using Eq. (5.10), for large τ,

$$\widetilde{R}(\lambda, \tau) \approx g(\lambda)\, \exp[\tau\mu(\lambda)], \tag{5.11}$$

where $g(\lambda) = \int \chi(\boldsymbol{U}_0, \lambda)\Psi(\boldsymbol{U}_0, 0)\, d\boldsymbol{U}_0 \int \Psi(\boldsymbol{U}, \lambda)\, d\boldsymbol{U}$, and we note that $g(0) = 1$.

The large τ behavior of the pdf $R(Q, \tau)$ can be obtained by the saddle-point approximation of the integral

$$R(Q, \tau) = (2\pi i)^{-1} \int_{-i\infty}^{i\infty} \widetilde{R}(\lambda, \tau) e^{\lambda Q}\, d\lambda,$$

while using the approximation given by Eq. (5.11) for the integrand. This leads to the large deviation form of the pdf, $R(Q, \tau) \sim \exp[-\tau\, F(Q/\tau)]$, meaning

$$\lim_{\tau\to\infty} \tau^{-1} \ln P(q\tau, \tau) = -F(q).$$

The large deviation function is given by, $F(q) = -[\mu(\lambda^*) + \lambda^* q]$, with $\lambda^*(q)$ implicitly given by the saddle point equation $\mu'(\lambda^*) = -q$, provided that $g(\lambda)$ is analytic along the real λ in the region $[0, \lambda^*]$, so that, (i) $g(\lambda)$ can be neglected from the above saddle-point calculation as sub-leading contribution, and (ii) the contour of the integration can be deformed smoothly through saddle point λ^*. In this case, if $\mu(\lambda)$ possesses the symmetry $\mu(\lambda) = \mu(a - \lambda)$ then the so-called fluctuation relation $F(q) - F(-q) = -aq$ is verified. On the other hand, if $g(\lambda)$ possesses any singularity in $[0, \lambda^*]$, then one needs to include $g(\lambda)$ in the saddle point calculation, and in that case even though $\mu(\lambda)$ possesses above mentioned symmetry, $F(q)$

may not satisfy the fluctuation relation. This has been discussed in great details in [117, 118, 109]. We shall not elaborate on this issue here. Rather, the aim is to obtain an exact expression for $\mu(\lambda)$, which according to Eq. (5.11),

$$\mu(\lambda) = \lim_{\tau\to\infty} \frac{1}{\tau} \ln\langle e^{-\lambda Q}\rangle. \tag{5.12}$$

Our main result is the exact expression

$$\mu(\lambda) = -\frac{1}{4\pi}\int_{-\infty}^{\infty} d\omega\, \ln\left[1 + \mathcal{T}(\omega)T_L T_R \lambda(\Delta\beta - \lambda)\right], \tag{5.13}$$

where $\Delta\beta = T_R^{-1} - T_L^{-1}$, and

$$\mathcal{T}(\omega) = 4\gamma_L\gamma_R\omega^2 G_{1,N}(\omega)G_{1,N}(-\omega), \tag{5.14}$$

$$\text{with} \quad G(\omega) = [\mathbf{\Phi} - \omega^2 \boldsymbol{M} + i\omega\mathbf{\Gamma}]^{-1}. \tag{5.15}$$

The function $\mathcal{T}(\omega)$ was introduced earlier in Eq.(2.38) and is the phonon transmission coefficient. From Eq. (5.13), we note that $\mu(0) = 0$ as required. It is also evident that Eq. (5.13) possesses the symmetry $\mu(\lambda) = \mu(\Delta\beta - \lambda)$. In general, if the operator $\mathcal{L}_\lambda$ and its adjoint $\mathcal{L}_\lambda^\dagger$ possess the symmetry $\mathcal{L}_\lambda^\dagger = \mathcal{L}_{a-\lambda}$, then it is easily shown that $\mu(\lambda) = \mu(a-\lambda)$, without requiring its explicit form. Even if after doing a similarity transformation the operator $\mathcal{L}_\lambda$ possess the symmetry $\mathcal{L}_\lambda^\dagger = \mathcal{L}_{a-\lambda}$, then also $\mu(\lambda)$ has the above symmetry. However, this is not the case for the system discussed here. In fact, even for the simplest case of just one particle connected to two heat reservoirs [109], the Fokker-Planck operator does not possesses the above mentioned symmetry. Although, in this case the Fokker-Planck operator (of one variable) can be transformed to a Hermitian operator of quantum harmonic oscillator, where the potential remains invariant under $\lambda \to (\Delta\beta - \lambda)$. We are not aware of such a transformation for the system having more than one particles discussed in this chapter.

Using Eq. (5.13), one can immediately find the expression for the average energy current,

$$\lim_{\tau\to\infty} \frac{\langle Q\rangle}{\tau} = -\mu'(0) = \frac{T_L - T_R}{4\pi}\int_{-\infty}^{\infty} d\omega\, \mathcal{T}(\omega).$$

which is in agreement with previous results [19, 17, 15, 69]. It is clear from the above expres-

sion that the average current is sum of the different contributions for different phonon modes which is determined by the individual phonon transmission coefficient $\mathcal{T}(\omega)$. In the next few sections we present the derivation of our results. We start by calculating $\widetilde{P}(\lambda, \boldsymbol{U}, \tau|, \boldsymbol{U}_0)$.

5.1.1 Derivation

We first obtain an expression for $\widetilde{P}(\lambda, \boldsymbol{U}, \tau|, \boldsymbol{U}_0)$, from which we get $\chi(\boldsymbol{U}_0, \lambda)$ $\Psi(\boldsymbol{U}, \lambda)$ and $\mu(\lambda)$ after proper identification with Eq. (5.10). From Eq. (5.8) we see that $\widetilde{P}(\lambda, \boldsymbol{U}, \tau|, \boldsymbol{U}_0)$ is actually noise average of $e^{-\lambda Q}\delta(X - X(\tau))\delta(V - V(\tau))$, where noises are chosen from a Gaussian distribution. As usual replacing the δ functions by their integral representations

$$\begin{aligned}
\delta(X - X(\tau)) &= \int .... \int \frac{d\sigma}{(2\pi)^N} e^{i\sigma.(X - X(\tau))}, \text{ where } \sigma = (\sigma_1, \sigma_2, ...\sigma_N)^T \\
\delta(V - V(\tau)) &= \int ... \int \frac{d\rho}{(2\pi)^N} e^{i\rho.(V - V(\tau))}, \text{ where } \rho = (\rho_1, \rho_2, ...\rho_N)^T. \qquad (5.16)
\end{aligned}$$

we write

$$\begin{aligned}
\widetilde{P}(\lambda, \boldsymbol{U}, \tau|, \boldsymbol{U}_0) &= \int ... \int \prod_{l=1}^{N} \frac{d\sigma_l}{2\pi} e^{i\sigma_l x_l} \prod_{l=1}^{N} \frac{d\rho_l}{2\pi} e^{i\rho_l v_l} \langle e^{A(\tau)} \rangle \\
\text{where, } A(\tau) &= -\lambda Q - i \sum_{l=1}^{N} [\sigma_l x_l(\tau) + \rho_l v_l(\tau)]. \qquad (5.17)
\end{aligned}$$

There are three steps to calculate $\langle e^A \rangle$.

- (i) At first, we express $X(\tau)$ and $V(\tau)$ in terms of noise configurations by solving the equations in (5.4) for given $X(0)$ and $V(0)$.
- (ii) Second, using these expressions of $X(\tau)$ and $V(\tau)$ we show that $Q(\tau)$ is quadratic in $\eta(t)$ and hence $A(\tau)$ has quadratic, linear and noise independent terms.
- (iii) Finally, we take average of e^A over noise configurations. Since $\eta(t)$ is Gaussian noise and $A(\tau)$ depends on the noise atmost quadratically, $\langle e^{A(\tau)} \rangle$ can be expressed as a Gaussian integral over noise variables.

It is more convenient to do the above procedure in the Fourier space, because while taking the noise average in the time domain one has to do a Gaussian path integration over noise

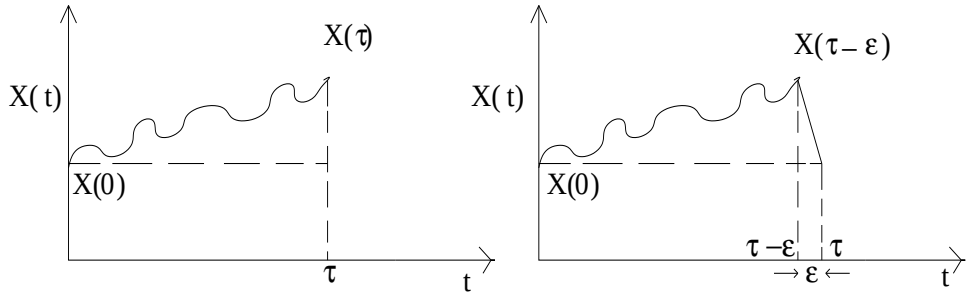

Figure 5.1: The function $X(t)$ is represented by a piece-wise continuous function.

configurations which are functions of continuous variable time t, whereas in the frequency space this path integral becomes product of Gaussian integrals over noise variables for each discrete Fourier mode. This will be clear after we define the Fourier transform rules.

The following defines the Fourier transform rules: let the Fourier transform of any function $h(t)$ defined over the interval $[0, \tau]$ be denoted by $\widetilde{h}(\omega)$. The relation between the Fourier transform pairs are defined by the following relations :

$$\widetilde{h}(\omega_k) = \frac{1}{\tau}\int_0^\tau h(t)\exp(-i\omega_k t)\,dt, \tag{5.18}$$

$$h(\tau) = \sum_{k=-\infty}^{\infty}\widetilde{h}(\omega_k)\,\exp(i\omega_k t), \quad \text{with } \omega_k = \frac{2\pi k}{\tau}. \tag{5.19}$$

So the noise configurations represented by $\{\eta(t) : 0 < t < \tau\}$, can now equivalently be described by the infinite sequence $\{\widetilde{\eta}(\omega_k) : k = -\infty... - 1.0, 1, ..\infty\}$ where $\widetilde{\eta}(\omega_k)$ denotes the Fourier transform of $\{\eta(t) : 0 < t < \tau\}$. Now we follow the three steps of calculating $\langle e^A \rangle$ as mentioned earlier.

First step: Let us denote the Fourier transforms of $X(t)$ and $V(t)$ by $\widetilde{X}(\omega_k)$ and $\widetilde{V}(\omega_k)$ respectively. After Fourier transforming Eqs. (5.4) and using these notations we get

$$\frac{\Delta X}{\tau} + i\omega_k\widetilde{\boldsymbol{X}}(\omega_k) = \widetilde{V}(\omega_k) \tag{5.20}$$

$$\boldsymbol{M}\frac{\Delta V}{\tau} + i\omega_k\boldsymbol{M}\widetilde{V}(\omega_k) = -\Gamma\widetilde{V}(\omega_k) - \Phi\widetilde{\boldsymbol{X}}(\omega_k) + \widetilde{\eta}(\omega_k), \tag{5.21}$$

$$\text{where, } \Delta X = X(\tau) - X_0, \quad \text{and} \quad \Delta V = V(\tau) - V_0. \tag{5.22}$$

Solving the above equations for $\widetilde{\boldsymbol{X}}(\omega_k)$ and $\widetilde{\boldsymbol{V}}(\omega_k)$ in terms of $\Delta X,\ \Delta V$ and $\widetilde{\boldsymbol{\eta}}$ we get :

$$\widetilde{\boldsymbol{X}} = G[\widetilde{\boldsymbol{\eta}} - \frac{1}{\tau}M\Delta V + \frac{1}{i\tau\omega_k}(\Phi - G^{-1})\Delta X], \tag{5.23}$$

$$\widetilde{\boldsymbol{V}} = G[i\omega_k\widetilde{\boldsymbol{\eta}} - \frac{i\omega_k}{\tau}M\Delta V + \frac{1}{\tau}\Phi\Delta X], \tag{5.24}$$

where,

$$\begin{aligned} X(\tau) &= \lim_{\epsilon\to 0}\sum_{k=-\infty}^{\infty}\widetilde{X}(\omega_k)\ \exp(-i\omega_k\epsilon) \\ V(\tau) &= \lim_{\epsilon\to 0}\sum_{k=-\infty}^{\infty}\widetilde{V}(\omega_k)\ \exp(-i\omega_k\epsilon). \end{aligned} \tag{5.25}$$

and G is given in Eq. (5.15). While representing the continuous function $\{X(t) : 0 \le t \le \tau\}$ in terms of Fourier series we have approximated the function $X(t)$ by a piecewise continuous function with $\epsilon \to 0$ as shown in the Fig. (5.1). Same holds for $V(\tau)$ also.

Using the above expressions for $\widetilde{\boldsymbol{X}}(\omega_k)$ and $\widetilde{\boldsymbol{V}}(\omega_k)$, one can easily show that for large τ

$$X(\tau) = \lim_{\epsilon\to 0}\sum_{k=-\infty}^{\infty}G\widetilde{\boldsymbol{\eta}}\exp(-i\omega_k\epsilon) \tag{5.26}$$

$$X(\tau) = \lim_{\epsilon\to 0}\sum_{k=-\infty}^{\infty}i\omega G\widetilde{\boldsymbol{\eta}}\exp(-i\omega_k\epsilon), \tag{5.27}$$

where we have used the fact that other terms of the form

$$\frac{1}{\tau}\sum_{k=-\infty}^{\infty}G(\omega_k)f(\Delta X, \Delta V, M, \omega_k)\exp(-i\omega_k\epsilon) \tag{5.28}$$

go to zero in the limit $\tau \to \infty$. It can easily be seen by converting the above summation into a contour integral on a semicircle in the lower half plane and noting that all the poles of $G(\omega_k)$ lie in the upper half plane.

Thus we have expressed all relevant variables in terms of new noise variables $\widetilde{\eta}_{L,R}(\omega_k)$, which have the following correlations:

$$\langle\widetilde{\eta}_\alpha(\omega_k)\widetilde{\eta}_{\alpha'}(\omega_k')\rangle = 2\delta_{\alpha,\alpha'}\frac{\gamma_\alpha T_\alpha}{\tau}\delta_{\omega_k,-\omega_k'}\ \text{ with, }\ \alpha,\alpha' = L,R. \tag{5.29}$$

Now we follow the remaining two [(ii) and (iii)] steps of calculating $\langle e^{A(\tau)}\rangle$. For convenience of calculation, from now onwards we suppress the subscript k in ω_k.

Second step : With the help of Eq. (5.19) we convert the two time integrals over $[0, \tau]$ in Eq. (5.5) into two infinite series summations over ω and finally get

$$Q(\tau) = \tau \sum_{k=-\infty}^{\infty} \Big[\widetilde{\eta}_L(\omega)\widetilde{v}_1(-\omega) - \gamma_L \widetilde{v}_1(\omega)\widetilde{v}_1(-\omega)\Big]. \tag{5.30}$$

Putting this expression of $Q(\tau)$ and expressions of $X(\tau)$ and $V(\tau)$ from Eqs. (5.26) and (5.27) into Eq. (5.17) we get

$$\begin{aligned} A(\tau) &= -\lambda\tau \sum_{k=-\infty}^{\infty} \Big[\{\widetilde{\eta}_L(\omega)\widetilde{v}_1(-\omega) - \gamma_L \widetilde{v}_1(\omega)\widetilde{v}_1(-\omega)\} \\ &\quad + i\big[g_1(\omega)\widetilde{\eta}_L(\omega) + g_2(\omega)\widetilde{\eta}_R(\omega)\big]e^{-i\omega\epsilon}\Big] \ . \qquad (5.31) \\ \text{where, } v_1(\omega) &= i\omega(G_{11}\widetilde{\eta}_L(\omega) + G_{1N}\widetilde{\eta}_R(\omega))e^{-i\omega\epsilon} + \frac{1}{\tau}\sum_{m=1}^{N} G_{1m} f_m(\omega) \qquad (5.32) \\ \text{with } f_m(\omega) &= \sum_j \Phi_{mj}\Delta X_j - i\omega M_m \Delta V_m. \end{aligned}$$

In the above we have introduced three new functions $g_1(\omega)$, $g_2(\omega)$ and $g(\omega)$ which are given by

$$\begin{aligned} g_1(\omega) &= \sum_{m=1}^{N} G_{m1}(\sigma_m + i\omega\rho_m), \\ g_2(\omega) &= \sum_{m=1}^{N} G_{mN}(\sigma_m + i\omega\rho_m) \\ \text{and} \qquad g(\omega) &= \sum_{m=1}^{N} G_{1m} f_m \qquad \text{respectively.} \end{aligned}$$

Now we show that $A(\tau)$ can be expressed as a sum of quadratic, linear and noise independent terms. Before doing that we introduce some more notations. We denote real and imaginary parts of $\widetilde{\eta}_{L,R}(\omega)$ as follows:

$$\widetilde{\eta}_L(\omega) = \xi_{L1}(\omega) - i\xi_{L2}(\omega) \ \text{ and } \ \widetilde{\eta}_R(\omega) = \xi_{R1}(\omega) - i\xi_{R2}(\omega) \tag{5.33}$$

where each $\xi's$ are independent Gaussian noise with zero mean and have the following correlations

$$\langle \xi_{Li}(\omega)\xi_{Lj}(\omega')\rangle = \delta_{ij}\frac{D_L}{\tau}[\delta_{\omega,\omega'} + \delta_{\omega,-\omega'}]$$

$$\begin{aligned}
\langle \xi_{Ri}(\omega)\xi_{Rj}(\omega')\rangle &= \delta_{ij}\frac{D_R}{\tau}[\delta_{\omega,\omega'} + \delta_{\omega,-\omega'}] \\
\langle \xi_{Li}(\omega)\xi_{Rj}(\omega')\rangle &= 0, \\
\text{where, } D_L = \gamma_L T_L \quad &\text{and} \quad D_R = \gamma_R T_R.
\end{aligned} \tag{5.34}$$

From Eq. (5.32) we note that $v_1(\omega)$ is linear in $\xi' s$. Hence it is clear from Eq. (5.31) that $A(\tau)$ has terms quadratic and linear in noise and as well as terms independent of noise. To write $A(\tau)$ as a sum of quadratic, linear and noise independent terms separately we first write $A(\tau)$ in the following form:

$$\begin{aligned}
A(\tau) &= s(0) + \sum_{k=1}^{\infty}[s(\omega) + s(-\omega)] \\
\text{where, } s(\omega) &= -\lambda\tau[\widetilde{\eta}_L(\omega)\widetilde{v}_1(-\omega) - \gamma_L\widetilde{v}_1(\omega)\widetilde{v}_1(-\omega)] \\
&\quad -i[g_1(\omega)\widetilde{\eta}_L(\omega) + g_2(\omega)\widetilde{\eta}_R(\omega)]e^{-i\omega\epsilon}.
\end{aligned} \tag{5.35}$$

Note that $s(-\omega)$ is the complex conjugate of $s(\omega)$. Putting $V_1(\omega)$ from Eq. (5.32) in the expression of $s(\omega)$ in Eq. (5.35) and using the expressions for $\widetilde{\eta}_{L,R}(\omega)$ given in Eq. (5.33), we write $A(\tau)$ in the following form

$$A(\tau) = s(0) + \sum_{k=1}^{\infty}[\,-\frac{\lambda\tau}{2}\xi^T(\omega)E(\omega)\xi(\omega) + J^T(\lambda,\omega)\xi(\omega) + c(\omega)]. \tag{5.36}$$

where $\xi(\omega) = [\xi_{L1}(\omega), \xi_{L2}(\omega), \xi_{R1}(\omega), \xi_{R2}(\omega)]^T$, $E(\omega)$ is a 4×4 matrix, $J(\lambda,\omega)$ is a 4×1 column vector and $c(\omega)$ is a complex number. From the above equation one can easily note that $E(\omega)$ does not depend on the initial and final configuration whereas $J_\lambda(\omega)$ and $c(\omega)$ do depend. In the appendix we give explicit forms of $E(\omega)$, $J(\lambda,\omega)$ and $c(\omega)$.

Third step : In this step we take average over noises to calculate $\langle e^{A(\tau)}\rangle$. Noise average of $e^{A(\tau)}$ can be written as

$$\begin{aligned}
\langle e^{A(\tau)}\rangle &= \prod_k \iiiint d\xi_{L1}(\omega)d\xi_{L2}(\omega)d\xi_{R1}(\omega)d\xi_{R2}(\omega)\;\; P(\xi_{L1},\xi_{L2},\xi_{R1},\xi_{R2})\;\; \exp[A(\tau)], \\
\text{where} \qquad P(\xi_{L1},\xi_{L2},\xi_{R1},\xi_{R2}) &= \frac{\tau^2}{4\pi^2 D_L D_R}\exp[\,-\frac{\tau}{2}\xi^T \text{diag}(\frac{1}{D_L},\frac{1}{D_L},\frac{1}{D_R},\frac{1}{D_R})\xi],
\end{aligned} \tag{5.37}$$

is the joint probability distribution of the noise variables $[\xi_{L1}(\omega), \xi_{L2}(\omega), \xi_{R1}(\omega), \xi_{R2}(\omega)]$. Now putting the expression of $A(\tau)$ from Eq. (5.36) in the argument of the exponential we get

$$\begin{aligned}
\langle e^{A(\tau)} \rangle &= [\frac{\tau}{2\pi\sqrt{D_1 D_2}} \iint d\xi_{L1}(0) d\xi_{R1}(0)\ \ P(\xi_{L1}, \xi_{R1})\ \ e^{-s(0)}] \\
&\quad \times \prod_{k=1}^{\infty} \frac{\tau^2}{4\pi^2 D_1 D_2} \iiiint d\xi_{L1}(\omega) d\xi_{L2}(\omega) d\xi_{R1}(\omega) d\xi_{R2}(\omega) \\
&\quad \exp\{\sum_{k=1}^{\infty} [-\frac{\tau}{2} \xi^T(\omega) \Sigma_\lambda(\omega) \xi(\omega) + J_\lambda^T(\omega) \xi(\omega) + c(\omega)]\} \\
\text{where} \qquad & \Sigma_\lambda(\omega) = \lambda E(\omega) + \text{diag}(\frac{1}{D_L}, \frac{1}{D_L}, \frac{1}{D_R}, \frac{1}{D_R}).
\end{aligned} \tag{5.38}$$

After doing the Gaussian integration over the noises and after some rearrangements we finally get

$$\begin{aligned}
\langle e^{A(\tau)} \rangle &= \sqrt[4]{\frac{\det\Sigma_0(0)}{\det\Sigma_\lambda(0)}} \exp[\frac{1}{4\tau} J^T(\lambda, 0) \Sigma_\lambda^{-1}(0) J(\lambda, 0) + \frac{1}{2} c(0)] \\
&\times \prod_{k=1}^{\infty} \sqrt{\frac{\det\Sigma_0(\omega)}{\det\Sigma_\lambda(\omega)}} \exp\{\sum_{k=1}^{\infty} [\frac{1}{2\tau} J^T(\lambda, \omega) \Sigma_\lambda^{-1}(\omega) J(\lambda, \omega) + c(\omega)]\}.
\end{aligned} \tag{5.39}$$

Including the $k = 0$ term one can write $\langle e^{A(\tau)} \rangle$ in the following compact form

$$\langle e^{A(\tau)} \rangle = \sqrt[4]{\frac{\det\Sigma_0(0)}{\det\Sigma_\lambda(0)}} \prod_{k=1}^{\infty} \sqrt{\frac{\det\Sigma_0(\omega)}{\det\Sigma_\lambda(\omega)}} \exp\{\sum_{k=-\infty}^{\infty} [\frac{1}{4\tau} J^T(\lambda, \omega) \Sigma_\lambda^{-1}(\omega) J(\lambda, \omega) + \frac{1}{2} c(\omega)]\}. \tag{5.40}$$

This completes the three steps of calculating $\langle e^{A(\tau)} \rangle$.

Now putting this expression for $\langle e^{A(\tau)} \rangle$ in Eq. (5.17) we get the following expression

$$\begin{aligned}
\widetilde{P}(\lambda, \boldsymbol{U}, \tau|, \boldsymbol{U}_0) &= \Big(\sqrt[4]{\frac{\det\Sigma_0(0)}{\det\Sigma_\lambda(0)}} \prod_{k=1}^{\infty} \sqrt{\frac{\det\Sigma_0(\omega)}{\det\Sigma_\lambda(\omega)}} \Big) \times \\
&\Big(\int \dots \int \prod_{l=1}^{N} \frac{d\sigma_l}{2\pi} e^{i\sigma_l x_l} \prod_{l=1}^{N} \frac{d\rho_l}{2\pi} e^{i\rho_l v_l} \\
&\exp\{\sum_{k=-\infty}^{\infty} [\frac{1}{4\tau} J^T(\lambda, \omega) \Sigma_\lambda^{-1}(\omega) J(\lambda, \omega) + \frac{1}{2} c(\omega)]\} \Big).
\end{aligned} \tag{5.41}$$

We Compare the *r.h.s.* of the above equation with *r.h.s.* of Eq. (5.10), while noting that Σ_λ does not depend on $\mu,\ \nu,\ \Delta X,\ \Delta V$ whereas the expression in the exponent does, and identify

$$\mu(\lambda) = \frac{1}{2\tau}\sum_{k=0}^{\infty} ln[\frac{\det\Sigma_0(\omega)}{\det\Sigma_\lambda(\omega)}] + \frac{1}{4\tau}\, ln[\frac{\det\Sigma_0(0)}{\det\Sigma_\lambda(0)}] \tag{5.42}$$

$$\text{and } \chi(\boldsymbol{U}_0,\lambda)\Psi(\boldsymbol{U},\lambda) = \int ... \int \prod_{l=1}^{N}\frac{d\sigma_l}{2\pi}e^{i\sigma_l x_l}\prod_{l=1}^{N}\frac{d\rho_l}{2\pi}e^{i\rho_l v_l}$$
$$\exp\Big\{\sum_{k=-\infty}^{\infty}[\frac{1}{4\tau}J_\lambda^T\Sigma_\lambda^{-1}J_\lambda + \frac{1}{2}(c(\omega)+c(-\omega))]\Big\}. \tag{5.43}$$

From the explicit form of $\Sigma_\lambda(\omega)$ one can calculate $\det\Sigma_\lambda(\omega)$ and get

$$\frac{\det\Sigma_\lambda(\omega)}{\det\Sigma_0(\omega)} = \left[1+\mathcal{T}(\omega)T_L T_R\lambda(\Delta\beta-\lambda)\right]^2. \tag{5.44}$$

Above we have made use of the identity:

$$\frac{i\omega}{2}[G_{1,1}(\omega)-G_{1,1}(-\omega)] = \omega^2[\gamma_L G_{1,1}(\omega)G_{1,1}(-\omega)+\gamma_R G_{1,N}(\omega)G_{1,N}(-\omega)] \tag{5.45}$$

which can be proved as follows. From Eq.(5.15) we have $G^{-1}(\omega)-G^{-1}(-\omega) = 2i\omega\Gamma$. Multiplying by $G(\omega)$ from left and by $G(-\omega)$ from right on the both sides of the equation in the previous line we get $G(-\omega)-G(\omega) = 2i\omega G(\omega)\Gamma G(-\omega)$. After multiplying both sides by $i\omega$ and comparing the 11^{th} element from both sides we get the above identity. Same identity has been obtained in Eq. (4.55) but in time domain and from this one can get the present one by Fourier transforming both sides.

In $\tau\to\infty$ limit, converting the summation over k in Eq. (5.42) into integration over ω we get the following exact expression for $\mu(\lambda)$:

$$\mu(\lambda) = -\frac{1}{4\pi}\int_{-\infty}^{\infty} d\omega\ \ln\left[1+\mathcal{T}(\omega)T_L T_R\lambda(\Delta\beta-\lambda)\right]. \tag{5.46}$$

For the case when all the masses are equal to m, after some algebra one gets $\det\boldsymbol{G}^{-1}(\omega) = [a(q)\sin Nq + b(q)\cos Nq]/\sin q$, where $2\cos q = 2-m\omega^2$, and

$$a(q) = (2-\omega^2\gamma_L\gamma_R)\cos q - 2 + i\omega(\gamma_L+\gamma_R)(1-\cos q),$$
$$b(q) = [\omega^2\gamma_L\gamma_R + i\omega(\gamma_L+\gamma_R)]\sin q.$$

Therefore, one has

$$\mathcal{T}(\omega) = \frac{4\gamma_L\gamma_R\omega^2 \sin^2 q}{\left|a(q)\sin Nq + b(q)\cos Nq\right|^2}. \tag{5.47}$$

Using Eq. (5.47), it is straight forward to numerically compute the integral in Eq. (5.46) for any finite N. The integration in Eq. (5.43) is actually a Gaussian integration over σ_i and ρ_i's, since the exponent of the exponential can be expressed as a quadratic polynomial in σ and ρ variables. It is very difficult to do the integrations in Eqs. (5.46) and (5.43) analytically for a general N particle harmonic chain. There are few cases where these two integrations can be done analytically. Below we consider one such case.

5.1.2 Single Brownian particle

The Langevin equation for a single Brownian particle is given by :

$$\dot{v} = -(\gamma_L + \gamma_R)v + \eta_L(t) + \eta_R(t), \tag{5.48}$$

where v is the velocity of the particle. Here we consider the velocity of the particle and not the position, since velocity v of the particle will have a normalized steady state distribution whereas position will not have one, and the heat transfer Q, in which we are interested, does not depend on position. For single Brownian particle the matrix defined in Eq. (5.15) becomes a complex number: $G^{-1}(\omega) = -\omega^2 + i\omega\gamma$ where $\gamma = \gamma_L + \gamma_R$. For this case explicit forms for the matrices $\mathcal{A}_{LL}$, $\mathcal{A}_{LL}$ and $\mathcal{A}_{LL}$ (defined in appendix 5.4.1) in terms of γ, D_L, and D_R are following :

$$\mathcal{A}_{LL} = \begin{pmatrix} D_L^{-1} + \frac{4\lambda\gamma_R}{(\gamma^2+\omega^2)} & 0 \\ 0 & D_L^{-1} + \frac{4\lambda\gamma_R}{(\gamma^2+\omega^2)} \end{pmatrix}, \quad \mathcal{A}_{RR} = \begin{pmatrix} D_R^{-1} - \frac{4\lambda\gamma_L}{(\gamma^2+\omega^2)} & 0 \\ 0 & D_R^{-1} - \frac{4\lambda\gamma_L}{(\gamma^2+\omega^2)} \end{pmatrix}.$$

$$\text{and} \quad \mathcal{A}_{LR} = \begin{pmatrix} \frac{2\lambda(\gamma_R-\gamma_L)}{(\gamma^2+\omega^2)} & \frac{-2\lambda\omega}{(\gamma^2+\omega^2)} \\ \frac{2\lambda\omega}{(\gamma^2+\omega^2)} & \frac{2\lambda(\gamma_R-\gamma_L)}{(\gamma^2+\omega^2)} \end{pmatrix} \tag{5.49}$$

The expression for phonon transmission coefficient is obtained from Eq. (5.47) and given by $\mathcal{T}(\omega) = 4\gamma_L\gamma_R[m^2\omega^2 + (\gamma_L + \gamma_R)^2]^{-1}$. We use this form in Eq. (5.46) to evaluate the integral and get

$$\mu(\lambda) = \frac{\gamma_L + \gamma_R}{2m}\left[1 - \sqrt{1 + \frac{4\gamma_L\gamma_R}{(\gamma_L + \gamma_R)^2}T_L T_R \lambda(\Delta\beta - \lambda)}\right].$$

This is the result obtained in [109]. We now give the expressions for $J(\lambda,\omega)$ and $c(\omega)$:

$$\begin{aligned} J(\lambda,\omega) &= \frac{-2}{(\gamma^2+\omega^2)}\begin{pmatrix} \lambda\Delta v(\gamma_R-\gamma_L) - i\varrho[\gamma\, cos(\omega\epsilon) - \omega\, sin(\omega\epsilon)] \\ \lambda\Delta v\omega + i\varrho[\gamma\, sin(\omega\epsilon) + \omega\, cos(\omega\epsilon)] \\ -2\lambda\Delta v\gamma_L - i\varrho[\gamma\, cos(\omega\epsilon) - \omega\, sin(\omega\epsilon)] \\ 0 + i\varrho[\gamma\, sin(\omega\epsilon) + \omega\, cos(\omega\epsilon)] \end{pmatrix}, \\ C(\omega) &= \frac{2\lambda}{\tau}\frac{\gamma_L\Delta v^2}{(\gamma^2+\omega^2)}. \end{aligned} \tag{5.50}$$

In this case one can actually find an explicit expression for $\sum_\omega J^T\Sigma_\lambda^{-1}J$ in terms of Δv, λ and ρ. After putting that expression along with $\sum_\omega c(\omega)$ in the exponent of the exponential in the integrand of Eq. (5.43), we do the integration to find $\chi(v_0,\lambda)\Psi(v,\lambda)$, where v is the velocity at time τ and v_0 is the velocity at time 0. After some manipulations and rearrangements we finally get the following expressions for $\chi(v_0,\lambda)$ and $\Psi(v,\lambda)$:

$$\begin{aligned} & \chi(v_0,\lambda) = e^{\alpha_1 v_0^2}\ ;\ \ \Psi(v,\lambda) = e^{\alpha_2 v^2} \\ \text{where, } \alpha_1 &= \frac{1}{4(D_L+D_R)}\Big[2\lambda D_L + \gamma\Big(1 - \sqrt{1+\frac{4D_LD_R}{\gamma^2}\lambda(\Delta\beta-\lambda)}\ \Big)\Big] \\ \text{and, } \alpha_2 &= -\frac{1}{4(D_L+D_R)}\Big[2\lambda D_L + \gamma\Big(1 + \sqrt{1+\frac{4D_LD_R}{\gamma^2}\lambda(\Delta\beta-\lambda)}\ \Big)\Big]. \end{aligned} \tag{5.51}$$

Two particles connected by a harmonic spring.— In this case from Eq. (5.47) we find $\mathcal{T}(\omega) = 4\gamma_L\gamma_R[\omega^2(m^2\omega^2 - \gamma_L\gamma_R - 2m)^2 + (\gamma_L+\gamma_R)^2(1-m\omega^2)^2]^{-1}$. Using this expression we are not able to evaluate the integral in Eq. (5.13) in general. However, for the special case $\gamma_L = \gamma_R = \sqrt{2m}$, the expression for $\mathcal{T}(\omega)$ becomes simpler, namely, $\mathcal{T}(\omega) = [m^3\omega^6/8+1]^{-1}$. Now the integral in Eq. (5.13) can be carried out, which yields

$$\mu(\lambda) = \sqrt{\frac{2}{m}}\Big[1-(1+T_LT_R\lambda(\Delta\beta-\lambda))^{1/6}\Big].$$

It is interesting to note the with the special value $\gamma_L = \gamma_R = \sqrt{2m}$, both the expressions, for the single particle as well as for the two particles are very similar, except the exponents $1/2$, and $1/6$. In this case we are not able to perform the integration in Eq. (5.43) to find $\chi(U_0,\lambda)\Psi(U,\lambda)$.

Thus we have obtained an exact expression for $\mu(\lambda)$ corresponding to heat flow through

harmonic chain, from which one can obtain the large deviation function $F(q)$ corresponding to the pdf of Q through Legendre transform. This $F(q)$ provides the large deviation form of $R(Q,\tau) \sim \exp[-\tau\, F(q)]$ and also provides the behavior of $R(Q,\tau)$ at the tails *i.e.* probabilities of rare fluctuations of Q. The pdf $R(Q,\tau)$ can also be obtained by simulating Langevin equations given in Eq. (5.2). We are interested in the tails of $R(Q,\tau)$, where probabilities are very small ($\approx 10^{-15}$) and hence events are very rare. It is very difficult to generate those rare events by direct simulations, because one has to take average over a large ($\approx 10^{15}$) no of repetitions which is very timeconsuming. In the next section we describe an algorithm using which one can easily generate rare events without such large number of repetitions.

5.2 Algorithm for finding probabilities of rare events

In this section we discuss about an algorithm for generating rare events and computing their probabilities. It is developed in the spirit of importance sampling algorithm. First we describe the algorithm for general purpose and next we apply this algorithm to different nonequilibrium processes, including heat transport process.

Consider a system with a time evolution described by the stochastic process $x(t)$. For simplicity we assume for now that $x(t)$ is a integer-valued variable and time is discrete. Let us denote a particular path in configuration space over a time period τ by the vector $\mathbf{x}(\tau) := \{x(t)\ |t = 1, 2, ..., \tau\}$ and let O be an observable which is a function of the path $\mathbf{x}(\tau)$. We will be interested in finding the probability distribution $P(O,\tau)$ of O, and especially in computing the probability of large deviations from the mean value $\langle O\rangle$. As a simple illustrative example consider the tossing of a fair coin. For $\tau = N$ tosses we have a discrete stochastic process described the time series $\mathbf{x}(N) = \{x_i\}$ where $x_i = 1$ if the outcome in i^{th} trial is head, and $x_i = -1$ otherwise. Suppose we want to find the probability of generating O heads (thus $O = \sum_{i=1}^{N} \delta_{x_i,1}$). An example of a rare event is, for example, the event $O = N$. The probability of this is 2^{-N} and if we were to simulate the coin toss experiment we would need lot more than 2^N repeats of the experiment to realize this event with sufficient frequency in order to calculate the probability reliably. For large N this is clearly very difficult. The

importance sampling algorithm is useful in such situations. The basic idea is to increase the occurrence of the rare events by introducing a bias in the dynamics. The rare events are produced with a new probability corresponding to the bias. However by keeping track of the relative weights of trajectories of the unbiased and biased processes it is possible to recover the probability corresponding to the original unbiased process.

5.2.1 The algorithm

We now describe the algorithm in the context of evaluating $P(O,\tau)$ for the stochastic process $\mathbf{x}(\tau)$. We denote the probability of a particular trajectory by $\mathcal{P}(\mathbf{x})$. By definition:

$$P(O,\tau) = \sum_{\mathbf{x}} \delta_{O,O(\mathbf{x})}\mathcal{P}(\mathbf{x}). \tag{5.52}$$

For the same system let us consider a biased dynamics for which the probability of the path $\mathbf{x}$ is given by $\mathcal{P}_b(\mathbf{x})$. Then we have:

$$P(O,\tau) = \sum_{\mathbf{x}} \delta_{O,O(\mathbf{x})} e^{-W(\mathbf{x})}\mathcal{P}_b(\mathbf{x}), \tag{5.53}$$

$$\text{where} \quad e^{-W(\mathbf{x})} = \frac{\mathcal{P}(\mathbf{x})}{\mathcal{P}_b(\mathbf{x})}. \tag{5.54}$$

Thus in terms of the biased dynamics, $P(O,\tau)$ is the average $\langle \delta_{O,O(\mathbf{x})} e^{-W}\rangle_b$ and in a simulation we estimate this by performing averages over M realizations to obtain:

$$P_e(O,\tau) = \frac{1}{M}\sum_{r} \delta_{O,O(\mathbf{x}_r)} e^{-W(\mathbf{x}_r)} \,, \tag{5.55}$$

where $\mathbf{x}_r$ denotes the path for the r^{th} realization. For $M \to \infty$ we obtain $P_e(O,\tau) \to P(O,\tau)$ which is the required probability. Note that the weight factor W is a function of the path. In a simulation we know the details of the microscopic dynamics for both the biased and unbiased processes. Thus we can evaluate W for every path $\mathbf{x}$ generated by the biased dynamics. A necessary requirement of the biased dynamics is that the distribution of O that it produces, i.e., $P_b(O,\tau) = \langle \delta_{O,O(\mathbf{x})}\rangle_b$, should be peaked around the desired values of O for which we want an accurate measurement of $P(O,\tau)$. As we will see the required dynamics can often be guessed from physical considerations.

We explain the algorithm for the coin tossing experiment. In this case we consider a biased dynamics where the probability of head is p and that of tail is $1-p$. If we take $p \approx 1$ then the event $O = N$, which was earlier rare, is now generated with increased frequency and we can use Eq. (5.55) to estimate the required probability $P(O = N, N)$. For any path consisting of O heads the weight factor is simply given by $e^{-W} = (1/2)^N/[p^O(1-p)^{N-O}]$. Choosing $p = 0.95$ it is easy to see that for $N = 100$ we can get the required probability $P(O = N, N)$ with more than 1% accuracy using only $M = 10^7$ realizations as opposed to at least $M = 10^{30}$ required by the unbiased dynamics. Note that for this example W has the same value for all paths with the same O. In general of course W depends on the details of the path, *e.g.* for a random walk with a waiting probability. We will now illustrate the algorithm with non-trivial examples of computing large deviations in two well known models in nonequilibrium physics. These are the (i) symmetric simple exclusion process (SSEP) with open boundaries and (ii) heat conduction across a harmonic system connected to Langevin reservoirs.

5.2.2 Symmetric simple exclusion process

This is a well studied example of an interacting stochastic system consisting of particles diffusing on a lattice with the constraint that each site can have at most one particle. Here we restrict ourselves to one dimension and study the case of an open system where a linear chain with L sites is connected to particle reservoirs at the two ends. The dynamics can be specified by the following rules: (a) a particle at any site $l = 1, 2, ..., L$ can jump to a neighboring empty site with unit rate , (b) at $l = 1$ a particle can enter the system with rate α (if it is empty) and leave with rate γ. At site N a particle can leave or enter the system with rates β and δ respectively. The biased dynamics can be realized in various ways, for example by introducing asymmetry in the bulk hopping rates or by changing the boundary hopping rates.

For SSEP, the configuration of the system at any time is specified by the set $C = \{n_1(t), n_1(t), ..., n_L(t)\}$ where $n_l(t)$ (0 or 1) gives the occupancy of the l^{th} site. The dynamical rules specify the matrix element $\mathcal{W}(C, C')$ giving the transition rate from configuration

C' to C. We write $\mathcal{W}(C,C') = \mathcal{W}_1 + \mathcal{W}_{-1} + \mathcal{W}_0$ where $\mathcal{W}_1$ and $\mathcal{W}_{-1}$ correspond to transitions whereby a particle enters the system from the left bath or leaves the system into the left bath respectively while $\mathcal{W}_0$ corresponds to all other transitions. At long times the system will reach a steady state with particles flowing across the system and we are here interested in the current fluctuations in the wire. Specifically let K be the net particle transfer from the left reservoir into the system during a time interval τ. For a fixed τ we want to obtain the distribution $P(K,\tau)$ of K, in the steady state of the system. It is useful to define the joint probability distribution function $R(K,C,\tau)$ for K number of particles transported and for the system to be in state C. Clearly $P(K,\tau) = \sum_C R(K,C,\tau)$. We also define the characteristic functions $\tilde{R}(z,C,\tau) = \sum_{-\infty}^{\infty} R(K,C,\tau)z^K$ and $\tilde{P}(z,\tau) = \sum_C \tilde{R}(z,C,\tau)$. It is then easy to obtain the following master equation [107]:

$$\frac{d\tilde{R}(z,C,\tau)}{d\tau} = \sum_{C'}\Big[z\mathcal{W}_1(C,C') + \mathcal{W}_0(C,C') + \frac{1}{z}\mathcal{W}_{-1}(C,C')\Big]\tilde{R}(z,C',\tau). \tag{5.56}$$

The general solution of this equation for arbitrary L is difficult but for $L = 1$ an explicit solution can be obtained for $\tilde{R}(z,C',\tau)$ and $\tilde{P}(z,\tau)$. We will here first discuss a special case $\alpha = \beta = \gamma = \delta$ for which $\tilde{P}(z,\tau)$ can be inverted explicitly. The choice of steady state initial conditions gives the solution: $P(K,\tau) = (e^{-2\alpha\tau}/2)[I_{2K-1}(2\alpha\tau)+2I_{2K}(2\alpha\tau)+I_{2K+1}(2\alpha\tau)]$, where $I_n(x)$ is the modified Bessel's function. In Fig. (5.2) we plot the exact distribution along with a direct simulation of the above process with averaging over 5×10^8 realizations. As we can see the direct simulation is accurate only for events with probabilities of $O(10^{-8})$. Now we illustrate our algorithm using a biased dynamics. We consider biasing obtained by changing the boundary transition rates. We denote the rates of the biased dynamics by $\alpha',\beta',\delta',\gamma'$ and these are chosen such that $P_b(K)$ has a peak in the required region. In our simulation we consider a discrete-time implementation of SSEP. For every realization of the process over a time τ (after throwing away transients) the weight factor W is dynamically evaluated. For instance every time a particle hops into the system from the left reservoir W is incremented by $-\ln(\alpha/\alpha')$. In Fig. (5.2) we see the result of using our algorithm with two different biases. Using the same number of realizations we are now able to find probabilities up to $O(10^{-16})$

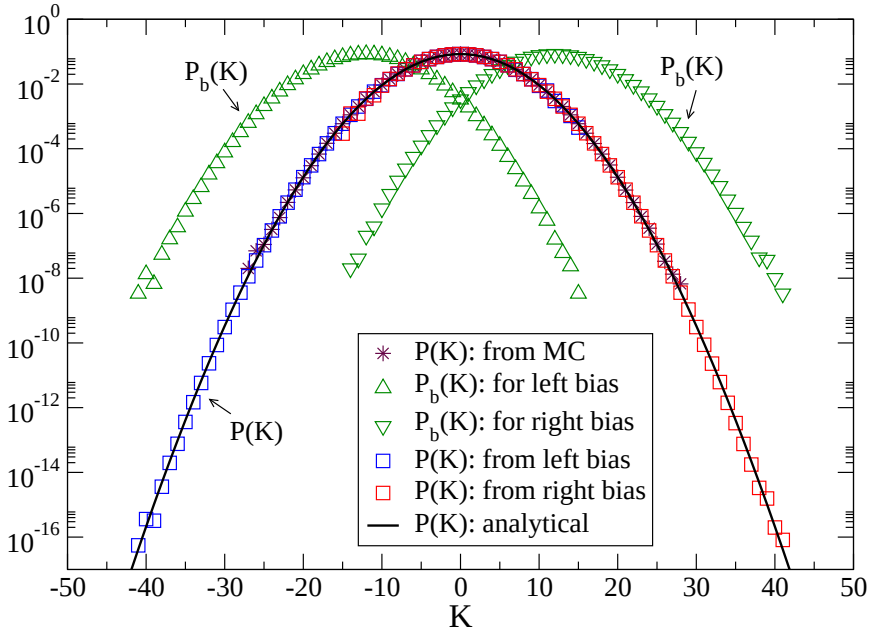

Figure 5.2: Plot of $P(K)$ for $\tau = 15$ for the one-site SSEP model with $\alpha = \beta = 3.0, \gamma = \delta = 3.0$. MC refers to direct Monte-Carlo simulations. Left bias corresponds to $\alpha' = \beta' = 3.8, \gamma' = \delta' = 2.2$ and right bias to $\alpha' = \beta' = 2.2, \gamma' = \delta' = 3.8$.

and the comparison with the exact result is excellent.

We next study the case with $L = 3$. In this case we consider a biased dynamics with asymmetric bulk hopping rates. Finding $\tilde{R}(z, C, \tau)$ analytically involves diagonalizing a 8×8 matrix. We do this numerically and after an inverse Laplace transform find $P(K, \tau)$. In Fig. (5.3) we show the numerical and direct simulation results for this case and also the results obtained using the biased dynamics. Again we find that the biasing algorithm significantly improves the accuracy of finding probabilities of rare events using the same number of realizations (5×10^8).

5.2.3 Heat conduction

Next we consider the problem of heat conduction across a system connected to heat reservoirs modeled by Langevin white noise reservoirs. Here we are interested in the distribution of the net heat transfer Q from the left bath into the system over time τ. First let us consider the simple example of a single Brownian particle connected to two baths at temperatures $T_L = \beta_L^{-1}$ and $T_2 = \beta_R^{-1}$ described in detail in sec. (5.1.2). The heat flow from the left bath

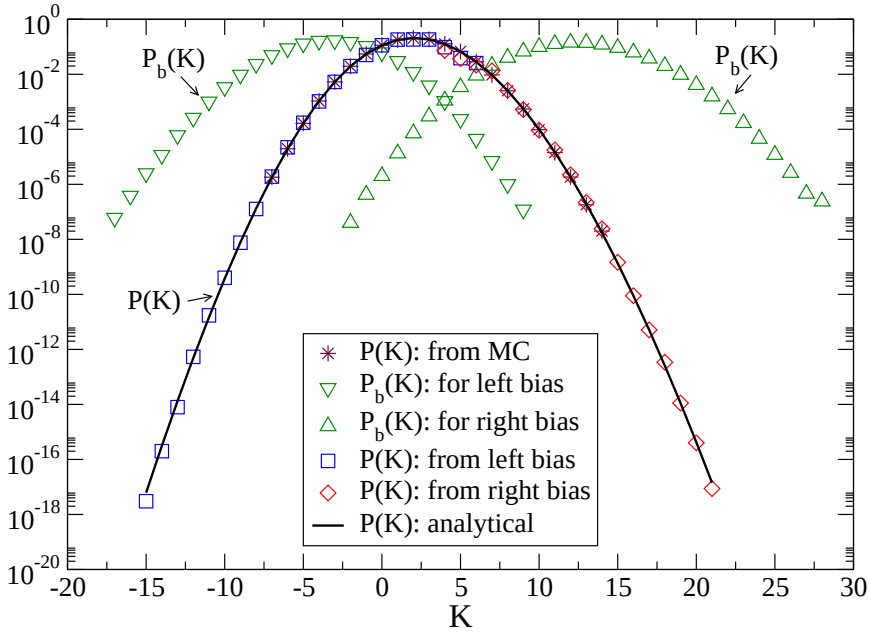

Figure 5.3: Plot of $P(Q)$ for $\tau = 15$ for the three-site SSEP model with $\alpha = \beta = 4.0, \gamma = \delta = 2.0$. MC refers to direct Monte-Carlo simulations. For left (right) bias simulations, the particles in bulk hop to the left (right) with rate 4 and to the right (left) with unit rate. The boundary rates are kept unchanged.

into the system in time τ is given by $Q(\tau) = \int_0^\tau (-\gamma_L v^2 + \sqrt{2D_L}\eta_L v)\, dt$. For the single Brownian particle in this problem it is sufficient to specify the state by the velocity $v(t)$ alone. If we choose $T_L > T_R$ then $P(Q,\tau)$ will have a peak at $Q > 0$. It is clear that in order to use the biasing algorithm to compute probabilities of rare events with $Q < 0$ we can choose a biased dynamics with temperatures of left and right reservoirs taken to be T'_L and T'_R with $T'_L < T'_R$. The calculation of the weight factor W is somewhat tricky since computing $\mathcal{P}(v(t))$ from $\mathcal{P}(\eta_L(t), \eta_R(t))$ is non-trivial. Also one cannot eliminate η_L to express Q as a functional of only the path v. To get around this problem we note the following mapping of the single-particle system to the over-damped dynamics of two coupled oscillators given by the equations of motion: $\dot{x}_1 = -\gamma_1(x_1 - x_2) + \sqrt{2D_L}\eta_L$, $\dot{x}_2 = -\gamma_2(x_2 - x_1) - \sqrt{2D_R}\eta_R$. The variable $x_1 - x_2 = x_{12}$ satisfies the same equation as v in Eq. (5.48). Thus with the same definition for Q as given earlier we can use above equations for x_1 and x_2 to find $P(Q,\tau)$. In this case we do not have the problem as earlier and both Q and W can be readily expressed in terms of $\{x_1, x_2\}$. Let us denote by γ'_i, T'_i, D'_i the parameters of the biased system. Also

let $\eta'_{L,R}$ be the noise realizations in the biased process that result in the same path $\{x_1, x_2\}$ as produced by $\eta_{L,R}$ for the original process. Choosing $D_i = D'_i$ for $i = L, R$ it can be shown that:

$$W = \int_0^\tau dt\, [(\eta_L^2/2 + \eta_R^2/2) - (\eta_L'^2/2 + \eta_R'^2/2)]. \tag{5.57}$$

Using the equations of motion we can express $\eta_{L,R}, \eta'_{L,R}$ in terms of the phase-space variables and this gives:

$$\begin{aligned} W &= \frac{1}{4D_L}\int_0^\tau dt[2(\gamma_L - \gamma'_L)\dot{x}_1 x_{12} + (\gamma_L^2 - \gamma_L'^2)x_{12}^2] \\ &\quad + \frac{1}{4D_R}\int_0^\tau dt[2(\gamma_R - \gamma'_R)\dot{x}_2 x_{12} + (\gamma_R^2 - \gamma_R'^2)x_{12}^2], \\ Q &= \int_0^\tau dt \dot{x}_1 x_{12}. \end{aligned}$$

Thus W and Q are easily evaluated in the simulation using the biased dynamics. In Fig. (5.4) we show results for $P(Q, \tau)$ obtained both directly and using the biased dynamics. Again we see that for the same number of realizations (10^9) one can obtain probabilities about 10^8 times smaller than using direct simulations. The comparison with the numerical results obtained from the exact expression for $\langle e^{-\lambda Q}\rangle$ [109] also shows the accuracy of the algorithm.

It is easy to apply the algorithm to more complicated cases. For example consider a one-dimensional chain of L particles connected to heat reservoirs at the two ends described by the Langevin equations given in Eq. (5.2). The net heat transfer from left bath into the system is given by $Q = \int_0^\tau(-\gamma_L v_1^2 + \sqrt{2D_L}\eta_L v_1)$ and using Eqs. (5.2) this can be expressed in terms of $\{x_l, v_l\}$ as $Q = \int_0^\tau dt v_1(m_1\dot{v}_1 + (x_1 - x_2))$. To apply our algorithm we consider a biased dynamics where the Hamiltonian evolution is unchanged while the bath dynamics has new parameters $\gamma'_L, \gamma'_R, T'_L, T'_R$ which are chosen so that $P_b(Q)$ has a peak in the required region. Choosing $D'_i = D_i$ we again find W by using Eqs. (5.2) in Eq. (5.57), as for the single particle case. Thus both Q and W can be expressed in terms of the path and so are readily evaluated for every realization of the biased dynamics.

As an example we study the case $L = 2$ with $U = (x_1 - x_2)^2/2$ and with $m_1 = m_2 = 1$. For the special parameters $\gamma_L = \gamma_R = \sqrt{2}$ we use the results in [100] to obtain $\langle e^{-\lambda Q}\rangle \sim e^{\mu(\lambda)\tau}$

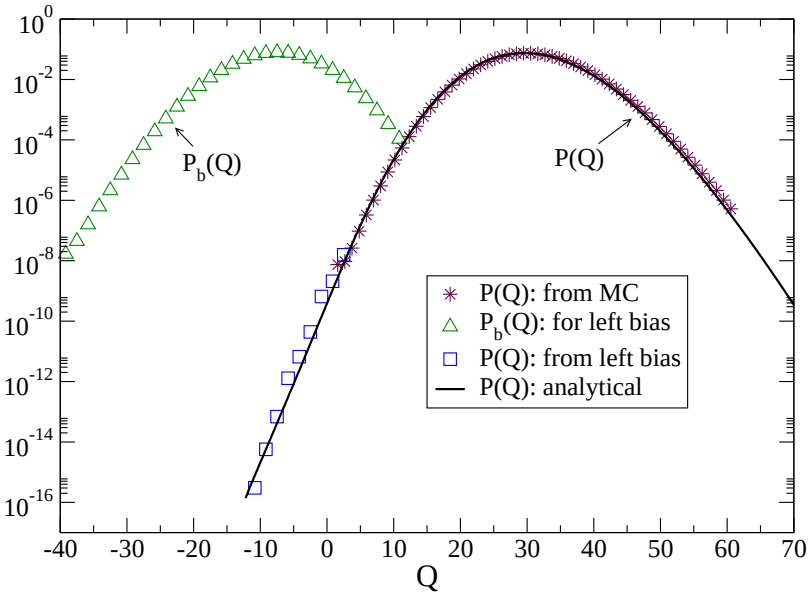

Figure 5.4: Plot of $P(Q)$ for $\tau = 200$ for heat conduction across a single free particle with $\gamma_L = 0.8, \gamma_R = 0.2, T_L = 1.1875, T_R = 0.25$. The parameters have been chosen to correspond to a region in parameter-space where the fluctuation theorem is not satisfied [109]. MC refers to direct Monte-Carlo simulations. The left bias corresponds to $\gamma'_L = \gamma_L, \gamma'_R = \gamma_2/20, T'_L = T_L, T'_R = 20T_R$.

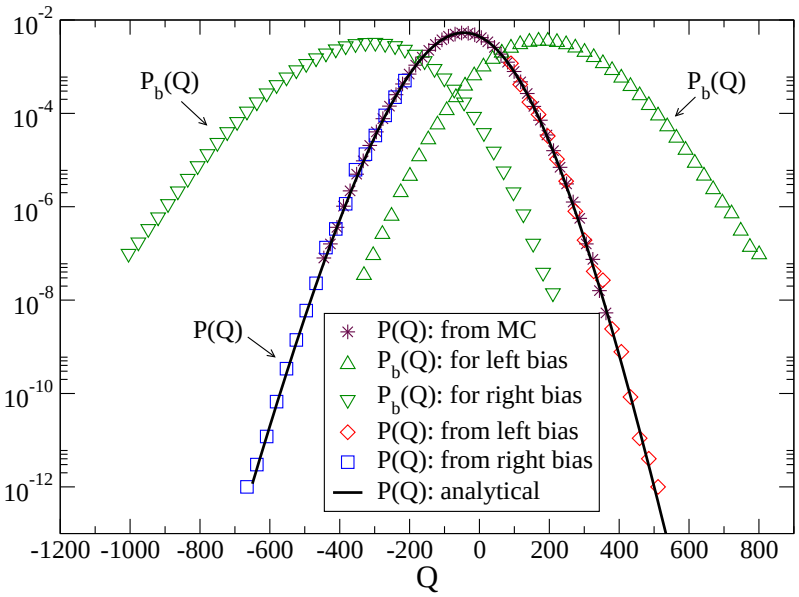

Figure 5.5: Plot of $P(Q)$ for $\tau = 100$ for heat conduction across two particles connected by a harmonic spring with unit spring constant and $\gamma_L = \gamma_R = \sqrt{2}, T_L = 10, T_R = 12$. MC refers to direct Monte-Carlo simulations. The left bias corresponds to $\gamma'_L = \gamma_L, \gamma'_R = \gamma_R/2, T'_L = T_L, T'_R = 2T_R$ and right bias to $\gamma'_L = \gamma_L/2, \gamma'_R = \gamma_R, T'_L = 2T_L, T'_R = T_R$.

with $\mu(\lambda) = \sqrt{2}\{1 - [1 + \beta_L^{-1}\beta_R^{-1}\lambda(\Delta\beta - \lambda)]^{1/6}\}$. This can be inverted to numerically compute $P(Q,\tau)$ at large τ. In Fig. (5.5) we give the comparison between the analytical distribution and that obtained by the biasing method.

5.3 Conclusions

We have calculated the large deviation function $\mu(\lambda)$ of the pdf of heat flow across a harmonic chain. The large deviation function $\mu(\lambda)$ is expressed in terms of integration of a function of the phonon transmission coefficient $\mathcal{T}(\omega)$. Two cases, (a)single Brownian particle and (b) two particles connected by harmonic spring were studied where for some special set of parameters the integration in the expression for $\mu(\lambda)$ were carried out. For single Brownian particle we also have obtained the steady state distribution.

We have presented an algorithm for computing the probabilities of rare events in various nonequilibrium processes. The algorithm is an application of importance sampling and consists in using a biased dynamics to generate the required rare events. The error in the estimate of $P(O,\tau)$ is $\approx \langle e^{-2W}\delta_{O,O_x}\rangle_b^{1/2}/(MP_b(O))^{1/2}$, and can be made small by choosing the biased dynamics carefully. We have applied the algorithm to two different models of particle and heat transport and shown that in both cases it gives excellent results. This algorithm is straightforward to understand and also to implement.

5.4 Appendix

5.4.1 Expression of the matrix $E(\omega)$:

Let us define vectors $\mathcal{G}_1(\omega) = i\omega e^{-i\omega\epsilon}(G_{11}^{-1}(\omega), -iG_{11}^{-1}(\omega), G_{1N}^{-1}(\omega), -iG_{1N}^{-1}(\omega))^T$ and $\Psi = (1, -i, 0, 0)^T$. In terms of these two vectors we can write $\widetilde{\eta}_L(\omega)$ and $\widetilde{v}_1(\omega)$ (Eq. (5.32)) in the following form :

$$\begin{aligned} \widetilde{\eta}_L(\omega) &= \Psi^T\xi(\omega) = \xi(\omega)\Psi \\ \widetilde{v}_1(\omega) &= \mathcal{G}_1^T(\omega)\xi(\omega) = \xi(\omega)^T\mathcal{G}_1(\omega). \end{aligned} \tag{5.58}$$

Here we have ignored $1/\tau$ dependent terms in the expression of $\widetilde{v}_1(\omega)$ in Eq. (5.32) since they do not contribute in the quadratic part in $A(\tau)$. It is clear that the quadratic part in $A(\tau)$ comes from $\sum_k [\widetilde{\eta}_L^*(\omega)\widetilde{v}_1(\omega) + \widetilde{v}_1^*(\omega)\widetilde{\eta}_L(\omega) - 2\gamma_L\widetilde{v}_1(\omega)\widetilde{v}_1^*(\omega)]$, where $*$ represents complex conjugate. Now putting the expressions for $\widetilde{\eta}_L(\omega)$ and $\widetilde{v}_1(\omega)$ (Eq. (5.58)) in the above expression we get

$$\sum_k [\widetilde{\eta}_L^*(\omega)\widetilde{v}_1(\omega) + \widetilde{v}_1^*(\omega)\widetilde{\eta}_L(\omega) - 2\gamma_L\widetilde{v}_1(\omega)\widetilde{v}_1^*(\omega)] = \frac{1}{2}\xi^T(\omega)E(\omega)\xi(\omega)$$
$$\text{where, } E(\omega) = [(\Psi\mathcal{G}_1^{*T}(\omega) + \mathcal{G}_1^*(\omega)\Psi^T + \Psi^*\mathcal{G}_1^T(\omega) + \mathcal{G}_1(\omega)\Psi^{*T})$$
$$- 2\gamma_L(\mathcal{G}_1(\omega)\mathcal{G}_1^{*T}(\omega) + \mathcal{G}_1^*(\omega)\mathcal{G}_1^T(\omega))]. \tag{5.59}$$

Let the real part of any complex number x is denoted by $\text{Re}[x] = (x + x^*)/2$ and the imaginary by $\text{Im}[x] = (x - x^*)/2i$. Using these notations the matrix $\Sigma_\lambda(\omega) = \lambda E(\omega) + diag(D_L^{-1}, D_L^{-1}, D_R^{-1}, D_R^{-1})$ can be written in the block matrix form

$$\Sigma_\lambda(\omega) = \begin{pmatrix} \mathcal{A}_{LL}(\omega) & \mathcal{A}_{LR}(\omega) \\ \mathcal{A}_{LR}^T(\omega) & \mathcal{A}_{RR}(\omega) \end{pmatrix}$$

where

$$\mathcal{A}_{LL}(\omega) = \begin{pmatrix} D_L^{-1} - 4\,\lambda\,(\omega Im[G_{11}] & 0 \\ +\gamma_L\omega^2|G_{11}|^2]) & \\ & D_L^{-1} - 4\,\lambda\,(\omega Im[G_{11}] \\ 0 & +\gamma_L\omega^2|G_{11}|^2]) \end{pmatrix} \tag{5.60}$$

$$\mathcal{A}_{RR}(\omega) = \begin{pmatrix} D_R^{-1} - 4\omega^2\lambda\gamma_L|G_{1N}|^2 & 0 \\ 0 & D_R^{-1} - 4\omega^2\lambda\gamma_L|G_{1N}|^2 \end{pmatrix}. \tag{5.61}$$

and

$$\mathcal{A}_{LR}(\omega) = \begin{pmatrix} 2\lambda\left(-\omega\, Im[G_{1N}] & 2\lambda\left(\omega\, Re[G_{1N}]\right. \\ -2\omega^2\,\gamma_L\, Re[G_{11}G_{1N}^*]\right) & +2\omega^2\,\gamma_L\, Im[G_{11}G_{1N}^*]\left.\right) \\ & \\ -2\lambda\left(\omega\, Re[G_{1N}]\right. & 2\lambda\left(-\omega\, Im[G_{1N}]\right. \\ +2\omega^2\gamma_L\, Im[G_{11}G_{1N}^*]\left.\right) & -2\omega^2\gamma_L\, Re[G_{11}G_{1N}^*]\left.\right) \end{pmatrix}. \tag{5.62}$$

Similarly $\Sigma_\lambda^{-1}(\omega)$ can also be written in the following block matrix form

$$\Sigma_\lambda^{-1}(\omega) = \frac{1}{D_L D_R \det\Sigma_\lambda} \begin{pmatrix} \mathcal{A}_{RR}(\omega) & -\mathcal{A}_{LR}(\omega) \\ -\mathcal{A}_{LR}^T(\omega) & \mathcal{A}_{LL}(\omega) \end{pmatrix}. \tag{5.63}$$

5.4.2 Expressions of the elements of $J(\lambda,\omega)$ and $c(\omega)$:

$$\begin{aligned} J_1(\lambda,\omega) &= \lambda[\{g(\omega)+g(-\omega)\} - 2i\omega\gamma_L\{G_{11}(\omega)g(-\omega) - G_{11}(-\omega)g(\omega)\}] \\ &\quad + i[e^{i\omega\epsilon}g_1(-\omega) + e^{-i\omega\epsilon}g_1(\omega)], \\ J_2(\lambda,\omega) &= i\lambda[\{g(\omega)-g(-\omega)\} + 2i\omega\gamma_L\{G_{11}(\omega)g(-\omega) + G_{11}(-\omega)g(\omega)\}] \\ &\quad - [e^{i\omega\epsilon}g_1(-\omega) - e^{-i\omega\epsilon}g_1(\omega)], \end{aligned} \tag{5.64}$$

$$\begin{aligned} J_3(\lambda,\omega) &= \lambda[- 2i\omega\gamma_L\{G_{1N}(\omega)g(-\omega) - G_{1N}(-\omega)g(\omega)\}] \\ &\quad + i[e^{i\omega\epsilon}g_2(-\omega) + e^{-i\omega\epsilon}g_2(\omega)], \\ J_4(\lambda,\omega) &= i\lambda[2i\omega\gamma_L\{G_{1N}(\omega)g(-\omega) + G_{1N}(-\omega)g(\omega)\}] \\ &\quad - [e^{i\omega\epsilon}g_2(-\omega) - e^{-i\omega\epsilon}g_2(\omega)], \\ \text{and } C(\omega) &= \frac{2\lambda}{\tau}\gamma_L|g(\omega)|^2. \end{aligned} \tag{5.65}$$

Bibliography

[1] N. W. Ashcroft and D. Mermin, Solid State Physics (Harcourt College Publishers, 1976).

[2] J. M. Ziman, Principles of the theory of solids (Second Edition, Cambridge University Press, 1972).

[3] J. M. Ziman, Electrons and Phonons (Clarendon Press, Oxford, 1960).

[4] R. E. Peierls, Quantum Theory of Solids, (Oxford University Press, London, 1955).

[5] H. Spohn, J. Stat. Phys. **124**, 1041, (2006).

[6] J. Lukkarinen and H. Spohn, Arch. Rat. Mech. Anal. **183**, 93, (2007).

[7] J. M. Luttinger, Phys. Rev. **135**, A1505, 1964

[8] C. Caroli, R. Combescot, P. Nozieres, and D. Saint-James, J. Phys. C **4** , 916, (1971).

[9] Y. Meir and N.S. Wingreen, Phys. Rev. Lett. **68**, 2512, (1992).

[10] R. Landauer, Philos. Mag. **21**, 863, (1970).

[11] Z. Rieder, J.L. Lebowitz, and E. Lieb, J. Math. Phys. **8**, 1073, (1967).

[12] H. Nakazawa, Prog. Theor. Phys. **39**, 236, (1968).

[13] D. Roy and A. Dhar, J. Stat. Phys. **131**, 535, (2008).

[14] H. Matsuda and K. Ishii, Prog. Theor. Phys. Suppl. **45**, 56, (1970).

[15] R.J. Rubin and W.L. Greer, J. Math. Phys. **12**, 1686, (1971).

[16] T. Verheggen, Commun. Math. Phys. **68**, 69, (1979).

[17] A. Casher and J.L. Lebowitz, J. Math. Phys. **12**, 1701, (1971).

[18] M. Rich and W.M. Visscher, Phys. Rev. B **11**, 2164, (1975).

[19] A. Dhar, Phys. Rev. Lett. **86**,5882, (2001).

[20] N. Likhachev et al., Phys. Rev. E **73**,016701, (2006).

[21] A. Dhar and J.L. Lebowitz, Phys. Rev. Lett. **100**,134301, (2008).

[22] D. Roy and A. Dhar, Phys. Rev. E **78**, 051112, (2008).

[23] M. Bolsterli, M. Rich, and W.M. Visscher, Phys. Rev. A **4**, 1086, (1970).

[24] Dhar and D. Roy, J. Stat. Phys. **125**, 801, (2006).

[25] S. John, H. Sompolinsky, and M.J. Stephen, Phys. Rev. B **27**, 5592, (1983).

[26] L. Yang, Phys. Rev. Lett. **88**, 094301, (2002).

[27] L.W. Lee and A. Dhar, Phys. Rev. Lett. **95**, 094302, (2005).

[28] O. Narayan and S. Ramaswamy, Phys. Rev. Lett. **89**, 200601, (2002).

[29] S. Lepri, R. Livi, and A. Politi, Europhys. Lett. **43**, 271, (1998).

[30] S. Lepri, Phys. Rev. E 58 (1998), p. 7165.

[31] L. Delfini, S. Lepri, R. Livi, and A. Politi, J. Stat. Mech. (2007).

[32] J.S. Wang and B. Li, Phys. Rev. Lett. **92**, 074302, (2004).

[33] J.S. Wang and B. Li, Phys. Rev. E **70**, 021204, (2004).

[34] S. Lepri, R. Livi, and A. Politi, Phys. Rev. E **68**, 067102, (2003).

[35] K. Aoki and D. Kusnezov, Phys. Rev. Lett. **86**, 4029, (2001).

[36] T. Mai, A. Dhar, and O. Narayan, Phys. Rev. Lett. **98**, 184301, (2007).

[37] A. Dhar and K. Saito, Phys. Rev. E vol. **78**, 061136 (2008).

[38] C. Giardina, R. Livi, A. Politi, and M. Vassalli, Phys. Rev. Lett. **84**, 2144, (2000).

[39] B. Li, H. Zhao, and B. Hu, Phys. Rev. Lett. **86**, 63, (2001).

[40] A. Dhar and K. Saito, Phys. Rev. E **78**, 061136 (2008).

[41] G. Casati, Found. Phys. **16**, 51, (1986).

[42] T. Hatano, Phys. Rev. E **59**, R1, (1999).

[43] P.L. Garrido, P.I. Hurtado, and B. Nadrowski, Phys. Rev. Lett. **86**, 5486, (2001).

[44] A. Dhar, Phys. Rev. Lett. **86**, 3554, (2001).

[45] P. Grassberger, W. Nadler, and L. Yang, Phys. Rev. Lett. **89**, 180601, (2002).

[46] A.V. Savin, G.P. Tsironis, and A.V. Zolotaryuk, Phys. Rev. Lett. **88**,154301, (2002).

[47] G. Casati and T. Prosen, Phys. Rev. E **67**, 015203, (2003).

[48] G. Casati, J. Ford, F. Vivaldi, and W.M. Visscher, Phys. Rev. Lett. **52**, 1861, (1984).

[49] T. Prosen and M. Robnik, J. Phys. A: Math. Gen. **25**, 3449, (1992).

[50] B. Hu, B. Li, and H. Zhao, Phys. Rev. E **57**, 2992, (1998).

[51] K. Aoki and D. Kusnezov, Phys. Lett. A **265**, 250, (2000).

[52] K. Aoki and D. Kusnezov, Ann. Phys. (N.Y.) **295**, 50, (2002).

[53] A. Lippi and R. Livi, J. Stat. Phys. **100**, 1147, (2000).

[54] L. Yang, P. Grassberger, and B. Hu, Phys. Rev. E **74**, 062101, (2006).

[55] H. Shiba and N. Ito, J. Phys. Soc. Jpn **77**, 054006, (2008).

[56] T. Shimada, T. Murakami, S. Yukawa, K. Saito, and N. Ito, J. Phys. Soc. Jpn **69**, 3150, (2000).

[57] K. Saito and A. Dhar, Phys. Rev. Lett. **104**, 040601, (2010).

[58] A. Dhar, Advances in Physics, **57**, 457, (2008).

[59] S. Lepri, R. Livi, and A. Politi, Phys. Rep. **377**, 1, (2003).

[60] G. W. Ford, M. Kac and P. Mazur, J. Math. Phys. **6**, 504, (1965).

[61] A. Dhar and B. S. Shastry, Phys. Rev. B **67**, 195405, (2003).

[62] A. Dhar and D. Sen, Phys. Rev. B **73**, 085119, (2006).

[63] Unpublished notes of Dr. Abhishek Dhar

[64] S. Datta, Electronic transport in mesoscopic systems (Cambridge University Press, 1995)

[65] L. G. C. Rego and G. Kirczenow, Phys. Rev. Lett. **81**, 232, (1998).

[66] M. P. Blencowe, Phys. Rev. B **59**, 4992, (1999).

[67] T. Yamamoto and K. Watanabe, Phys. Rev. Lett. **96**, 255503, (2006).

[68] J. S. Wang, J. Wang and N. Zeng, Phys. Rev. B **74**, 033408, (2006).

[69] A. J. O'Connor and J. L. Lebowitz, J. Math. Phys. **15**, 692, (1974).

[70] P. W. Anderson, Phys. Rev. **109**, 1492, (1958).

[71] I. Savic, N. Mingo and D. A. Stewart, Phys. Rev. Lett. **101**, 165502, (2008).

[72] G. Stoltz, M. Lazzeri and F. Mauri, Jn. Phys. Cond. Matt. **21** 245302, (2009).

[73] N. F. Mott and W. D. Twose, Adv. Phys. **10**, 107, (1961).

[74] R. E. Borland, Proc. R. Soc. London, Ser. A **274**, 529, (1963).

[75] I. Ya. Goldsheid, S. A. Molchanov and L. A. Pastur, Funct. Anal. Appl. **11**, 1, (1977).

[76] P. A. Lee and T. V. Ramakrishnan, Rev. Mod. Phys. **57**, 287, (1985).

[77] J. Callaway, Phys. Rev. **113**, 1046, (1959).

[78] P. B. Allen and J. L. Feldman, Phys. Rev. Lett. **62**, 645, (1989).

[79] N. Xu *et al.*, Phys. Rev. Lett. **102**, 038001, (2009).

[80] D. N. Payton and W. M. Visscher, Phys. Rev. **154**, 802, (1967).

[81] P. Dean, Rev. Mod. Phys. **44**, 127, (1972).

[82] A. Kundu, A. Chaudhuri and A. Dhar, to be published.

[83] G. Basile, C. Bernardin, S. Olla, Phys. Rev. Lett. **96**, 204303 (2006).

[84] M. S. Green, J. Chem. Phys. **22**, 398, (1954).

[85] R. Kubo, M. Yokota, and S. Nakajima, J. Phys. Soc. Jpn. **12**, 1203, (1957);

[86] H. Mori, Phys. Rev. **112**, 1829 (1958); M. S. Green, Phys. Rev. **119**, 829 (1960); L.P Kadanoff and P. C. Martin, Annals of Physics **24**, 419 (1963); J. M. Luttinger, Phys. Rev. **135**, A1505, (1964); W. M. Visscher, Phys. Rev. A. **10**, 2461 (1974).

[87] K. R. Allen and J. Ford, Phys. Rev. **176**, 1046 (1968).

[88] D. S. Fisher and P. A. Lee, Phys. Rev. B **23**, 6851 (1981).

[89] G. Gallavotti, Phys. Rev. Lett. **77**, 4334 (1996).

[90] J.L. Lebowitz and H. Spohn, J. Stat. Phys. **95**, 333 (1999).

[91] L. Rey-Bellet and L. E. Thomas, Annales Henri Poincare **3**, 483 (2002); L. Rey-Bellet, in: XIVth International Congress on Mathematical Physics, World Sci. Publ., Hackensack, NJ, 2005 pp. 447-454.

[92] D. Andrieux and P. Gaspard, J. Stat. Mech. P02006, (2007).

[93] H. Haken, Rev. Mod. Phys. **47**, 67 (1975).

[94] H. Risken, *The Fokker-Planck Equation: Methods of solutions and applications*, Springer-Verlag Berlin Heidelberg, Second Edition, 1989.

[95] J. Kurchan, arxiv:0901.1271.

[96] E. A. Novikov, Zh. Eksp. Teor. Fiz. **47**, 1919 (1964); Sov. Phys. JETP **20**, 1290 (1965); V. V. Konotop and L. Vazquez, *Nonlinear Random Waves*, WorldScientific (Singapore) 1994, pp 14-15..

[97] P. Mazur and E Montroll, J. Math. Phys. **1**, no.1, (1960).

[98] D. W. Jepsen, J. Math. Phys. **6**, no.3, (1965).

[99] W. A. M. Morgado and D. O. Soares-Pinto, Phys. Rev. E **79** (2009) 051116.

[100] K. Saito, A. Dhar, Phys. Rev. Lett. **99**, 180601 (2007).

[101] R. Rubin and W. Greer, J. Math. Phys. (N.Y.) **12**, 1686 (1971).

[102] T. Verheggen, Commun. Math. Phys. **68**, 69, (1979).

[103] M. Rich and W. M. Visscher, Phys. Rev. B **11**, 2164, (1975).

[104] D. J. Evans, E. G. D. Cohen, and G. P. Morriss, Phys. Rev. Lett. **71**, 2401 (1993); D. J. Evans and D. J. Searles, Phys. Rev. E **50**, 1645 (1994); G. Gallavotti and E.G.D. Cohen, Phys. Rev. Lett. **74**, 2694 (1995); J. L. Lebowitz and H. Spohn, J. Stat. Phys. **95**, 333 (1999);

[105] C. Jarzynski and D. K. Wojcik, Phys. Rev. Lett. **92**, 230602 (2004).

[106] T. Bodineau, B. Derrida, Phys. Rev. Lett. **92**, 180601 (2004); C. Enaud, B. Derrida, J. Stat. Phys. **114**, 537 (2004).

[107] B. Derrida, B. Doucot and P.-E. Roche J. Stat. Phys. **115**, 717-748 (2004).

[108] B. Derrida, J.L. Lebowitz, Phys. Rev. Lett. **80**, 209 (1998).

[109] P. Visco, J. Stat. Mech. P06006 (2006).

[110] C. Jarzynski, Phys. Rev. Lett. **78**, 2690 (1997); G. E. Crooks, Phys. Rev. E **60**, 2721 (1999); T. Hatano and S. Sasa, Phys. Rev. Lett. **86**, 3463 (2001); U. Seifert, Phys. rev. lett. **95**, 040602, (2005).

[111] C. Giardina, J. Kurchan and L. Peliti, Phys. Rev. Lett. **96**, 120603 (2006)

[112] P. I. Hurtado and P. L. Garrido, Phys. Rev. Lett. **102**, 250601 (2009); J. Stat. Mech. (2009) P02032.

[113] O. Mazonka, C. Jarzyski and J. Bocki, Nucl. Phys. A **641**, 335 (1998).

[114] C. Dellago, P. G. Bolhuis, F. S. Csajka, and D. Chandler, J. Chem. Phys. **108**, 1964 (1998).

[115] R. J. Allen, P. B. Warren, and P. R. ten Wolde, Phys. Rev. Lett. **94**, 018104 (2005).

[116] H. Touchette, Phys. Rep. **478**, 1 (2009).

[117] J. Farago, J. Stat. Phys., **107**, 781 (2002).

[118] R. van Zon and E. G. D. Cohen, Phys. Rev. Lett. **91**, 110601 (2003); *ibid.* Phys. Rev. E **69**, 056121 (2004).

[119] J. Kurchan, J. Phys. A: Math. Gen. **31**, 3719 (1998)

[120] F. van Wijland, Phys. Rev. E **74**, 063101 (2006).

[121] Details will be published elsewhere.